

LIU A'CHENG

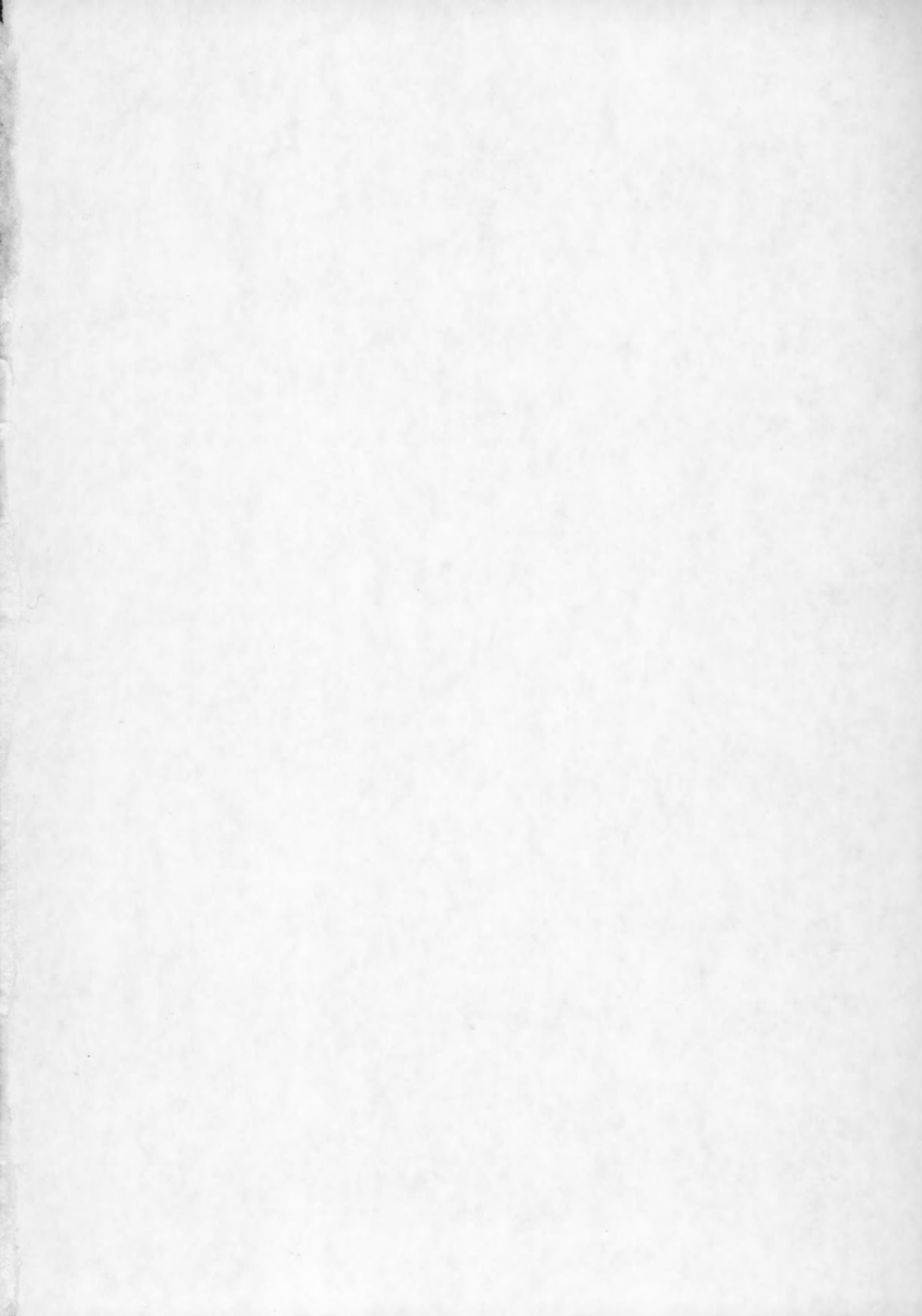
**A SEISMIC AND GEOMORPHOLOGICAL STUDY
OF THE EROSION SURFACE AT THE TOP OF
THE TERTIARY IN THE SOUTHERN NORTH SEA
(BELGIAN AND NORTHERN FRENCH SECTORS)**

VOLUME 1: TEXT

Proefschrift ingediend by de Faculteit van de Wetenschappen
van de Rijksuniversiteit te Gent voor het verkrijgen van
de graad van Doctor in de Wetenschappen
(Groep Aard- en Delfstofkunde)

Promotor: Prof. Dr. R. Marechal

Co-Promotor: Dr. J. P. Henriët



LIU A'CHENG

呈给 T. Missaen

作者 刘阿成

一九九〇年七月二十五日

**A SEISMIC AND GEOMORPHOLOGICAL STUDY
OF THE EROSION SURFACE AT THE TOP OF
THE TERTIARY IN THE SOUTHERN NORTH SEA
(BELGIAN AND NORTHERN FRENCH SECTORS)**

VOLUME 1: TEXT

Proefschrift ingediend by de Faculteit van de Wetenschappen
van de Rijksuniversiteit te Gent voor het verkrijgen van
de graad van Doctor in de Wetenschappen
(Groep Aard- en Delfstofkunde)

Promotor: Prof. Dr. R. Marechal

Co-Promotor: Dr. J. P. Henriët

TABLE OF CONTENTS

Volume 1: Text

ACKNOWLEDGEMENT

1. INTRODUCTION	1
1.1 General	1
1.2 The study area	1
1.3 Former seismic research	2
1.4 Purpose of the study	3
2. THE METHOD	4
2.1 Introduction	4
2.2 High resolution reflection seismic exploration	5
22.1 Basic principles	5
221.1 Reflection coefficient	5
221.2 Reflection time	5
221.3 Seismic velocity	6
2213.1 General	6
2213.2 Average velocity model	7
2213.3 Interval velocity model	7
221.4 Seismic profiles	8
221.5 Features and events	8
221.6 Multiple reflections	9
221.7 Resolution	9
22.2 Field equipment	10
222.1 General	10
222.2 Energy sources	10
222.3 Detection	11
222.4 Registration	11
222.5 Positioning	12
2.3 Seismic stratigraphy	12
23.1 Introduction	12
23.2 Seismic sequence analysis	13
232.1 Depositional sequences	13

232.2	Boundaries of depositional sequences	13
2322.1	General	13
2322.2	Lower boundaries	14
2322.3	Upper boundaries	14
23.3	Seismic facies analysis	15
233.1	Seismic facies	15
233.2	Geometrical configuration	15
233.3	Shape of seismic facies units	16
23.4	Chronostratigraphic significance	16
23.5	Sea-level analysis	17
23.6	Sequence stratigraphy	18
2.4	Seismic velocity measurements	19
24.1	Introduction	19
24.2	Uphole-downhole shooting	19
242.1	Principle	19
242.2	Acquisition	20
242.3	Velocity calculations	20
24.3	Calibration with boreholes	20
3.	INTERPRETATION PROCEDURE	22
3.1	Introduction	22
3.2	Interpretation of the seismic profiles	23
3.3	Creation of geological cross-sections	23
33.1	Digitization of the interpreted profiles	23
33.2	Processing of the digitized profiles	24
332.1	Converting speed to distance	24
332.2	Velocity effects	24
332.3	Converting reflection time to depth	25
3.4	Contour maps	26
4.	GEOLOGICAL HISTORY OF THE SOUTHERN NORTH SEA	27
4.1	Introduction	27
4.2	Pre-Tertiary	28
42.1	Paleozoic	28
42.2	Mesozoic	28
4.3	Tertiary	29
43.1	General	29
43.2	Paleogene	29
43.3	Neogene	30

4.4 Quaternary	31
44.1 General	31
44.2 Pleistocene	32
442.1 Early Pleistocene	32
442.2 Middle Pleistocene	33
442.3 Late Pleistocene	35
44.3 Holocene	37
5. SEDIMENTATION IN THE SOUTHERN NORTH SEA	40
5.1 Introduction	40
5.2 Cretaceous	41
5.3 Paleogene	41
53.1 Paleocene	41
53.2 Eocene	42
532.1 Ypresian	42
532.2 Ypresian-Lutetian	43
532.3 Lutetian	44
532.4 Bartonian	45
532.5 Priabonian	45
53.3 Oligocene	45
5.4 Neogene	46
5.5 Quaternary	47
55.1 General	47
55.2 Pleistocene	48
55.3 Holocene	49
6. MORPHOLOGY OF THE TOP-TERTIARY EROSION SURFACE IN THE BELGIAN AND NORTHERN FRENCH SECTORS OF THE NORTH SEA	52
6.1 Contour maps	52
6.2 General morphological considerations	53
6.3 Morphological features	53
63.1 General	53
63.2 First order features	54
63.3 Second order features	54
63.4 Third order features	55
6.4 Morphological units	55
6.5 Planation surfaces and their boundaries	57
65.1 The Offshore Platform	57
65.2 The Offshore Scarp	58

65.3 The Middle Platform	59
65.4 The Middle Scarp	60
65.5 The Nearshore Slope	60
65.6 The Nearshore Slope Break	61
65.7 The Marginal Platform	62
6.6 Paleovalleys	62
66.1 The Coastal Valley	62
66.2 The Western Valley	63
66.3 The Ostend-Northern valley system	63
663.1 The Ostend Valley	63
663.2 The Northern Valley	64
663.3 The Northern Low Surface	65
66.4 The Axial Channel	65
6.7 Scour hollows	67
67.1 The Zeebrugge Pit	67
67.2 The Sepia Pits	68
67.3 The Dunkerque Pit	69
67.4 Isolated pits in the planation surfaces	69
67.5 Isolated pits in the paleovalleys	70
7. GEOLOGICAL CONTROL ON THE MORPHOLOGY	71
7.1 Introduction	71
7.2 Regional lithological control	71
72.1 General	71
72.2 Effect of vertical lithological contrasts	72
722.1 Cuestas	72
722.2 Slope breaks and scarps	73
722.3 Valleys	73
72.3 Effect of lateral lithofacies contrasts	74
7.3 Local lithological control	74
7.4 Dip control	75
7.5 Structural control	75
8. POSSIBLE GENETIC SCENARIO'S	78
8.1 Introduction	78
8.2 The Axial Channel	78
8.3 The planation surfaces	80
8.4 The paleovalleys	81

9. BEDROCK CONTROL ON THE QUATERNARY SEDIMENTATION	84
9.1 Introduction	84
9.2 Influence of valleys on the distribution pattern	84
9.3 Influence of bedrock highs on Quaternary accumulations	85
CONCLUSION	86
SAMENVATTING	88
LIST OF ILLUSTRATIONS	94
BIBLIOGRAPHY	106

Volume 2: Illustrations

LIST OF ILLUSTRATIONS

ACKNOWLEDGEMENT

On bringing this thesis to a conclusion, I would like to express my sincere gratitude to my promotor, Prof. Dr. R. Marechal, head of the Laboratory of Earth Sciences of the State University of Gent (RUG). He offered me the possibility for research work in his laboratory and has supported me implicitly all through this study.

I also owe a great debt of gratitude to my co-promotor, Dr. J. P. Henriët, who allowed me to join the Renard Centre of Marine Geology (RCMG). Thanks to his dedication I had the disposal of all possible facilities of the marine seismic team. The many fruitful discussions with him provided an important contribution to this thesis.

I am much obliged to the RUG and the Science Policy Office (SPO) of Belgium, for their financial support which enabled me to carry out this research. Also a large part of the data acquisition was made possible by the research grant "Geconcentreerde Onderzoeksakcie Mariene Geologie, Fase 1" of the SPO.

I would like to render thanks to the State Oceanic Administration of China, not only for supporting my study here in Belgium but also for taking care of my family in China.

I am also very grateful to the Belgian, Dutch and British Geological Surveys for providing me with a lot of valuable information. Several studies of the RCMG in the Southern Bight of the North Sea have been supported by the Department of Economic Affairs, the Administration of Mines and the Belgian Geological Survey.

A special word of thanks to the captain and the crew of the oceanic vessel R.V. Belgica for their cooperation and the pleasant atmosphere during the seismic cruises. Also the

Management Unit of the Mathematical Model of the North Sea and Scheldt Estuary is gratefully acknowledged for its logistic support.

I am very much indebted to T. Missiaen, whose constant assistance during the final stage of my research was of incalculable value. The many suggestions and comments from her contributed in a large way to this study.

Dr. M. De Batist has given me a lot of information concerning Tertiary sedimentation in the Southern Bight, for which I am very thankful. The many discussions with him have been extremely useful to me.

I would also like to express my thanks to Dr. F. Mostaert of the Ministerie van de Vlaamse Gemeenschap, Administratie van de Natuurlijke Rijkdommen en Energie, for his persistent advices, based on his particular expertise on the Quaternary geology of the Belgian coastal plain.

Special thanks also to M. Bogaert for giving the so important finishing touches to this thesis.

My gratitude also goes to M. Verschuren, A. Moons, E. Maes, W. Versteeg, E. Van Heuverswyn and all other colleagues of the Laboratory of Earth Sciences who contributed to the pleasant working atmosphere.

Last but certainly not least I wish to thank my wife Lü Wenying and my son Liu Siyuan for their moral support in China during these hard years.

1. INTRODUCTION

1.1. General

High resolution reflection seismic investigations are commonly used to study the stratigraphical and structural build-up of the uppermost part of the substratum. They may however also be used to study shallow buried morphologies over large areas. The present study involves a reconstruction of the topography of the base of the Quaternary deposits in the Southern Bight of the North Sea, based on such stratigraphical and structural information. In this region, the erosion surface at the top of the Tertiary is marked by an unconformity, which results from tectonic deformation and erosion of the Tertiary strata before and/or during the Quaternary.

This study aims the definition and analysis of the morphological aspects of the erosion surface and the interpretation of these morphological features in the length of the present knowledge of the Quaternary history.

1.2. The study area

The study area is geographically located in the Southern Bight of the North Sea. Its boundaries more or less coincide with the borders of the Belgian and Northern French sectors of the continental shelf (fig. 1.1).

The seismic grid available by 1988 covers a much larger area. Its boundaries are roughly formed by the French-Belgian-Dutch coast-line in the south, the latitude 52°N in the north, the meridian 2°E in the west and the meridian 3°30'E in the east (fig. 3.1). However, the high resolution profiles which yield the most information concerning the studied morphologies

are mainly confined to the central and southern part of this area, and therefore the geological study presented here only concerns this part of the seismic grid.

The southern part of the study area is marked by the occurrence of numerous sand banks. The water depth ranges from a few meters in the nearshore zone and on top of the sand banks to some 40 to 50 m in the north.

The study area is geologically located in the southern margin of the Cenozoic North Sea basin, on top of the London-Brabant Massif (fig. 1.1). This massif came into existence during the Palaeozoic and formed a topographic high throughout a considerable part of the geological history, probably preventing the study area from being flooded until the Cretaceous.

1.3. Former seismic research

One of the first systematic marine geological studies in the Southern Bight which involved reflection seismics was carried out by Houbolt (1968), who used it to describe the sand banks in this area.

A reflection seismic study of the Tertiary deposits in the Belgian sector of the continental shelf was carried out by Bastin (1974).

In 1975-76 marine seismic investigations were carried out for the expansion of the Zeebrugge harbour, yielding some 400 km of seismic profiles, which did not only cover the harbour area but reached as far as 30 km offshore Zeebrugge. This resulted in a preliminary reconstruction of the base of the Quaternary, although the main purpose of the survey concerned a more general geological site study (Yates, 1977; Henriët, 1978, unpublished report).

During the following years, the Renard Centre of Marine Geology (RCMG) of the State University of Gent (RUG) has

gathered more than 12000 km of high resolution seismic profiles in the Southern Bight, which is greatly due to the recent availability of a very well equipped oceanic vessel, the R.V. Belgica. These seismic studies mostly involved the stratigraphy and structure of the Tertiary and Quaternary sediments (Mostaert et al., 1989; Henriët et al., 1989; De Batist, 1989).

1.4. Purpose of the study

The purpose of the geological study presented here was threefold. A first aim was to obtain a detailed description of the top-Tertiary erosion surface. A second aim was to describe possible controlling factors of the Tertiary substratum on the morphology of the erosion surface. The last purpose concerned a tentative reconstruction of the evolution of the erosion surface. Possible influences of the bedrock morphology on the distribution of Quaternary sediments are briefly mentioned.

2. THE METHOD

2.1 Introduction

The geological study presented here has been based on information from seismic research. Because the seismic method offers wide possibilities of stratigraphic resolution and penetration, it forms one of the most important geophysical techniques to provide information about the structure and distribution of rock types.

The data used in this thesis have been acquired with a marine high resolution reflection seismic method. This method offers a very detailed picture of the sedimentary succession of layers down to a depth of 500 meters, making it a perfect tool to study sedimentary sequences and buried morphologies.

The reflection seismic method is based on the propagation of artificially generated waves through the earth. These seismic waves will be partly reflected at each interface between beds with a different acoustic impedance. From the observed arrival times of the reflected waves, i.e. the time required to travel from the source to the receiver, information can be deduced concerning the depth of the interfaces which gave rise to the reflections.

Seismic velocity plays an important role in calculating the location and attitude of the interfaces. Patterns in the seismic data are interpreted in terms of stratigraphical features. The results are translated into geological cross-sections and contour maps, representing the structure of the main geological interfaces.

2.2 High resolution reflection seismic exploration

22.1 Basic principles

221.1 Reflection coefficient

The acoustic impedance Z of a medium depends on the velocity of propagation V of the seismic wave in the considered medium and the density ρ of the medium:

$$Z = V \cdot \rho \quad 2.1$$

A difference in acoustic impedance between two beds causes part of the energy of the seismic wave to be reflected at the interface between those beds. The strength of this reflection depends on the impedance difference, i.e. the bigger the difference, the stronger the reflection, and can be expressed in terms of the reflection coefficient R . In the case of normal incidence on an interface between two beds with impedances Z_1 and Z_2 , the reflection coefficient is given by:

$$R = \frac{Z_2 - Z_1}{Z_2 + Z_1} \quad \text{with} \quad -1 \leq R \leq +1 \quad 2.2$$

In the case of oblique incidence expression 2.1 will become more complicated, due to the partitioning of energy over 4 resultant waves. The variation of this energy partition as a function of the angle of incidence is given by the Zoeppritz equations, which are best known under their graphical representation. However, since these curves change slowly for small incident angles (up to 20°), the results for normal incidence have wide application (Sheriff & Geldart, 1982).

221.2 Reflection time

Reflection seismics is based on measuring the time required for the wave to travel from the source to the receiver

via a reflection at some point. This two-way traveltime is called reflection time. In the case of normal incidence the reflection time is given by (fig. 2.1a):

$$T_0 = \frac{\text{travelled distance}}{\text{velocity}} = \frac{2H}{V} \quad 2.3$$

H denotes the depth of the interface which generates the reflection, and V denotes the velocity of the seismic wave.

In the case of non-normal incidence, the reflection time will also depend on the distance between the source and the receiver, also called offset (X). From the geometry of the reflection path (fig. 2.1a) we can deduce the following relations:

$$T = \frac{\sqrt{2(H^2 + (X/2)^2)}}{V} \quad 2.4$$

$$\Rightarrow T^2 = T_0^2 + \frac{X^2}{V^2} \quad 2.5$$

The difference $T - T_0$ is called normal moveout.

Formulas 2.4 and 2.5 only hold for reflection at a horizontal interface. In the case of a dipping interface the reflection time will also depend on the magnitude of the dip. However, because the present study area mainly consists of very gently dipping beds the above formulas still hold.

221.3 Seismic velocity

2213.1 General

A real, multi-layered earth is marked by lateral and vertical velocity fluctuations, due to changes in lithology, compaction, temperature, etc...

Lateral variations in velocity are generally rather slow and can be taken into account by dividing the area into smaller areas with a negligible variation.

Vertical variations in velocity can be quite rapid, and are generally linearly related to depth, i.e. the seismic velocity will increase in deeper sediments. Sometimes a certain layer will exhibit a lower velocity than the overlying layer, causing a velocity inversion. Vertical velocity variations can be taken into account in various ways, two of which will be discussed here.

2213.2 Average velocity model

One of the simplest ways is to replace the actual section above a certain reflecting horizon by an equivalent single layer of constant velocity, equal to the average velocity between the surface and the horizon. In other words, the section is assigned a different constant velocity for each reflecting horizon beneath the surface. For small angles of incidence, the average velocity is given by (fig. 2.1b):

$$\bar{V} = \frac{2D}{T} \quad 2.6$$

D denotes the thickness of the section, and T denotes the reflection time between surface and horizon.

2213.3 Interval velocity model

Another approach consists of representing the section by a number of horizontal layers of different velocities, the velocity being constant within each layer. The raypaths will now be broken at each interface. This means we have to replace the (average) velocity by its root-mean-square value V_{rms} , which depends on the velocities and traveltimes within each layer. This rms velocity is given by (fig. 2.1c):

$$V_{rms} = \sqrt{\frac{\sum_i v_i^2 t_i}{\sum_i t_i}} \quad 2.7$$

V_i and t_i denote the resp. interval velocity and reflection time in layer i .

221.4 Seismic profiles

The reflected seismic wave is plotted under the form of a seismic trace. As marine seismics involves continuous shooting and registration along a track, a continuous seismogram (seismic profile) is obtained by alignment of traces from successive shots.

The basic problem in reflection seismics is to determine the position of the beds which give rise to reflections on a seismic profile. In order to do so we must be able to recognize different seismic events on the profile and identify which events are primary reflections and which not. The actual position of the bed, associated with the primary reflection, can then be calculated using an appropriate seismic velocity model. Different methods to measure the seismic velocity are described in section 2.4.

221.5 Features and events

Recognition of seismic events is based on the following characteristics: coherence, amplitude standout and character (fig. 2.2). Coherence is determined by the similarity in appearance from trace to trace, and is by far the most important factor in recognizing an event. Amplitude standout refers to an increase of amplitude due to the arrival of coherent energy, while character involves the distinctive appearance of the waveform (Sheriff & Geldart, 1982).

221.6 Multiple reflections

Multiple reflections are events which have undergone more than one reflection. Interfaces exhibiting a large impedance contrast can generate multiples strong enough to be recognized as distinctive events. We can distinguish so-called long-path and short-path multiples.

Long-path multiples have travel paths which are long compared to the primary reflections from the same interface. They appear as separate events on the seismogram. Short-path multiples, on the other hand, arrive so soon after the associated primary reflection that they interfere with it. Hence they merely change the waveshape of the primary reflection. Possible raypaths for long-path and short-path multiples are shown in figure 2.3.

221.7 Resolution

Resolution refers to the minimum separation between two features such that we can speak of two separate features rather than only one. In reflection seismics vertical resolution relates to the question how far apart (in space or time) two interfaces must be to show up as separate reflectors on a seismic profile.

According to Rayleigh, two reflecting interfaces can be distinguished if their separation is larger than about a quarter of the dominant wavelength of the seismic signal (Dobrin, 1976). As a consequence, the wavelength is kept as short as possible, which implies a broad frequency bandwidth.

Resolution will deteriorate due to different processes affecting the shape of the seismic signal. The most important one is absorption. As a seismic wave penetrates in the subsoil, absorption takes place, reducing the frequency bandwidth of the signal while at the same time shifting the central frequency to lower values. This results in wavelet stretching, and thus

resolution deteriorates as depth increases. Because this study did involve only rather shallow Tertiary and Quaternary sediments, absorption was not prohibitive and high resolution seismics was possible.

22.2 Field equipment

222.1 General

The seismic profiles used in this thesis have been obtained during different marine reflection seismic investigations carried out from 1980 up to 1988 in the Southern Bight of the North Sea. The seismic acquisition system, developed at the RCMG, is shown on fig. 2.4.

The oldest seismic profiles were only recorded in an analogue mode. The more recent profiles have been recorded both in analogue and digital modes. The seismic data presented in this study are based on analogue profiles. Consequently, the digital registration system is merely discussed in brief terms.

222.2 Energy sources

Different types of sources have been used during the campaigns, depending on penetration and resolution demands of the survey in question.

The watergun SODERA model S15 has been used for data acquisition with a high penetration (up to more than 500 m). It has the advantage of a very high signal repetitivity, which makes it particularly convenient for digital data acquisition. The resolution is however not the highest among the available sources.

The boomer, model EG&G 230 UNIBOOM, has a lower penetration (some 50-80 m) but yields a very good resolution (up to 0.5 m in clays).

Multi-electrode sparkers can be used at different energy levels. Higher energy will result in a better penetration but also reduce the resolution.

222.3 Detection

Detection of the reflected seismic signals was generally done with a single-channel streamer. Alternatives were two TELEDYNE 8-channel streamers of resp. 50 and 100 m active length. The depth of each 8-channel streamer was regulated by two SYNTRON depth controllers attached to the streamer. A depth sensor was attached to the front end of the single- and multi-channel streamers. This allowed continuous registrations of the streamer depth, which was visually displayed on a TELEDYNE depth monitor on board of the ship.

222.4 Registration

The raw signals coming from the hydrophones were generally recorded in digital format with a seismograph model EG&G GEOMETRICS ES 2420, and recorded in SEG-D format on one of two CIPHER tape drives. Visual control of the first trace was possible on a digital NICOLET oscilloscope. Noise monitoring on all 8 channels of the 100 m streamer was done with a TEKTRONIX oscilloscope.

During digital registration the first channel was tapped for analogue monitoring. Before recording, the single-channel signals passed through various frequency filters, in order to remove electronic noise and to prevent aliasing, as well as through a time-variant gain amplifier, in order to reduce the effect of absorption. Analogue registration was done on the EPC

1600S paper recorder, and resulted in a continuous seismic profile.

222.5 Positioning

Positioning on board the R.V. Belgica was based on the Decca Mainchain system, a hyperbolic radiopositioning method measuring the difference in phase between signals from two or more shore stations. The RS4000 Radio Navigation herefrom calculated the actual position of the ship in terms of latitude and longitude. Positions were noted every ten minutes on a recording sheet. At this same moment a fix was made on the analogue recording paper.

2.3 Seismic stratigraphy

23.1 Introduction

Seismic stratigraphy, as introduced by Vail et al. (1977), offers a practical geological-stratigraphical interpretation tool for seismic data. The unique properties of seismic reflections allow the direct application of geologic concepts based on physical stratigraphy, leading to a possible interpretation of depositional environments, geologic time correlations, postdepositional structural deformation, etc...

The original approach in seismic stratigraphy involves 3 major steps: seismic sequence analysis, seismic facies analysis and sea-level analysis. More recently, seismic stratigraphic concepts were implemented with sedimentological models, leading to the sequence stratigraphic approach (Vail, 1987).

23.2 Seismic sequence analysis

232.1 Depositional sequences

A depositional sequence is a stratigraphical unit composed of a relatively conformable succession of genetically related strata, which is bounded at its top and base by unconformities or their correlative conformities (fig. 2.5). It is determined by a single objective criterion -the physical relations of the strata themselves- which makes it a fundamental and very practical tool for the interpretation of seismic profiles (Mitchum et al., 1977).

232.2 Boundaries of depositional sequences

2322.1 General

In order to identify and correlate depositional sequences adequately, boundaries are defined at unconformities and traced where possible to their relative conformities. If the strata above and below a surface are concordant (i.e. essentially parallel to it), then there is no physical evidence for an unconformity. If the strata are discordant (i.e. they terminate against the surface), then there is physical evidence for an unconformity (Mitchum et al., 1977).

Both concordance and discordance may be seen at the upper or lower boundary of a depositional sequence. There are two types of discordance: lapout and truncation. Lapout is the lateral termination of a stratum at its original depositional limit. Truncation is the lateral termination of a stratum as a result of being cut off from its original depositional limit. Lapout may occur at both the upper and lower boundary (and is then resp. referred to as toplap and baselap), while truncation only occurs at the upper boundary (Mitchum et al., 1977).

2322.2 Lower boundaries

We can identify different types of baselap or concordance at the lower boundary of depositional sequences (fig. 2.6).

Onlap is a baselap in which an initially horizontal stratum laps out against an initially inclined surface, or in which an initially inclined stratum laps out updip against a surface of greater initial inclination (Mitchum et al., 1977).

Downlap is a baselap in which an initially inclined stratum terminates downdip against an initially horizontal or inclined surface (Mitchum et al., 1977).

In most cases onlap and downlap can be easily identified, except for structurally complicated areas, where a reconstruction of the initial depositional surface is difficult.

2322.3 Upper boundaries

Different types of toplap, truncation and concordance may occur at the upper boundary of depositional sequences (fig. 2.6).

Toplap is a lapout in which an initially inclined stratum terminates updip against an initially horizontal or inclined surface. It results from a depositional base-level being too low to permit the strata to extend further updip (Mitchum et al., 1977).

Erosional truncation is the lateral termination of a stratum by erosion. Structural truncation is the lateral termination of a stratum by a structural disruption caused by faulting, salt flowage, gravity sliding, etc... (Mitchum et al., 1977).

23.3 Seismic facies analysis

233.1 Seismic facies

The next step in seismostratigraphical analysis is the description and mapping of the so-called seismic facies units. Each seismic facies unit may represent a distinct depositional environment. It is defined on the basis of the appearance of seismic reflections, characterised by parameters like reflection configuration, continuity, amplitude and frequency. The boundaries of seismic facies units can, but do not have to, coincide with the boundaries of the depositional sequences (Mitchum et al., 1977).

Reflection configuration refers to the geometrical relationship between the different reflectors, as well as to the mode of termination of the reflections against the unconformities. Individual reflection characteristics such as continuity, amplitude and frequency offer incidental information about lateral changes in stratification, thickness or lithology (Mitchum et al., 1977).

233.2 Geometrical configurations

Major groups of geometrical configurations include parallel, subparallel, divergent, prograding and chaotic patterns (fig. 2.7).

Parallel and subparallel patterns suggest uniform rates of deposition on a uniformly subsiding shelf or stable basin setting (Mitchum et al., 1977).

Divergent patterns indicate lateral variations in depositional rate or a progressive tilting of the depositional surface (Mitchum et al., 1977).

Prograding patterns generally form through the progressive lateral development of gently sloping depositional surfaces, called clinoforms. Differences in clinoform patterns are largely due to variations in rate of deposition and water depth (Mitchum et al., 1977).

Chaotic patterns indicate deposition in a variable, relatively high-energy setting, or post-depositional deformation of initially continuous strata (Mitchum et al., 1977).

Reflection-free areas suggest homogeneous, nonstratified or steep dipping geologic units (Mitchum et al., 1977).

233.3 Shape of seismic facies units

External forms of seismic facies units are identified by the termination of a series of reflections against a common reflection, by a conformable reflection that bounds a particular configuration or by an arbitrary boundary within a sequence across a gradational change in reflection characteristics. We can distinguish between mounds, fills, sheets and sheet drapes, banks, lenses and wedges (fig. 2.8). Most of these external forms are subdivided into different types, depending on internal reflection configuration and genesis (Mitchum et al., 1977).

23.4 Chronostratigraphic significance

Seismic reflections are caused by stratal surfaces and unconformities if sufficient velocity and/or density contrasts occur. Stratal surfaces are major bedding surfaces and represent periods of nondeposition or change in the depositional sequence. Unconformities are surfaces of erosion or nondeposition and represent a significant geologic time gap (Vail et al., 1977).

Both stratal surfaces and unconformities have chronostratigraphic (time) significance. Reflections from stratal surfaces are approximate time-synchronous events, while reflections from unconformities are commonly time-variable, but do have time significance because they separate younger rocks from older rocks (Vail et al., 1977).

Boundaries between time-transgressive formations, such as lithostratigraphic units, generally do not cause seismic reflections. They are crossed by stratal surfaces. Lithostratigraphic boundaries may however yield changes in the reflection coefficient and the signal shape, for instance due to lateral changes in absorption.

23.5 Sea-level analysis

Relative sea-level changes may be inferred from patterns of onlapping and toplapping reflections.

A relative rise in sea-level is indicated by coastal onlap (fig 2.9a). The amount of sea-level rise can be determined from the vertical component of the sedimentary onlap, but should be adjusted for any thickening due to differential basinward subsidence. This can be done by measuring increments over small horizontal intervals, close to the former shoreline ("coastal" onlap) (Vail et al., 1977).

A relative fall of sea-level is indicated by a downward shift in coastal onlap from the highest position in a sequence to the lowest position in the overlying sequence (fig. 2.9b). The amount of sea-level drop can be determined by the vertical component of basinward shift of the sedimentary onlap, provided the underlying sequence has not been eroded too intensely (Vail et al., 1977).

A relative stillstand of sea-level is indicated by toplap (fig. 2.9c) (Vail et al., 1977).

Relative sea-level changes are the result of the superposition of three independent processes: eustatic sea-level changes, tectonic subsidence/uplift of the basin and sediment inflow. Of all these processes the eustatic sea-level generally proves to be the most important, due to its ability to change rapidly and in a reversible way, and therefore forms the main control of the relative sea-level changes in sedimentary basins. A combination of different relative sea-level curves determined in basins all over the world has led to a global eustatic sea-level curve (Vail et al., 1977).

23.6 Sequence stratigraphy

The application of seismic stratigraphy to sedimentary basin analysis has resulted in a new way to subdivide, correlate and map sedimentary rocks (Vail, 1987). This technique is called sequence stratigraphy. It groups seismic reflections into so-called system tracts, which correspond to chronostratigraphically constrained genetic depositional intervals (Brown & Fisher, 1977; Vail, 1987). System tracts are related to relative changes of sea-level and according to Vail (1987) they can be divided into four groups: lowstand, highstand, transgressive and shelf margin.

The different system tracts may then be grouped into a so-called "depositional sequence"* (Vail, 1987), which can be correlated with one full cycle of relative sea-level change. Due to the predictable strata patterns and lithofacies of these "depositional sequences" and system tracts, their identification on seismic sections offers a more accurate prediction method of depositional environments and lithofacies (Vail, 1987).

(*) The term depositional sequence, as introduced by Mitchum et al. (1977), has been newly defined in terms of a sedimentological-genetical approach by Vail (1987). To avoid confusion the new term is put between quotationmarks.

2.4 Seismic velocity measurements

24.1 Introduction

A knowledge of the velocity of seismic waves in different sediments is essential for a correct interpretation of the seismic profiles. Errors in seismic velocity can cause quite serious errors in layer thicknesses and reflector depths, which can eventually lead to a wrong representation of certain geological features. This will be discussed in more detail in chapter 3.

Different methods can be used in order to determine the seismic velocity. They include uphole-downhole shooting, reflection seismic calibration on boreholes, refraction measurements and wide-angle reflection measurements. Only the first two methods will be discussed here, being the most simple and widely used methods.

24.2 Uphole-downhole shooting

242.1 Principle

The most direct measurement of seismic velocity is done in boreholes. By placing a seismic device at different depths inside a borehole, the effect of the different layers on the velocity can be determined. In uphole shooting the source is lowered in the borehole, while the detector remains at the surface (fig. 2.10b). Downhole shooting is just a reverse procedure, i.e. the detector is lowered in the borehole and the source remains at the surface (fig. 2.10a). Uphole-downhole shooting measurements are useful for spotting possible velocity inversions.

242.2 Acquisition

The energy source in downhole shooting measurements carried out by the RCMG generally consists of a sparker. Detection for both methods generally happens with a single channel hydrophone cable. The arrival times of the direct waves are recorded on paper. The depth of the source/receiver is read from a gauged cable and marked on the paper.

242.3 Velocity calculations

A first step in determining the velocity from downhole shooting measurements is to calculate the distance between the borehole hydrophone and the source. From the calculated distance and the known hydrophone depth the raypaths of the seismic waves can be determined. Together with the arrival times at different depths this allows the calculation of the average velocity at these depths, and eventually the interval velocities within the different layers.

A velocity calculation in the uphole shooting method is based on the same principles.

24.3 Calibration with boreholes

In order to get a better idea of the variation of the seismic velocity in the Quaternary sediments, results from reflection seismic profiles have been calibrated on borings in the Southern Bight of the North Sea. On the profile closest to boring sites the reflection time was measured to the base of the Quaternary. From this reflection time the average velocity was determined using the following formula:

$$\bar{V} = \frac{2D}{T} \quad 2.8$$

D denotes the thickness of the Quaternary, as derived from the boring. T denotes the reflection time, as derived from the seismic profile.

This method had to cope with several problems. First of all, the borings were sometimes located in an area without seismic penetration. Secondly, only few borings were deep enough to reach the base of the Quaternary. And thirdly, quite often the interpretation of the borings was not very reliable. Together with the possible errors in the measured reflection times (often with non-normal incidence on shallow sand banks) this resulted in rather inaccurate velocity values.

3. THE INTERPRETATION PROCEDURE

3.1 Introduction

Seismic profiles give a two-dimensional picture of the sea-bottom and the underlying reflectors. The horizontal axis of the profile is a function of the ship's speed and the firing rate of the source. The vertical axis represents the reflection time.

Marine seismic operations involve continuous profiling along certain seismic tracks. Together these tracks form what is called a seismic grid. The grid which covers the southern part of the Southern Bight totalizes about 12000 km (fig. 3.1). It mainly consists of orthogonally oriented seismic lines, which allows a rough three-dimensional geological representation of the area.

The seismic profiles have different recording lengths of 100, 200, 400 and 800 ms (two-way traveltime). The 400 and 800 ms records however hardly provide any information about relatively shallow sediments, due to a deteriorating resolution. Therefore mostly 100 and 200 ms profiles were used for this study. These profiles are mainly confined to the central and southern part of the grid, i.e. to the Belgian and Northern French sectors of the continental shelf.

Transformation of the seismic profiles into geological profiles takes place in two steps. The first step consists of the interpretation of the seismic profiles, i.e. identification of reflectors, depositional sequences and structural deformations. During the second step the interpreted profiles are digitized, and their resp. horizontal and vertical scales converted into distance and depth scales. The thus obtained geological cross-sections can be used to create different types of contour maps.

3.2 Interpretation of the seismic profiles

A first major step in the interpretation of the seismic profiles is the identification of the most significant reflectors, as described in chapter 2. These reflectors are then marked ("picked") and followed throughout the complete seismic grid. Special attention is hereby paid to the reflectors on the tie-points of the grid.

Subsequently the reflectors are grouped according to the principles of seismic stratigraphy, as described in chapter 2. Reflectors corresponding to unconformities help to define the different depositional sequences. The identified sequences are labeled with a character-digit symbol, suggesting their most probable chronostratigraphic identity. Main reflectors are labeled with the character-digit symbol of the overlying depositional sequence, accompanied by a rank number. First order ranks are given to significant sequence boundaries, higher rank numbers to significant internal reflectors. Within each sequence attention is also paid to the seismic facies units (De Batist, 1989).

A last step consists of the identification of different structural deformations, such as faults, folds and diapirs.

3.3 Creation of geological cross-sections

33.1 Digitization of the interpreted profiles

Digitization of profiles is storing the x- and z-coordinates of certain points on the profiles in the computer memory. It is done by fixing the profile onto a magnetic digitizing table and subsequently marking the different points with a cursor or magnetic pen.

In order to calibrate the digitizing table before further use, three corner points of the profile are digitized first. In

the case of a non-linear horizontal scale of the profile, the intersections of all fix lines with the reference time line have to be digitized too. After this the sea-bottom reflector and the other identified reflectors are digitized.

33.2 Processing of the digitized profiles

332.1 Converting speed to distance

The horizontal scale of the seismic profile is quite often a non-linear time scale, depending on the line density, firing rate and the ship's speed. Whereas the first two factors mostly remain constant, the last one, speed, may vary along the track. In this case the distance between two fix lines on the profile will no longer be constant. In order to keep things simple the ship's speed is supposed to remain constant between two fix lines.

Each x-coordinate lies between two fix lines. The x' - and y' -coordinates of all the fix lines have been stored in a positioning file. By interpolation between the x' - and y' -coordinates of the two fix lines each x-coordinate can be converted into an x' - and y' -coordinate. Every digitized reflector point can now be expressed in (x', y', z) - coordinates.

332.2 Velocity effects

The depth of a reflector on the seismic profile depends on the velocity model that is used, as discussed in section 221.3. Different velocity models will yield different reflector depths, and therefore the importance of an accurate velocity model becomes quite obvious.

The study presented here mainly concerns the top-Tertiary erosion surface. The depth of this surface is calculated by using the two-layered interval velocity model. The upper layer

consists of sea-water and has a velocity of 1500 m/s. The lower layer consists of Quaternary deposits. The velocity of these deposits may vary from 1650 to 2000 m/s. In general the Quaternary layer is very thin (less than 20 m), and consequently the velocity variation will not cause strong effects in the surface morphology. In some places, however, the Quaternary may reach a considerable thickness (up to 40 m), and here the velocity effect will become more pronounced.

The apparent effect of different velocities of the Quaternary layer on the morphology of the erosion surface is illustrated by the following examples. Fig 3.2 shows a flat surface covered by sand banks. The depth of the surface has been calculated for velocities ranging from 1600 to 2000 m/s. For larger velocities (1800 m/s and more) the shape of the surface becomes clearly deformed, in such that depressions and hills show up in those places where the sand bank locally becomes very thin or very thick. Fig. 3.3 shows a slightly dipping surface covered by sand banks, and again a similar deformation of the surface can be observed for larger velocities. From these examples it is quite clear that a low Quaternary velocity yields the best representation of the actual erosion surface morphology.

332.3 Converting reflection time to depth

Before converting the vertical time scale to depth, an extra correction has to be made for a possible signal delay and for tidal fluctuations. The datum plane for all height reductions is the mean lowest low water-level at spring-tide.

The vertical scale of the seismic profile is a linear time scale representing the arrival times of the reflected waves. It depends on the distance travelled by the wave and its velocity. In order to determine the travelled distance a constant small offset was assumed, turning the distance into roughly twice the reflector depth. The velocity of the wave was derived from the two-layered interval velocity model, as described in the

previous section, with a value of 1700 m/s for the Quaternary layer.

With these seismic velocities and travel distances, one can convert the time corresponding with every reflector point for successive deeper reflectors on the profile to real depth, resulting in a linear vertical depth scale. Every digitized reflector point is then stored in real (x', y', z') -coordinates.

3.4 Contour maps

The interpreted geological profiles can be translated into different types of contour maps. Digitization of the reflector representing the top-Tertiary erosion surface has lead to an isobath map of the top of the Tertiary. Additional digitization of the sea-bottom reflector and some internal Quaternary reflectors has lead to an isopach map of the Quaternary cover. The maps will be discussed in more detail in chapter 6.

4. GEOLOGICAL HISTORY OF THE SOUTHERN NORTH SEA

4.1 Introduction

The geological history of the North Sea area is strongly related to the tectonic evolution of NW Europe. During this evolution the North Sea was occupied by a number of genetically different sedimentary basins caused by different megatectonic settings. The North Sea basin came into existence as a structural entity during the Early Tertiary. Its geometry is strongly influenced by tectonic patterns established during the Late Paleozoic and Mesozoic, and reflects the subsidence pattern of an aborted rift.

The southern North Sea is closely related to the London-Brabant Massif. This massif is believed to be of Pre-Cambrian or Early Paleozoic age, and persisted as a highland and a sediment source to the surrounding basins during the subsequent geological history. From the Late Cretaceous on the massif has been frequently flooded, in consequence of the numerous transgressions during the Tertiary and Quaternary. This resulted in the deposition of a thick sequence of Late Mesozoic and Cenozoic sediments in the study area.

A drastical variation in Quaternary deposits from the north to the south in the Southern Bight implies a rather different recent geological history between the study area, situated in the southern part, and the rest of the Bight.

4.2 Pre-Tertiary

42.1 Paleozoic

The Belgian sector is located on top of the London-Brabant Massif. During Late Pre-Cambrian and Early Paleozoic times this massif formed a huge triangular unit, expanding from Kingston upon Hull in the north to the Bristol channel and Brabant in the west and east. It was surrounded by Caledonian fold belts and acted as a stable micro-continent (fig. 4.1). Subsequent orogenic events during the Devonian, Carboniferous and Early Permian were of minor influence on the configuration of the London-Brabant Massif (P. Ziegler, 1981).

42.2 Mesozoic

During the Triassic the Caledonian tectonic framework was thoroughly changed by the subsidence of a complex graben system which gradually opened up during the Mesozoic (fig. 4.2), eventually resulting in the drifting apart of the North American - Greenland and the European plate during the Late Mesozoic and earliest Cenozoic (P. Ziegler, 1981).

Throughout the Jurassic and Cretaceous major eustatic sea-level changes took place, which in combination with the tectonic instability caused several transgressions and regressions in the North Sea area. Due to a presumed acceleration of sea-floor spreading rates, a significant rise of global sea-levels took place during this period, which reached its peak during the Late Cretaceous (Pitman, 1978). The sea-level reached a maximum high stand of some 100-300 m above present level* (a.p.l.), inundating the London-Brabant Massif (fig. 4.3), and seaways were opened which linked the basin with the North Atlantic and Tethys oceans (P. Ziegler & Louwerens, 1979; Tröger, 1978; Wiedmann, 1979). A sheet of chalk, varying in thickness from 50 to 200 m, was deposited in a shallow sea environment (fig. 4.4) (Kockel, 1988).

(*) The term present level refers to the mean lowest low water-level at spring-tide.

4.3 Tertiary

43.1 General

During the drifting apart of the European and the North America - Greenland plate the North Sea rift had not been affected by extensional stresses. With the onset of sea-floor spreading in the Norwegian-Greenland sea during the Early Tertiary, the North Sea rift gradually became an inactive, but still subsiding branch of the North Atlantic - Arctic rift (P. Ziegler, 1979). The great thickness of Quaternary sediments demonstrates that this subsidence movement is still going on at this very moment. A final tectonic pulse occurred during the Early Tertiary, and probably corresponds to an early phase of the Alpine orogeny (P. Ziegler, 1982).

As a result of the subsidence movement the North Sea basin became an elongated, saucer-shaped basin, with its axis above the Mesozoic rift system (P. Ziegler & Louwerens, 1979). The transgressions and regressions associated with the repeated sea-level changes in the Southern Bight during the Paleogene and Neogene (fig. 4.5) covered the chalk on top of the London-Brabant Massif with a thick sequence of Tertiary beds.

43.2 Paleogene

Subsidence of the North Sea basin, combined with warmer climatic conditions, led to a first Tertiary transgression during the Early Paleocene, which covered nearly the entire NW European basin (fig. 4.6). The subsequent Mid-Paleocene fall in sea-level coincided with the Laramide deformation of the Alpine foreland, resulting in a wide-spread regression which removed the Early Paleocene deposits from much of the basin, except for

the areas of extreme subsidence (Gramann & Kockel, 1988). Moreover, this regression caused the separation of the Atlantic-Tethys and the Arctic seas (P. Ziegler, 1982). During the much cooler Late Paleocene several smaller transgressions took place, the last two of which barely flooded the London-Brabant Massif.

Rising sea-levels and progressive degradation of tectonically uplifted areas caused a severe transgression during Mid-Eocene times, and most likely a seaway was re-opened between the basin and the Atlantic via the Channel (fig. 4.7) (Gramann, 1988). After this the basin slowly shallowed, until a new Late Eocene transgression flooded the area, inundating many areas formerly above sea-level (fig. 4.8) and creating a southern seaway with the Tethys (Gramann & Kockel, 1988).

The Early Oligocene transgression covered a much smaller area than the previous transgressions, and together with the upwarping of the Weald-Artois anticline this caused a temporary interruption of the seaways that had been established during the Eocene (P. Ziegler, 1982). The last severe transgression of the Paleogene took place during the Middle Oligocene (fig. 4.9), under markedly warmer climatic conditions, and caused a re-opening of the southern and western seaways (Gramann, 1988).

The following regional Mid- to Late Oligocene regression was possibly induced by the onset of the first major glaciation of Antarctica, and again separated the NW European basin from the Atlantic and the Tethys. According to P. Ziegler (1982) the passage through the Channel to the Atlantic was only to be re-opened during the Quaternary.

43.3 Neogene

The onset of the Miocene was marked by several small transgressions, which barely influenced the Belgian sector. Most likely these transgressions only reached the margin of the London-Brabant Massif, never actually flooding the massif.

A sudden, big rise of sea-level took place during the Middle Miocene, flooding most of the Southern Bight and big parts of Belgium (fig. 4.10). It was mainly due to a glacio-eustatic sea-level rise, but may also have been influenced by tectonic activity in the Alpine region (Zagwijn & Doppert, 1978).

During this period the area south of the present Thames estuary was tectonically uplifted (Weald-Artois anticline), and a complex river system was formed, which flowed NE across this area towards the North Sea (Briquet, 1921). The Lobourg river, which formed the most eastward river of this system, was rising off the NE flank of the uplift in the area of the Dover Strait, whereas the Thames river flowed further north (Stamp, 1972; Balson & D'Olier, 1988).

The Late Miocene was marked by a comprehensive temperature drop, and the sea regressed from large parts of the Southern Bight, removing most of the Miocene deposits in the study area (Zagwijn & Doppert, 1978).

The last Tertiary transgression took place during the Early Pliocene, and flooded most of the Southern Bight (fig. 4.11). During this period the rivers Medway and Stour formed the tributaries of the Lobourg river, which became subject to strong erosion and shaping (Balson & D'Olier, 1988). Many of the Early Pliocene deposits were eroded again during the following severe regression at the end of the Pliocene.

4.4 Quaternary

4.4.1 General

The sea-level changes in the southern North Sea area during the Quaternary are the combined effect of tectonic, eustatic and isostatic movements. The tectonic movements were due to the slow subsidence of the entire NW-European basin and to some regional uplifting/subsidence caused by tectonic

activity in the Central European hinterland, and resulted in a gradual narrowing of the southern North Sea basin. The eustatic movements of sea-level were caused by the alternating glacial and interglacial periods, very typical of the Quaternary era (fig. 4.12), and are believed to be the major controlling factor for the position of the shorelines. Isostatic movements connected to loading and unloading of ice sheets are still a much disputed subject (Jelgersma, 1979), and will be neglected in this study .

44.2 Pleistocene

442.1 Early Pleistocene

The first Pleistocene glacial stage started at the end of the Pliocene and lasted throughout the Praetiglian. It was marked by a sea-level drop up to 100 m, transforming the Southern Bight into land. According to Graman & Kockel (1988) this regression was not only due to a glacio-eustatic sea-level drop, but was also influenced by a substantial uplift of the marginal areas on the NW European basin at this time.

The following Tiglian interglacial is subdivided into 3 subcycles. During the Early Tiglian the climate was still very cold, as indicated by the periglacial phenomena observed at the bottom of Early Pleistocene sandy sediments in northern Belgium (Paepe et al., 1981).

By the beginning of the Middle Tiglian the coastline had shifted towards the Belgian-Dutch border (fig. 4.13), due to tectonic activity in the area of the Central graben Rhine embayment (Zagwijn, 1979). Big parts of the Southern Bight were under intertidal conditions and a sheet of sandy and clayey sediments was deposited, which reached the northern part of the Belgian sector (Cameron et al., 1989).

During the Late Tiglian the coastline shifted to the west (fig. 4.14). Its convex shape was probably related to the

formation of the large delta of the River Rhine and the North German rivers combined (Zagwijn, 1979). The Mid-Tiglian sediments became overlain by a layer of deltaic sediments in the northeastern part of the Bight and marine sands in the northwestern part of the Bight, both of which barely reached the Belgian sector (Cameron et al., 1989).

During the Eburonian glacial a huge ice sheet covered North America, resulting in a considerable eustatic lowering of sea-level. Melting of the ice sheet during the following Waalian interglacial caused sea-level to rise again. Together with the further narrowing of the southern North Sea basin this resulted in the coastline shown in fig. 4.16. The NW European delta complex expanded across the Southern Bight, depositing a layer of mainly fluviatile sediments which might have reached the northeastern part of the study area (Cameron et al., 1989). The subsequent glacial stage during the Menapian can again be correlated with a large North American glaciation, and was marked by a global sea-level drop.

Throughout the entire Early Pleistocene the routes of the rivers Thames, Medway, Stour and Lobourg kept a more or less stable course (fig. 4.15) (Balson & D'Olier, 1988).

442.2 Middle Pleistocene

The first interglacial stage of the Middle Pleistocene is referred to as the Cromerian complex. It is generally believed that the sea withdrew completely from the southern part of the North Sea basin during early Cromerian, and could not, even during high sea-level stands of the Cromerian interglacials I and II, penetrate into this part of the North Sea basin (Zagwijn, 1979). In a later phase, however, the southern part of the basin was flooded again during the Cromerian interglacials III and IV (fig. 4.17) (Zagwijn & Doppert, 1978). By this time the coastline had been shifted towards the Belgian-French border, probably due to a tilting of the marginal basin to the west (Paepe & Baeteman, 1979).

There is still some speculation concerning a possible connection between the North Sea and the sea south of the Strait of Dover during these last interglacials. According to Zagwijn and Doppert (1978), the Dover Strait did not open again until the Holsteinian. The believed presence of marine sediments of Late Cromerian age in the Belgian-French border area (see chapter 5) seems to contradict this assumption (Sommé, 1979; Paepe & Baeteman, 1979). It suggests that the sea flooded from the Channel through the Dover Strait and the Lobourg Channel into a precursor of the Yzer Valley (Mostaert et al., 1989).

During the Elsterian glacial stage inland ice invaded the southern North Sea (fig. 4.18). The ice blocked the route of the river Thames to the north, causing it to shift progressively eastward and southward until it joined the river Medway (fig. 4.15) (Gibbard, 1977; Balson & D'Olier, 1988). According to Zagwijn (1979) the land ice did not reach the southernmost part of the Bight.

During the Holsteinian interglacial sea-level rose considerably (fig. 4.19). According to Paepe & Baeteman (1979) a large bay existed from Ostend to the Cliff of Sangatte. It is still not certain whether the North Sea extended to the south, or the Channel extended northward through the Strait of Dover, or perhaps the North Sea was connected with the Channel (Zagwijn, 1979). However, from the presence of marine deposits of Holsteinian age near the French-Belgian border (see chapter 5) (Sommé, Paepe et al., 1978) and in southeast Britain (Pike & Godwin, 1953; Stevens, 1960) it is believed that the sea flooded from the Channel through the Dover Strait and the Lobourg Channel into the southernmost part of the Southern Bight, eventually inundating the Yzer Valley for the second time. Similar sediments of Holsteinian age have so far not been found in the middle coastal plain (Paepe et al., 1981), which may indicate that this area might have formed a high during this period.

Throughout the Holsteinian the river Thames moved further towards the south (fig. 4.15), possibly under the influence of

differential subsidence (D'Olier, 1981; Balson & D'Olier, 1988).

The Saalian glaciation forms the last episode of the Middle Pleistocene. During this period sea-level dropped to a minimum of some 130 m below the present level (b.p.l.) (Jelgersma, 1979), and the Southern Bight became land once more. The Scandinavian ice sheet covered the northern half of the Dutch territory (fig. 4.20), forcing the rivers Rhine and Meuse to flow along the front of the ice sheet before they turned southwards (Oele & Schüttenhelm, 1979). A huge longitudinal glacial valley reached the northern margin of the Southern Bight, but did not affect the study area (Jelgersma, 1979).

During this period the area of the Flemish Valley formed the mouth of the river Scheldt and its tributaries. Strong erosion took place in the axial part of the valley, causing a gradual deepening of the valley (De Moor & Tavernier, 1978).

According to Kellaway et al. (1975), the land ice also penetrated from the south into the North Sea through both the Channel and the Strait of Dover during the later part of the Saalian. Although his view has been challenged by other authors (a.o. Kidson & Bowen, 1976), the results of the present study are in favour of this interpretation (see chapter 8).

442.3 Late Pleistocene

After the retreat of the land ice during the Early Eemian interglacial, sea-level rose and the North Sea region became an open sea again. The maximum Eemian sea-level is believed to have been higher than the present level, as suggested by pollen analysis and oxygen-isotopic records (Jelgersma, 1979), and a layer of sandy and clayey sediments was deposited in large parts of the Southern Bight. Most likely the Strait of Dover was open at this time. But the absence of southern elements in the Eemian sediments in the Dutch sector indicates the

transgression from the south must have passed very quietly, if at all (Oele & Schüttenhelm, 1979).

The position of the maximum Eemian sea-level varies considerably between the different countries surrounding the southern North Sea basin. A rise of the top of the marine Eemian deposits is noticed from the Netherlands towards Belgium. This is most likely due to differences in tectonic downwarping in and around the basin (Jelgersma, 1979).

In Belgium the coastline most likely extended east of Ostend, inundating the middle and eastern coastal plain and interfingering along the Flemish Valley until Gent, and further towards the north (Paepe & Baeteman, 1979). It hereby locally eroded the Saalian sediments in the Flemish Valley, which resulted in the formation of Eemian terraces (De Moor & Tavernier, 1978; De Moor, 1988). According to Oele & Schüttenhelm (1979) the southern margin of the Eemian transgression was formed by the south side of the more recently discovered Ostend Valley. This seems to be confirmed by the absence of Eemian deposits in the coastal area south of the Thames (Jardine, 1979) and the western Belgian coastal plain (Paepe & Baeteman, 1979).

Nevertheless, sediments of believed Eemian age are reported to be present in a basin infill in the Sandettie area (Kirby & Oele, 1975), but this was later contested by Oele & Schüttenhelm (1979) who believed the sediments could also be Late Saalian (see also chapter 5). Up to this very day it remains strongly disputed whether or not the southernmost part of the Southern Bight and the western coastal plain have actually been flooded during the Eemian transgression.

Mostaert & De Moor (1984, 1989) provided an Eemian mean sea-level curve based on geological studies in the eastern part of the coastal plain. According to this curve at least one sea-level lowering occurred during the period of Eemian highest sea-level stand.

The Late Eemian was marked by a considerable drop in sea-level. During the Early Weichselian the sea retreated further

from the southern part of the North Sea. This was probably due to an eustatic lowering of sea-level caused by the growth of the Laurentic ice sheet in North America (Dreimanis, 1960). Sediments from the Southern Bight, which was a large fresh-water lake at this time, indicate a sea-level stand at 40 m b.p.l., even during the interstadials (Jelgersma et al., 1979; Jansen et al., 1979).

The land ice reached its maximum extension during the Middle Weichselian, and sea-level dropped to 130 m b.p.l. (fig. 4.21). Still, this ice extension was much smaller than during the Saalian, and did not reach the Belgian and Dutch sectors (Jelgersma et al., 1979). The sediments deposited in the Southern Bight throughout this period are entirely of terrestrial origin (fluvial, lacustrine, aeolian) and do not contain any marine material (Jansen et al., 1979). Fluvioperiglacial erosion removed part of the Eemian deposits in the middle and eastern coastal plain, and in the Flemish Valley (De Moor & Tavernier, 1978; Mostaert & De Moor, 1989).

During the early Late Weichselian the land ice started to melt and the sea transgressed southward over the North Sea. At the onset of the Holocene about half of the ice sheet had disappeared, and sea-level was at 60 to 70 m b.p.l. (Jelgersma, 1979).

Throughout the entire Late Pleistocene the Thames/Medway route shifted further towards the south, most likely due to differential subsidence (D'Olier, 1981). Eventually it ran eastwards, joined by the river Stour, into the Lobourg channel (fig 4.15) (Balson & D'Olier, 1988).

44.3 Holocene

Sea-level changes during the Holocene have been discussed by a number of authors over the past years (a.o. Fairbridge, 1961; Jelgersma, 1979; Köhn, 1988; Mostaert & De Moor, 1989), and different sea-level curves have been put forward. Most curves indicate a rapid rising of sea-level until the Late

Atlantic (6600 before present (B.P.)), followed by a slight slowing down until the Subboreal (5000 B.P.) and eventually further slowing down up to the present day (fig. 4.22). In the southern North Sea this continuous sea-level rise is believed to be largely due to an eustatic sea-level rise, and to a much smaller extent to tectonic downwarping (Jelgersma et al., 1979).

During the Preboreal the southern and northern part of the North Sea were separated by a narrow land bridge. Sea-level stood about 50 m b.p.l. and only the deepest parts of the Southern Bight were believed to be tidal flats (Jelgersma et al., 1977). During the Late Boreal, when the southern and northern North Sea were recently connected, sea-level rose to about 30 m b.p.l., and the Southern Bight turned into a tidal flat (Jelgersma et al., 1961, 1966). Most likely a first ingression of the lower western part of the Belgian coastal plain took place at the end of the Late Boreal period by penetrating the Yzer Valley (Köhn, 1988).

During the Early Atlantic the sea penetrated a small system of gullies near Nieuwpoort. The coastline east of Nieuwpoort was probably situated more seaward than today (Köhn, 1988). According to Baeteman (1981) a coastal barrier may have been formed at the end of the Early Atlantic, which gradually reduced the marine influence. During the Middle Atlantic the sea-level rise slackened and the sedimentation area became more extended, resulting in the formation of a moor which extended from the Belgian/French border to Zeeland (Köhn, 1988). During the Late Atlantic the coastal barrier was broken by several tidal inlets, transforming parts of the moor into tidal flats (Köhn, 1988). According to De Ceuninck (1985) the first dunes were formed at the end of this period.

All through the Subboreal and Subatlantic sea-level kept rising very slowly, flooding the moor and turning the area into a tidal flat near the sea or a swamp in other places (Köhn, 1988). By the building of dikes since 1000 B.P. the tidal flat area was reclaimed, and the whole coastal plain now became a marshland.

Already during the flooding of the southern North Sea, strong tidal currents from the Channel caused serious reworking of Pleistocene and probably also Tertiary deposits into tidal flat sands, estuarine sand banks and beach deposits. According to some authors certain sand banks (Brown Bank, Sandettie Bank) can be considered as ancient beach barriers of Early Holocene age (Kirby & Oele, 1975; Oele, 1971).

During the later part of the Holocene a repeated reworking and removing of the fine-grained material led to the deposition of the so-called Young Sands on top of the tidal flat deposits (Oele, 1971; Jelgersma et al., 1977; Jansen et al., 1979). These sands form the present sea-floor, and recent tidal currents have shaped them into nearly planar beds, megaripples, sand waves and linear sand ridges (Eisma et al., 1979).

At present only fine-grained material (200-300 μm) is transported in suspension over large distances in the Southern Bight (Mc Cave, 1971; Eisma et al., 1979). Due to the combined effect of a large river supply, heavy coastal erosion and a strong current, this suspended material reaches high concentrations in the coastal waters (Dietrich, 1955; Ramster, 1965).

5. SEDIMENTATION IN THE SOUTHERN NORTH SEA

5.1 Introduction

The strata in the Belgian sector of the North Sea can be subdivided into three major units: a Paleozoic basement, a cover of Cretaceous and Tertiary sediments and a Quaternary drift mantle (Marechal, 1972). In the study area the basement corresponds to the London-Brabant Massif, which is composed of intensively folded Cambrian, Ordovician and Silurian rocks (mainly shales and phyllites), maybe with a core of Pre-Cambrian rocks. The cover sediments are almost undeformed and mostly unconsolidated (chalk, sand, clay). They are mainly of marine origin and extend continuously, only with gradual changes in thickness and composition. The drift mantle includes relatively recent sediments which are marked by abrupt and strong variations in thickness, related to the present day sea-floor morphology.

Only few borings are located on the Belgian continental shelf, and consequently no lithostratigraphic division of the sediments in this area is possible as yet. However, the application of seismic-stratigraphic analysis (Vail et al., 1977), which was correlated with the existing borings, has recently lead to a seismostratigraphic division of the sediments in the Southern Bight into 17 depositional sequences of which one belongs to the Cretaceous, 14 to the Paleogene, one to the Neogene and one to the Quaternary (fig. 5.1) (De Batist, 1989; Henriët et al., 1989). The seismostratigraphic terminology used in this study has originally been introduced by De Batist (1989).

The Paleogene sediments exhibit a general strike of some 40-45° NW and a dip of some 0.5-1° NE, which is most likely caused by the subsidence movement of the North Sea basin together with some regional tectonic activities (Henriët et

al., 1989). As a consequence, progressively younger sequences are subcropping at the top-Tertiary erosion surface from southwest to northeast (fig. 5.2). The dip increases suddenly to some 2-3° NE towards the northeastern border of the Belgian continental shelf, near the margin of the London-Brabant Massif, where the Paleogene deposits are overlain by Neogene sediments. A thin layer of Quaternary sediments covers the larger part of the top-Tertiary erosion surface (De Batist, 1989).

Both the structure and the stratification and lithology of the Tertiary sedimentary sequences are important controlling factors of the morphology of the top-Tertiary erosion surface, as will be discussed in chapter 7. Therefore a rather detailed description of these sequences will be given in this chapter.

5.2 Cretaceous

The lowermost identified depositional sequence C0 consists of Late Cretaceous chalk and chalky limestone. It is bounded resp. by unconformities at the top of the Paleozoic basement and at the base of the Tertiary (De Batist, 1989). Due to the lithological homogeneity of these Cretaceous sediments and the rather great depths at which they are found, very few internal reflectors show up on the seismic profiles. The lack of internal structural deformation patterns suggests that tectonic quiet conditions prevailed during the Late Cretaceous.

5.3 Paleogene

5.3.1 Paleocene

The first three sequences (T1, T2 and T3) overlying the Cretaceous chalk on the Northern French continental shelf belong to the Late Paleocene (Late Thanetian) and can be correlated with the Landen Formation in Belgium. The thickness

of the lowermost T1 sequence decreases from about 30 m to 18.5 m towards the southwest. It consists of marine silts and clays, and its rather homogeneous facies suggests a quiet depositional environment (De Batist, 1989).

The T1 sequence is separated from the overlying T2 sequence by an erosion surface, which on its turn is scoured on some places by the basal reflector of the uppermost T3 sequence (De Batist, 1989) (fig. 5.3). The T2-T3 interval consists of sand with silt, clay and shells and has a constant thickness of about 20 m. Its rather irregular facies suggests a more complex intertidal marine or continental depositional environment, as caused by alternating transgressions and regressions (De Batist, 1989).

53.2 Eocene

532.1 Ypresian

The Paleocene deposits are overlain by a thick sequence of clayey sediments (Y1) of Ypresian (Early Eocene) age. This Y1 sequence can be correlated with the lower part of the Yper Formation (Orchies Member, Roubaix Member, Aalbeke Member) in Belgium and the London Clay in England (De Batist, 1989). Its facies is generally characterized by weak parallel internal reflections, suggesting a low-energy marine depositional environment (Henriet et al., 1989).

The most striking feature though is the occurrence of strong internal deformations, often showing a vertical zonation (De Batist et al., 1989). The lowest interval is marked by intensive block-faulting, with tilted and bent blocks and randomly dipping fault planes. The throw is about 2 m (fig. 5.4). In the second interval this movement is amplified and develops into a convolute structure, with alternation of narrow, cusped anticlines and broad, rounded synclines (fig. 5.5). The upper interval displays a pattern of faulted blocks with dipping fault planes. Near the top of the sequence the

faulted blocks no longer exhibit significant tilting or displacement (fig. 5.6) (De Batist et al., 1989).

Henriet et al. (1989) established a genetic model for these clay-tectonic processes (fig. 5.7). Due to the easy expulsion of pore water in the bottom and top part, the clay body sealed itself, thus causing an overpressure in the locked pore water. This overpressure reduced the effective normal stress acting on the interparticle contact and consequently the shear strength of the sediments, leading to deformation. Relaxation of the pore water overpressure froze some initial, wave-like deformations in the shape we observe nowadays.

An interesting question is to what extent such deformations might have influenced the resistance of the clays to marine and fluviatile erosion. This will be discussed in more detail in chapter 7.

532.2 Ypresian - Lutetian

The Ypresian Clay is overlain by the transition sequences Y2, Y3, Y4 and Y5. The Y2 sequence consists of silty to sandy sediments and can be correlated with the middle and upper part of the Yper Formation (Kortemark Member, Egem Member) in Belgium (De Batist, 1989). It varies in thickness from some 30 m in the north to about 15 m near the coast, and is separated from the overlying Y3 sequence by a distinct erosion surface, locally marked by deep scouring.

The Y3 sequence consists of rather resistant clayey sediments and can be correlated with the Merelbeke Member of the Panisel Formation. The facies of both the Y2 and Y3 sequences is marked by weak to rather strong parallel and prograding internal reflectors, suggesting a low- to medium high-energetic marine depositional environment (De Batist, 1989).

The rather sandy Y4 sequence occurs only locally offshore Ostend as a complex fill of an erosive depression, which scours

the underlying sequences Y3, Y2 and even the top of the Y1 sequence (fig. 5.8) (De Bruyne, 1984). Its facies is marked by southeastward prograding internal reflectors, suggesting a high-energetic, intertidal to shallow marine depositional environment with a sediment supply mainly coming from the northwest (Mitchum, 1977; De Batist, 1989).

The scouring of the Merelbeke Clay Member (Y3) by the Y4 sequence may have had a pronounced morphological effect on the top-Tertiary erosion surface, as discussed later in chapter 7.

The Y5 sequence can only be observed in the southern part of the Belgian sector, offshore Blankenberge (De Batist, 1989). It varies in thickness from some 15-17 m near the coast to some 5 m in the north, and consists of sandy sediments which can probably be correlated with the lower part of the Panisel Formation (Vlierzele Member) (Steurbaut & Nolf, 1986; De Batist, 1989). Its facies is marked by parallel and eastward prograding reflectors, suggesting a low- to medium high-energetic depositional environment (De Batist, 1989).

532.3 Lutetian

The next two depositional sequences are believed to be of Lutetian (early Middle Eocene) age and can be correlated with the upper part of the Panisel Formation (Oedelem Member) (De Batist, 1989). The lower sequence, L1, consists of sand with calcareous limestone and sandstone beds, and varies in thickness from 30 m near the coast to about 25 m in the north. It is separated from the underlying Ypresian-Lutetian sediments by truncation (De Batist, 1989).

The internal facies of the L1 sequence is marked by oblique prograding clinoforms and (sub)parallel reflectors, which suggests a rather uniform deposition in a shallow marine environment. Towards the upper part of the sequence several strong, high-amplitude reflections show up, which probably mark the resistant sandstone/limestone beds (fig. 5.9) (De Batist, 1989).

The upper L2 sequence only occurs very locally as a thin, lens-like infilling (De Batist, 1989).

532.4 Bartonian

The Lutetian sediments are overlain by a layer of sediments of believed Bartonian (late Middle Eocene) age, which can probably be correlated with the Meetjesland Formation in Flanders (De Batist, 1989). This B1 sequence is built up of alternating sand and massif clay layers, as reflected by the distinct facies units on the profiles (fig. 5.10). Towards the top the internal facies is marked by draping reflectors with decreasing amplitudes, possibly due to differential compaction processes (Henriet et al., 1989).

532.5 Priabonian

The next depositional sequence, P1, is probably of Priabonian (Late Eocene) age and can be correlated with the lower part of the Zelzate Formation in Flanders (Bassevelde Member, Watervliet Member) (De Batist, 1989). This sequence, which mainly consists of sandy sediments, is only present in the northeasternmost part of the study area. Its facies exhibits a pattern of parallel and wavy reflectors which vary laterally in amplitude, suggesting a shallow marine depositional environment (De Batist, 1989).

53.3 Oligocene

The depositional sequences overlying the Priabonian sediments can only be identified in the northeastern part of the Belgian continental shelf, but do not extend into the study area. They will therefore be discussed rather briefly in this study.

The two depositional sequences belonging to the Oligocene are most likely of Rupelian age. The lowermost sequence, R1, is very thin and consists of sandy sediments. It can be correlated with the upper part of the Zelzate Formation in Flanders (Ruisbroek Member) (De Batist, 1989). This R1 sequence is bounded at its bottom by a weak erosion surface, making it difficult to distinguish it from the underlying Priabonian Sands (De Batist, 1989).

The upper R2 sequence is very thick and consists of clayey sediments. It can be correlated with the Boom Member of the Rupel Formation in Belgium (De Batist, 1989).

5.4 Neogene

The Neogene depositional sequence N0 only occurs near the northeastern border of the Belgian continental shelf, where it overlies the erosion surface at the top of the R2 sequence, and in the so-called Murray Pit in the northwestern part of the Belgian sector, where it scours the Lutetian and Bartonian sequences.

Micropaleontological investigations have dated the Neogene sediments in the Murray Pit as being of Early Pliocene age, and they may be correlated with a lateral equivalent of the lowermost facies of the British Coralline Crag Formation. The northeastern, more continuous part of the N0 sequence however is believed to be of Pliocene to Plio-Pleistocene age, and may be correlated with the British Red Crag Formation (Balson, 1989; Cameron et al., 1984 and 1989).

So far no Miocene deposits have been found in the study area and its surroundings, but this does not exclude the possibility of some Miocene relics in certain deeper parts of the top-Tertiary erosion surface.

In Belgium, however, deposits of both Miocene and Pliocene age have been found in different places.

Marine Early Miocene sediments show up in the north of Belgium, near the margin of the London-Brabant Massif (Bolderberg Formation) and near Antwerp (Berchem Formation), where they overlie and locally scour the Rupelian deposits (Laga & Lauwaert, 1988). The pronounced Middle Miocene sea-level change is most likely represented by the marine Diest Formation, which is found in the northeast of Belgium and on the so-called Flemish Hills, and which locally cuts down in channels into the Middle Eocene (Laga, 1988).

Marine Early Pliocene sediments occur near Antwerp (Kattendijk Formation and the lowermost part of the Lillo Formation (Luchtbal sand Member)) and in the north of Belgium (Kattendijk-Kasterlee Formation) (Laga, 1988). The latter possibly correlates with the transgressive Coralline Crag in East Anglia (Kockel, 1988). Middle and Late Pliocene deposits include the littoral-transitional Poederlee-Mol Formation in the northeast of Belgium and the upper part of the marine Lillo Formation near Antwerp, and most likely represent the regressive phase at the end of the Pliocene (Laga & Lauwaert, 1988).

5.5 Quaternary

55.1 General

In the present study area the surface which truncates the sequence of Paleogene strata coincides with the base of the Quaternary deposits. In the Strait of Dover, this erosional surface also truncates Mesozoic deposits. In the northeastern corner of the Belgian continental shelf however, the truncation surface coincides with the base of the Neogene deposits, and quite often the base of the Quaternary cannot be recognized without borehole control (Mostaert et al., 1989).

The Quaternary in the study area is characterized by a laterally as well as vertically complex facies. It can be regarded as the agglomerate of individual morphological

subunits with a very distinct stratigraphical build-up and lithological complexity (Bastin, 1974; Eisma et al., 1979). The seismic profiles in themselves do not yet allow us to draw any conclusions concerning the age of the different Quaternary sediments. This can only be done by micropaleontological and paleomagnetic investigation of the sediments from borings.

55.2 Pleistocene

Up to now only few Quaternary sediments have been identified in the Belgian and Northern French sectors, due to a lack of borings in this area.

According to Kirby & Oele (1975) sediments of Late Eemian age occur in the Sandettie area as a basin infill scoured into the Paleogene, where they are overlain and locally reworked by Weichselian deposits. The Late Eemian age is suggested by the presence of mollusc species indicating cool to cold climatic conditions, and seems to be supported by earlier information from Paepe & Vanhoorne (1972) who described similar closed asymmetrical depressions cut into the Tertiary and infilled by Eemian sediments. According to Oele & Schüttenhelm (1979), however, the sediments could also be of Late Saalian age.

Sediments of Eemian age also show up in the southern margin of the Lobourg Channel and in some scour hollows offshore Ostend. These borings will be discussed in more detail in chapter 6.

In Belgium, Quaternary deposits of Early, Middle and Late Pleistocene age have been found in different places.

In the north the Poederlee-Mol Formation is covered by a series of continental and estuarine deposits of Early Pleistocene age, also called the Campine Formation (Paepe, 1979). It contains the lower Rijkevorsel (estuarine) clay Member, the middle Beerse (continental) Member consisting of sand and peat, and the upper Turnhout (estuarine) clay Member (Dricot, 1961; Paepe & Vanhoorne, 1970; Paepe & Baeteman,

1979). Paleobotanical and paleomagnetic investigations have dated these layers as being of resp. Tiglian, Eburonian and Waalian age (Van Montfrans, 1971; Hus et al., 1976). They are overlain by the Campine High Terrace, which is believed to be of Menapian and Cromerian age.

In the western coastal plain near the Belgian-French border the Yper Formation is directly overlain by a series of marine deposits of Middle Pleistocene age, also called the Herzelee Formation (Sommé, 1974). Its lowermost layer is believed to be of Late Cromerian age, whereas the two upper layers are most likely of Holsteinian age (Zagwijn, 1971; Paepe et al., 1981). The Cromerian and Holsteinian sediments are separated by a peat layer formed during a warmer period (Paepe et al., 1981).

In Melle, on the southern margin of the Flemish Valley, sediments of Holsteinian age have been found, which can probably be correlated with the uppermost layer of the Herzelee Formation (Tavernier & De Moor, 1974; Paepe et al., 1981).

In both the middle and eastern coastal plain marine tidal-flat deposits of believed Eemian age, also called the Oostende Formation, have been found. Near Ostend these sediments directly cover the Tertiary Panisel and Yper Formations, and are overlain by loamy Weichselian coversands (Paepe et al., 1981). In the eastern coastal plain the Eemian sediments are covered by aeolian coversands of Weichselian age (Gent Formation) (Paepe et al., 1981). More inland, along the Flemish Valley, the Oostende Formation laterally changes into the fluvial Zemst Formation, where it covers older Saalian and Holsteinian deposits (Paepe, 1971; De Moor & Tavernier, 1978; Paepe et al., 1981).

55.3 Holocene

The most important Quaternary deposits in the Southern Bight include Holocene sand waves and tidal sand banks, also called linear sand ridges. The sand waves can be up to 10 m

high and several hundreds of meters long. Their crests are oriented normal to the principle direction of ebb and flood. The sand banks vary in height from about 10 m to 40 m, and can be up to tens of kilometers long (Eisma et al., 1979).

The tidal sand banks in the Belgian sector include four groups: the Hinder group, the Flemish Banks, the Coastal Banks and the Zeeland ridges (fig 5.11). The banks within each group are linear and parallel to each other, and are covered with megaripples and sand waves. The seismic facies inside the banks is often characterized by cross-bedding and unconformities, indicating the development stages (fig. 5.12). The upmost set of cross-bedding reflectors, if any, has a dip which is usually similar to the dip of the steep side of the bank. Nuclei of older sediments are found in some banks (fig. 5.13).

The banks of the Hinder group are generally symmetric, and exhibit a NNE direction. They are covered by south-pointing asymmetric ripples. The base* of the banks is at a depth of about 40 m b.p.l.. The sand banks have a maximum thickness of some 25 m, which reduces to a few meters in the swales between the banks (fig. 5.13).

The NE oriented Flemish banks generally have an asymmetrical, wide-crested form. The western flank of the banks is concave, while the eastern flank is convex at the top but concave at the bottom (fig. 5.14). The concave side makes a sharp angle with the crest, which gradually decreases in height towards the other side. The base of the banks, which is at about 30 m b.p.l., is approximately at the same level as the surrounding sea-floor. On both sides the crest is covered by small sand waves.

* The Zeeland ridges also have a NE orientation, but contain rather short and small banks. The Tertiary stratum is widely exposed in the swales between the different banks, particularly between the Goote and Akkaert Bank, where it is deeply incised. The southeastern margin of the Thornton Bank is bounded by a valley (fig. 5.15).

The small and tightly gathered Coastal Banks are separated from the Flemish Banks by a 20 m deep water channel (fig. 5.16). The banks, which range in height from a few meters to 10 m, merely represent slight fluctuations of the thickness of the sand sheet. The base of the banks varies strongly in depth, from 15 m to about 30 m b.p.l., and shallows towards the shore. The internal facies of the banks is marked by foresets at three different levels (fig. 5.16). The lower foresets, which are found in the Oostende Bank, are dipping seaward. They are truncated at the top by a landward dipping reflector. The middle foresets, which can be observed in the Nieuwpoort Bank and in between the Middelkerke and Oostende Bank, also exhibit a seaward dipping direction. The upper foresets, which are present in the Nieuwpoort Bank, are dipping landward. They are separated from the middle foresets by a reflector which truncates the latter.

(*) The term base here refers to the top-Tertiary erosion surface underlying the sand bank.

6. MORPHOLOGICAL DESCRIPTION OF THE TOP-TERTIARY EROSION SURFACE IN THE STUDY AREA

6.1 Contour maps

From the digitization of the reflectors marking the top-Tertiary erosion surface, the sea-floor and some internal Quaternary layers, and the subsequent conversion to depth sections (based on an interval velocity of 1700 m/s), information can be obtained concerning the depth of the erosion surface, the depth of the sea-floor and the thickness of the Quaternary sediments. On the basis of this information two different contour maps have been made. The first, isobath map represents the depth of the top-Tertiary erosion surface (fig.6.1). The second, isopach map represents the thickness of the Quaternary sediments (fig.9.1).

Both maps are in Mercator projection. The scale of these original contour maps is 1/50000 at the reference latitude of 51°20'N. The contour interval of the isobath map is 2.5 m, whereas the isopach map has a contour interval of 5.0 m. The reference level for both maps is the mean lowest low water-level at spring-tide. Digitization of the contour lines of the original maps enabled reproduction of the maps on a reduced scale of 1/100000, as presented in this study.

The landward part of the contour maps was derived from former work by De Moor & De Breuck (1973), Sommé (1979), Baeteman (1981), Depret (1983), Devos (1984), Mostaert (1985) and De Batist (1989).

6.2 General morphological considerations

The morphological evolution of the top-Tertiary erosion surface in the study area is closely related to the sea-level changes and coastal shifts during the Quaternary. The various morphological features of the erosion surface were formed by different genetic processes. In general, each feature can be related to more than one genetic process.

Based on the identification of these morphological features, we can define different morphological units. Each of these units is marked by one certain main feature, which can be superimposed by several smaller features. Sometimes, however, a unit may be marked by more than one main feature. This unit will then be named after the feature which characterizes the greater part of the unit.

6.3 Morphological features

63.1 General

The top-Tertiary erosion surface off the Belgian coast roughly consists of a flat surface nearshore which becomes inclined towards the sea, and about halfway turns flat again until it deepens into a channel. The erosion surface off the Northern French coast is generally flat.

In general the morphology of the erosion surface is not controlled by the strike of the Tertiary substratum. However, some morphological features in the study area have quite clearly been influenced by the structure and lithology of the Tertiary sequences, as will be discussed in chapter 7.

The different morphological features showing up in the erosion surface can be divided into three categories: first order features, which are mainly planar, second order features,

which are mainly linear, and third order features, which are more or less singularities.

63.2 First order features

First order features include planation surfaces and their boundaries. Planation surfaces are fundamentally even, flat or level surfaces (Bates & Jackson, 1980). They can be either horizontal or gently sloping, in which case they are resp. called platforms and slopes. Their boundaries can be either formed by ridges, slope breaks or scarps (fig. 6.2). Ridges are relatively narrow elevations. Slope breaks merely mark a change in slope. Scarps mark any steep change in elevation between two planation surfaces, which are not necessarily marked by a slope change.

Sometimes a scarp may form the steep side of an asymmetric ridge. In the special case when the strike of such a ridge is parallel to the strike of the bedding of the substratum, and its scarp face dips in a direction opposite to that of the underlying strata, the ridge is called a cuesta.

In general, the first order features in the study area exhibit a SW-NE orientation. The ridges, slope breaks and scarps are marked by drops of less than ten meters. Figures 6.3, 6.4, 6.5 and 6.6 show the resp. distribution of ridges, cuestas, slope breaks and scarps in the study area.

63.3 Second order features

Second order features include paleovalleys. A paleovalley is any low-lying land bordered by higher ground, which is usually developed by stream erosion, but may be formed by faulting (Bates & Jackson, 1980). Paleovalleys may have cross-sections displaying either a V-shape, a curved shape or an asymmetric shape, and may be partly or wholly buried by Quaternary deposits. Their depth below the surrounding erosion

surface ranges from a few meters to a few tens of meters. Figure 6.7 shows the distribution of paleovalleys in the study area.

63.4 Third order features

Third order features include scour hollows or pits. They are small depressions, which have been formed by erosion due to flowing water, ice or air (Bates & Jackson, 1980). Most of the scour hollows or pits are located in valleys. When they display an elongation, the large axis is generally parallel with the axis of the valley in which they occur. Exceptionally, deep pits may also show up in planation surfaces. In general, the scour hollows in the northernmost part of the study area are deeper than those near the shore, which are less developed and only incise a few meters into the Tertiary substratum. Figure 6.8 shows the distribution of scour hollows in the study area.

A combined map of the distribution of the main morphological features, such as ridges, cuerdas, slope breaks, scarps, paleovalleys and scour hollows, is shown in figure 6.9.

6.4 Main morphological units

Based on the identification of the different features, as described in the previous section, 13 main morphological units can be defined in the study area (fig. 6.10). They include the Marginal Platform, the Nearshore Slope Break, the Nearshore Slope, the Middle Scarp, the Middle Platform, the Offshore Scarp, the Offshore Platform, the Western Valley, the Coastal Valley, the Ostend Valley, the Northern Valley, the Northern Low Surface and the Axial Channel. Figures 6.11a-i show some different NW-SE and NE-SW oriented cross-sections of the study area.

The names of some of these morphological units have been based on former terminology introduced by other authors. The

Ostend Valley was first described and named by Henriët et al. (1982). The term Axial Channel has been inherited from former work by Balson & D'Olier (1988) and Mostaert et al. (1989). The Coastal Valley and the Marginal Platform were introduced by Mostaert et al. (1989). All other units have been introduced by the present author.

The NE-SW oriented Axial Channel is located in the northwestern part of the study area. It forms the northern part of the Lobourg Channel, which stretches from the Strait of Dover to the Southern Bight. Its depth varies from 45 m to 50 m b.p.l., locally increasing up to 60 m in depressions (fig. 6.10).

The Ostend Valley, the Northern Valley and the Northern Low Surface will be referred to as the Ostend-Northern valley system. The Ostend Valley stretches NW from Ostend to some 20 km offshore. The valley is rather narrow near the coast and widens towards the sea (figs. 6.10 & 6.11c-d). Towards the northeast the Ostend Valley changes into the southern part of the Northern Valley, which exhibits a SW-NE orientation (figs. 6.10 & 6.11a-b). The northern part of the Northern Valley stretches SE-NW and extends towards the north into the Northern Low Surface (figs. 6.10 & 6.11g-h).

The Coastal Valley follows the general direction of the coastline. Two inland branches are formed by the Yzer Valley and the Flemish Valley. The Coastal Valley joins the Ostend Valley offshore Ostend, and extends into the Western Valley towards the west (fig 6.10). This Western Valley is located just off Dunkerque on the Northern French coast and exhibits a general SE-NW orientation (fig. 6.10).

The Offshore Platform in the western part of the study area has a SW-NE orientation, and its depth varies between 35 m and 40 m b.p.l. (figs. 6.10, 6.11b-d & 6.11g). It is bounded to the north by the Axial Channel, locally via an elongated mound (figs. 6.10 & 6.11a). Towards the east it is cut by the Northern Valley, which divides it into an eastern and a western part (figs. 6.10 & 6.11g-h).

The Offshore Scarp forms the boundary between the Offshore Platform and the Middle Platform, and has an average drop of some 5 m. The Middle Platform exhibits a SW-NE orientation, and has a depth of some 32 m b.p.l.. The platform is very wide off the Northern French coast but gradually narrows towards the east (figs. 6.10, 6.11a-f & 6.11h).

The boundary between the Middle Platform and the Nearshore Slope is formed by the Middle Scarp, which locally changes into a slope break or a ridge. The Nearshore Slope varies in depth between some 25 m b.p.l. in the seaward part and some 15-20 m b.p.l. towards the land. It is cut by the Ostend Valley, resulting in a separated eastern and western part (figs. 6.10, 6.11a-b & 6.11e-f).

The Nearshore Slope Break forms the boundary between the Nearshore Slope and the Marginal Platform. This Marginal Platform, which generally has a depth of some 15-20 m b.p.l., consists of two different parts, located east and west of the Ostend Valley. Both the Eastern and Western Marginal Platform are bounded towards the south by the Coastal Valley. The Western Marginal Platform is also bounded towards the west by the Western Valley (fig. 6.10).

6.5 Planation surfaces and their boundaries

65.1 The Offshore Platform

The Offshore Platform is bounded to the north by the Axial Channel, locally via a slope break (fig. 6.13a) or a ridge (fig. 6.13b), and to the south by the Offshore Scarp (fig. 6.13c). The Northern Valley cuts through the eastern part of the platform, creating a large Western Offshore Platform and a small Eastern Offshore Platform.

The Western Offshore Platform has a SW-NE orientation. Its surface is rather flat and has depth of some 35-40 m b.p.l., increasing up to some 43 m near the southwestern margin of the

platform (figs. 6.13c & 6.13d). It truncates the Ypresian clay, except for the westernmost part where it also truncates the Thanetian sequences, and the easternmost part where it locally truncates the Y2 and Y3 sequences. The southern half of the platform is overlain by the sand banks of the Hinder group (figs. 6.13b-d).

The surface of the Eastern Offshore Platform is also rather flat, and has a depth of some 37 m b.p.l.. It truncates the Bartonian sequence, and exhibits an orientation which is more or less parallel to the strike. Its eastern margin is marked by several slope breaks, and will be discussed in more detail in chapter 7.

65.2 The Offshore Scarp

The Offshore Scarp, separating the Offshore Platform from the Middle Platform, is characterized by a drop of some 5 m, locally increasing up to 10 m (fig. 6.13c). The scarp is oriented NE-SW in the west, changes to an E-W orientation in the middle part and eventually turns NE-SW towards the east.

Towards the southwest, in the Sandettie area, Kirby and Oele (1975) described a SW-NE trending Quaternary basin, as mentioned in chapter 5. The surface of this basin is roughly at the same depth as the Offshore Platform. The southeast margin of the basin exhibits a drop of some 5-10 m, quite similar to the Offshore Scarp. Moreover, the landward margin of both the Offshore Platform and the basin is formed by a shallow valley which flattens out towards the north. This seems to suggest that the margin of the basin probably forms a part of the Offshore Scarp, and most likely the Quaternary basin may well be regarded as an integrated part of the Offshore Platform.

65.3 The Middle Platform

The SW-NE stretching Middle Platform is bounded to the northwest by the Offshore Scarp, to the southwest by the Middle Scarp, and to the southeast by the Ostend Valley and the Northern Valley. Its surface is very wide off the Northern French coast, and gradually narrows towards the east until it wedges out almost completely (fig. 6.10). The surface truncates the Ypresian clay, except for the westernmost part where it truncates the Thanetian sequences, and the easternmost part where it locally truncates the Y2 and Y3 sequences.

The western part of the Middle Platform is cut by a valley which runs E-W in the westernmost part, and then turns NE-SW until it reaches the Middle Scarp. The E-W trending part of the valley is rather shallow, except for the westernmost part, and has a rather steep seaward flank and a more gentle landward flank (fig. 6.15a). The surfaces on both sides of the valley are more or less at the same height (fig. 6.15a). The NE-SW trending part of the valley is somewhat deeper than the first part, and also here the seaward flank is quite steeper than the landward flank (fig. 6.15c). The surface on the landward side of the valley is some 5-6 m higher than on the seaward side (fig. 6.15b).

In general, the surface north of the valley is rather flat, with only a few meters fluctuation. South of the valley the surface exhibits a slight NNW dip and is incised by shallow gullies. These gullies run more or less parallel to the valley and are well buried by Quaternary sediments (figs. 6.1, 6.15c & 6.15d).

The narrow eastern part of the surface is characterized by shallow depressions and an inclined surface (fig. 6.11b). This surface is locally incised by gullies, which are either exposed on the sea-floor or poorly covered with Quaternary sediments.

65.4 The Middle Scarp

The Middle Scarp runs parallel to the French coastline until Dunkerque, where it is cut by the Western Valley, and then turns NE-SW, forming the boundary between the Middle Platform and the Nearshore Slope, the Ostend Valley and the Northern Valley (fig. 6.10). Its main part roughly coincides with the 30 m contour line (fig. 6.1).

The western part of the Middle Scarp, south of the valley in the Middle Platform, is formed by a rather gentle scarp with a drop of some 5 m (figs. 6.10 & 6.15e). The dip of the scarp gradually decreases towards the northeast. Between the valley in the Middle Platform and the Ostend Valley the boundary becomes rather unclear, and is locally marked by small slope breaks. Further north, where it bounds the Ostend Valley and the southern part of the Northern Valley, the boundary is roughly marked by a ridge (fig. 6.11c).

65.5 The Nearshore Slope

The Nearshore Slope forms a gently NW declining surface, with a depth of some 25 m b.p.l. near the Middle Scarp and of some 15 m b.p.l. near the Marginal Platform. In the easternmost part, near the border of the Belgian/Dutch sector, its surface locally drops down some 10 m. It is cut by the Ostend Valley, and the parts on both sides of the valley are referred to as the Eastern and Western Nearshore Slope (fig. 6.10). They are characterized by a quite different morphology, which is most likely related to the lithology of the underlying Tertiary stratum, as will be further discussed in chapter 7.

The Western Nearshore Slope is underlain by the Ypresian clay. Its surface is more or less regular, as indicated by the alignment of the contour lines in figure 6.1. Near Ostend the slope becomes steeper, where it bounds the Ostend Valley in a NW-SE direction.

The Eastern Nearshore Slope truncates the Ypresian to Priabonian sequences. Its surface is rather irregular and strongly eroded. The landward part is marked by two elliptic depressions. The western depression is 7 km long and 3 to 4 km wide, and is incised some 3 m into the upper part of the Ypresian clay (fig. 6.17c). It has an asymmetric cross-section with a steep eastern flank and a rather gentle western flank and the main part of its surface is exposed or poorly concealed by Quaternary sediments. The depression is connected with the Ostend Valley via an opening on the west side. The rather shallow eastern depression is almost 10 km long and 3.5 km wide, and is cut into the Bartonian clay (fig. 6.17f). The main part of this depression is filled and overlain by the shoal of Vlakte van de Raan. Due to the fact that only few profiles of good quality cross this area further details remain unknown.

The seaward part of the Eastern Nearshore Slope is marked by a valley which runs more or less parallelly to the Middle Scarp and separates the Akkaert Bank and the Goote Bank. It is scoured into the Y5, L1 and B1 sequences. The eastern part of the valley has a more or less symmetric cross-section with two gentle flanks (fig. 6.17e). The western part of the valley has a somewhat asymmetric shape with a rather steep southern flank and a very gentle northern flank (fig. 6.17d).

65.6 The Nearshore Slope Break

The Nearshore Slope Break, which separates the Nearshore Slope from the Marginal Platform, consists of two different parts (fig. 6.10). The western part of the slope break, situated west of the Ostend Valley, is marked by a rather gentle dip change and is fully covered by Quaternary sediments (figs. 6.17a-b). The eastern part of the slope break, situated east of the Ostend Valley, is marked by a somewhat bigger slope change and is fully exposed (fig. 6.17c). The latter may be due the steepness of the Nearshore Slope bounding this part of the slope break.

65.7 The Marginal platform

The Marginal Platform also consists of two parts, separated by the Ostend Valley (fig. 6.10). Towards the south the Eastern and Western Marginal Platform are bounded by the Coastal Valley. The Western Platform is also bounded by the Western Valley towards the west. Both parts of the platform have a depth of some 15 m b.p.l..

The Eastern Marginal Platform is rather flat (figs. 6.11a-b), and truncates the Ypresian to Bartonian sequences. It is 20 km long and about 10 km wide, and runs somewhat parallelly to the coastline (fig. 6.10). The easternmost part of this platform is not very clear due to a lack of seismic penetration in this area.

The Western Marginal Platform has a rather irregular surface marked by several hills and depressions (figs. 6.11e & 6.17a), and truncates the Ypresian clay. It is somewhat lens-shaped, about 6 km wide and 15 km long (fig. 6.10).

6.6 Paleovalleys

66.1 The Coastal Valley

The Coastal Valley extends along the Belgian coastline from the Belgian/Dutch border, where it joins the Flemish Valley, to the French/Belgian border, where it joins the Yzer Valley (fig. 6.10). The section between the Belgian/Dutch border and Ostend is referred to as the Eastern Coastal Valley, whereas the section between Ostend and the French/Belgian border is referred to as the Western Coastal Valley. The Western Coastal Valley is carved into the Ypresian clay, whereas the Eastern Coastal Valley is scoured into the Ypresian-Lutetian, Lutetian, and Bartonian sequences.

The bottom of the valley is generally at a depth of some 20-25 m b.p.l., except for the Flemish Valley and a pit near the Ostend Valley where it is locally deeper (fig. 6.1). The cross-section of the valley is asymmetric, with a rather steep landward flank and a more gentle seaward flank. Its northern flank bounds the Marginal Platform, whereas its southern flank is formed by the coastal margin, reaching a level of up to 20 m (Mostaert et al. 1989). Due to the geographical location of the valley, the seismic grid only covers an extremely small part of the valley.

66.2 The Western Valley

The Western Valley is located to the west of the French/Belgian border, and is scoured into the Ypresian clay. It stretches east-west from the border until Dunkerque, and then turns towards the northwest. The morphology of the valley is not very clear, as profiles of good quality are lacking in this region. Only the extreme northwestern part, containing a deep scour hollow, is covered by several good quality profiles. It will be described in more detail in section 6.7.

66.3 The Ostend-Northern valley system

663.1 The Ostend Valley

The Ostend Valley is situated offshore Ostend, and stretches SE-NW. Its rather steep eastern flank is marked by a scarp, which forms the boundary with the Eastern Nearshore Slope (figs. 6.19a-b). Its western flank is rather gentle (figs. 6.16a-b), and its margin is roughly defined by the 25 m contour line. The valley is narrow near Ostend (5-7 km wide, 40-45 m b.p.l.) (figs. 6.19d-e) and widens towards the sea (up to 20 km wide), where it also becomes shallow and flat (25-30 m b.p.l.) (figs. 6.19a-b).

The Ostend Valley is carved into the Ypresian clay, running more or less parallel to the strike, and is heavily covered by Quaternary sediments. The nearshore part is overlain by the Coastal Banks. Horizontal or subhorizontal internal reflectors are present at least at two different levels in the sediments (figs. 6.19a-b), indicating a minimum of three different infilling stages. The lower infill has a depth of some 25-27 m b.p.l., while the upper one has a depth of 15-20 m b.p.l. (fig. 6.19a).

Two borings have been made in the Oostende Bank (fig. 6.10). The core of the northernmost boring (RGD 74) reaches from 11.05 to 23.0 m b.p.l.. Mollusc analysis has dated the uppermost 0.85 m as Late Boreal, and the rest of the core as Late Holocene (Spaink & Sliggers, 1979, unpublished report). The core of the second boring (RGD 57) reaches from 8.2 to 18.7 m b.p.l.. Mollusc analysis again indicated a thin, very young upper layer, underlain by older, Late Holocene sediments (Spaink & Sliggers, 1979, unpublished report).

663.2 The Northern Valley

The Northern Valley extends towards the NE north of the Ostend Valley, then swings NW along the Offshore Platform and keeps this direction until it reaches the southern limit of the North Low Surface. It is incised into the mainly sandy Ypresian, Ypresian-Lutetian and Lutetian sequences.

The southern, NE trending Northern Valley seems to follow the Y4/Y2 and Y4/Y3 boundaries. It is quite shallow, some 30-35 m b.p.l., and its rather irregular surface is exposed or poorly concealed by overlying Quaternary sediments (figs. 6.21a-b).

The northern, NW trending Northern Valley mainly follows the Y3/L1 boundary, except for those places where the Y5 sequence is present and where it follows the Y5/L1 boundary (see also chapter 7). It is somewhat deeper than the NE trending part, reaching depths of up to some 45 m b.p.l.. Its surface is locally quite rough, and is completely buried by

Quaternary sediments (figs. 6.21c-e). The southern part of the valley is locally overlain by the Thornton Bank. Towards the north the valley gradually widens and eventually changes into the Northern Low Surface.

663.3 The Northern Low Surface

The Northern Low Surface is located in the north of the study area and has a depth of some 40-45 m b.p.l.. The surface is rather flat, with only a few meters of fluctuation. The southernmost part of the surface is scoured into the Ypresian-Lutetian sequences. More towards the east the surface is incised into the Bartonian, Priabonian and Rupelian sequences. The boundary between the surface and the Western Offshore Platform is not very clear, due to a lack of profiles crossing this boundary. The boundary which is marked on figure 6.10 roughly coincides with the 40 m contour line of the erosion surface (fig. 6.1). The northern part of the surface remains rather unknown, as the profiles crossing this area are of rather dubious quality.

According to Mostaert et al. (1989) the Northern Low Surface may well be bounded towards the northeast by a NE dipping slope. This slope is related to an early Quaternary erosion surface, which is covered by Plio-Pleistocene deposits (N1 sequence), as mentioned in chapter 5.

66.4 The Axial Channel

The Axial Channel stretches SW-NE and has a width of some 17 to 20 km (fig. 6.10). Because the seismic profiles only crossed the southeastern part of the channel, only this area will be discussed in detail.

The southeastern part has a general depth of some 50 m b.p.l., locally up to 58 m b.p.l. (figs. 6.23a-e). The southern margin of the channel is characterized by three pronounced

lobes, two of which are oriented to the north, and the third one is oriented to the south. The northern and southern lobes are separated by a narrow, elongated hill (figs. 6.1 & 6.10), which forms the northwest extension of the Offshore Platform.

The northernmost lobe is 4-5 km wide, incising the Ypresian clay over a depth of some 5-8 m (fig. 6.23b). Its cross-section has a rough "W" shape, due to the fact that the two margins of the lobe are noticeably deeper (over 50 m b.p.l.) than the middle part (some 47 m b.p.l.). The bottom of the lobe is very irregular (fig. 6.23b). Towards the west it is separated from the Axial Channel by a ridge of about 1 km wide and 10 m high.

The largest southernmost lobe is some 2 km wide and has a depth of some 50 m b.p.l., incising the Ypresian clay over only a few meters. Its cross-section has a more or less curved shape (figs. 6.23d-e). Towards the west the lobe is separated from the Axial Channel by a ridge of 3 km wide and some 10 m high. Further south, the lobe widens drastically and joins the Axial Channel. East of this lobe a smaller, rather shallow lobe can be observed (fig. 6.23e).

The Axial Channel is poorly covered by Quaternary sediments, which are locally absent. The two lobes however are completely buried by Quaternary sediments, superimposed with sand waves. The occurrence of an internal reflector in the infilling material of the largest southern lobe suggests that at least two stages of infilling must have taken place here (fig. 6.23e).

A borehole (RGD 80MK127) is located immediate south of the southern lobe (fig. 6.10). The core, which has a length of some 8 m, consists mainly of coarse sands. Mollusc analysis has indicated the upper 4 m to be of marine Holocene origin, whereas the lower 4 m is believed to be of marine Eemian origin (Spaink, 1981, unpublished report). Most likely these two layers correspond with the two infilling stages observed in the southern lobe.

This borehole is also located rather close to the Sandettie area. As already mentioned in chapter 5, the basin infill in this area probably consists of Eemian or Late Saalian sediments. There is however an important elevation difference between the erosion surface in the borehole area (50 m b.p.l.) and in the Sandettie area (34-40 m b.p.l.). This may suggest that although the Eemian transgression possibly flooded the area in the channel, it may not have been able to reach the higher land of the Sandettie area. Therefore the lower infilling sediments in the southern lobe can most likely be dated as marine Eemian, whereas the upper infilling sediments are probably Holocene.

In some places the infilling material of the marginal lobes is marked by two horizontal internal reflectors, i.e. three stages of infilling must have taken place. The upper two infillings are believed to correspond with the Eemian and Holocene stages described above.

More information about the age of the lowest infilling, which is 1-3 m thick, can be obtained from recent research by Balson & D'Olier (1988). According to these authors the sand-sized sediments at the bottom of the outer Thames Estuary region mainly consist of reworked younger Thames/Medway fluvial deposits of possible Early Miocene age, whereas sediments of fluvio-glacial origin may be particularly present in the Lobourg Channel. This may suggest that the lowest infilling material in the lobes could possibly be of Saalian fluvio-glacial origin or maybe even older, although this does not preclude a younger, Eemian age.

6.7 Scour hollows

67.1 The Zeebrugge Pit

The Zeebrugge Pit is located in the Coastal Valley, just offshore Zeebrugge (figs. 6.1 & 6.8). It has a depth of some 35 m b.p.l., and a rather elongated, NW trending shape. The bottom

of the pit is formed by the sandy L1 sequence. Its northeastern flank is marked by a very steep slope, and scours the Bartonian clay, whereas its southern flank is very gentle and follows the resistant limestone and sandstone beds in the L1 sequence (Henriet, 1978, unpublished report). The infilling sediments exhibit some subhorizontal and gently dipping internal reflectors, suggesting that several infilling stages must have taken place. The main part of the pit is marked by three different infillings, which can be dated from bottom to top as Eemian, Weichselian and Middle Holocene (Henriet, 1978, unpublished report).

67.2 The Sepia Pits

The nearshore part of the Ostend Valley is marked by several scour hollows, called the Sepia Pits, which are all cut into the Ypresian clay. These pits were first described and named by Mostaert et al. (1989). The most seaward hollow, Sepia Pit 1, has a depth of some 52.5 m b.p.l. and a width of 3 km (fig. 6.1). It has a rather symmetric cross-section (fig. 6.19c). The second hollow, Sepia Pit 2, is located further landward and has a depth of over 47.5 m b.p.l. (fig. 6.1). It is about 3.5 km wide and has an asymmetric cross-section, with a steep eastern flank and gentle western flank (fig. 6.19e). The third and deepest hollow, Sepia Pit 3, is located about 1 km east of Sepia Pit 2 (fig. 6.1). This pit has a depth of some 60 m b.p.l. (fig. 6.19e). Unfortunately only few profiles of good quality cross this pit, leaving further details unknown.

The relation between Sepia Pits 1 and 2 is not clear so far. According to Mostaert et al. (1989) the two pits are isolated. But the present author believes that they might be linked by a shallow valley, as seems to be suggested by some seismic profiles. However, the profiles near Sepia Pit 1 are very obscure due to strong absorption of the sediments, making it impossible to draw any definite conclusions.

Sepia Pit 1 is overlain by the Oostende Bank. The foresets of the reflectors showing up in its infilling are dipping to

the north (fig. 6.19c). The reflectors showing up inside Sepia Pit 2, however, exhibit a southwest direction (fig. 6.19d). This indicates at least two major infilling stages must have taken place in the Sepia Pits.

A boring (RGD 72) is located between Sepia Pits 2 and 3 (fig. 6.10). Its core reaches from 10 to 12.4 m b.p.l., of which the upper 0.9 m could be dated as Late Holocene, and the rest as Late Eemian (Spaink & Sliggers, 1979, unpublished report). This suggests that the sediments in Sepia Pits 2 and 3 may well belong to the Eemian. Most likely the same conclusion may be drawn for the infilling sediments of Sepia Pit 1.

67.3 The Dunkerque Pit

The Dunkerque Pit is located on the northwestern margin of the Western Valley. The pit, which cuts into the Ypresian clay, has a depth of some 42 m b.p.l., and is heavily buried by Quaternary sediments. The foresets of the reflectors showing up in the pit are dipping towards the southeast (figs. 6.25a-b).

67.4 Isolated pits in the planation surfaces

A small pit can be observed in the western depression of the Eastern Nearshore Slope (fig. 6.1). The pit is cut some 5 m into the Ypresian clay, and is completely filled by Quaternary sediments. The facies of its infilling sediments is marked by several internal reflectors (fig. 6.17b).

Two pits show up in the western margin of the valley in the western part of the Middle Platform, where they are scoured into the T2 and Y1 sequences (fig. 6.1). The western pit is quite deep (50 m b.p.l.) and is incised some 7 m into the valley bottom. It has an asymmetric V-shaped cross-section. The more elongated eastern pit runs parallel with the direction of the valley, and is less deep (47 m b.p.l.). It is incised some 5 m into the valley bottom, and has a more or less symmetric V-shaped cross-section.

Two scour hollows show up just east of the Eastern Offshore Platform (figs. 6.1 & 6.8). The northern hollow is the deepest one (50 m b.p.l.), and cuts some 8 m into the P1 sequence. The southern hollow is less deep (45 m b.p.l.) and incises the B1 and P1 sequences over a depth of some 8 m.

67.5 Isolated pits in the paleovalleys

The Axial channel is marked by several rather deep hollows. First of all two large, elongated hollows show up in the southeastern part of the channel (fig. 6.1). They both have a SW-NE orientation, and locally increase the depth of the channel up to resp. 55 and 60 m b.p.l.. Few seismic profiles are crossing this area, leaving further details of the pits unknown.

Two hollows can be observed in the eastern and western margin of the northern lobe in the Axial Channel, causing the "W"-shaped cross-section as described in section 66.4. Both of these hollows have a more or less elongated form, and exhibit a N-S orientation (figs. 6.1 & 6.8). The western hollow is somewhat deeper than the eastern one (resp. 55 m and 50 m b.p.l.).

Several small pits can be observed in the Ostend Valley and Northern Valley (figs. 6.1 & 6.8). The two pits in the northwestern part of the Ostend Valley are scoured some 4-8 m into the Ypresian clay. They both have a rather flat bottom and their cross-sections exhibit a curved shape. The scour hollows in the Northern Valley are rather shallow. Their depth is less than 5 m below the valley bottom, and they all have a more or less V-shaped cross-section.

A deep, elongated pit shows up in the southern part of the Northern Low Surface, near the Offshore Platform (fig. 6.1). The pit is oriented SW-NE and scours some 15 m into the underlying Y3 and L1 sequences (fig. 6.21f). It has a more or less asymmetric cross-section, with a rather steep southeast flank and a more gentle northwest flank.

7. GEOLOGICAL CONTROL ON THE MORPHOLOGY

7.1. Introduction

A remarkable result of this study is the observation that the morphology of the top-Tertiary erosion surface is to a certain extent influenced by the geology of the substratum. The overall structure of this substratum consists of a monoclinical sequence of dipping beds. The combination of lithology and local structures can cause certain differential erosion processes, eventually resulting in some outspoken effects on the morphology of the erosion surface.

We can distinguish four different kinds of geological control, though usually without sharp distinction: regional lithological control, local lithological control, dip control and structural control. Regional lithological control is mainly on a km scale and involves the general correlation between lithology and morphology, whereas local lithological control is more confined and operates on a somewhat smaller scale. Dip control may also occur on a large scale and is caused by a change in dip of the Tertiary substratum. Structural control is often more or less incidental and mostly occurs on a rather small scale. It is mainly caused by structural deformations in the substratum, sometimes in combination with lithological control.

7.2 Regional lithological control

72.1 General

Regional lithological control can involve both vertical and lateral changes in lithology. Vertical changes in lithology

are generally abrupt, and may occur along sequence boundaries as well as along lithological boundaries within sequences. They mostly cause differential erosion, which may eventually result in the formation of bedrock highs, valleys anduestas, parallel to the strike of the substratum.

Lateral changes in lithology are generally more gradual, and therefore mostly do not cause differential erosion processes. Sometimes they even may reduce the vertical lithological contrast, preventing the development of differential erosion.

72.2. Effect of vertical lithological contrasts

722.1. Cuestas

As we already mentioned in chapter 6, a cuesta can be considered as an asymmetric ridge with a steep scarp face and a more gentle dip slope. Its strike is roughly parallel to the strike of the bedding surfaces in the substratum, whereas the scarp face dips in a direction opposite to the slope of the stratal surfaces. A cuesta results from the differential erosion of gently dipping beds, in which resistant beds alternate with softer beds. The uppermost bedding surface of a resistant bed forms the gentle dip slope, and its eroded outcrop forms the steep face of the cuesta.

Cuestas are especially well developed at different levels in the Lutetian and Bartonian sequences (figs. 6.4 & 7.1). The cuestas which occur in the L1 sequence are related to the strong reflectors which have been identified as calcareous sandstone and limestone beds (see chapter 5). The part of the NW trending Northern Valley bottom which is scoured into the L1 sequence is marked by several cuestas. (figs. 7.2 & 7.3). Part of the southern flank of the valley in the northern part of the Nearshore Slope is a cuesta scarp, which has been formed by a more resistant bed in the L1 sequence (fig. 6.17d).

The *cuestas* showing up in the Bartonian sequence are related to the reflectors which mark the alternating sand and clay layers (see chapter 5). The steep flank of the Zeebrugge Pit, which has been discussed in chapter 6, is a *cuesta* scarp which has been formed by the rather resistant lower seismic facies unit in the B1 sequence. The Eastern Offshore Platform is marked by several *cuestas* at different levels, which have been formed by the heavy clay layers in the B1 sequence (fig. 7.4). Isolated *cuestas* show up east of the Eastern Offshore Platform and in the southern part of the Nearshore Slope, where they occur in the resp. upper and lower part of the B1 sequence (figs. 7.5 & 7.6).

The southern flank of the western depression in the Eastern Nearshore Slope is marked by a *cuesta*-like feature, which has probably been caused by differential erosion of the facies units in the Y1 sequence (fig. 6.17b).

722.2. Slope breaks and scarps

The eastern margin of the Eastern Offshore Platform is marked by several slope breaks, as mentioned in chapter 6 (fig. 7.5). The strike of the slope breaks is parallel to the strike of the bedding of the substratum, which indicates that the slope breaks probably resulted from differential erosion between the sand and clay beds in the B1 sequence.

The scarp which shows up in the southern part of the Eastern Nearshore Slope has probably been formed by a resistant clay layer in the B1 sequence (fig. 7.6).

722.3. Valleys

A vertical lithological change may also initiate the formation of a valley, incised in the softer bed. In this case one of the flanks of such a valley is often formed by a *cuesta* scarp. This can be observed in the NW trending Northern Valley,

the eastern flank of which is often marked by a cuesta scarp. The main part of the eastern flank roughly coincides with the L1/B1 boundary, which indicates it may have been formed by differential erosion between the relatively soft L1 sequence and the more resistant B1 sequence.

The Ostend Valley is parallel to the strike of the Tertiary substratum, but it is hard to identify which phenomenon of geological control has caused its formation. However, the fact that the valley has a more or less asymmetric shape with a steep flank and a more gentle flank, suggests that it may have resulted from differential erosion caused by vertical lithological contrasts.

72.3. Effect of lateral lithological contrasts

Towards the north the Northern Valley gradually widens into the Northern Low Surface, while the cuesta forming its eastern flank also fades out (figs. 6.4 & 7.1). This is probably caused by a lateral lithofacies change in the L1 sequence from sandy to more clayey sediments, which eventually reduced the vertical lithological contrast between the L1 and B1 sequences.

7.3 Local lithological control

Basin fills exhibit a typical local lithofacies. Any relatable morphology of the erosion surface, caused by the lithology of the basin fill, consequently has a local character. Such local fill sequences are found in the Tertiary substratum off the Belgian coast (Henriet et al., 1989; De Batist, 1989).

Figure 7.7 shows the transition sequence Y4 in a scoured basin. The basin forms part of the Eastern Nearshore Slope and the NE trending Northern Valley. It is carved into the Y3 and Y2 sequences, and into the top of the Y1 sequence (see chapter

5). It roughly has a SSW-NNE orientation and is some 15 km long and 5 km wide. The fill sequences form a high in the erosion surface, probably due to the presence of more resistant material.

The origin of the offset between the Ostend Valley and the NE trending Northern Valley is still unclear. It may possibly be related to the presence of this basin fill, although a regional lithological control cannot be ruled out.

7.4 Dip control

A sudden change in dip of the substratum may result in the formation of a scarp, which runs parallel to the strike of the substratum. Fig. 7.8 shows such a scarp which forms part of the southern flank of the NW trending Northern Valley. The steeper dipping strata are truncated by the erosion surface, whereas the more gentle dipping strata are more or less parallel to the erosion surface and form the bottom of the valley.

7.5 Structural control

Local structural deformations in the Tertiary strata, such as synclines, anticlines and faults may, in combination with lithological contrasts, exert certain effects on the morphology of the erosion surface.

Differential erosion of the folded layers may result in the formation of depressions and/or highs in the erosion surface overlying the core of the synclines and/or anticlines. Figure 7.9 shows an isolated syncline in the Eastern Nearshore Slope. It is overlain by a depression which is scoured into the Y5 sequence. Figure 7.10 shows two rather weak synclines in the NE trending Northern Valley, the cores of which are overlain by highs made up of Y4. Figure 7.11 shows an anticline in the Eastern Nearshore Slope underlying a depression which cuts into the Y3 sequence.

A large number of synclines, anticlines and faults can be observed in the northern part of the study area, which are commonly referred to as the Noordhinder deformation zone (fig. 5.2) (Henriet et al., 1989). The most remarkable feature of the deformation zone is the occurrence of five NE trending synclinal depressions, roughly circular in shape, affecting the Y1 to P1 sequences (De Batist, 1989). Most of these synclines seem to coincide with highs in the erosion surface (fig. 6.1).

The southernmost syncline stands out as an isolated feature and affects the Y2 and Y3 sequences in the Western Offshore Platform. It has an amplitude of some 150 m and a diameter of some 5 km, and is bordered to the east by a fault zone (fig. 7.12). The erosion surface which truncates the steep northwest limb of the syncline forms a local high, probably due to differential erosion. The erosion surface truncating the core of the syncline also forms somewhat of a local high in the Y3 sequence. The seismic facies of this sequence consists of a lower, reflection free unit and an upper unit marked by continuous, low amplitude reflectors. Most likely the lower unit is softer than the upper one, resulting in the formation of the local high. The presence of a fault in the core of the syncline might however also have contributed to the morphology of the erosion surface.

The three central synclines seem to be structurally connected, forming a complex, elongated and asymmetrical synclinal trough (Henriet et al., 1989). This trough is marked by a pattern of smaller-scale dense block-faulting superimposed on the main folds, which may be due to a reactivation of pre-existing clay-tectonic deformations (see chapter 5) (Henriet et al., 1988). The northernmost of these depressions affects the B1 and L1 sequences (fig. 7.13). The erosion surface overlying the fold is marked by a high with an amplitude of some 5 to 10 m, which is most likely caused by differential erosion. Local fluctuations in this high may possibly be due to the presence of the smaller-scale deformations.

The northernmost syncline is situated just outside the present study area. It is unconformably covered by the

undeformed R1 sequence and therefore cannot be observed in the top-Tertiary subcrop map shown in figure 5.2 (De Batist, 1989).

8. POSSIBLE GENETIC SCENARIO'S

8.1 Introduction

In order to reconstruct the morphological evolution of the top-Tertiary erosion surface, adequate sedimentological and paleontological information about the overlying sediments is essential. Due to severe erosion the Quaternary cover in the study area is relatively thin. Moreover, only few borings exist in the area. Therefore, very little sedimentological and paleontological data are available in the study area. However, a combination of these limited data with the seismic data and the recent knowledge of the Quaternary history enabled us to make a tentative reconstruction of the evolution of certain morphological units.

Most units in the study area were formed during the Quaternary. The Axial Channel, however, is believed to be of Neogene age (Balson & D'Olier, 1988). According to the present author the Nearshore Slope also could have originated in pre-Quaternary times.

The planation surfaces and their boundaries were probably mainly formed by marine abrasion, although some influence of glacial erosion may not be ruled out. The paleovalleys, on the other hand, were most likely mainly formed by fluvial and estuarine erosion.

8.2 The Axial Channel

Recently, Balson & D'Olier (1988) reviewed the Quaternary history of the Lobourg Channel, as based on borings and seismic investigations (see chapter 4). According to these authors the Lobourg Channel, including the Axial Channel, came into

existence during the Middle Miocene. It formed the most eastward branch of a complex river system related to a tectonically uplifted area, flowing off the flank of the uplift towards the northeast. During the Pliocene the channel was further eroded and shaped, and it is most likely that the Murray Pit was formed by fluvial erosion during this period, as indicated by the Early Pliocene age of some infilling sediments of the pit (see chapter 5). It is difficult to reconstruct the exact configuration of the Axial/Lobourg Channel at this initial stage, due to subsequent marine, glacial and fluvial erosion during later times. It is generally believed that the channel kept a more or less stable course throughout the Pleistocene (fig. 4.15).

Apart from the Murray Pit, several overdeepened hollows can be observed in the channel, as mentioned in chapter 6. The presence of Eemian deposits in the southern margin of the Axial Channel indicates that the channel may have been scoured by tidal currents during the Eemian transgression. Most likely some of the hollows can be related to this scouring, although an initial fluvial origin (maybe even during the Neogene, as is the case for the Murray Pit) can not be entirely excluded (Mostaert et al., 1989). According to Destombes et al. (1975) the Fosse Dangeard Pit, which is located in the southernmost part of the Lobourg Channel, was probably formed by fluvial erosion from meltwater during the Late Saalian. Maybe this could also be the case for similar deep pits in the southeastern part of the channel.

The Axial Channel is poorly covered by Quaternary sediments which are locally absent, suggesting that it must have been scoured during the Holocene. Because very little information is available about the age of these sediments, the extent of this Holocene scouring remains rather unclear. The recent paleochannel system is shown in fig. 8.1 (Bridgland & D'Olier, 1989).

8.3 The planation surfaces

The original top-Tertiary erosion surface in the study area probably consisted of a slightly seaward dipping surface, which extended from the present coastal area down to the Axial Channel. This original morphology is probably still reflected in the Nearshore Slope and in the landward part of the Coastal Valley above the 15m contour line.

Except for the Axial Channel and the northeast corner of the study area, no Pliocene sediments have been found in the Belgian sector (see chapter 4). This may suggest that the original dipping surface was eroded as a whole after the Pliocene, whereby the Pliocene deposits were completely removed.

It is generally believed that a certain period of relative stillstand or very slow rise of sea-level is needed in order to cause abrasion of a platform. During the Holocene the sea-level rose rapidly, and only slowed down after 6000 B.P., during which time the sea-level was only barely below the present level. This seems to suggest that the planation surfaces have most likely been formed before the Holocene, probably by one or more transgressions during the Pleistocene.

The Early Pleistocene transgressions did not reach the study area, as discussed in chapter 4. During the Middle Pleistocene transgressions, however, the study area was flooded several times, and it is quite possible that the Marginal Platform and the Middle Platform were formed during these transgressions, the latter extending down to the Axial Channel at that time.

According to Kellaway (1975), at least part of the study area was invaded by land ice during the later period of the Saalian. This suggests that the northern part of the Middle Platform may possibly have been covered by an ice lobe during that time. Subsequent glacial abrasion may then have resulted in the formation of the Offshore Scarp and the Offshore Platform (fig. 8.2), and possibly the small depression along

the landward margin of the Western Offshore Platform was due to erosion by meltwater. However, an initial stage of formation of both platform and scarp during the Middle Pleistocene transgressions cannot be ruled out.

During the Saalian a layer of fluviatile sand was deposited in the study area by the rivers Rhine and Meuse, the northern outlet of which had been blocked by land ice, so that they were now forced to flow southward (see chapter 4). These sands probably protected the main part of the erosion surface from severe marine abrasion during the Eemian and Holocene transgression.

The valley which crosses the western part of the Middle Platform may well have been created during the Holocene, as suggested by the orientation of the valley, which is more or less parallel to the general NE direction of the tidal currents off the French coast during that time. In an early stage the valley may have developed towards the east, but was probably blocked by the Middle Scarp. Most likely this forced the currents at the bottom to turn north along the scarp, which may have resulted in the formation of the SW-NE oriented part of the valley (fig. 8.3). Nevertheless, a formation during Eemian or even pre-Eemian times cannot be totally ruled out.

It is uncertain whether the valley in the northern part of the Eastern Nearshore Slope was formed during the Eemian or during the Holocene. The SW-NE direction of the valley may well indicate that it was formed by present regional tidal currents, but this does not exclude an initial forming during the Eemian.

8.4 The paleovalleys

During the Middle Pleistocene the middle coastal plain probably formed a high, and even was not flooded during the severe Holsteinian transgression (see chapter 4). This may indicate that the paleovalleys probably did not come into existence before the Saalian.

It has already been mentioned that the Scandinavian ice sheet of the Saalian covered large parts of the Dutch territory. During this period the area of the Flemish Valley formed the mouth of the Scheldt river and its tributories. The ice never reached the southernmost part of the Netherlands and northern Belgium, which indicates that the deepening of the Flemish Valley was only due to fluvial erosion, and not to glacial and/or marine erosion.

During the early part of the Saalian glacial the water coming from the Flemish Valley probably turned towards the west, hereby possibly creating the eastern part of the Coastal Valley, and then could have turned NW towards the Axial Channel, hereby creating the Ostend Valley, the Northern Valley and the Northern Low Surface. Meanwhile, part of the high around Ostend may have been removed by fluvial erosion.

During the later part of the Saalian, when the land ice reached its maximum extension, the water coming from the Flemish Valley could have been locked from the Axial Channel by an ice lobe extending along the present Offshore Scarp (see section 8.3). This probably caused severe erosion of the remaining part of the Ostend high by the water from the Flemish Valley, and eventually could have resulted in the formation of the western part of the Coastal Valley and the Western Valley (fig. 8.2).

During this time the Ostend Valley was probably not as wide as it is nowadays. The presence of infilling sediments of Eemian age in the Sepia Pits, as described in chapter 6, indicates that the valley was probably deepened and widened by marine erosion during the Eemian. This may also have been the case for the Coastal Valley, the northern flank of which got fairly but not entirely flattened during this period (Mostaert et al., 1989). Most likely the Yzer Valley, which had kept an independent course during the earlier inundations, now joined the Coastal Valley in the west (fig. 8.3).

During the Holocene the paleovalleys were further deepened and widened. This seems to be confirmed by the presence of Holocene sediments more or less directly overlying the bottom

of the Ostend Valley north of Sepia Pit 1 (see chapter 6). The Dunkerque Pit at the mouth of the Western Valley probably was also created by tidal currents during the Holocene transgression, as indicated by the foresets of the infilling sediments which exhibit a dipping direction consistent with the direction of the Holocene transgression, although a formation during the Eemian cannot be completely ruled out.

9. BEDROCK CONTROL ON THE QUATERNARY SEDIMENTATION

9.1. Introduction

The Quaternary deposits in the study area are mainly composed of Holocene tidal sand banks. The Quaternary sedimentation therefore will largely depend on the distribution pattern of the sand banks, which have a general SW-NE alignment (fig.9.1). Nevertheless, several major morphological features of the top-Tertiary erosion surface have imposed some outspoken effects on the Quaternary distribution pattern

9.2. Influence of valleys on the distribution pattern

The most pronounced influence on the Quaternary deposits is exerted by large paleovalleys, such as the Ostend Valley and the Coastal Valley. These valleys formed a kind of large sediment trap, and consequently became completely filled with sediments (figs. 6.19a-e & 9.1). An exception to this rule is the Axial Channel, where complete infilling can only be observed in the lobes on the southern margin of the channel (figs. 6.23b & 6.23d-e). This is probably due to strong tidal currents in the channel, which removed most of the infilling sediments.

Smaller, local paleovalleys have a more limited influence on the Quaternary distribution. This can especially be observed in the valley bounding the southern margin of the Offshore Scarp (fig. 9.2).

9.3 Influence of bedrock highs on Quaternary accumulations

A remarkable feature seems to be related to certain scarps in the erosion surface: in many cases an internal Quaternary reflector can be observed which abutts against the scarp (figs. 9.2 & 6.15e), forming a somewhat foreset-like sedimentary lens along the scarp. Most likely this reflector represents a depositional surface rather than an erosional one. Such scarps are quite often overlain by sand banks, which might suggest a possible relationship between the sedimentary lens and some initial stage of the sand bank.

In some cases Tertiary ridges and slope breaks are overlain by sand banks. This can be clearly observed in the northern part of the Akkaert Bank (fig. 9.3), where the ridge underlying the bank forms the nucleus of the sand bank. Foresets can be observed on one side of the ridge, which may indicate that the ridge possibly formed some sort of initial stage of the sand bank. The Thornton bank is underlain by a rather broad, irregular ridge (fig. 9.4). The boundary between the Offshore Platform and the southeastern part of the Axial Channel, which is locally marked by a ridge and a slope break, is overlain by NE oriented sand banks (figs. 6.13a-b & 9.1). The sand bank overlying the ridge is some 5 m thicker than the one overlying the slope break. This may be due to the fact that the slope break probably formed a somewhat smaller obstacle during the initial stage of the sand bank, causing less sediments to be deposited.

CONCLUSIONS

The analysis of more than 12000 km of high resolution reflection seismic profiles has allowed to gain a better insight into the character of the top-Tertiary erosion surface in the Belgian and Northern French sectors of the North Sea. The detailed study of the morphological features of the erosion surface has lead to the identification of 13 morphological units in the study area. They include 6 paleovalleys (Axial Channel, Northern Low Surface, Northern Valley, Ostend Valley, Coastal Valley and Western Valley), 4 planation surfaces (Offshore Platform, Middle Platform, Nearshore Slope and Marginal Platform) and their boundaries (Offshore Scarp, Middle Scarp and Nearshore Slope Break).

Most morphological units exhibit a SW-NE orientation, i.e. roughly parallel to the present Belgian coastline, except for the Ostend and Northern Valley which are mainly trending SE-NW. In general, the morphology of the erosion surface is not controlled by the strike of the substratum. Nevertheless, the combination of lithological contrasts, dip variations and structural deformations of the Tertiary strata have lead to some outspoken effects on the surface morphology.

Such geological control is very distinct in the Ostend-Northern valley system, the formation of which has clearly been influenced by vertical and lateral lithological contrasts. It is also explicitly expressed in the morphology of the northern part of the Offshore Platform, which has been affected by the occurrence of a large deformation zone.

The combination of the seismic study with the scarce sedimentological and paleontological information, taking into account the recent knowledge of the Quaternary history, has lead to a tentative reconstruction of the evolution of the main morphological units. Most units apparently have been formed during the Quaternary. The formation of the planation surfaces

and their boundaries is probably to a great extent due to marine abrasion and glacial erosion during the Middle Pleistocene. The initial formation of the paleovalleys is most likely caused by fluvial erosion during the Middle Pleistocene, except for the Axial Channel which probably originated during the Neogene.

The Quaternary sedimentation in the study area mainly consist of Holocene tidal sand banks, and therefore its distribution pattern will largely depend on the distribution pattern of these sand banks. Nevertheless, certain morphological features have had pronounced effects on the Quaternary distribution. The most distinct influence is exerted by large valleys, which acted as some sort of sediment trap. In some cases bedrock highs can most likely be related to the initial stages of sand banks.

The present thesis forms a base for further study of the Quaternary sedimentation and sea-level changes in the southern North Sea. This will however require many more borings.

SAMENVATTING

1. Inleiding

Het hier gepresenteerde onderzoek betreft een seismische en geomorfologische studie van het erosieoppervlak aan de top van het Tertiair in de Zuidelijke Noordzee (Belgische en Noordfranse sectoren). Het doel van deze studie was drieledig:

1. Een gedetailleerde beschrijving van de morfologie van het post-Tertiaire erosieoppervlak.
2. Een beschrijving van de invloed van de Tertiaire afzettingen op het erosieoppervlak.
3. Een poging tot reconstructie van de geologische evolutie van het erosieoppervlak.

Daarbij werd ook nog kort ingegaan op de mogelijke invloed van het erosieoppervlak op de Kwartaire sedimentatie.

Het studiegebied bevindt zich in het zuidelijke randgebied van het Cenozoische Noordzeebekken, bovenop het Paleozoische London-Brabant Massief. Tijdens het Tertiair en Kwartair werd dit gebied het toneel van veelvuldige transgressies en regressies. In het Tertiair heeft dit geleid tot een vrij continue reeks van afzettingen, met betrekkelijk geringe dikte (enkele honderden meter). In het Jong Kwartair van de zuidelijke baai van de Noordzee domineren echter erosieprocessen onder invloed van sterke getijdestromingen, en zijn de Kwartaire afzettingen erg diskontinu. De erosiemorfologie aan de top van het Tertiair is dan ook één van de belangrijkste informatiebronnen voor de recentste geologische evolutie van dit gebied.

De seismische gegevens werden verzameld d.m.v. continue mariene hoge-resolutie reflektieseismiek. De aldus bekomen profielen werden na interpretatie en digitalisatie omgezet in geologische dieptesekties, waarbij gebruik gemaakt werd van het 'interval velocity' snelheidsmodel. De gedigitaliseerde

profielen vormden tevens de basis voor een isobathenkaart van de top van het Tertiair en een isopachenkaart van de dikte van het Kwartair.

2. Morfologie van het top-Tertiaire erosieoppervlak

2.1 Algemeen

De morfologische karakteristieken van het post-Tertiaire erosieoppervlak kunnen onderverdeeld worden in eerste, tweede en derde orde kenmerken. Eerste orde kenmerken zijn veelal planair en omvatten al dan niet lichtjes hellende planatieoppervlakken en hun grenzen, zoals hellingsveranderingen, ruggen en steile flanken. Tweede orde kenmerken zijn veelal lineair en omvatten voornamelijk paleovalleien. Derde orde kenmerken zijn veelal singulier en omvatten putten en kleine depressies. Op basis van deze morfologische kenmerken kunnen 13 morfologische eenheden gedefinieerd worden in het studiegebied, waaronder 4 planatieoppervlakken en hun grenzen (3), en 6 paleovalleien. De planatieoppervlakken en hun grenzen hebben allemaal ruwweg een ZW-NO oriëntatie.

In deze Nederlandse samenvatting wordt gebruik gemaakt van de Engelse benaming van de eenheden, dit om eventuele problemen in terminologie te vermijden.

2.2 Planatieoppervlakken en hun grenzen

Het meest noordelijke gesitueerde planatieoppervlak is het zgn. 'OFFSHORE PLATFORM'. Het bestaat uit twee verschillende delen die van elkaar gescheiden worden door een paleovallei. Beide delen zijn tamelijk vlak. In het westelijke deel dagzomen Landenian- en Ieperiaanreeksen (De Batist, 1989), terwijl in het oostelijke deel enkel het Bartoon dagzoomt.

Het 'OFFSHORE PLATFORM' wordt naar het zuiden toe begrensd door een steile flank, de zgn. 'OFFSHORE SCARP', met een gemiddeld verval van 5 m. Ten zuiden van deze flank ligt het zgn. 'MIDDLE PLATFORM'. Dit oppervlak is relatief breed voor de Franse kust, en wordt naar het oosten toe geleidelijk aan smaller. Het westelijke deel wordt gekenmerkt door een ruwweg O-W georiënteerde, asymmetrische vallei. Het oostelijke deel vertoont een lichte helling en wordt gekenmerkt door ondiepe depressies.

Het 'MIDDLE PLATFORM' wordt landwaards begrensd door een steile flank, de zgn. 'MIDDLE SCARP', met een verval van ongeveer 5 m. Op bepaalde plaatsen gaat de flank over in een rug of vervaagt tot een nauwelijks waarneembare hellingsverandering. Deze flank vormt tevens de zeewaardse begrenzing van een zwak hellend planatieoppervlak, de zgn. 'NEARSHORE SLOPE'. Net zoals het 'OFFSHORE PLATFORM' bestaat ook de 'NEARSHORE SLOPE' uit twee verschillende delen, die van elkaar gescheiden worden door een paleovallei. Deze delen vertonen een opvallend verschillende morfologie. Het westelijke deel is relatief vlak en ligt op een substraat van Ieperse klei. Aan het oostelijke, sterk geërodeerde deel van het oppervlak dagzomen Ieperiaan- tot Priaboniaanreeksen. Dit deel wordt tevens gekenmerkt door een kleine paleovallei en een aantal elliptische depressies.

De overgang tussen de 'NEARSHORE SLOPE' en het meest zuidelijke planatieoppervlak, de zgn. 'MARGINAL PLATFORM', wordt gevormd door de zgn. 'NEARSHORE SLOPE BREAK'. Deze tamelijk zwakke hellingsverandering wordt naar het oosten toe meer geprononceerd. Het westelijke deel van het 'MARGINAL PLATFORM' ligt op de Ieperse klei en wordt gekenmerkt door verscheidene heuvels en depressies. Aan het oostelijke deel, dat van het westelijke gescheiden is door een paleovallei, dagzomen Ieperiaan- tot Bartoonreeksen.

2.3 Paleovalleien

Onder de kustvlakte en parallel met de kust loopt de zgn. 'COASTAL VALLEY'. Deze vallei heeft een sterk asymmetrische vorm, met een steile zuidflank en een zachte noordflank, en is uitgeschuurd in Ieperiaan- tot Bartoonreeksen. Ten westen van de Belgisch/Franse grens gaat de 'COASTAL VALLEY' over in de zgn. 'WESTERN VALLEY'. Deze vallei heeft grotendeels een ZO-NW oriëntatie, en wordt gekenmerkt door een depressie voor de kust van Duinkerke.

De volgende 3 valleien hebben grotendeels een ZO-NW oriëntatie, en maken deel uit van het zgn. 'OSTEND-NORTHERN VALLEY SYSTEM'.

De meest zuidelijke paleovallei van dit systeem, de zgn. 'OSTEND VALLEY', is relatief smal en diep nabij de kust en wordt naar zee toe geleidelijk aan breder en minder diep. De vallei is uitgeschuurd in de Ieperse klei en volgt ruwweg de strekking van deze afzettingsreeks. Naar het noordoosten toe gaat de 'OSTEND VALLEY' over in het zuidelijke, ZW-NO georiënteerde deel van de zgn. 'NORTHERN VALLEY'. Dit deel van de vallei volgt ruwweg de Y4/Y2 en Y4/Y3 grens. Het noordelijke, ZW-NO georiënteerde deel van de vallei volgt grotendeels de Y3/L1 grens, en wordt gekenmerkt door een onregelmatige bodem. Naar het noorden toe wordt de 'NORTHERN VALLEY' geleidelijk aan breder, om vervolgens langzaam over te gaan in het zgn. 'NORTHERN LOW SURFACE'. Het westelijke deel van deze vallei is uitgeschuurd in Y2- tot Y5-sekwenties, het oostelijke deel daarentegen snijdt Bartoon- tot Rupeliaanreeksen aan.

De meest noordelijke paleovallei, de zgn. 'AXIAL CHANNEL', heeft een ZW-NO oriëntatie en is zo'n 17-20 km breed. De zuidelijke rand van deze paleovallei wordt gekenmerkt door verscheidene 'lobben'. Deze 'lobben' zijn grotendeels opgevuld met Kwartaire sedimenten, in tegenstelling tot het meer centrale deel van de vallei dat weinig of niet bedekt is.

2.4 Putten

De meeste putten en kleine depressies komen voor in paleovalleien, en meer uitzonderlijk in planatieoppervlakken. Het landwaardse gedeelte van de 'OSTEND VALLEY' wordt gekenmerkt door verscheidene putten, de zgn. 'SEPIA PITS'. Voor de kust van Zeebrugge ligt de zgn. 'ZEEBRUGGE PIT', die is uitgeschuurd in Lutetiaan- en Bartoonreeksen. De zgn. 'DUNKERQUE PIT' is gelegen in het zeewaardse gedeelte van de 'WESTERN VALLEY'.

3. Invloed van het Tertiair substraat op het erosieoppervlak

De lithologie, helling en structuur van de Tertiaire afzettingen beïnvloeden op vele punten de morfologie van het erosieoppervlak.

Vertikale, regionale contrasten in lithologie veroorzaken meestal differentiële erosie, hetgeen vervolgens kan leiden tot de vorming van hellingsveranderingen, flanken, valleien en cuestas. Laterale lithologische variaties daarentegen leiden bijna nooit tot differentiële erosie, en kunnen in sommige gevallen zelfs eventuele verticale lithologische contrasten teniet doen. Dit is waarschijnlijk het geval voor de overgang van de 'NORTHERN VALLEY' in het 'NORTHERN LOW SURFACE'.

Lokale lithologische contrasten zijn meer plaatsgebonden, en kunnen aanleiding geven tot kleinschaliger morfologische kenmerken. Een mooi voorbeeld hiervan is de erosieve depressie in het zuidelijke deel van de 'NORTHERN VALLEY', die is uitgeschuurd in de afzettingsreeksen Y3, Y2 en zelfs de top van de Y1-sekwentie.

Een verandering in de helling van de Tertiaire strata kan o.a. aanleiding geven tot de vorming van een steile flank, zoals te zien in een deel van de zuidelijke flank van het ZO-NW georiënteerde deel van de 'NORTHERN VALLEY'.

Lokale structurele deformaties, vaak in combinatie met bepaalde lithologische contrasten, kunnen tevens aanleiding geven tot differentiële erosie. Een goed voorbeeld daarvan is de vervormingszone van de Noordhinder.

4. Mogelijke genetische scenario's

De combinatie van seismische gegevens, sedimentologische en/of paleontologische informatie en recente kennis van de geschiedenis van het Kwartair heeft geleid tot een voorlopige rekonstructie van de evolutie van het post-Tertiaire erosieoppervlak. De planatieoppervlakken en hun grenzen zijn waarschijnlijk ontstaan door mariene abrasie, en misschien ook glaciale erosie, tijdens het Midden Pleistoceen. Een eerste vorming van de paleovalleien is vermoedelijk gebeurd door fluviale erosie tijdens het Saaliaan. Verdere uitschuring vond waarschijnlijk plaats gedurende het Eemiaan en het Holoceen. De 'AXIAL CHANNEL' vormt echter hierop een uitzondering. Deze paleovallei is meer dan waarschijnlijk ontstaan tijdens het Neogeen, en werd verder uitgeschuurd door latere fluviale en mariene erosie.

5. Invloed van het erosieoppervlak op het Kwartair

De Kwartaire sedimentatie in het centrale tot noordelijke deel van de Belgischesector en in de Noordfranse sector hangt in belangrijke mate samen met de verspreiding van de zandbanken in het gebied. In sommige gevallen echter heeft de morfologie van het erosieoppervlak een merkbare invloed op de verdeling van het Kwartair. Verreweg de grootste invloed wordt uitgeoefend door de paleovalleien, die als het ware fungeren als een soort van 'vergaarbak' voor sedimenten. In bepaalde gevallen kunnen flanken en ruggen in het erosieoppervlak geassocieerd worden met een eerste stadium in de vorming van zandbanken.

LIST OF ILLUSTRATIONS

Chapter 1

Figure 1.1 Location of the study area.

Chapter 2

- Figure 2.1 Geometry of the reflection path
 a. For constant velocity
 b. For average velocity model
 c. For interval velocity model
 (after Sheriff & Geldart, 1982).
- Figure 2.2 Characteristics of seismic events (after Sheriff & Geldart, 1982).
- Figure 2.3 Types of multiples (after Sheriff & Geldart, 1982).
- Figure 2.4 Schematic of the RCMG seismic system.
- Figure 2.5 Definition of a depositional sequence and its boundaries (after Mitchum et al., 1977).
- Figure 2.6 Relations of strata to boundaries of depositional sequences (after Mitchum et al., 1977).
- Figure 2.7 Different types of reflection configurations (after Mitchum et al., 1977).
- Figure 2.8 External forms of some seismic facies units (after Mitchum et al., 1977).
- Figure 2.9 Relative changes of sea-level
 a. Coastal onlap indicates a relative rise of sea-level
 b. Downward shift in coastal onlap indicates a relative drop of sea-level
 c. Coastal toplap indicates a relative stillstand of sea-level
 (after Vail et al., 1977).

- Figure 2.10 a. Downhole shooting in offshore conditions
 b. Uphole shooting in offshore conditions
 (after Vercoutere, 1987).

Chapter 3

- Figure 3.1 The seismic grid covering the Belgian, Dutch, French and UK sectors of the continental shelf (after Henriët et al., 1988).
 Figure 3.2 Velocity effect on a flat surface covered by sand banks.
 Figure 3.3 Velocity effect on a gently dipping surface covered by sand banks.

Chapter 4

- Figure 4.1 Spatial relationship of the Paleozoic orogenic belt during the Late Paleozoic. L.B.M. = London-Brabant Massif (after P. Ziegler, 1981).
 Figure 4.2 Schematic graben pattern of the Mesozoic North Atlantic - Arctic rift system. NS = North Sea rift (after P. Ziegler & Louwerens, 1979).
 Figure 4.3 Paleogeography of the southern North Sea area during the Late Cretaceous (after Kockel, 1988).
 Figure 4.4 Thickness of the Late Cretaceous chalk (after Roorda Van Eysinga, 1982 and Legrand, 1968).
 Figure 4.5 Assumed basin-wide sea-level changes in the NW European basin (after Kockel, 1988).
 Figure 4.6 Paleogeography of the southern North Sea area during the Early Paleocene (after P. Ziegler, 1982 and Kockel, 1988).
 Figure 4.7 Paleogeography of the southern North Sea area during the Middle Eocene (after P. Ziegler, 1982 and Kockel, 1988).
 Figure 4.8 Paleogeography of the southern North Sea area during the Late Eocene (after P. Ziegler, 1982 and Kockel, 1988).
 Figure 4.9 Paleogeography of the southern North Sea area during the Middle Oligocene (after P. Ziegler, 1982 and Kockel, 1988).

- Figure 4.10 Paleography of the southern North Sea area during the Middle Miocene (after P.Ziegler, 1982 and Kockel, 1988).
- Figure 4.11 Paleography of the southern North Sea area during the Early Pliocene (after Zagwijn & Doppert, 1978 and P.Ziegler, 1982).
- Figure 4.12 Paleomagnetic measurements, climatic curve and stratigraphic subdivision of the Quaternary in The Netherlands and East Anglia (after Zagwijn, 1979).
- Figure 4.13 Paleography of the southern North Sea area during the Middle Tiglian (after Zagwijn, 1979).
- Figure 4.14 Paleography of the southern North Sea area during the Late Tiglian (after Zagwijn, 1979).
- Figure 4.15 Development of the Thames-Lobourg river system during the Quaternary (after Balson & D'Olier, 1988).
- Figure 4.16 Paleography of the southern North Sea area during the Waalian (after Zagwijn, 1979).
- Figure 4.17 Paleography of the southern North Sea area during the later part of the Cromerian Complex (after Zagwijn, 1979).
- Figure 4.18 Paleography of the southern North Sea area during the Elsterian (after Zagwijn, 1979).
- Figure 4.19 Paleography of the southern North Sea area during the Holsteinian (after Zagwijn, 1979).
- Figure 4.20 Paleography of the southern North Sea area during the Saalian (after Zagwijn, 1979). The extension of British land ice is after West (1977).
- Figure 4.21 Paleography of the southern North Sea area during the Middle to Late Weichselian (after Jelgersma, 1979).
- Figure 4.22 Curve for the relative sea-level rise during the Holocene, based on data from the Belgian coastal plain. MSL = mean lowest low water-level at spring-tide (after Köhn, 1988).

Chapter 5

- Figure 5.1 Schematic seismic-stratigraphic sequence chart and correlation table of the Paleogene deposits in the Southern Bight (after De Batist, 1989).
- Figure 5.2 Seismic-stratigraphic solid map of the Paleogene deposits in the Southern Bight (after De Batist, 1989).
- Figure 5.3 Analog record of a sparker section and interpreted line-drawing showing Thanetian gully erosion features (after Henriët et al., 1989).
- Figure 5.4 Analog record of a sparker section and interpreted line-drawing showing the lower interval of Ypresian clay-tectonic deformations (after De Batist et al., 1989)*.
- Figure 5.5 Analog record of a sparker section and interpreted line-drawing showing the middle interval of Ypresian clay-tectonic deformations (after De Batist et al., 1989)*.
- Figure 5.6 Analog record of a sparker section and interpreted line-drawing showing the upper interval of Ypresian clay-tectonic deformations (after De Batist et al., 1989)*.
- Figure 5.7 Genetic model of the clay-tectonic deformations in the Ypresian Clay (after Henriët et al., 1988).
- Figure 5.8 Schematic representation of the Ypresian basin-fill sequences offshore Ostend (after De Batist, 1989).
- Figure 5.9 Analog record of a sparker section and interpreted line-drawing showing the L1 sequence (after De Batist, 1989).
- Figure 5.10 Analog record of a boomer section and interpreted line-drawing showing the different seismic facies units in the B1 sequence (after Henriët et al., 1989).

- Figure 5.11 Location of tidal sand banks in the study area
 1. The Coastal Banks and mouth of the river Scheldt
 2. The Flemish Banks
 3. The Hinder group
 4. The Zeeland ridges
 (after Bastin, 1974).
- Figure 5.12 Analog record of a sparker section and interpreted line-drawing showing the seismic facies of a tidal sand bank.
- Figure 5.13 Analog record of a sparker section and interpreted line-drawing showing sand banks of the Hinder group, containing sedimentary nuclei.
- Figure 5.14 Analog record of a sparker section and interpreted line-drawing showing the Flemish Banks.
- Figure 5.15 Analog record of a sparker section and interpreted line-drawing showing a valley bounding the Thornton Bank.
- Figure 5.16 Analog record of a sparker section and interpreted line-drawing showing the Coastal Banks.

(*) Depth calculated with an interval velocity of 1620 m/s.

Chapter 6

- Figure 6.1 Isobath map of the top-Tertiary erosion surface. Mercator projection at 51°20'N. Scale 1/100000. Reference level is the mean lowest low water-level at spring-tide. Landward part after De Moor & De Breuk (1973), Sommé (1979), Baeteman (1981), Depret (1983), Devos (1984), Mostaert (1985) and De Batist (1989).
- Figure 6.2 Schematic 3D representation of different types of planation surface boundaries.
 a. slope break
 b. scarp
 c. ridge
 d. cuesta
- Figure 6.3 Distribution of ridges in the study area.

- Figure 6.4 Distribution of cuestras in the study area.
- Figure 6.5 Distribution of slope breaks in the study area.
- Figure 6.6 Distribution of scarps in the study area.
- Figure 6.7 Distribution of paleovalleys in the study area.
- Figure 6.8 Distribution of pits in the study area.
- Figure 6.9 Distribution of different morphological features
in the study area.
- Figure 6.10 Distribution of morphological units in the study
area.
- Figure 6.11a Interpreted line-drawing of cross-section A-A'.
- Figure 6.11b Interpreted line-drawing of cross-section B-B'.
- Figure 6.11c Interpreted line-drawing of cross-section C-C'.
- Figure 6.11d Interpreted line-drawing of cross-section D-D'.
- Figure 6.11e Interpreted line-drawing of cross-section E-E'.
- Figure 6.11f Interpreted line-drawing of cross-section F-F'.
- Figure 6.11g Interpreted line-drawing of cross-section G-G'.
- Figure 6.11h Interpreted line-drawing of cross-section H-H'.
- Figure 6.11i Interpreted line-drawing of cross-section I-I'.
- Figure 6.12 Location of profiles across the Offshore
Platform and the Offshore Scarp.
- Figure 6.13a Analog record of a sparker section and
interpreted line-drawing showing the seaward
part of the Offshore Platform. For location of
the profile see fig. 6.12.
- Figure 6.13b Analog record of a sparker section and
interpreted line-drawing showing the seaward
part of the Offshore Platform. For location of
the profile see fig. 6.12.
- Figure 6.13c Analog record of a sparker section and
interpreted line-drawing showing the landward
part of the Offshore Platform and the Offshore
Scarp. For location of the profile see fig.
6.12.
- Figure 6.13d Analog record of a sparker section and
interpreted line-drawing showing the landward
part of the Offshore Platform. For location of
the profile see fig. 6.12.
- Figure 6.14 Location of profiles across the Middle Platform
and the Middle Scarp.

- Figure 6.15a Analog record of a sparker section and interpreted line-drawing showing the southwestern part of the Middle Platform. For location of the profile see fig. 6.14.
- Figure 6.15b Analog record of a sparker section and interpreted line-drawing showing the southwestern part of the Middle Platform. For location of the profile see fig. 6.14.
- Figure 6.15c Analog record of a sparker section and interpreted line-drawing showing the northwestern part of the Middle Platform. For location of the profile see fig. 6.14.
- Figure 6.15d Analog record of a sparker section and interpreted line-drawing showing the northwestern part of the Middle Platform. For location of the profile see fig. 6.14.
- Figure 6.15e Analog record of a sparker section and interpreted line-drawing showing the western part of the Middle Scarp. For location of the profile see fig. 6.14.
- Figure 6.16 Location of profiles across the Nearshore Slope, the Nearshore Slope Break and the Marginal Platform.
- Figure 6.17a Analog record of a sparker section and interpreted line-drawing showing the Western Nearshore Slope Break. For location of the profile see fig. 6.16.
- Figure 6.17b Analog record of a sparker section and interpreted line-drawing showing the Western Nearshore Slope Break. For location of the profile see fig. 6.16.
- Figure 6.17c Analog record of a sparker section and interpreted line-drawing showing the western depression in the Eastern Nearshore Slope. For location of the profile see fig. 6.16.
- Figure 6.17d Analog record of a sparker section and interpreted line-drawing showing the western part of the valley in the Nearshore Slope. For location of the profile see fig. 6.16.

- Figure 6.17e Analog record of a sparker section and interpreted line-drawing showing the eastern part of the valley in the Nearshore Slope. For location of the profile see fig. 6.16.
- Figure 6.17f Analog record of a sparker section and interpreted line-drawing showing the eastern depression in the Eastern Nearshore Slope. For location of the profile see fig. 6.16.
- Figure 6.18 Location of profiles across the Ostend Valley.
- Figure 6.19a Analog record of a sparker section and interpreted line-drawing showing the seaward part of the Ostend Valley. For location of the profile see fig. 6.18.
- Figure 6.19b Analog record of a sparker section and interpreted line-drawing showing the seaward part of the Ostend Valley. For location of the profile see fig. 6.18.
- Figure 6.19c Analog record of a sparker section and interpreted line-drawing showing the middle part of the Ostend Valley. For location of the profile see fig. 6.18.
- Figure 6.19d Analog record of a sparker section and interpreted line-drawing showing the landward part of the Ostend Valley. For location of the profile see fig. 6.18.
- Figure 6.19e Analog record of a sparker section and interpreted line-drawing showing the landward part of the Ostend Valley. For location of the profile see fig. 6.18.
- Figure 6.20 Location of profiles across the Northern Valley and the Northern Low Surface.
- Figure 6.21a Analog record of a sparker section and interpreted line-drawing showing the NE trending Northern Valley. For location of the profile see fig. 6.20.
- Figure 6.21b Analog record of a sparker section and interpreted line-drawing showing the NE trending Northern Valley. For location of the profile see fig. 6.20.

- Figure 6.21c Analog record of a sparker section and interpreted line-drawing showing the NW trending Northern Valley. For location of the profile see fig. 6.20.
- Figure 6.21d Analog record of a sparker section and interpreted line-drawing showing the NW trending Northern Valley. For location of the profile see fig. 6.20.
- Figure 6.21e Analog record of a sparker section and interpreted line-drawing showing the NW trending Northern Valley. For location of the profile see fig. 6.20.
- Figure 6.21f Analog record of a sparker section and interpreted line-drawing showing the Northern Low Surface. For location of the profile see fig. 6.20.
- Figure 6.22 Location of profiles across the Axial Channel.
- Figure 6.23a Analog record of a sparker section and interpreted line-drawing showing the southeastern part of the Axial Channel. For location of the profile see fig. 6.22.
- Figure 6.23b Analog record of a sparker section and interpreted line-drawing showing the northern lobe in the Axial Channel. For location of the profile see fig. 6.22.
- Figure 6.23c Analog record of a sparker section and interpreted line-drawing showing the part of the Axial Channel between the northern and southern lobes. For location of the profile see fig. 6.22.
- Figure 6.23d Analog record of a sparker section and interpreted line-drawing showing the southern lobe in the Axial Channel. For location of the profile see fig. 6.22.
- Figure 6.23e Analog record of a sparker section and interpreted line-drawing showing the southern lobe in the Axial Channel. For location of the profile see fig. 6.22.
- Figure 6.24 Location of profiles across the Dunkerque Pit.

Figure 6.25a Analog record of a sparker section and interpreted line-drawing showing the Dunkerque Pit in the Western Valley. For location of the profile see fig. 6.24.

Figure 6.25b Analog record of a sparker section and interpreted line-drawing showing the Dunkerque Pit in the Western Valley. For location of the profile see fig. 6.24.

Chapter 7

Figure 7.1 Paleogene sequences subcropping against the top-Tertiary erosion surface of the different morphological units (partly after De Batist, 1989).

Figure 7.2 Analog record of a sparker section and interpreted line-drawing showing cuestas in the L1 sequence.

Figure 7.3 Analog record of a sparker section and interpreted line-drawing showing cuestas in the L1 sequence.

Figure 7.4 Analog record of a sparker section and interpreted line-drawing showing cuestas at different levels in the B1 sequence.

Figure 7.5 Analog record of a sparker section and interpreted line-drawing showing a cuesta and a slope break in the upper part of the B1 sequence.

Figure 7.6 Analog record of a sparker section and interpreted line-drawing showing a cuesta and a scarp in the lower part of the B1 sequence.

Figure 7.7 Analog record of a sparker section and interpreted line-drawing showing the high overlying the basin fill offshore Ostend.

Figure 7.8 Analog record of a sparker section and interpreted line-drawing showing a scarp in the NW trending Northern Valley.

Figure 7.9 Analog record of a sparker section and interpreted line-drawing showing a syncline overlain by a depression.

- Figure 7.10 Analog record of a sparker section and interpreted line-drawing showing two weak synclines overlain by highs.
- Figure 7.11 Analog record of a sparker section and interpreted line-drawing showing an anticline overlain by a depression.
- Figure 7.12 Analog record of a sparker section and interpreted line-drawing showing the most southern synclinal depression of the Noordhinder deformation zone.
- Figure 7.13 Analog record of a sparker section and interpreted line-drawing showing the northernmost central synclinal depression of the Noordhinder deformation zone.

Chapter 8

- Figure 8.1 The recent Lobourg paleochannel system (after Bridgland & D'Olier, 1989).
- Figure 8.2 Tentative reconstruction of the study area during the Saalian.
- Figure 8.3 Tentative reconstruction of the study area during the Holocene.

Chapter 9

- Figure 9.1 Isopach map of the thickness of the Quaternary sediments. Mercator projection at 51°20'N. Scale 1/100000. Reference level is the mean lowest low water-level at spring-tide. Landward part after De Moor & De Breuck (1973), Sommé (1979), Baeteman (1981), Depret (1983), Devos (1984), Mostaert (1985) and De Batist (1989).
- Figure 9.2 Analog record of a sparker section and interpreted line-drawing showing the Oosthinder overlying the Offshore Scarp .
- Figure 9.3 Analog record of a sparker section and interpreted line-drawing showing a ridge underlying the northern part of the Akkaert Bank.

Figure 9.4 Analog record of a sparker section and interpreted line-drawing showing a broad ridge underlying the Thornton Bank.

BIBLIOGRAPHY

- ALLEN, J.R.L., 1973. Phase differences between bed configuration and flow in natural environments, and their geological relevance. *Sedimentology*, 20, 323-329.
- ALLEN, J.R.L., 1982. Sedimentary structures : Their character and physical basis. Volume 2, 101-131. Elsevier.
- BAETEMAN, C., 1981. De Holocene ontwikkeling van de westelijke kustvlakte. Unpublished doctoral thesis, Free University of Brussels, 297 pp.
- BALSON, P.S., 1989. Tertiary phosphorites in the southern North Sea Basin : Origin, evolution and stratigraphic correlation. In: HENRIET, J.P. & DE MOOR, G. (eds.) *The Quaternary and Tertiary Geology of the Southern Bight, North Sea*, 51-70.
- BALSON, P.S., 1989. Neogene deposits of the UK sector of the southern North Sea (51°-53°N). In: HENRIET, J.P. & DE MOOR, G. (eds.) *The Quaternary and Tertiary Geology of the Southern Bight, North Sea*, 89-96.
- BALSON, P.S. & D'OLIER, B., 1988. Thames Estuary, sheet 51°N-00°E. Solid Geology. 1:250000 series.
- BANKS, N.L., 1973. The origin and significance of some downcurrent-dipping cross-stratified sets. *J. Sed. Petrol.*, 43, 423-427.
- BASTIN, A., 1974. Regionale sedimentologie en morfologie van de zuidelijke noordzee en van het schelde estuarium. Unpublished doctoral thesis, Catholic University of Leuven, 91 pp.
- BATES, R.L. & JACKSON, J.A., 1980. Glossary of geology. American Geological Institute, 751 pp.
- BRIDGLAND, D.R. & D'OLIER, B., 1989. A preliminary correlation of the onshore and offshore courses of the Rivers Thames and Medway during the Middle and Upper Pleistocene. In: HENRIET, J.P. & DE MOOR, G. (eds.) *The Quaternary and Tertiary Geology of the Southern Bight, North Sea*, 161-172.
- BRIQUET, A., 1921. Sur l'origine du Pas-de Calais. *Ann. Soc. Geol. Nord.*, 46, 141-157.
- BROWN, L.F.^R & FISGER, W.L., 1977. Seismic-stratigraphic interpretation of depositional surfaces : Examples from Brazilian rift and pull-apart basin. In: PAYTON, C.E. (ed.) *Seismic stratigraphy - applications to hydrocarbon exploration*. AAPG Memoir, 26, 213-248.

CAMERON, T.D.J., BONNY, A.P., GREGORY, D.M. & HARLAND, R., 1984. Lower Pleistocene dinoflagellate cyst, foraminiferal and pollen assemblages in four boreholes in the southern North Sea. *Geol. Mag.*, 121, 85-97.

CAMERON, T.D.J., LABAN, C. & SCHÜTTENHELM, R.T.E., 1989. Upper Pliocene and Lower Pleistocene stratigraphy in the Southern Bight of the North Sea. In: HENRIET, J.P. & DE MOOR, G. (eds.) *The Quaternary and Tertiary Geology of the Southern Bight, North Sea*, 97-110.

CAMERON, T.D.J., SCHÜTTENHELM, R.T.E. & LABAN, C., 1989. Middle and Upper Pleistocene and Holocene stratigraphy in the southern North Sea between 52° and 54°N, 2° to 4°E. In: HENRIET, J.P. & DE MOOR, G. (eds.) *The Quaternary and Tertiary Geology of the Southern Bight, North Sea*, 119-136.

CASTON, V.N.D., 1972. Linear sand banks in the southern North Sea. *Sedimentology*, 18, 63-78.

CASTON, V.N.D., 1979. The Quaternary sediments of the North Sea. In: BANNER, F.T., COLLINS, M.B. & SASSIE, K.S. (eds.) *The North-West European shelf seas : The sea bed and the sea in motion. I. Geology and sedimentology*, 195-270. Elsevier Scientific Publishing Company.

CURRY, D., ADAMS, C.G., BOULTER, M.C., DILLEY, F.C., EAMES, F.E., FUNNELL, B.M. & WELLS, M.K., 1978. A correlation of Tertiary rocks in the British Isles. *Spec. Aep. Geol. Soc. London*, 12, 72 pp.

DAVIS, A.G. & ELLIOT, G.F., 1957. The paleogeography of the London Clay Sea. *Proc. Geol. Ass.*, 68, 255-277.

DE BATIST, M., 1989. Seismostratigrafie en structuur van het paleogeen in de zuidelijke noordzee. Unpublished doctoral thesis, State University of Gent. Volume 1: Text, 107 pp.

DE BATIST, M., 1989. Seismostratigrafie en structuur van het paleogeen in de zuidelijke noordzee. Unpublished doctoral thesis, State University of Gent. Volume 2: Figures, 136 figs.

DE BATIST, M., DE BRUYNE, H., HENRIET, J.P. & MOSTAERT, F., 1989. Stratigraphic analysis of the Ypresian off the Belgian coast. In: HENRIET, J.P. & DE MOOR, G. (eds.) *The Quaternary and Tertiary Geology of the Southern Bight, North Sea*, 75-88.

DE BRUYNE, H., 1984. Een seismisch-stratigrafische studie van het Tertiair op het oostlijk deel van het Belgisch Continentaal Plat. Unpublished thesis, State University of Gent, 30 pp.

DE CEUNINCK, R., 1985. The evolution of the coastal dunes in the western Belgian coastal plain. *Eiszeitalter und Gegenwart*, 35, 33-41, Hanover.

DE COCK, V., 1985. Een ontwerp van een seismisch-geologisch gegevensbestand voor het Belgisch Continentaal Plat. Unpublished thesis, State University of Gent, 49 pp.

DE MEUTER, F.J. & LAGA, P.G., 1976. Lithostratigraphy and biostratigraphy based on benthonic foraminifera of the Neogene deposits of northern Belgium. *Bull. Soc. Belge Geol.*, 85(4), 133-152.

DE MOOR, G. & DE BREUCK, W., 1973. Sedimentologie en stratigrafie van enkele Pleistoceen afzettingen in de Belgische kustvlakte. *Nat. Wet. Tijdschr.*, 55, 3-96.

DE MOOR, G. & TAVERNIER, R., 1978. Periglacial and paleogeography of the Quaternary : Periglacial deposits and sedimentary structures in the Upper-Pleistocene infilling of the Flemish Valley. Unpublished excursion.

DE MOOR, G., 1988. The Flemish Valley and the Quaternary river morphology in northern Belgium. *BEVAS-SOBEG*, 57, 31-85.

DE MOOR, G., 1989. Maintenance on the Flemish Banks. In: HENRIET, J.P. & DE MOOR, G. (eds.) *The Quaternary and Tertiary Geology of the Southern Bight, North Sea*, 185-216.

DEPRET, M., 1981. Litostratigrafie van het Kwartair en van het Tertiaire substraat te Zeebrugge. Lithologische en stratigrafische interpretatie van diepsonderingen met de konus van Begemann. Unpublished doctorate thesis, State University of Gent, 338 pp.

DEPRET, M., 1983. Studie van de litostratigrafie van het Kwartair en van het Tertiaire substraat te Zeebrugge onder meer met diepsonderingen. *Belg. Geol. Dienst, Prof. Paper*, 201, 235 pp.

DE ROUCK, 1978. Globaal grondonderzoek. deelrapport 1. 31 pp, 17 figs. Unpublished report.

DESTOMBES, J.P., SHEPARD-THORN, E.R. & REDDING, J.H., 1975. A buried valley system in the Strait of Dover. *Philos. Trans. R. Soc. Lond.*, A270, 243-256.

DEVOS, J., 1984. Hydrogeologie van het Duinengebied ten oosten van De Haan. Unpublished doctoral thesis, State University of Gent, 219 pp.

DEVOS, K., 1981. Een reflectieseismische studie op de zuidelijke Noordzee - Sector Sandettie-Noordhinder. Unpublished thesis, State University of Gent, 32 pp.

DIETRICH, G., 1955. Ergebnisse synoptischer ozeanographischer Arbeiten in der Nordsee. *Tagungsber. und wissenschaft. Abh. Dtsch. Geografentag.*, Hamburg 1955, 30, 376-383. Steiner, Wiesbaden.

DINGLE, R.V., 1965. Sand waves in the North Sea mapped by continuous reflection profiles. *Mar. Geol.*, 3, 391-400.

DIX, C.H., 1955. Seismic velocities from surface measurements. *Geophysics*, 20, 68-86.

- DOBRIN, M.B., 1976. Introduction to geophysical prospecting, 3rd ed. New York, McGraw-Hill.
- D'OLIER, B., 1975. Tunnel valleys and associated features of the Southern Bight of the North Sea. *Quaternary Newsletter*, 17, p 5.
- D'OLIER, B., 1981. Sedimentary events during Flandrian sea-level rise in the south-west corner of the North Sea. *Spec. Publ. Int. Ass. Sediment.*, 5, 221-227.
- DONOVAN, D.T., 1973. The geology and origin of the Silver Pit and other closed basins in the North Sea. *Proc. Yorkshire Geol. Soc. Vol. 39, Part 2, 13*, 267-293.
- DOPPERT, J.W.CHR., LAGA, P.G. & DE MEUTER, F.J., 1979. Correlation of the biostratigraphy of marine Neogene deposits, based on benthonic foraminifera, established in Belgium and the Netherlands. *Meded. Rijks Geol. Dienst*, 31-1, 1-8.
- DOPPERT, J.W.CHR., 1980. Lithostratigraphy and biostratigraphy of marine Neogene deposits in the Netherlands. *Meded. Rijks Geol. Dienst.*, 32, 255-312.
- DREIMANIS, A., 1960. Pre-Lassical Wisconsin in the eastern portion of the Great Lake Region, North America. *21st Intern. Geol. Congress Copenhagen*, 4, 108.
- DRICOT, E., 1961. Micro-stratigraphie des argiles de Campine. *Bull. Soc. Belg. Geol.*, 20, 113-141.
- EISMA, D., JANSEN, J.H.F. & VAN WEERING, T.C.E., 1979. Sea-floor morphology and recent sediment movement in the North Sea. In: OELE, E., SCHÜTTENHELM, R.T.E. & WIGGERS, A.J. (eds.) *The Quaternary history of the North Sea. Acta Univ. Ups. Symp. Univ. Ups. Annum Quingentesimum Celebrantis*, 2, 217-232.
- FAIRBRIDGE, R.W., 1961. Eustatic changes in sea level. In: AHRENE, L.H., PRESS, F., RANKAMA, K. & RUNCORN, S.K. (eds.) *Physics and chemistry of the earth*, 99-185. Pergamon, London.
- FAUST, L.T., 1951. Seismic velocity as a function of depth and geologic time. *Geophysics*, 16, 192-206.
- FUNNEL, B.M., 1972. The history of the North Sea. *Bull. Geol. Soc. Norfolk*, 22, 2-10.
- GEYS, J.F., 1978. The paleoenvironment of the Kempenland clay deposits (Lower Quaternary, N. Belgium). *Geol. Mijnbouw*, 57, 33-43.
- GIBBARD, P.L., 1977. Pleistocene History of the Vale of St. Albans. *Philosophical Transactions of the Royal Society, London*, B 280, 445-483.
- GODWIN, H., 1960. Radiocarbon dating and Quaternary history in Britain. *Proc. R. Soc. Lond.*, B 153, 287-320.

GRAMANN, F., 1988. Major paleontological events and biostratigraphical correlations. In: VON DANIELS, C., GRAMANN, F., KÖTHE, A., KNOX, R.W.O'B., KOCKEL, F., MEYER, K-J., VINKEN, R. & WEISS, W. (eds.) *Geologisches Jahrbuch, Reihe A, Heft 100, The Northwest European Tertiary basin*, 410-422. Hannover, 1988.

GRAMANN, F. & KOCKEL, F., 1988. Paleontological, lithological, paleoecological and paleoclimatic development of the Northwest European Tertiary Basin. In: VON DANIELS, C., GRAMANN, F., KÖTHE, A., KNOX, R.W.O'B., KOCKEL, F., MEYER, K-J., VINKEN, R. & WEISS, W. (eds.) *Geologisches Jahrbuch, Reihe A, Heft 100, The Northwest European Tertiary basin*, 428-440. Hannover, 1988.

GREEN, C.H., 1938. Velocity determinations by means of reflection profiles. *Geophysics*, 3, 295-305.

GREENSMITH, J.T. & TUCKER, E.V., 1973. Holocene transgressions and regressions on the Essex coast outer Thames estuary. *Geol. Mijnbouw*, 52(4), 193-202.

HAGEMAN, B.P., 1969. Development of the western part of the Netherlands during the Holocene. *Geol. Mijnbouw*, 48(4), 373-388.

HAMILTON, A., 1979. The geology of the English Channel, south Celtic Sea and continental margin, south western approaches. In: BANNER, F.T., COLLINS, M.B. & MASSIE, K.S. (eds.) *The North-West European shelf seas : The sea bed and the sea in motion. I. Geology and sedimentology*, 61-88. Elsevier Scientific Publishing Company.

HANCOCK, J.M. & SCHOLLE, P.A., 1975. Chalk of the North Sea. In: WOODLAND, A.W. (ed.) *Petroleum and the continental shelf of North West Europe*. Applied Science Publisher Ltd.

HELDENS, P., 1979. Een reflectieseismische studie van de Boomse klei tussen Temse en Antwerpen. Unpublished thesis, State University of Gent, 38 pp.

HELDENS, P., 1983. Een seismische studie van de Klei van Boom en de Klei van Ieper. Unpublished doctorate thesis, State University of Gent, 237 pp.

HENRIET, J.P., BASTIN, A. & DE BROUCK, J., 1978. Integration of continuous seismic profiling in geotechnical investigations of the Belgian coast. K.VIV, 7th Intern. Harbour Congress, 1.18/1-1.18/13.

HENRIET, J.P., DE ROUCK, J. & DE WOLF, P., 1981. Morfologie van het tertiair substraat ter plaatse van de nieuwe buitenhaven te Zeebrugge. *Colloquium Belgisch Comité voor Ingenieursgeologie. Excursiegids havenwerken Zeebrugge*, 9 October 1981.

HENRIET, J.P., D'OLIER, B. & ANDERSEN, H.L., 1982. Seismic tracking of geological hazards related to clay tectonics in the Southern Bight of the North Sea. *Royal Society of Flemish Engineers (K.VIV) Symposium engineering in marine environment*, Brugge (Belgium).

HENRIET, J.P., DE BATIST, M., VAN VAERENBERGH, W. & VERSCHUREN, M., 1988. Seismic facies and clay tectonic features of the Ypresian clay in the southern North Sea. *Bull. Belg. Ver. Geol.*, 97-4.

HENRIET, J.P., DE BATIST, M., D'OLIER, B. & AUFFRET, J.P., 1989. A northeast trending structural deformation zone near North Hinder. In: HENRIET, J.P. & DE MOOR, G. (eds.) *The Quaternary and Tertiary Geology of the Southern Bight, North Sea*, 9-16.

HENRIET, J.P., DE BATIST, M., DE BRUYNE, H., HELDENS, P., HUYLEBROECK, J.P., MOSTAERT, F., SEVENS, E., AUFFRET, J.P. & D'OLIER, B., 1989. Preliminary seismic-stratigraphic maps and type sections of the Paleogene deposits in the Southern Bight of the North Sea. In: HENRIET, J.P. & DE MOOR, G. *The Quaternary and Tertiary Geology of the Southern Bight, North Sea*, 29-44.

HOUBOLT, J.J.H.C., 1968. Recent sediments in the Southern Bight of the North Sea. *Geol. Mijnbouw*, 47, 245-273.

HUBBARD, D.K., OERTEL, G. & NOMMENDAL, D., 1979. The role of waves and tidal currents in the development of tidal inlet sedimentary structures and sand body geometry : examples from N. Carolina, S. Carolina and Georgia. *J. Sed. Petrol.*, 49, 1073-1092.

HUS, J., PAEPE, R., GEERAERTS, R., SOMME, J. & VANHOORNE, R., 1976. Preliminary magnetostratigraphical results of Pleistocene sequences in Belgium and northwest France. *Quaternary glaciation in the northern hemisphere, I.G.C.P.*, 24, report 3, 99-128, (Bellingham, 1975), Prague.

HUYLEBROECK, J.P., 1986. Seismisch-stratigrafisch onderzoek van het Paleoceen in de Zuidelijke Baai van de Noordzee. Unpublished thesis, State University of Gent, 91 pp.

JANSEN, J.H.F., VAN WEERING, T.C.E. & EISMA, D., 1979. Late Quaternary sedimentation in the North Sea. In: OELE, E., SCHÜTTENHELM, R.T.E. & WIGGERS, A.J. (eds.) *The Quaternary history of the North Sea. Acta Univ. Ups. Symp. Univ. Ups. Annum Quingentesimum Celebrantis*, 2, 175-188.

JARDINE, W.G., 1979. The western (United Kingdom) shore of the North Sea in Late Pleistocene and Holocene times. In: OELE, E., SCHÜTTENHELM, R.T.E. & WIGGERS, A.J. (eds.) *The Quaternary history of the North Sea. Acta Univ. Ups. Symp. Univ. Ups. Annum Quingentesimum Celebrantis*, 2, 159-174.

JELGERSMA, S., 1961. Holocene sea level changes in the Netherlands. *Meded. Geol. Sticht. C*, VI, 7, 100 pp.

JELGERSMA, S., 1966. Sea level changes during the last 10000 years. In world climate from 8000 to 0 B.C. Proceedings of the International Symposium Held at Imperial College, London, 18 and 19 April 1966, 54-71, Royal Meteorological Society, London.

JELGERSMA, S., OELE, E. & WIGGERS, A.J., 1979. Depositional history and coastal development in the Netherlands and the adjacent North Sea since the Eemian. In: OELE, E., SCHÜTTENHELM, R.T.E. & WIGGERS, A.J. (eds.) *The Quaternary history of the North Sea. Acta. Univ. Ups. Symp. Univ. Ups. Annum Quingensimum Celebrantis*, 2, 115-142.

JELGERSMA, S., 1979. Sea-level changes in the North Sea basin. In: OELE, E., SCHÜTTENHELM, R.T.E. & WIGGERS, A.J. (eds.) *The Quaternary history of the North Sea. Acta Univ. Ups. Symp. Univ. Ups. Annum Quingentesimum Celebrantis*, 2, 233-248.

JORDAN, G.F., 1962. Large submarine sand waves. *Science*, 126, 839-848.

KELLAWAY, G.A., REDDING, J.H., SHEPARD-THORN, E.R. & DESTOMBES, J.-P., 1975. The Quaternary history of the English Channel. *Philos. Trans. R. Soc. Lond.*, A279, 189-218.

KENNETT, P., 1979. Well geophone survey and calibration of acoustic velocity logs. Developments in geophysical exploration. Method - 1, 93-114. Applied Science Publisher Ltd, London.

KENT, P.E., 1975. Review of the North Sea Basin development. *J. Geol. Soc.*, 131, 435-468.

KENT, P.E., 1975. The tectonic development of Great Britain and the surrounding seas. In: WOODLAND, A.W. (ed.) *Petroleum and the continental shelf of North West Europe. Volume 1 : Geology*, 3-28. Applied Science Publishers Ltd.

KENYON, N.H., BELDERSON, R.H., STRIDE, A.H. & JOHNSON, M.A., 1981. Offshore tidal sand-banks as indicators of net sand transport and as potential deposits. *Spec. Publs int. Ass. Sediment.*, 5, 257-268.

KIDSON, C. & BOWEN, D.Q., 1976. Some comments on the history of the English Channel. *Quatern. Newslett.*, 18, 8-9.

KIRBY, R. & OELE, E., 1975. The geological history of the Sandettie-Fairy Bank area, southern North Sea. *Phil. Trans. R. Soc. Lond.*, A279, 257-267.

KNOX, R.W.O'B., 1989. The Paleogene of the UK souther North Sea, 50°N-53°N : a survey of stratigraphical data. In: HENRIET, J.P. & DE MOOR, G. *The Quaternary and Tertiary Geology of the Southern Bight, North Sea*, 17-28.

KOCKEL, F., 1988. The paleogeographical maps. In: VON DANIELS, C., GRAMANN, F., KÖTHE, A., KNOX, R.W.O'B., KOCKEL, F., MEYER, K.-J., VINKEN, R. & WEISS, W. (eds.) *Geologisches Jahrbuch, Reihe A, Heft 100, The Northwest European Tertiary basin*, 410-422. Hannover, 1988.

KÖHN, W., 1988. The Holocene transgression of the North Sea as exemplified by the southern Jade Bay and the Belgian coastline. Unpublished report.

KOKESH, F.P. & BLIZARD, R.B., 1959. Geometrical factors in sonic logging. *Geophyscs*, XXIV, 1, 64-76.

KOMAR, P.D., 1971. The mechanics of sand transport on beaches. *J. Geophys. Res.*, 75, 5914-5927.

LABAN, C. & SCHÜTTENHELM, R.T.E., 1981. Some new evidence on the origin of the Zeeland ridges. *Spec. Publs int. Ass. Sediment.*, 5, 239-245.

LABAN, C., CAMERON, T.D.J. & SCHÜTTENHELM, R.T.E., 1984. Geologie van het Kwartair van de zuidelijke bocht van de Noordzee. *Meded. Werkgr. Tert. Kwart. Geol.*, 21(3), 139-154.

LAGA, P.G., 1973. The Neogene deposits of Belgium - Guide book for the field meeting of the Geologists' Association London. *Geol. Surv. Belg.*, 1-31. Brussels.

LAGA, P., 1988. The description of regional lithostratigraphy : Belgium. In: VON DANIELS, C., GRAMANN, F., KÖTHE, A., KNOX, R.W.O'B., KOCKEL, F., MEYER, K-J., VINKEN, R. & WEISS, W. (eds.) *Geologisches Jahrbuch, Reihe A, Heft 100, The Northwest European Tertiary basin*, p48. Hannover, 1988.

LAGA, P., 1988. Description of cross-section A-A': Belgium, River Maas (ESE) - Oostende (WNW). In: VON DANIELS, C., GRAMANN, F., KÖTHE, A., KNOX, R.W.O'B., KOCKEL, F., MEYER, K-J., VINKEN, R. & WEISS, W. (eds.) *Geologisches Jahrbuch, Reihe A, Heft 100, The Northwest European Tertiary basin*, p115. Hannover, 1988.

LAGA, P. & LAUWAERT, B., 1988. Description of cross-section B-B': Belgium, Mons (SW) - Mol (NE). In: VON DANIELS, C., GRAMANN, F., KÖTHE, A., KNOX, R.W.O'B., KOCKEL, F., MEYER, K-J., VINKEN, R. & WEISS, W. (eds.) *Geologisches Jahrbuch, Reihe A, Heft 100, The Northwest European Tertiary basin*, p115. Hannover, 1988.

LAGA, P., 1988. Description of cross-section C-C': Belgium, Brussels (S) - Antwerpen (N). In: VON DANIELS, C., GRAMANN, F., KÖTHE, A., KNOX, R.W.O'B., KOCKEL, F., MEYER, K-J., VINKEN, R. & WEISS, W. (eds.) *Geologisches Jahrbuch, Reihe A, Heft 100, The Northwest European Tertiary basin*, p116. Hannover, 1988.

LAGA, P. & VANDENBERHE, N., 1989. A geological profile along the Belgian coast. In: HENRIET, J.P. & DE MOOR, G. (eds.) *The Quaternary and Tertiary Geology of the Southern Bight, North Sea*, 5-8.

LUGG, R., 1979. Marine seismic sources. Developemnts in geophysical exploration. Method - 1, 143-203. Applied Science Publisher Ltd. London.

MARECHAL, R., 1972. Geology. Unpublished lecture, Intern. Training Centre for Post-graduate Soil Scientists, State University of Gent.

MARECHAL, R., HENRIET, J.P., MOSTAERT, F., DE BATIST, M., MOONS, A. & VERSCHUREN, M., 1986. Studie oppervlaktelaag van het Belgisch Continentaal Plat. Seismisch prospectie Sector B. Onuitgegeven Rapport, Ministerie voor Economische Zaken, 52 pp.

McCAYE, I.N., 1971. Sand waves in the North Sea off coast of Holland. *Mar. Geol.*, 10, 199-225.

McCAYE, I.N., 1979. Tidal currents at the North Hinder lightship, southern North Sea : Flow directions and turbulence in relation to maintenance of sand banks. *Mar. Geol.*, 31, 101-104.

McQUILLIN, R., BACON, M. & BARCLAY, W., 1984. An introduction to seismic interpretation : Reflection seismics in petroleum exploration. Graham & Trotman Limited Sterling House, London, 287 pp.

MITCHUM, R.M.JR. VAIL, P.R. & THOMPSON, S., 1977. The depositional sequence as a basic unit for stratigraphic analysis. In: PAYTON, C.E. (ed.) *Seismic stratigraphy - applications to hydrocarbon exploration*. AAPG Memoir, 26, 53-62.

MITCHUM, R.M.JR. & VAIL, P.R., 1977. Seismic stratigraphic interpretation procedure. In: PAYTON, C.E. (ed.) *Seismic stratigraphy - applications to hydrocarbon exploration*. AAPG Memoir, 26, 135-144.

MITCHUM, R.M.JR., 1977. Glossary of terms used in seismic stratigraphy. In: PAYTON, C.E. (ed.) *Seismic stratigraphy - applications to hydrocarbon exploration*. AAPG Memoir, 26, 205-212.

MOSTAERT, F. & DE MOOR, G., 1984. Eemian deposits in the neighbourhood of Brugge ; a paleogeographical and sea-level reconstruction. *Bull. Soc. Belg. Geol.*, 93, 297-287.

MOSTAERT, F., 1985. Bijdrage tot de kennis van de kwartaairgeologie van de oostlijke kustvlakte op basis van sedimentologisch en lithostratigrafisch onderzoek. Unpublished doctoral thesis, State University of Gent.

MOSTAERT, F., AUFERET, J.P., DE BATIST, M., HENRIET, J.P., MOONS, A., SEVENS, E., VAN DEN BROEKE, I. & VERSCHUREN, M., 1989. Quaternary shelf deposits and drainage patterns off the French and Belgian coasts. In: HENRIET, J.P. & DE MOOR, G. (eds.) *The Quaternary and Tertiary Geology of the Southern Bight, North Sea*, 111-118.

MOSTAERT, F. & DE MOOR, G., 1989. Eemian and Holocene sedimentary sequences on the Belgian coast and their meaning for sea level reconstruction. In: HENRIET, J.P. & DE MOOR, G. (eds.) *The Quaternary and Tertiary Geology of the Southern Bight, North Sea*, 137-148.

NIO, S.D., 1976. Marine transgressions as a factor in the formation of sandwave complex. *Geol. Mijnbouw*, 55(1-2), 18-40.

OELE, E., 1969. The Quaternary geology of the Dutch part of the North Sea, north of the Frisian isles. *Geol. Mijnbouw*, 48(5), 467-480.

OELE, E., 1971. The Quaternary geology of the southern area of the Dutch part of the North Sea. *Geol. Mijnbouw*, 50(3), 461-474.

OELE, E. & SCHÜTTENHELM, R.T.E., 1979. Development of the North Sea after the Saalian glaciation. In: OELE, E., SCHÜTTENHELM, R.T.E. & WIGGERS, A.J. (eds.) *The Quaternary history of the North Sea. Acta Univ. Ups. Symp. Univ. Ups. Annum Quingentesimum Celebrantis*, 2, 191-216.

OFF, T., 1963. Rhythmic linear sand bodies caused by tidal currents. *Bull. AAPG*, 47, 324-341.

OLSON, J.C., 1987. Tectonic evolution of the North Sea region. In: BROOKS, J. & GLENNIE, K.W. (eds.) *Petroleum geology of North West Europe*, 389-402. Graham & Trotman, London.

PAEPE, R., 1965. On the presence of 'Tapes senscens' in some borings of the coastal plain and the Flemish Valley of Belgium. *Bull. Soc. Belge. Geol.*, 74, 249-254.

PAEPE, R. & VANHOORNE, R., 1967. The stratigraphy and paleontology of the Late Pleistocene in Belgium. *Toelicht. Verh. Geol. Kaart en Mijnkaart Belgie*, 8, 96 pp.

PAEPE, R. & VANHOORNE, R., 1970. Stratigraphical position of periglacial phenomena in the Campine Clay of Belgium, based on paleobotanical analysis and paleomagnetic dating. *Bull. Soc. Belg. Geol.*, 79, 201-211.

PAEPE, R. & VANHOORNE, R., 1972. An outcrop of Eemian Wadden deposits at Meetkerke (Belgian Coast Plain). *Belgian geol. Survey Prof. Paper.*, 7, 9 pp.

PAEPE, R., VANHOORNE, R. & DERAYMAEKER, D., 1972. Eemian sediments near Brugge (Belgian Coast Plain). *Belgian Geol. Survey Prof. Paper.*, 9, 12 pp.

PAEPE, R. & SOMME, J., 1975. Marine Pleistocene transgressions along the Flemish coast (Belgian and France). *Quaternary glaciations in the northern hemisphere, I.G.C.P. project*, 2, 108-116, (Salzburg, 1974), Prague.

PAEPE, R. & BAETEMAN, C., 1979. The Belgian coastal plain during the Quaternary. In: OELE, E., SCHÜTTENHELM, R.T.E. & WIGGERS, A.J., 1979. *The Quaternary history of the North Sea. Acta Univ. Ups. Symp. Univ. Ups. Annum Quingentesimum Celebrantis*, 2, 143-146.

PAEPE, R., BAETEMAN, C., MORTIER, R., VANHOORNE, R. & CENTRE FOR QUATERNARY STRATIGRAPHY, 1981. The marine Pleistocene sediments in the Flanders area. *Geol. Mijnbouw*, 60, 321-330.

- PIKE, K. & GODWIN, H., 1953. The interglacial at Clacton-on-Sea, Essex, *Quat. J. Geol. Soc. Lond.*, 108, 261-272.
- PITMAN, W.C.III, 1978. Relationship between eustacy and stratigraphic sequences of passive margins. *Bull. Geol. Soc. Am.*, 89, 1389-1403.
- RAMSTER, JH.W., 1965. Studies with the Woodhead sea-bed drifter in the southern North Sea. *Lab. Leaflet. Fish. Lab. Lowesoft (New Ser.)*, 6, 1-4.
- RIJKS GEOLOGISCHE DIENST, 1988. Description of cross-section E-E': Belgium - The Netherlands, Mol (S) - Terschelling (N). In: VON DANIELS, C., GRAMANN, F., KÖTHE, A., KNOX, R.W.O'B., KOCKEL, F., MEYER, K-J., VINKEN, R. & WEISS, W. (eds.) *Geologisches Jahrbuch, Reihe A, Heft 100, The Northwest European Tertiary basin*, p119. Hannover, 1988.
- SHARP, F.P., 1974. Holocene sea-level changes : a discussion. *Geol. Mijnbouw*, 53, 71-73.
- SHERIFF, R.E., 1977. Limitations on resolution of seismic reflections and geologic detail derivable from them. In: PAYTON, C.E. (ed.) *Seismic stratigraphy - applications to hydrocarbon exploration. AAPG Memoir*, 26, 3-14.
- SHERIFF, R.E. & GELDART, L.P., 1982. Exploration seismology. Volume 1 : History, theory, data acquisition. Cambridge University Press, Cambridge, 253 pp.
- SHERIFF, R.E. & GELDART, L.P., 1982. Exploration seismology. Volume 2 : Data-processing and interpretation. Cambridge University Press, Cambridge, 221 pp.
- SMITH, J.D., 1969. Geomorphology of a sand bank. *J. Geol.*, 77, 39-55.
- SOMME, J., 1974. Les formations Quaternaires de la région du Nord. *Ann. Sci. Univ. Besançon, Géol.*, 3^e série, 21, 97-102.
- SOMME, J., PAEPE, R. ET AL., 1978. La Formation d'Herzeele: un nouveau stratotype du Pleistocène Moyen marin de la Mer du Nord. *Bull. Ass. Franç. Etude Quaternaire*, 1-2-3, 81-149.
- SOMME, J., 1979. Quaternary coastline in northern France. In: OELE, E., SCHÜTTENHELM, R.T.E. & WIGGERS, A.J. (eds.) *The Quaternary history of the North Sea. Acta Univ. Ups. Symp. Univ. Ups. Annum Quingentesimum Celebrantis*, 2, 147-158.
- SPAINK, G., 1973. De 'Fauna van Angulus pygmaeus' en de 'Fauna van Spisila subtruncata' in de zuidelijke noordzeekom. *Rijks Geol. Dienst Afd. Macropalaeontol., Int. Rep.* 578.
- SPAINK, G. & SLIGGERS, B.C., 1979. Boring RGD57. *Rijks Geol. Dienst Afd. Macropalaeontol., Int. Rep.* 211.
- SPAINK, G. & SLIGGERS, B.C., 1979. Boring RGD72. *Rijks Geol. Dienst Afd. Macropalaeontol., Int. Rep.* 219.

- SPAINK, G. & SLIGGERS, B.C., 1979. Boring RGD74. *Rijks Geol. Dienst Afd. Macropalaeontol., Int. Rep.* 221.
- SPAINK, G., 1981. Boring RGD 80MK127. *Rijks Geol. Dienst Afd. Macropalaeontol., Int. Rep.* 1395.
- STAMP, L.D., 1972. The Thames drainage system and the age of the Strait of Dover. *Geographical Journal*, 50, 386-390.
- STEURBAUT, E. & NOLF, D., 1986. Revision of Ypresian stratigraphy of Belgium and northwestern France. *Meded. Werkgr. Ter. Kwart. Geol.*, 23(4), 115-172.
- STEVENS, L.A., 1960. The interglacial of the Nar Valley, Norfolk. *Quat. J. Geol. Soc. Lond.*, 115, 291-315.
- STRIDE, A.H., 1970. Shape and size trends for sand waves in a depositional zone of the North sea. *Geol. Mag.*, 107, 469-477.
- TAVERNIER, R. & DEMOOR, G., 1974. L'Evolution du Bassin de l'Escaut. In: *L'Evolution Quaternaire des bassins fluviaux de la Mer du Nord méridionale. Centenaire Soc. Géol. Belg.*, 159-231.
- TRÖGER, K.A., 1978. Probleme der palaeontologie, biostratigraphie und palaeogeographie oberkretazischer fauna (Cenoman-Turon) Westeuropas und der Russischen Tafel. *Z. Geol. Wiss. Berlin*, 6, 557-570.
- VAIL, P.R., MITCHUM, R.M.JR. & THOMPSON, S., 1977. Relative changes of sea level from coastal onlap. In: PAYTON, C.E. (ed.) *Seismic stratigraphy - applications to hydrocarbon exploration. AAPG Memoir*, 26, 63-82.
- VAIL, P.R., TODD, R.G. & SANGREE, J.B., 1977. Chronostratigraphic significance of seismic reflections. In: PAYTON, C.E. (ed.) *Seismic stratigraphy - applications to hydrocarbon exploration. AAPG Memoir*, 26, 99-116.
- VAIL, P.R., 1987. Seismic stratigraphy interpretation utilizing sequence stratigraphy. Part 1 : Seismic stratigraphy interpretation procedure. In: BALLY, A.W. (ed.) *Atlas of seismic stratigraphy. AAPG, Studies in geology series*, 27.
- VANDENBERGHE, J., VANDENBERGHE, N. & GULLENTOPS, F., 1974. Late Pleistocene and Holocene in the neighbourhood of Brugge. *Med. Kon. Acad. Wet. Klasse Wet.*, 36, 77 pp.
- VAN DEN BROEKE, I., 1984. Een seismisch-stratigrafische studie van het kwartair van de zandbanken van de Hindergroep in het westelijk deel van het Belgisch continentaal plat. Unpublished thesis, State University of Gent, 43 pp.
- VANDEN DAELE, M.M., 1982. Morfologie van het post-Tertiair erosieoppervlak en omvang van het Kwartair dek in de zuidelijke Noordzee : een reflectieseismische benadering. Unpublished thesis, State University of Gent, 29 pp.

VAN MONTFRANS, H.M., 1971. Paleomagnetic dating in the North Sea Basin. Unpublished thesis, University of Amsterdam, 113 pp.

VANNESTE, L., 1987. Seismisch stratigrafische interpretatie van een Laat-Cenozoische erosiemorfologie in de zuidelijke baai van de Noordzee. Unpublished thesis, State University of Gent, 102 pp.

VANNEY, J.R., 1977. Geomorphologie des plates-formes continentales. Doin, Paris. 300 pp.

VAN STAALDUINEN, C.J., VAN ADRICHEM BOOGAERT, H.A., BLESS, M.J., DOPPERT, J.W.CHR., HARSVELDT, H.M., VAN MONTFRANS, H.M., OELE, E., WERMUTH, R.A. & ZAGWIJN, W.H., 1979. The geology of the Netherlands. *Meded. Rijks Geol. Dienst*, 31-2, 9-49.

VERCOUTERE, C., 1987. Voorbereidende studie tot het opstellen van een seismisch snelheidsmodel voor het Belgisch continentaal plat. Unpublished thesis, State University of Gent, 129 pp.

WIEDMANN, J., 1979. Prä-Driftzusammenhänge und Faunenprovinzen in der Kreide. *Neues Jb. Geol. Paläont. Abh.*, 157, 213-218.

WINGFIELD, R.T.R., 1989. Glacial incisions indicating Middle and Upper Pleistocene ice limits off Britain. *Terra Nova*, 6, 538-548.

YATES, J., 1977. Geophysical survey : Zeebrugge harbour investigation. Report, Volume 1.

ZAGWIJN, W.H., VAN MONTFRANS, H.M. & ZANDSTRA, J.G., 1971. Subdivision of the "Cromerian" in the Netherlands : pollen analysis, paleomagnetism and sedimentary petrology. *Geol. Mijnbouw*, 50, 41-58.

ZAGWIJN, W.H., 1971. Stratigrafische interpretatie van boringen tot circa 90 m onder zeeniveau in het Noordzeegebied (blokken L2, F17, F18, F14, F11, F3.) *Rijks Geol. Dienst, Afd. Palaeobot., Intern. Rep.* 615.

ZAGWIJN, W.H., 1974. The paleogeographic evolution of the Netherlands during the Quaternary. *Geol. Mijnbouw*, 53(6), 369-385.

ZAGWIJN, W.H. & DOPPERT, J.W.CHR., 1978. Upper Cenozoic of the southern North Sea Basin : Paleoclimatic and paleogeographical evolution. *Geol. Mijnbouw*, 57, 577-588.

ZAGWIJN, W.H., 1979. Early and Middle Pleistocene coastlines in the southern North Sea basin. In: OELE, E., SCHÜTTENHELM, R.T.E. & WIGGERS, A.J. (eds.) *The Quaternary history of the North Sea. Acta Univ. Ups. Symp. Univ. Ups. Annum Quingentesimum Celebrantis*, 2, 31-42.

ZAGWIJN, W.H., 1985. An outline of the Quaternary stratigraphy of the Netherlands. *Geol. Mijnbouw*, 64, 17-24.

ZAGWIJN, W.H., 1989. The Netherlands during the Tertiary and the Quaternary : a case history of Coastal Lowland evolution. *Geol. Mijnbouw*, 68, 107-120.

ZIEGLER, P.A., 1975. North Sea Basin history in the tectonic framework of North-Western Europe. In: WOODLAND, A.W. (ed.) *Petroleum and the continental shelf of North West Europe*. Applied Science Publisher Ltd.

ZIEGLER, P.A., 1978. North-Western Europe: Tectonics and basin development. *Geol. Mijnbouw*, 57, 589-626.

ZIEGLER, P.A. & LOUWERENS, C.J., 1979. Tectonics of the North Sea. In: OELE, E., SCHÜTTENHELM, R.T.E. & WIGGERS, A.J. (eds.) *The Quaternary history of the North Sea*. Acta. Univ. Ups. Symp. Univ. Ups. Annum Quingentesimum Celebrantis, 2, 7-22.

ZIEGLER, P.A., 1981. Evolution of sedimentary basin in North-West Europe. In: ILLING, L.V. & HOBSON, G.D. (eds.) *Petroleum geology of the continental shelf of North-west Europe*, 3-43. Institute of Petroleum, London.

ZIEGLER, P.A., 1982. Geological atlas of western and central Europe. Shell International Petroleum Maatschappij B.V., Den Haag, 130 pp.

ZIEGLER, P.A., 1983. Tectonics of the North Sea Basin and their possible relation to historical earthquakes. In: RITSEMA, A.R. & GÜRPINAR, A. (eds) *Seismicity and Seismic Risk in the Offshore North Sea Area*, 3-13. D. Reidel Publishing Company.

ZIEGLER, W.H., 1975. Outline of the geological history of the North Sea. In: WOODLAND, A.W. (ed.) *Petroleum and the continental shelf of North West Europe. Volume 1 : Geology*. Applied Science Publisher Ltd.

LIST OF ERRATA

1. p.57, section 65.1, § 1, line 2-3.
... fig. 6.13a ... should be ... fig. 6.13b ..., and vice versa.
2. p.65, section 663.3, § 1, line 1.
... north of he ... should be ... north of the ...
3. p.65, section 663.3, § 2, last line.
... N1 sequence ... should be ... N0 sequence ...
4. p.69, section 67.4, § 1, last line.
... fig. 6.17b ... should be ... fig. 6.17c ...
5. p.73, section 722.1, § 4, last line.
... fig. 6.17b ... should be ... fig. 6.17c ...

LIU A'CHENG

**A SEISMIC AND GEOMORPHOLOGICAL STUDY
OF THE EROSION SURFACE AT THE TOP OF
THE TERTIARY IN THE SOUTHERN NORTH SEA
(BELGIAN AND NORTHERN FRENCH SECTORS)**

VOLUME 2: ILLUSTRATIONS

Proefschrift ingediend by de Faculteit van de Wetenschappen
van de Rijksuniversiteit te Gent voor het verkrijgen van
de graad van Doctor in de Wetenschappen
(Groep Aard- en Delfstofkunde)

**Promotor: Prof. Dr. R. Marechal
Co-Promotor: Dr. J. P. Henriët**

- 1990 -

LIST OF ILLUSTRATIONS

Chapter 1

Figure 1.1 Location of the study area.

Chapter 2

- Figure 2.1 Geometry of the reflection path
a. For constant velocity
b. For average velocity model
c. For interval velocity model
(after Sheriff & Geldart, 1982).
- Figure 2.2 Characteristics of seismic events (after Sheriff & Geldart, 1982).
- Figure 2.3 Types of multiples (after Sheriff & Geldart, 1982).
- Figure 2.4 Schematic of the RCMG seismic system.
- Figure 2.5 Definition of a depositional sequence and its boundaries (after Mitchum et al., 1977).
- Figure 2.6 Relations of strata to boundaries of depositional sequences (after Mitchum et al., 1977).
- Figure 2.7 Different types of reflection configurations (after Mitchum et al., 1977).
- Figure 2.8 External forms of some seismic facies units (after Mitchum et al., 1977).
- Figure 2.9 Relative changes of sea-level
a. Coastal onlap indicates a relative rise of sea-level
b. Downward shift in coastal onlap indicates a relative drop of sea-level
c. Coastal toplap indicates a relative stillstand of sea-level
(after Vail et al., 1977).

- Figure 2.10 a. Downhole shooting in offshore conditions
 b. Uphole shooting in offshore conditions
 (after Vercoutere, 1987).

Chapter 3

- Figure 3.1 The seismic grid covering the Belgian, Dutch, French and UK sectors of the continental shelf (after Henriët et al., 1988).
- Figure 3.2 Velocity effect on a flat surface covered by sand banks.
- Figure 3.3 Velocity effect on a gently dipping surface covered by sand banks.

Chapter 4

- Figure 4.1 Spatial relationship of the Paleozoic orogenic belt during the Late Paleozoic. L.B.M. = London-Brabant Massif (after P. Ziegler, 1981).
- Figure 4.2 Schematic graben pattern of the Mesozoic North Atlantic - Arctic rift system. NS = North Sea rift (after P. Ziegler & Louwerens, 1979).
- Figure 4.3 Paleogeography of the southern North Sea area during the Late Cretaceous (after Kockel, 1988).
- Figure 4.4 Thickness of the Late Cretaceous chalk (after Roorda Van Eysinga, 1982 and Legrand, 1968).
- Figure 4.5 Assumed basin-wide sea-level changes in the NW European basin (after Kockel, 1988).
- Figure 4.6 Paleogeography of the southern North Sea area during the Early Paleocene (after P. Ziegler, 1982 and Kockel, 1988).
- Figure 4.7 Paleogeography of the southern North Sea area during the Middle Eocene (after P. Ziegler, 1982 and Kockel, 1988).
- Figure 4.8 Paleogeography of the southern North Sea area during the Late Eocene (after P. Ziegler, 1982 and Kockel, 1988).
- Figure 4.9 Paleogeography of the southern North Sea area during the Middle Oligocene (after P. Ziegler, 1982 and Kockel, 1988).

- Figure 4.10 Paleography of the southern North Sea area during the Middle Miocene (after P.Ziegler, 1982 and Kockel, 1988).
- Figure 4.11 Paleography of the southern North Sea area during the Early Pliocene (after Zagwijn & Doppert, 1978 and P.Ziegler, 1982).
- Figure 4.12 Paleomagnetic measurements, climatic curve and stratigraphic subdivision of the Quaternary in The Netherlands and East Anglia (after Zagwijn, 1979).
- Figure 4.13 Paleography of the southern North Sea area during the Middle Tiglian (after Zagwijn, 1979).
- Figure 4.14 Paleography of the southern North Sea area during the Late Tiglian (after Zagwijn, 1979).
- Figure 4.15 Development of the Thames-Lobourg river system during the Quaternary (after Balson & D'Olier, 1988).
- Figure 4.16 Paleography of the southern North Sea area during the Waalian (after Zagwijn, 1979).
- Figure 4.17 Paleography of the southern North Sea area during the later part of the Cromerian Complex (after Zagwijn, 1979).
- Figure 4.18 Paleography of the southern North Sea area during the Elsterian (after Zagwijn, 1979).
- Figure 4.19 Paleography of the southern North Sea area during the Holsteinian (after Zagwijn, 1979).
- Figure 4.20 Paleography of the southern North Sea area during the Saalian (after Zagwijn, 1979). The extension of British land ice is after West (1977).
- Figure 4.21 Paleography of the southern North Sea area during the Middle to Late Weichselian (after Jelgersma, 1979).
- Figure 4.22 Curve for the relative sea-level rise during the Holocene, based on data from the Belgian coastal plain. MSL = mean lowest low water-level at spring-tide (after Köhn, 1988).

Chapter 5

- Figure 5.1 Schematic seismic-stratigraphic sequence chart and correlation table of the Paleogene deposits in the Southern Bight (after De Batist, 1989).
- Figure 5.2 Seismic-stratigraphic solid map of the Paleogene deposits in the Southern Bight (after De Batist, 1989).
- Figure 5.3 Analog record of a sparker section and interpreted line-drawing showing Thanetian gully erosion features (after Henriët et al., 1989).
- Figure 5.4 Analog record of a sparker section and interpreted line-drawing showing the lower interval of Ypresian clay-tectonic deformations (after De Batist et al., 1989)*.
- Figure 5.5 Analog record of a sparker section and interpreted line-drawing showing the middle interval of Ypresian clay-tectonic deformations (after De Batist et al., 1989)*.
- Figure 5.6 Analog record of a sparker section and interpreted line-drawing showing the upper interval of Ypresian clay-tectonic deformations (after De Batist et al., 1989)*.
- Figure 5.7 Genetic model of the clay-tectonic deformations in the Ypresian Clay (after Henriët et al., 1988).
- Figure 5.8 Schematic representation of the Ypresian basin-fill sequences offshore Ostend (after De Batist, 1989).
- Figure 5.9 Analog record of a sparker section and interpreted line-drawing showing the L1 sequence (after De Batist, 1989).
- Figure 5.10 Analog record of a boomer section and interpreted line-drawing showing the different seismic facies units in the B1 sequence (after Henriët et al., 1989).

- Figure 5.11 Location of tidal sand banks in the study area
1. The Coastal Banks and mouth of the river Scheldt
2. The Flemish Banks
3. The Hinder group
4. The Zeeland ridges
(after Bastin, 1974).
- Figure 5.12 Analog record of a sparker section and interpreted line-drawing showing the seismic facies of a tidal sand bank.
- Figure 5.13 Analog record of a sparker section and interpreted line-drawing showing sand banks of the Hinder group, containing sedimentary nuclei.
- Figure 5.14 Analog record of a sparker section and interpreted line-drawing showing the Flemish Banks.
- Figure 5.15 Analog record of a sparker section and interpreted line-drawing showing a valley bounding the Thornton Bank.
- Figure 5.16 Analog record of a sparker section and interpreted line-drawing showing the Coastal Banks.

(*) Depth calculated with an interval velocity of 1620 m/s.

Chapter 6

- Figure 6.1 Isobath map of the top-Tertiary erosion surface. Mercator projection at 51°20'N. Scale 1/100000. Reference level is the mean lowest low water -level at spring-tide. Landward part after De Moor & De Breuck (1973), Sommé (1979), Baeteman (1981), Depret (1983), Devos (1984), Mostaert (1985) and De Batist (1989).
- Figure 6.2 Schematic 3D representation of different types of planation surface boundaries.
a. slope break
b. scarp
c. ridge
d. cuesta
- Figure 6.3 Distribution of ridges in the study area.

- Figure 6.4 Distribution of cuestras in the study area.
- Figure 6.5 Distribution of slope breaks in the study area.
- Figure 6.6 Distribution of scarps in the study area.
- Figure 6.7 Distribution of paleovalleys in the study area.
- Figure 6.8 Distribution of pits in the study area.
- Figure 6.9 Distribution of different morphological features
in the study area.
- Figure 6.10 Distribution of morphological units in the study
area. The dashed lines indicate scour hollows.
- Figure 6.11a Interpreted line-drawing of cross-section A-A'.
- Figure 6.11b Interpreted line-drawing of cross-section B-B'.
- Figure 6.11c Interpreted line-drawing of cross-section C-C'.
- Figure 6.11d Interpreted line-drawing of cross-section D-D'.
- Figure 6.11e Interpreted line-drawing of cross-section E-E'.
- Figure 6.11f Interpreted line-drawing of cross-section F-F'.
- Figure 6.11g Interpreted line-drawing of cross-section G-G'.
- Figure 6.11h Interpreted line-drawing of cross-section H-H'.
- Figure 6.11i Interpreted line-drawing of cross-section I-I'.
- Figure 6.12 Location of profiles across the Offshore
Platform and the Offshore Scarp.
- Figure 6.13a Analog record of a sparker section and
interpreted line-drawing showing the seaward
part of the Offshore Platform. For location of
the profile see fig. 6.12.
- Figure 6.13b Analog record of a sparker section and
interpreted line-drawing showing the seaward
part of the Offshore Platform. For location of
the profile see fig. 6.12.
- Figure 6.13c Analog record of a sparker section and
interpreted line-drawing showing the landward
part of the Offshore Platform and the Offshore
Scarp. For location of the profile see fig.
6.12.
- Figure 6.13d Analog record of a sparker section and
interpreted line-drawing showing the landward
part of the Offshore Platform. For location of
the profile see fig. 6.12.
- Figure 6.14 Location of profiles across the Middle Platform
and the Middle Scarp.

- Figure 6.15a Analog record of a sparker section and interpreted line-drawing showing the southwestern part of the Middle Platform. For location of the profile see fig. 6.14.
- Figure 6.15b Analog record of a sparker section and interpreted line-drawing showing the southwestern part of the Middle Platform. For location of the profile see fig. 6.14.
- Figure 6.15c Analog record of a sparker section and interpreted line-drawing showing the northwestern part of the Middle Platform. For location of the profile see fig. 6.14.
- Figure 6.15d Analog record of a sparker section and interpreted line-drawing showing the northwestern part of the Middle Platform. For location of the profile see fig. 6.14.
- Figure 6.15e Analog record of a sparker section and interpreted line-drawing showing the western part of the Middle Scarp. For location of the profile see fig. 6.14.
- Figure 6.16 Location of profiles across the Nearshore Slope, the Nearshore Slope Break and the Marginal Platform.
- Figure 6.17a Analog record of a sparker section and interpreted line-drawing showing the Western Nearshore Slope Break. For location of the profile see fig. 6.16.
- Figure 6.17b Analog record of a sparker section and interpreted line-drawing showing the Western Nearshore Slope Break. For location of the profile see fig. 6.16.
- Figure 6.17c Analog record of a sparker section and interpreted line-drawing showing the western depression in the Eastern Nearshore Slope. For location of the profile see fig. 6.16.
- Figure 6.17d Analog record of a sparker section and interpreted line-drawing showing the western part of the valley in the Nearshore Slope. For location of the profile see fig. 6.16.

Figure 6.17e Analog record of a sparker section and interpreted line-drawing showing the eastern part of the valley in the Nearshore Slope. For location of the profile see fig. 6.16.

Figure 6.18 Location of profiles across the Ostend Valley.

Figure 6.19b Analog record of a sparker section and interpreted line-drawing showing the seaward part of the Ostend Valley. For location of the profile see fig. 6.18.

Figure 6.19d Analog record of a sparker section and interpreted line-drawing showing the landward part of the Ostend Valley. For location of the profile see fig. 6.18.

Figure 6.20 Location of profiles across the Northern Valley and the Northern Low Surface.

Figure 6.21b Analog record of a sparker section and interpreted line-drawing showing the NE trending Northern Valley. For location of the profile see fig. 6.20.

- Figure 6.21c Analog record of a sparker section and interpreted line-drawing showing the NW trending Northern Valley. For location of the profile see fig. 6.20.
- Figure 6.21d Analog record of a sparker section and interpreted line-drawing showing the NW trending Northern Valley. For location of the profile see fig. 6.20.
- Figure 6.21e Analog record of a sparker section and interpreted line-drawing showing the NW trending Northern Valley. For location of the profile see fig. 6.20.
- Figure 6.21f Analog record of a sparker section and interpreted line-drawing showing the Northern Low Surface. For location of the profile see fig. 6.20.
- Figure 6.22 Location of profiles across the Axial Channel.
- Figure 6.23a Analog record of a sparker section and interpreted line-drawing showing the southeastern part of the Axial Channel. For location of the profile see fig. 6.22.
- Figure 6.23b Analog record of a sparker section and interpreted line-drawing showing the northern lobe in the Axial Channel. For location of the profile see fig. 6.22.
- Figure 6.23c Analog record of a sparker section and interpreted line-drawing showing the part of the Axial Channel between the northern and southern lobes. For location of the profile see fig. 6.22.
- Figure 6.23d Analog record of a sparker section and interpreted line-drawing showing the southern lobe in the Axial Channel. For location of the profile see fig. 6.22.
- Figure 6.23e Analog record of a sparker section and interpreted line-drawing showing the southern lobe in the Axial Channel. For location of the profile see fig. 6.22.
- Figure 6.24 Location of profiles across the Dunkerque Pit.

Figure 6.25a Analog record of a sparker section and interpreted line-drawing showing the Dunkerque Pit in the Western Valley. For location of the profile see fig. 6.24.

Figure 6.25b Analog record of a sparker section and interpreted line-drawing showing the Dunkerque Pit in the Western Valley. For location of the profile see fig. 6.24.

Chapter 7

Figure 7.1 Paleogene sequences subcropping against the top-Tertiary erosion surface of the different morphological units (partly after De Batist, 1989).

Figure 7.2 Analog record of a sparker section and interpreted line-drawing showing cuervas in the L1 sequence.

Figure 7.3 Analog record of a sparker section and interpreted line-drawing showing cuervas in the L1 sequence.

Figure 7.4 Analog record of a sparker section and interpreted line-drawing showing cuervas at different levels in the B1 sequence.

Figure 7.5 Analog record of a sparker section and interpreted line-drawing showing a cuesta and a slope break in the upper part of the B1 sequence.

Figure 7.6 Analog record of a sparker section and interpreted line-drawing showing a cuesta and a scarp in the lower part of the B1 sequence.

Figure 7.7 Analog record of a sparker section and interpreted line-drawing showing the high overlying the basin fill offshore Ostend.

Figure 7.8 Analog record of a sparker section and interpreted line-drawing showing a scarp in the NW trending Northern Valley.

Figure 7.9 Analog record of a sparker section and interpreted line-drawing showing a syncline overlain by a depression.

- Figure 7.10 Analog record of a sparker section and interpreted line-drawing showing two weak synclines overlain by highs.
- Figure 7.11 Analog record of a sparker section and interpreted line-drawing showing an anticline overlain by a depression.
- Figure 7.12 Analog record of a sparker section and interpreted line-drawing showing the most southern synclinal depression of the Noordhinder deformation zone.
- Figure 7.13 Analog record of a sparker section and interpreted line-drawing showing the northernmost central synclinal depression of the Noordhinder deformation zone.

Chapter 8

- Figure 8.1 The recent Lobourg paleochannel system (after Bridgland & D'Olier, 1989).
- Figure 8.2 Tentative reconstruction of the study area during the Saalian.
- Figure 8.3 Tentative reconstruction of the study area during the Holocene.

Chapter 9

- Figure 9.1 Isopach map of the thickness of the Quaternary sediments. Mercator projection at 51°20'N. Scale 1/100000. Reference level is the mean lowest low water-level at spring-tide. Landward part after De Moor & De Breuck (1973), Sommé (1979), Baeteman (1981), Depret (1983), Devos (1984), Mostaert (1985) and De Batist (1989).
- Figure 9.2 Analog record of a sparker section and interpreted line-drawing showing the Oosthinder overlying the Offshore Scarp .
- Figure 9.3 Analog record of a sparker section and interpreted line-drawing showing a ridge underlying the northern part of the Akkaert Bank.

Figure 9.4 Analog record of a sparker section and
interpreted line-drawing showing a broad ridge
underlying the Thornton Bank.

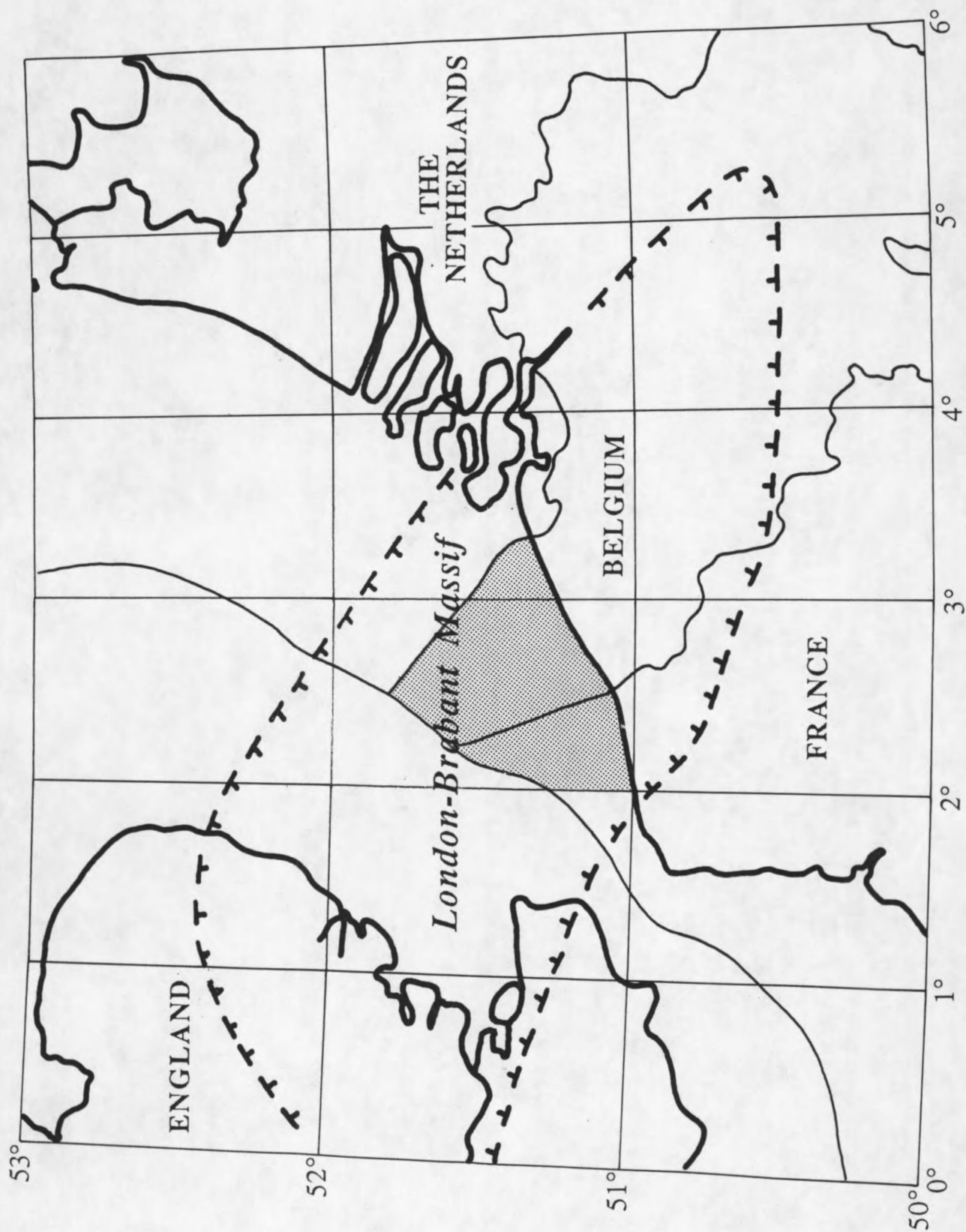


Figure 1.1 Location of the study area.

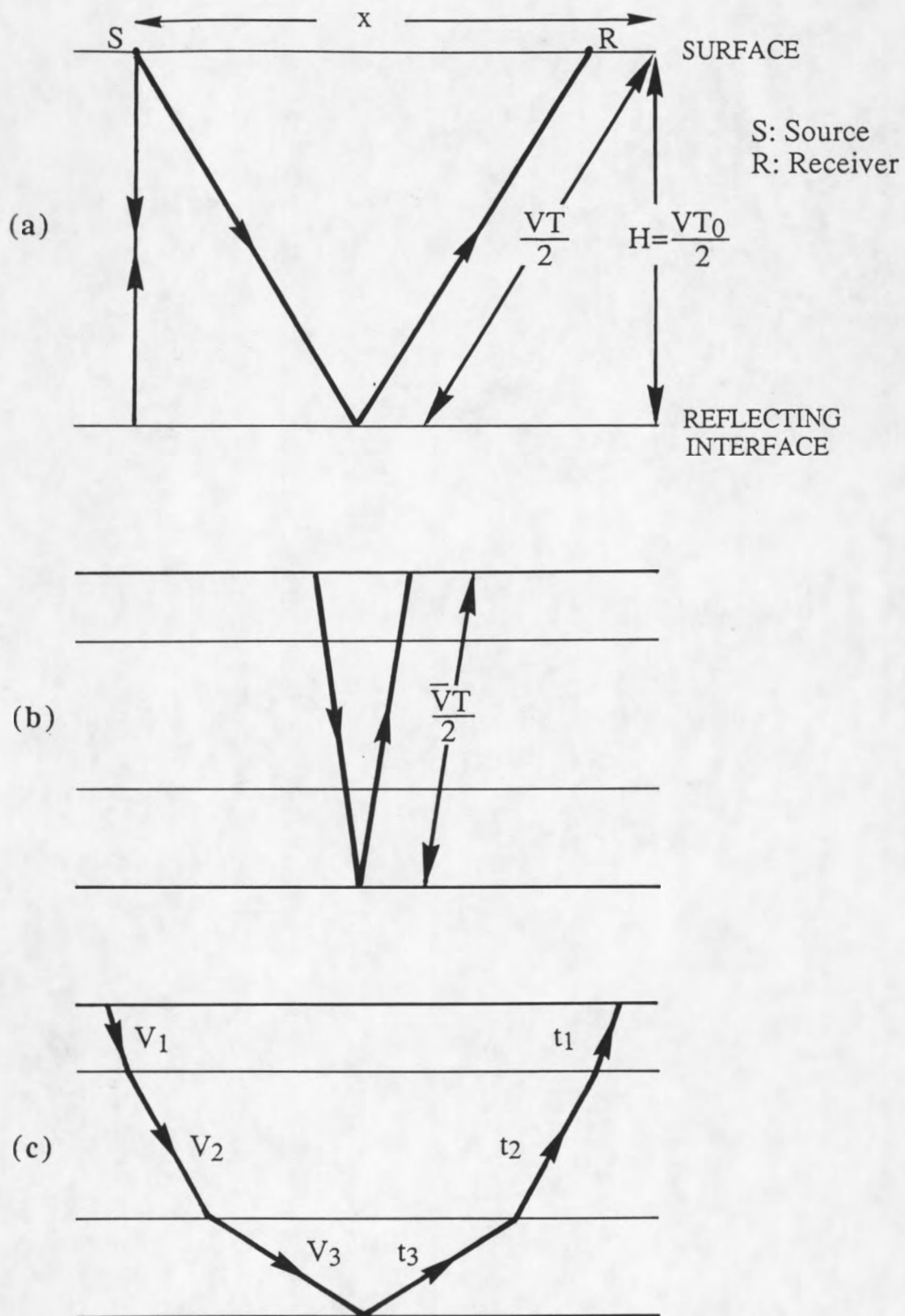


Figure 2.1 Geometry of the reflection path
a. For constant velocity
b. For average velocity model
c. For interval velocity model (after Sheriff & Geldart, 1982).

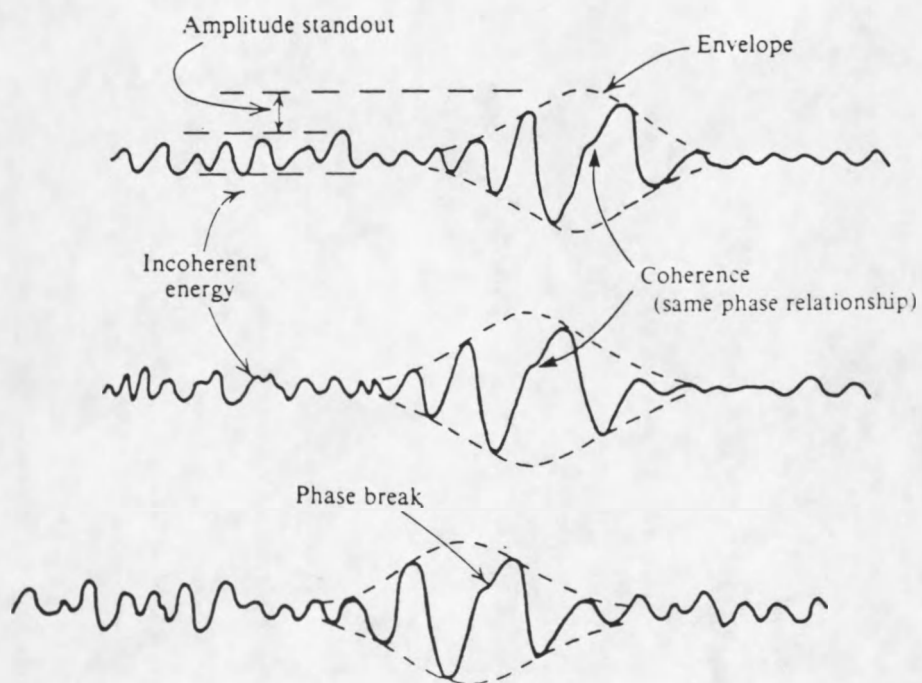


Figure 2.2 Characteristics of seismic events (after Sheriff & Geldart, 1982).

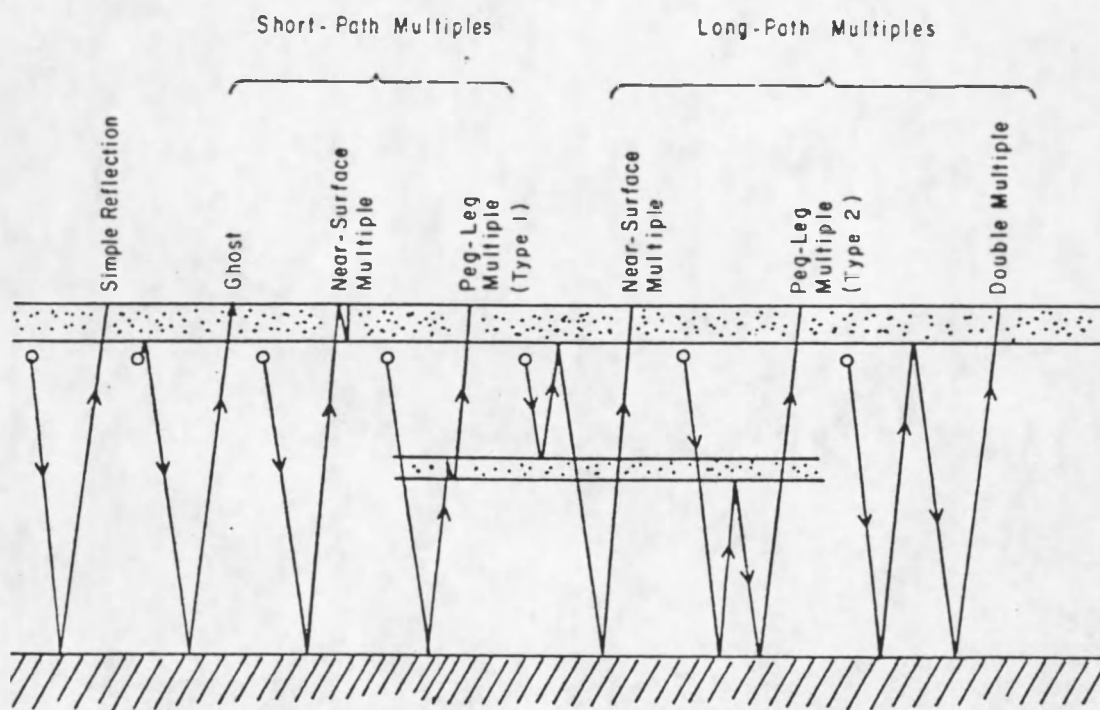


Figure 2.3 Types of multiples (after Sheriff & Geldart, 1982).

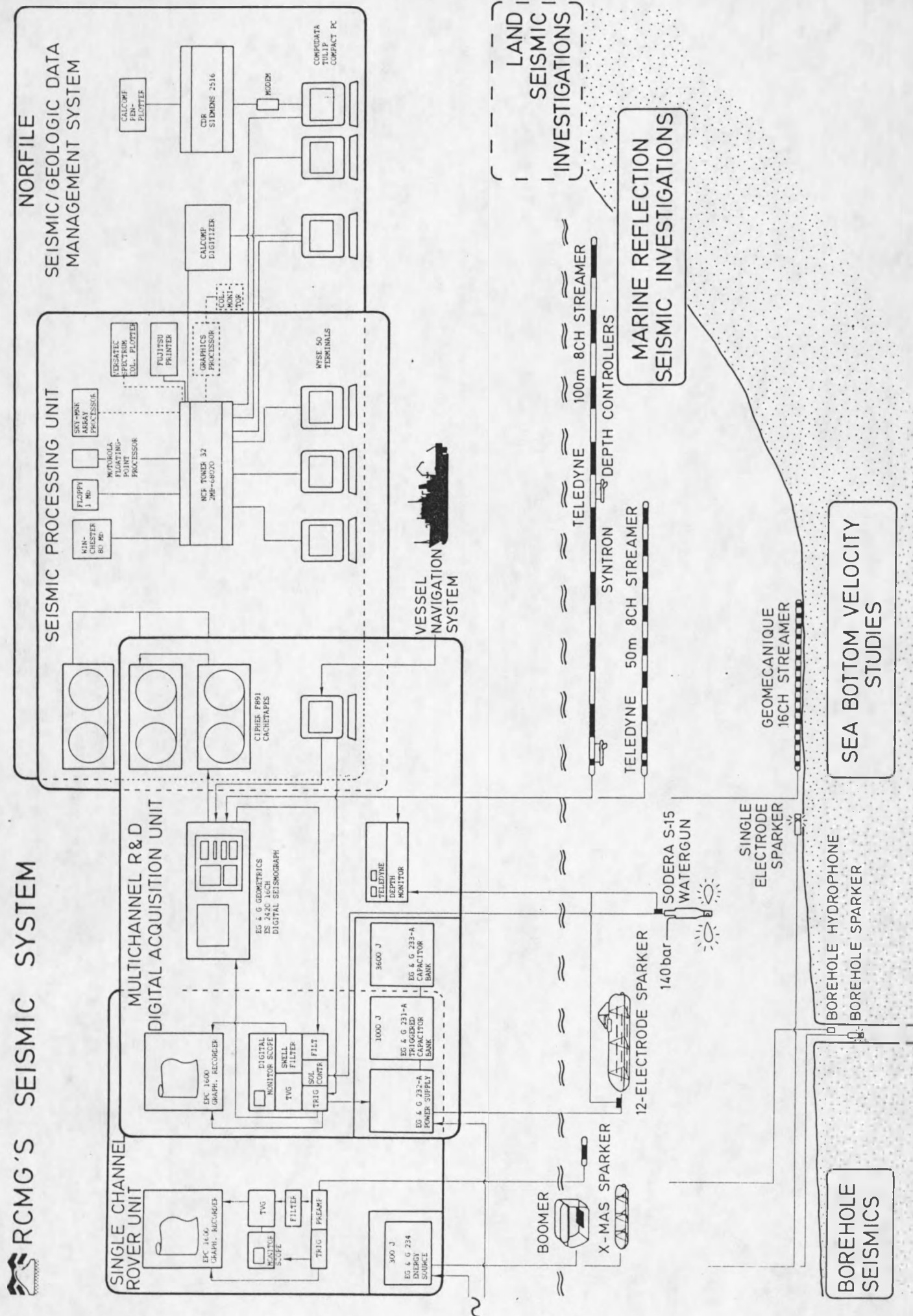
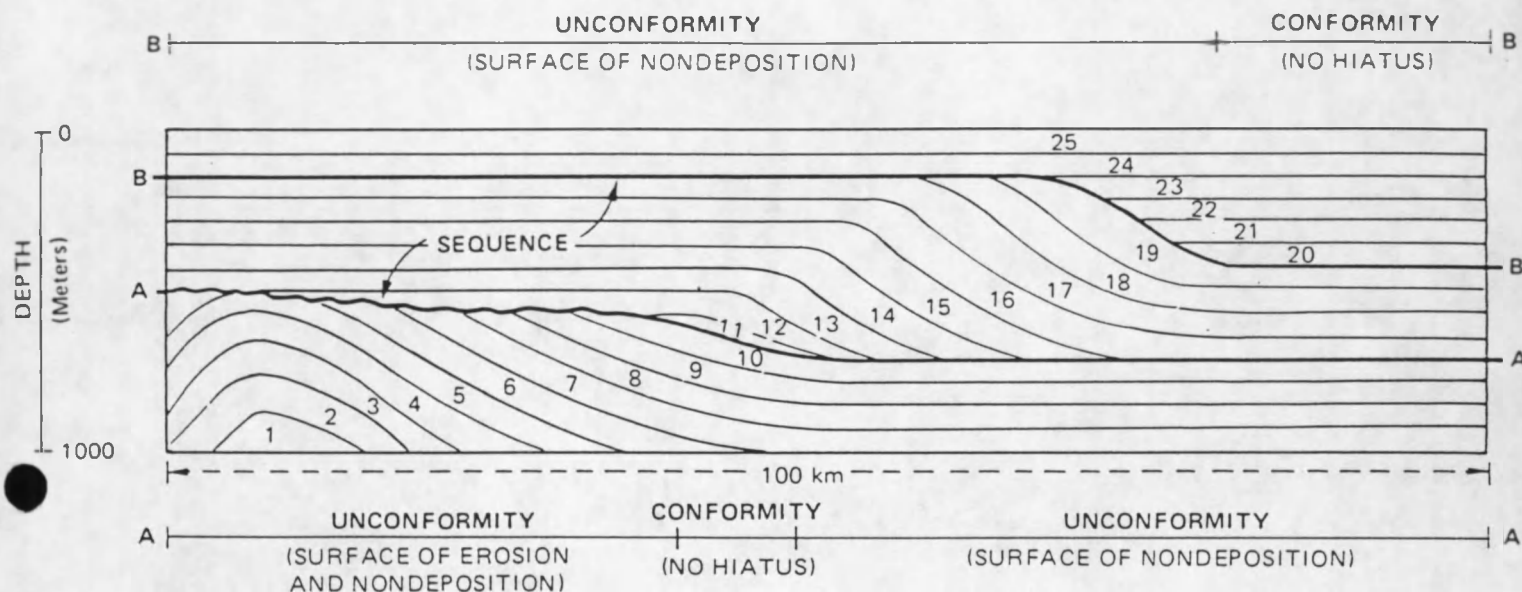
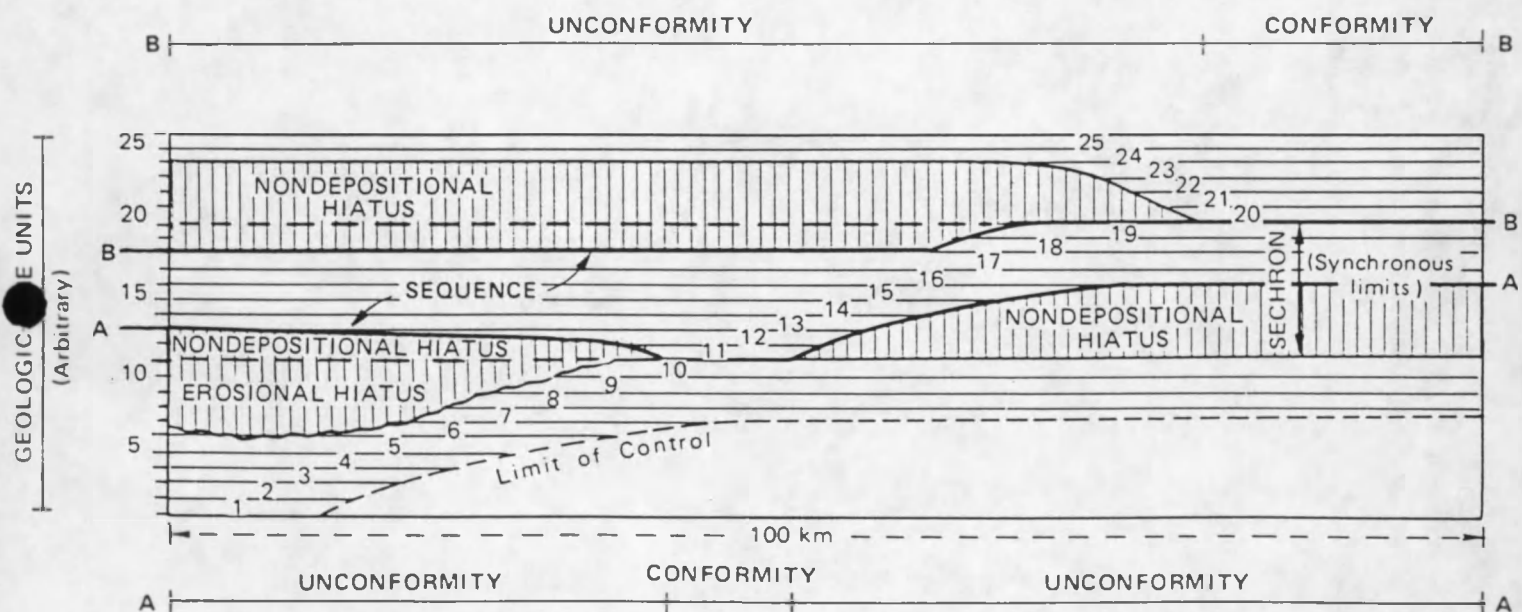


Figure 2.4 Schematic of the RCMG seismic system.



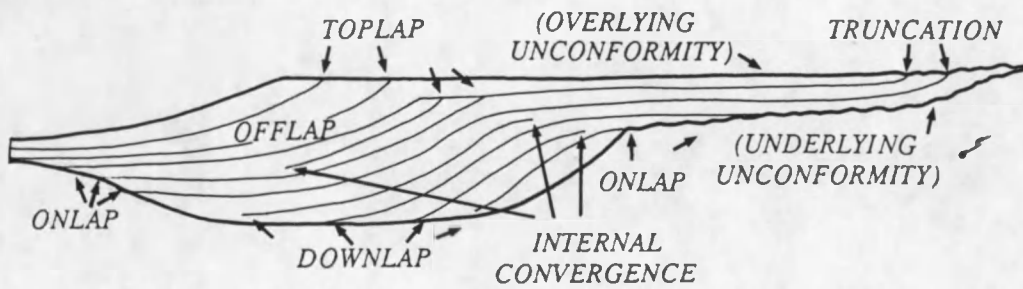
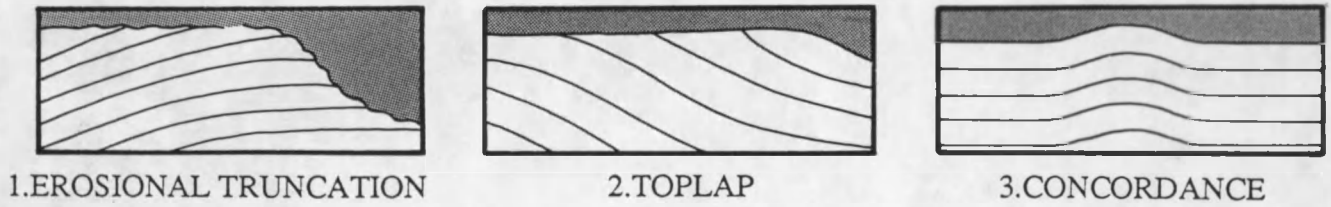
1a



1b

Figure 2.5 Definition of a depositional sequence and its boundaries (after Mitchum et al., 1977).

UPPER BOUNDARY



LOWER BOUNDARY

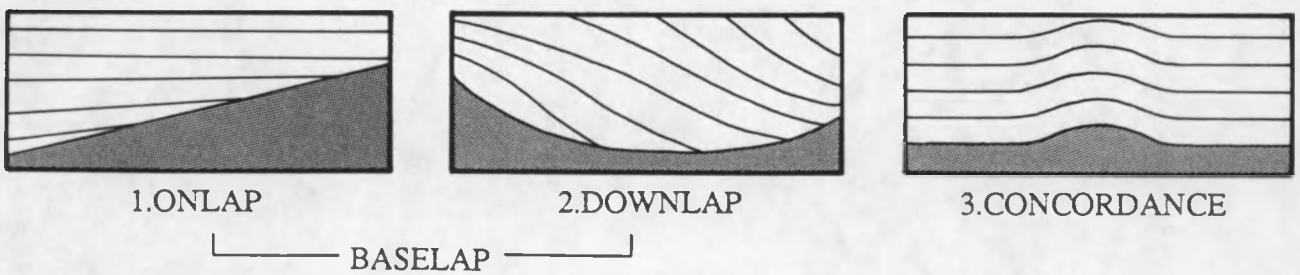


Figure 2.6 Relations of strata to boundaries of depositional sequences (after Mitchum et al., 1977).

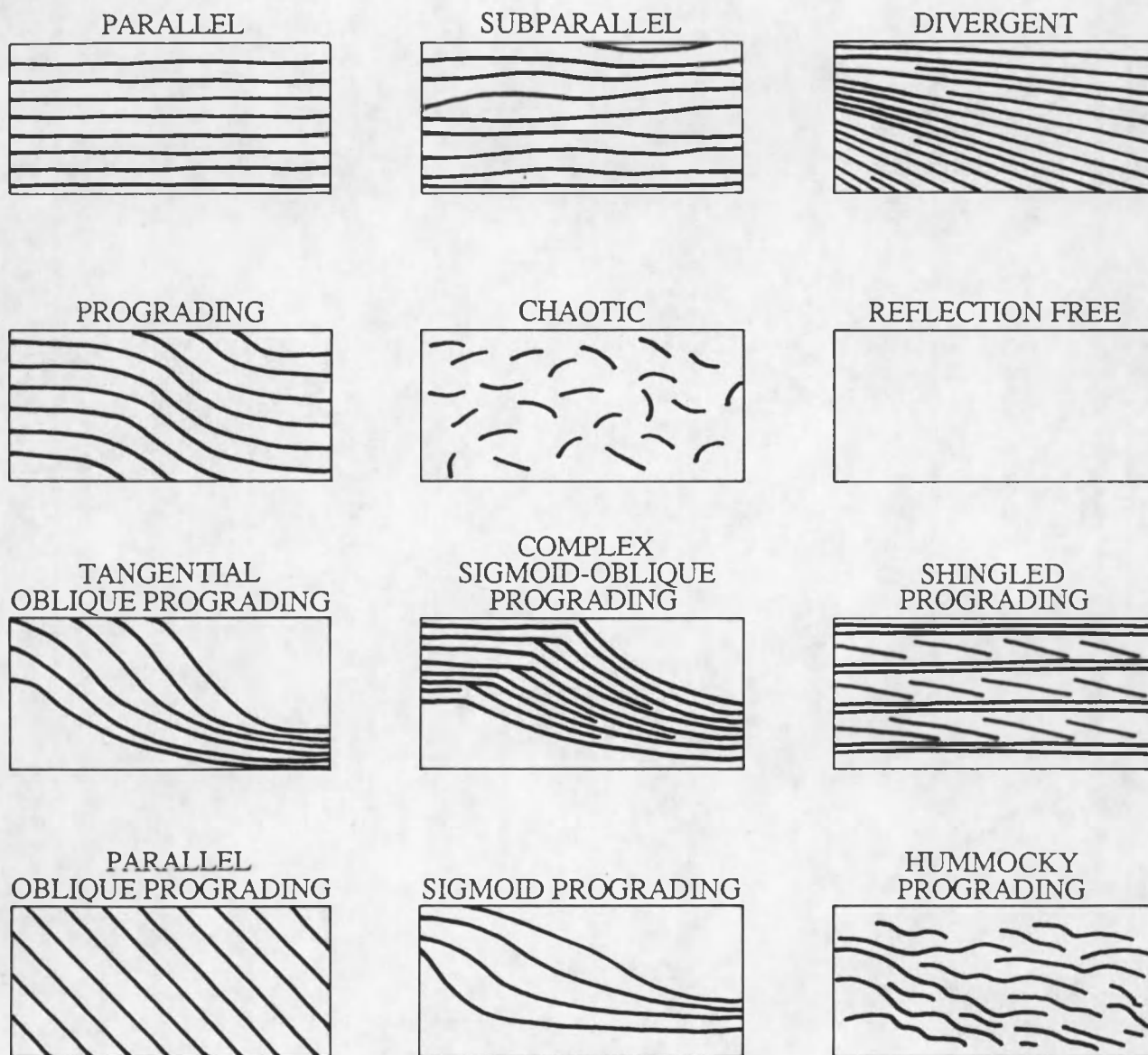


Figure 2.7 Different types of reflection configurations (after Mitchum et al., 1977).

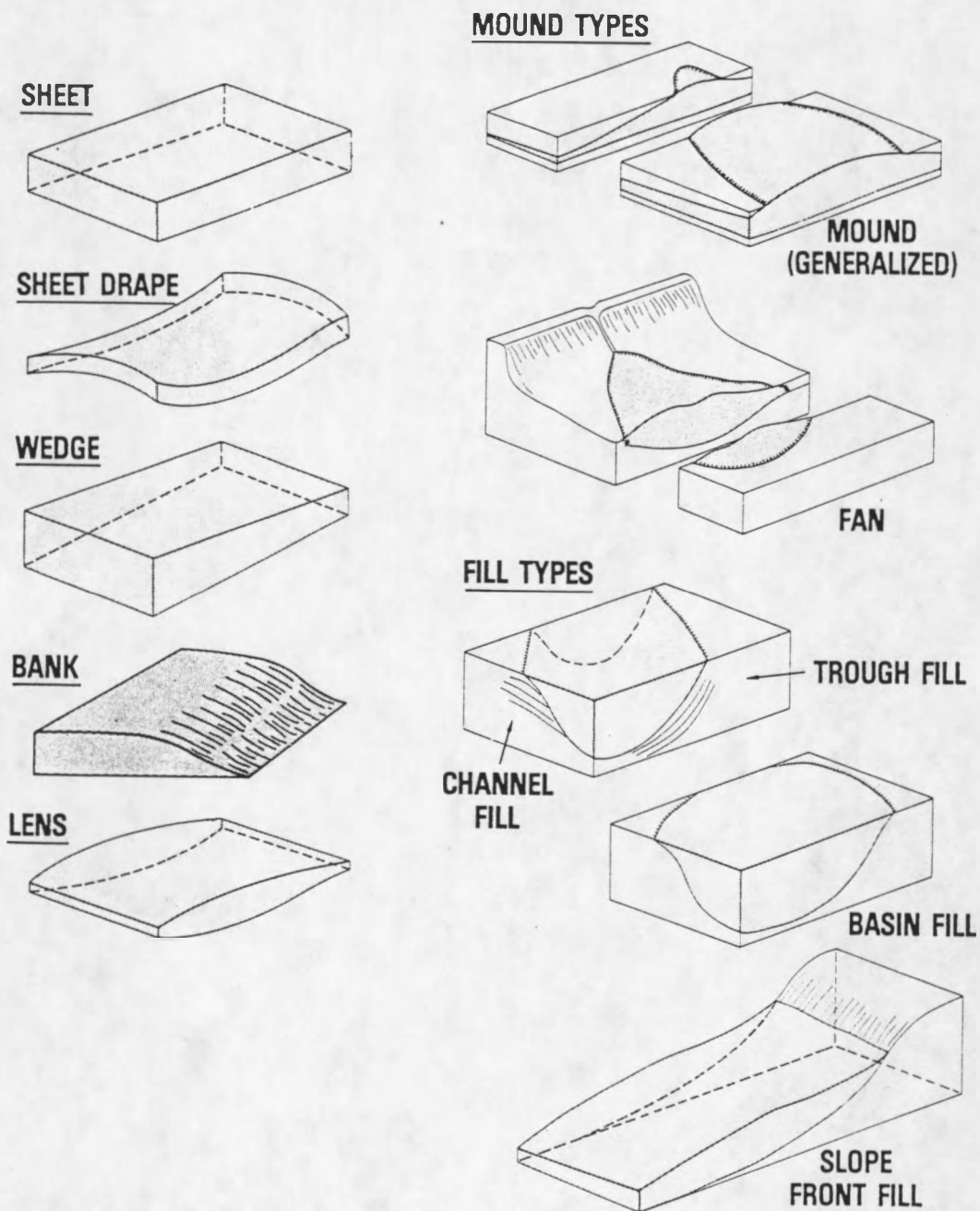


Figure 2.8 External forms of some seismic facies units (after Mitchum et al., 1977).

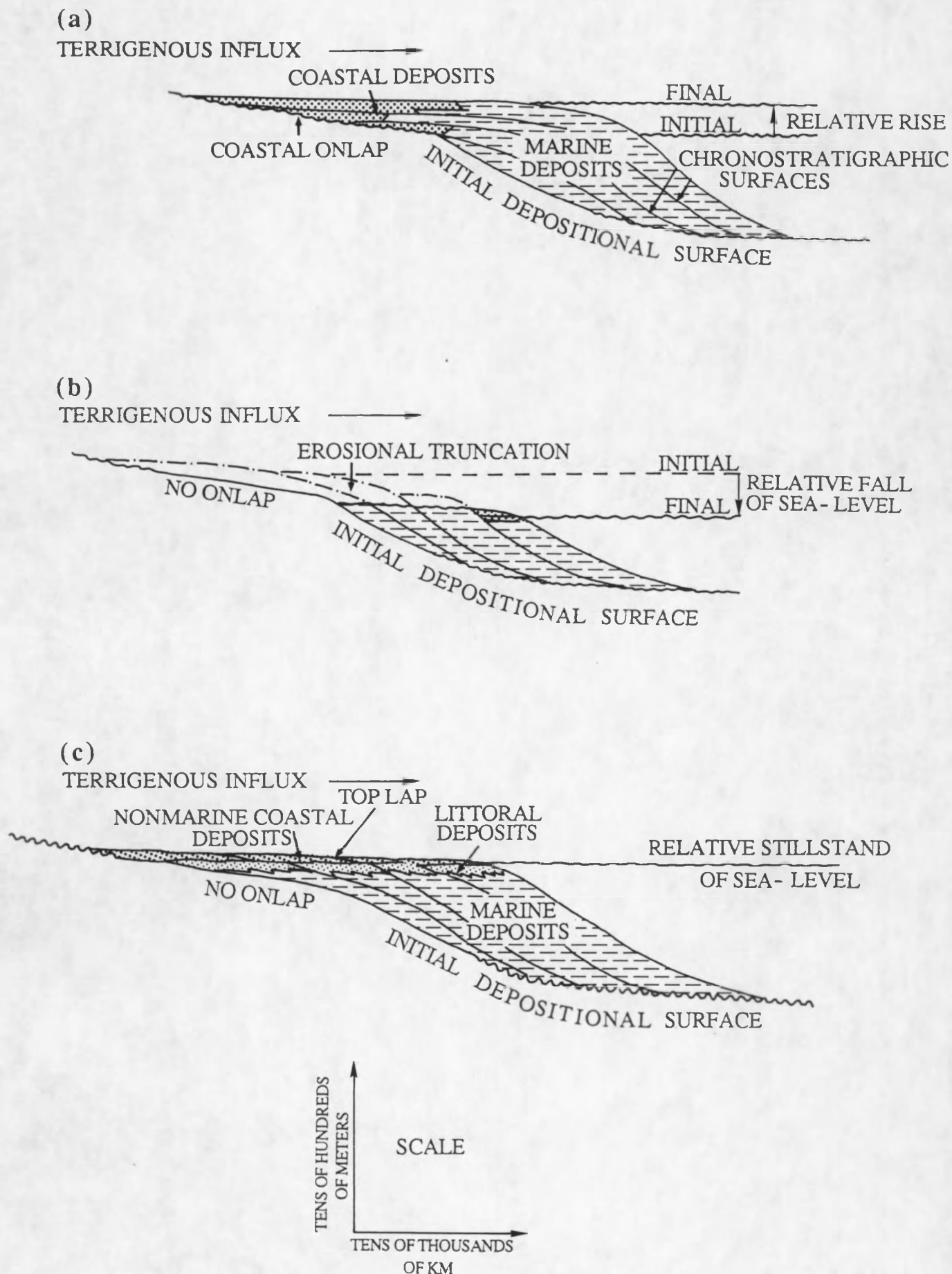


Figure 2.9 Relative changes of sea-level

- a. Coastal onlap indicates a relative rise of sea-level
- b. Downward shift in coastal onlap indicates a relative drop of sea-level
- c. Coastal toplap indicates a relative stillstand of sea-level (after Vail et al., 1977).

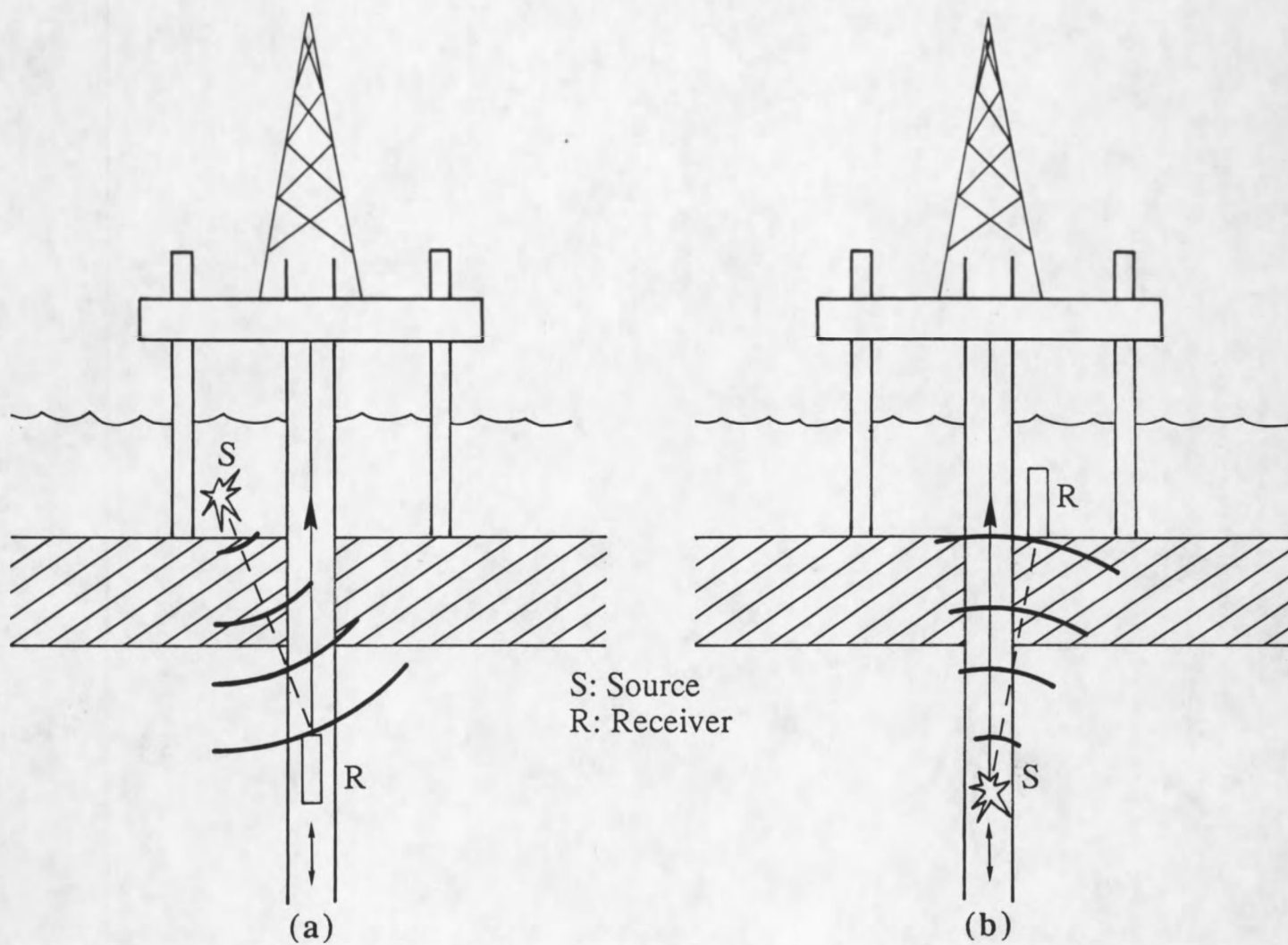


Figure 2.10

a. Downhole shooting in offshore conditions
b. Uphole shooting in offshore conditions
(after Vercoutere, 1987).



Figure 3.1 The seismic grid covering the Belgian, Dutch, French and UK sectors of the continental shelf (after Henriët et al., 1988).

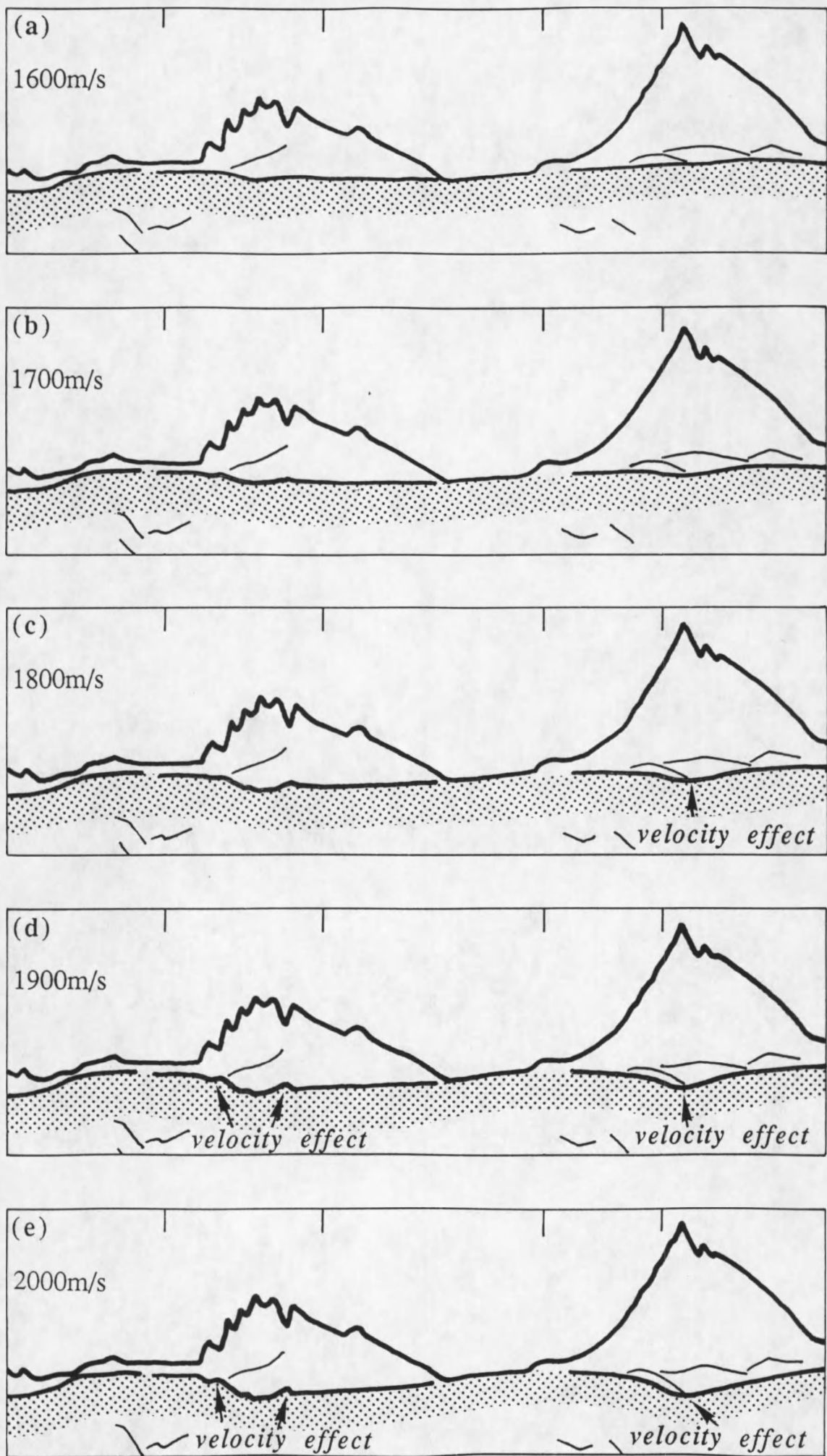


Figure 3.2 Velocity effect on a flat surface covered by sand banks.

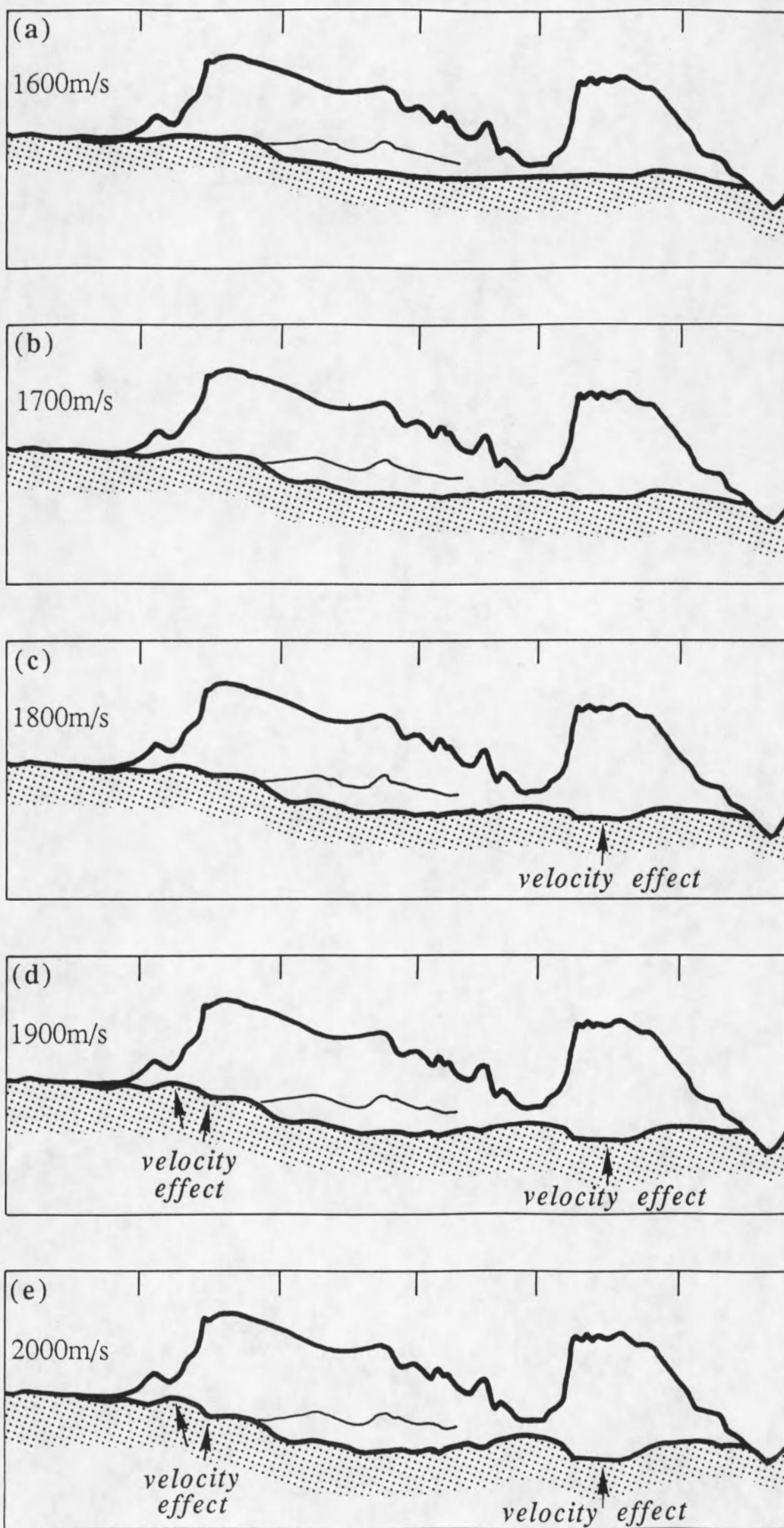


Figure 3.3 Velocity effect on a gently dipping surface covered by sand banks.

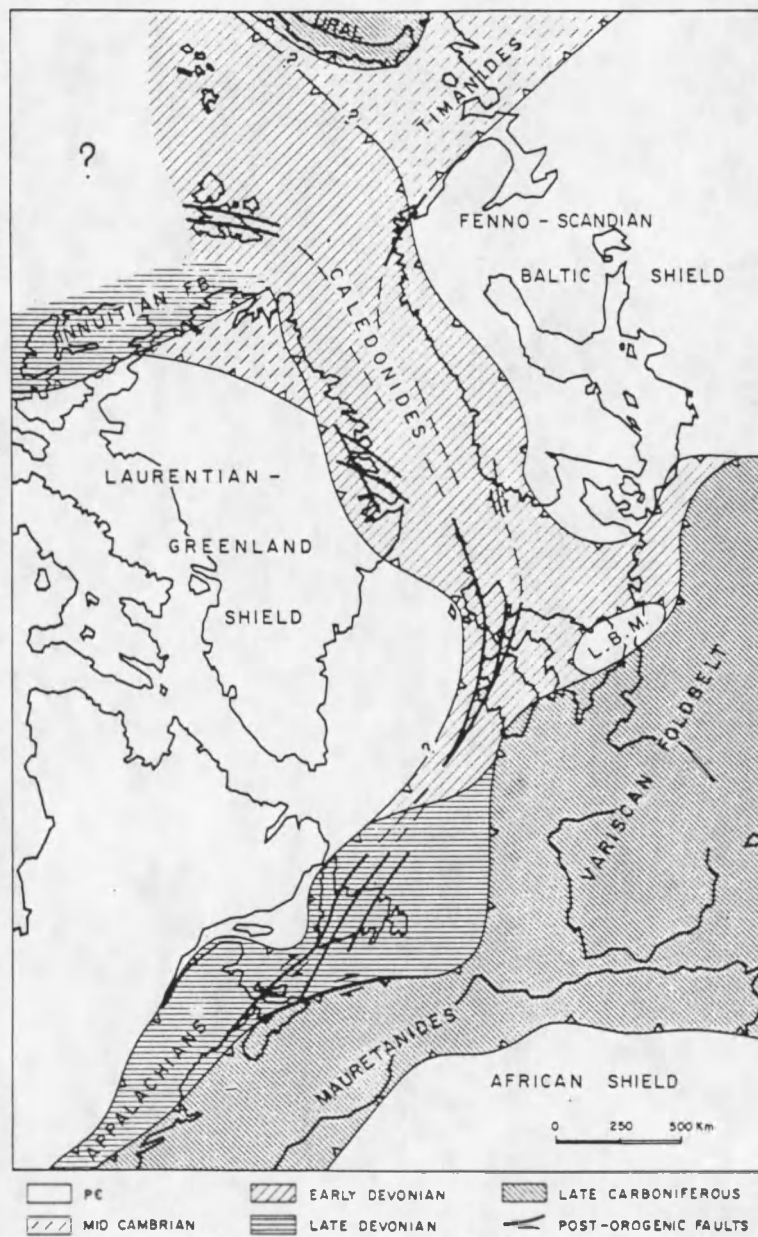


Figure 4.1 Spatial relationship of the Paleozoic orogenic belt during the Late Paleozoic. L.B.M. = London-Brabant Massif (after P. Ziegler, 1981).

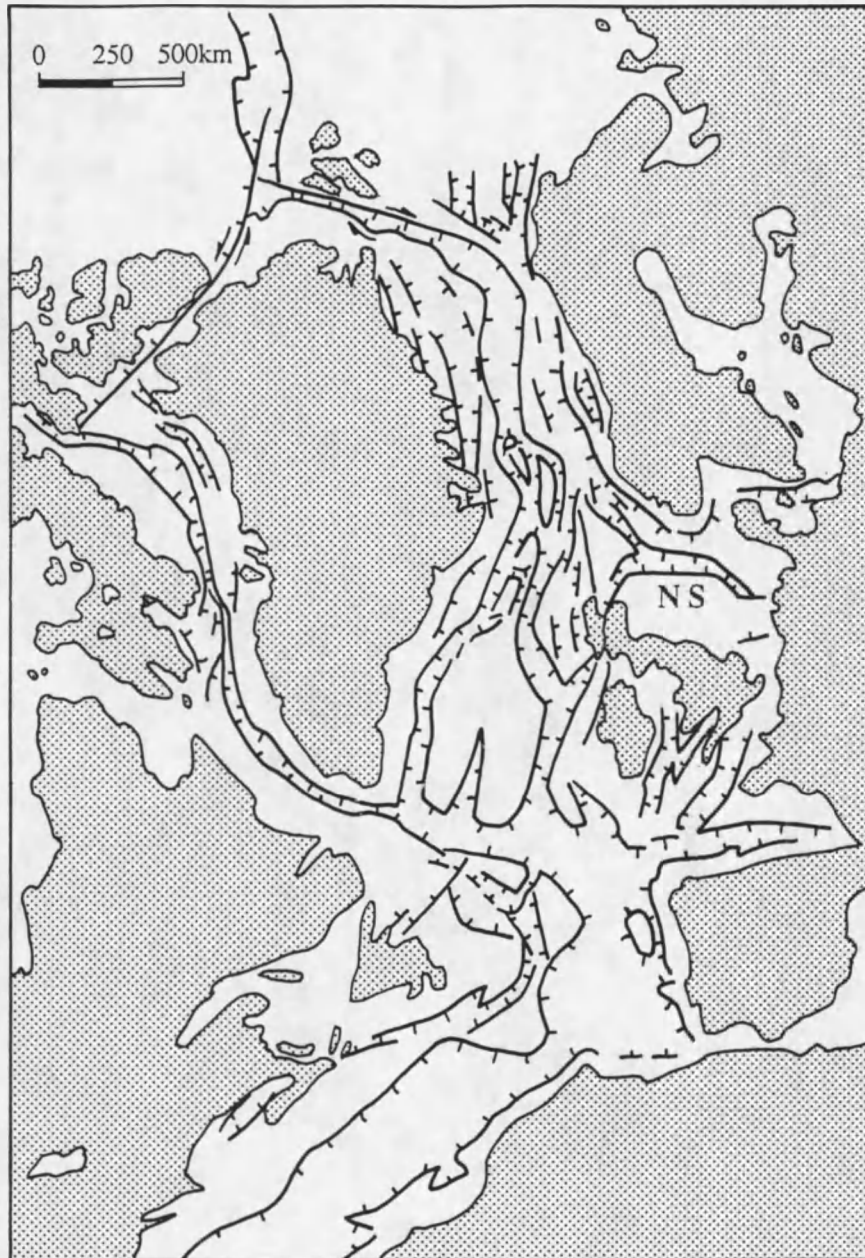


Figure 4.2 Schematic graben pattern of the Mesozoic North Atlantic - Arctic rift system. NS = North Sea rift (after P. Ziegler & Louwerens, 1979).

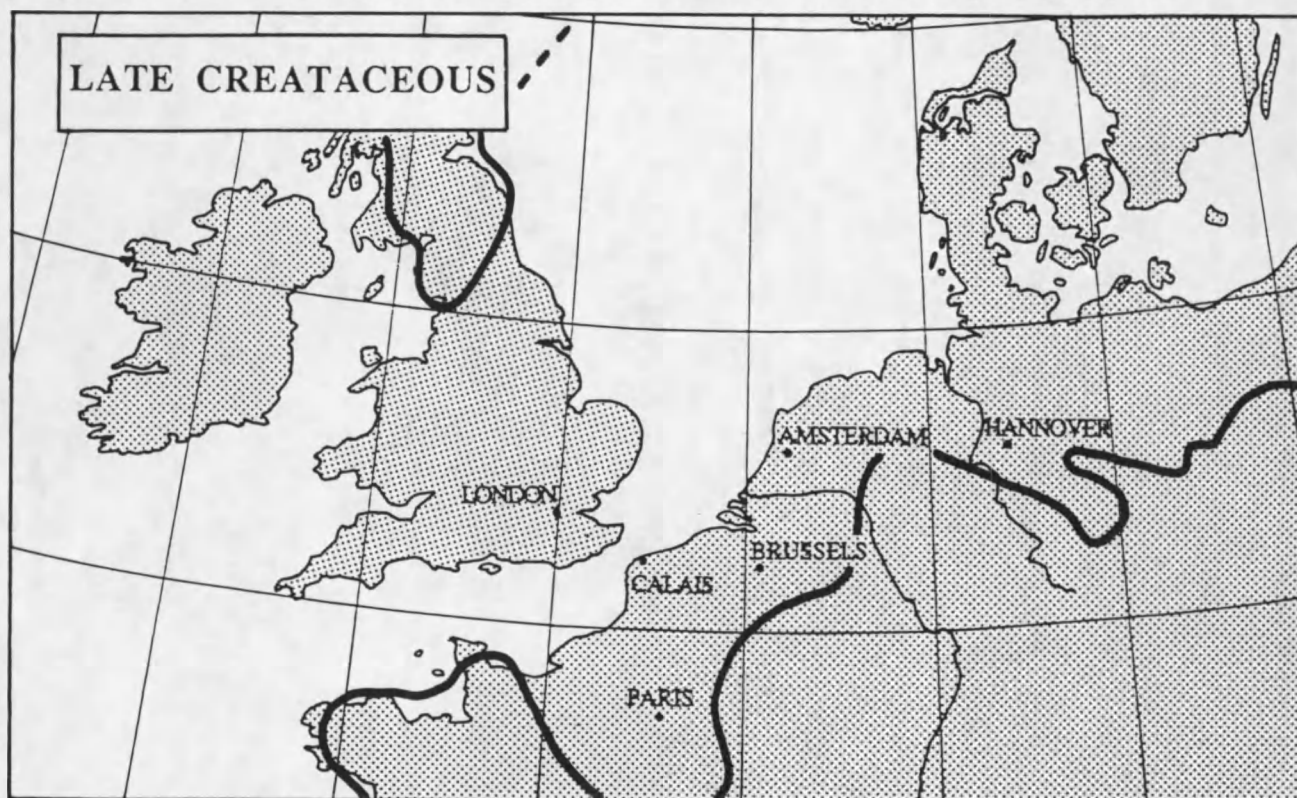


Figure 4.3 Paleogeography of the southern North Sea area during the Late Cretaceous (after Kockel, 1988).

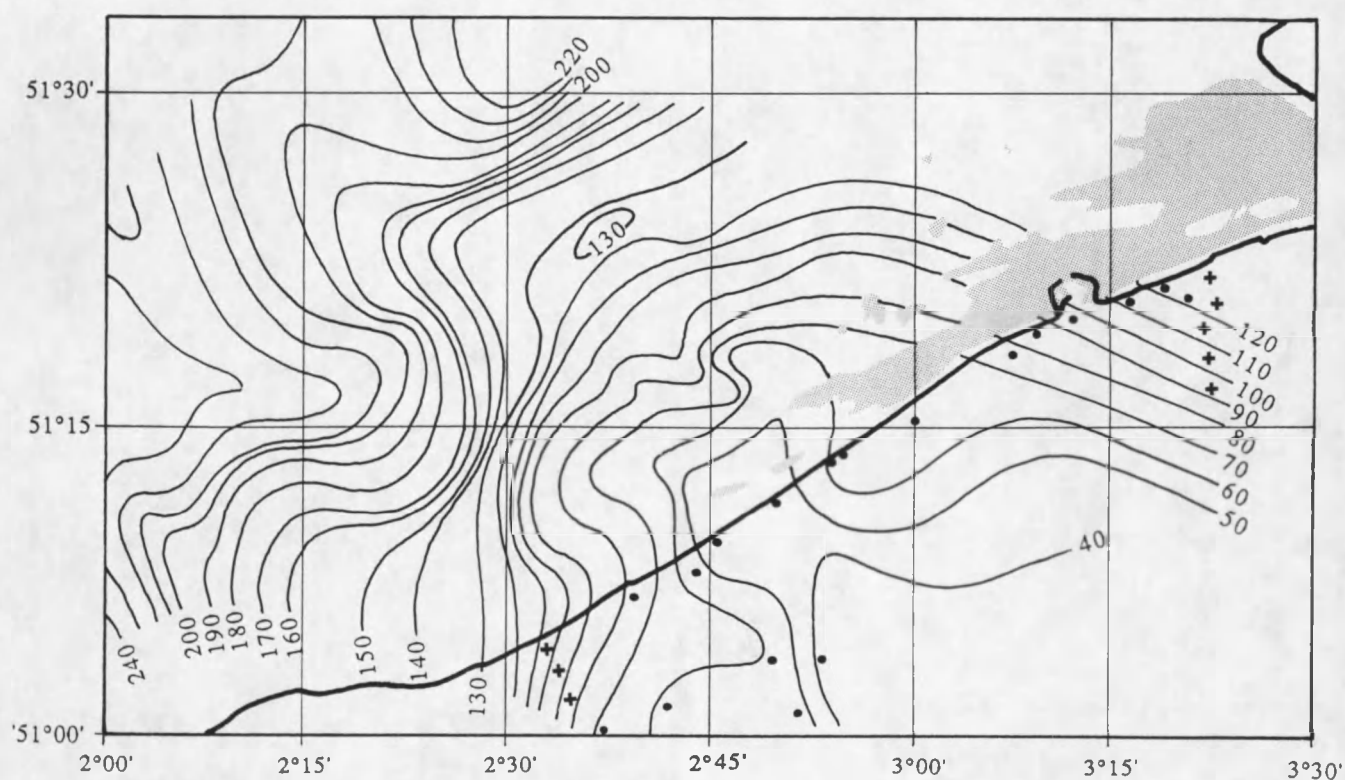


Figure 4.4 Thickness of the Late Cretaceous chalk (after Roorda Van Eysinga, 1982 and Legrand, 1968).

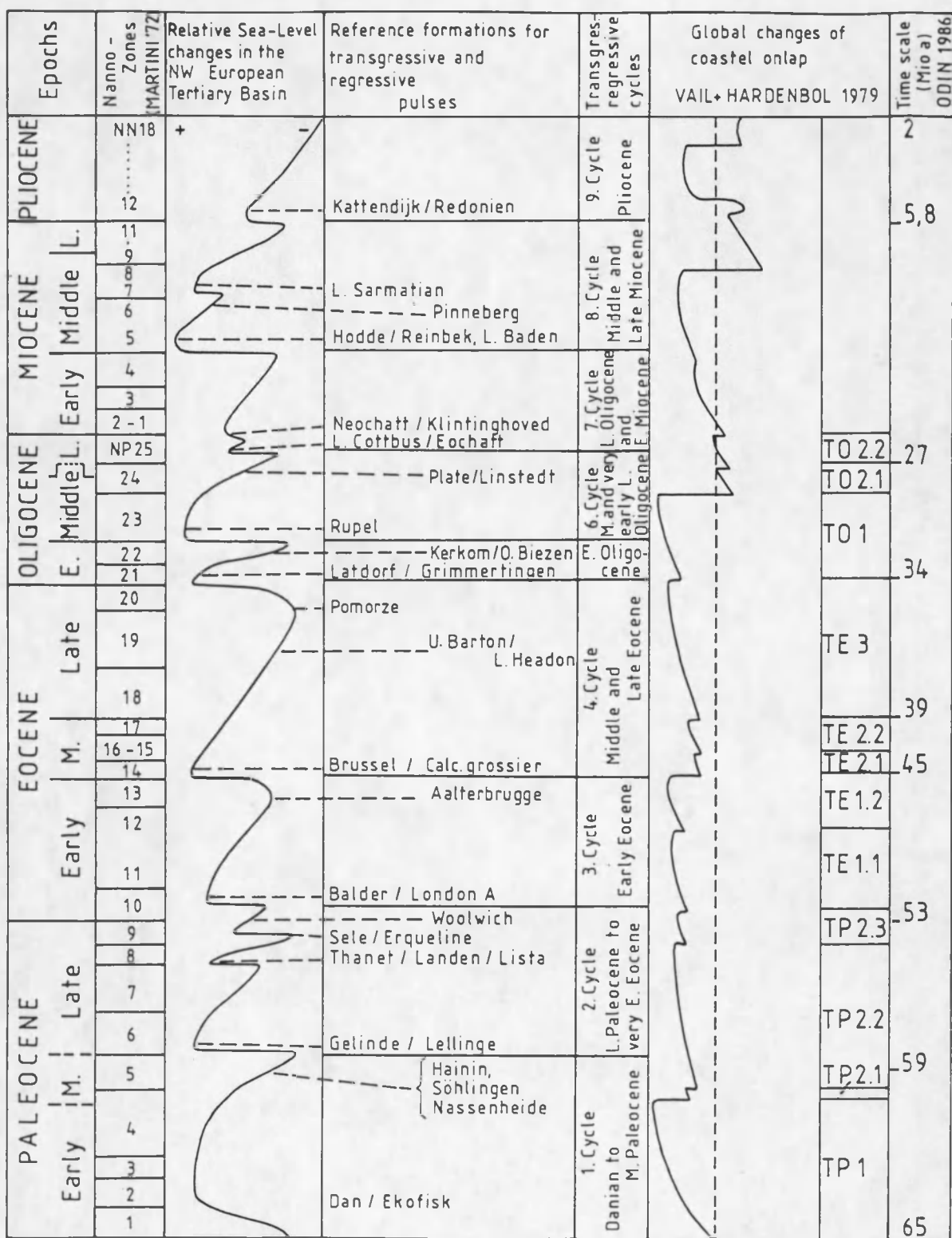


Figure 4.5 Assumed basin-wide sea-level changes in the NW European basin (after Kockel, 1988).

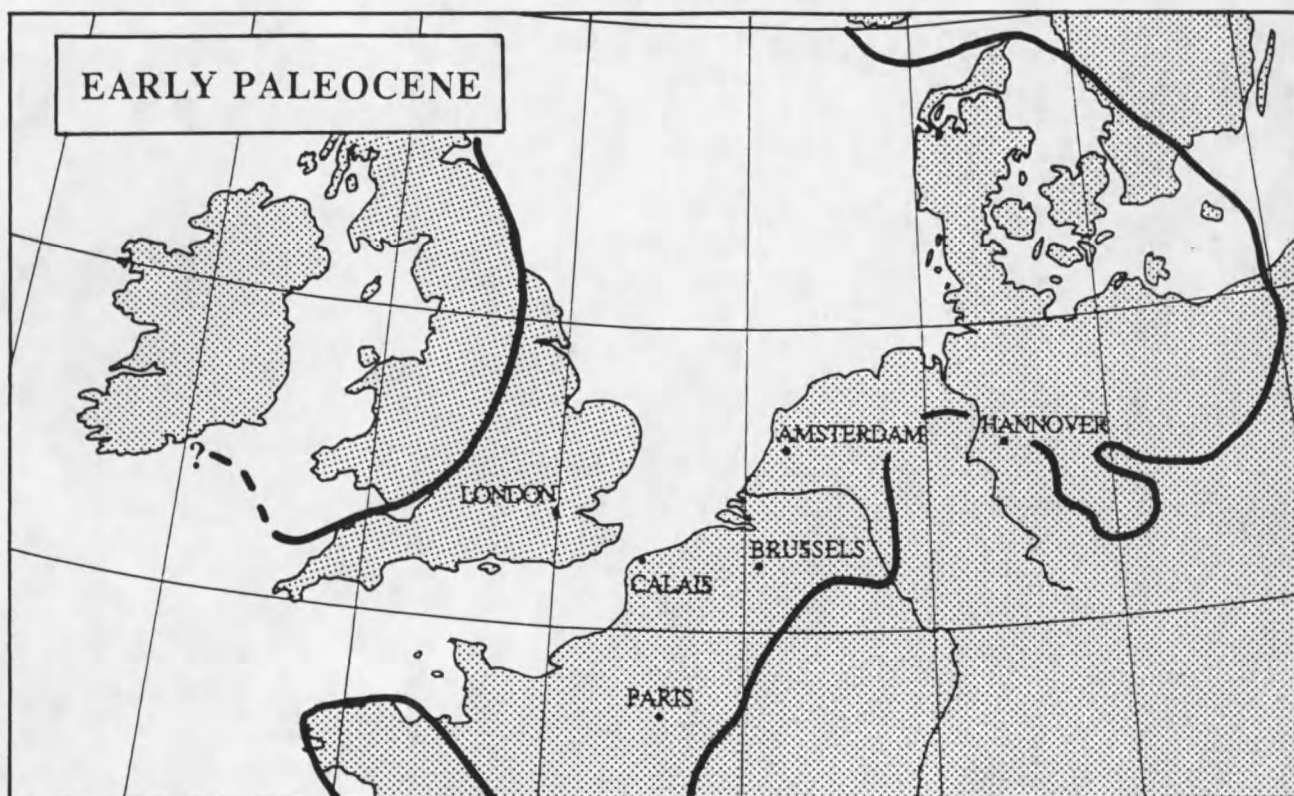


Figure 4.6 Paleography of the southern North Sea area during the Early Paleocene (after P.Ziegler, 1982 and Kockel, 1988).

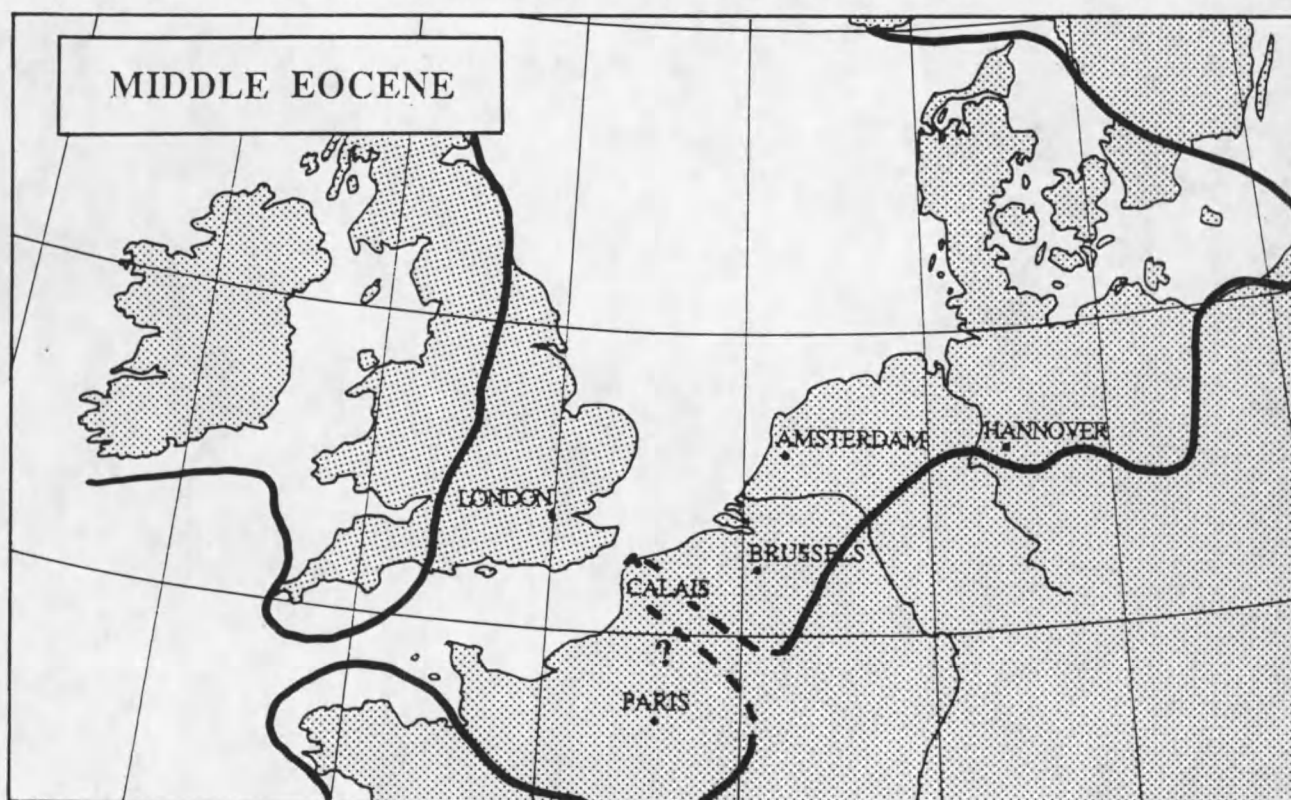


Figure 4.7 Paleography of the southern North Sea area during the Middle Eocene (after P.Ziegler, 1982 and Kockel, 1988).

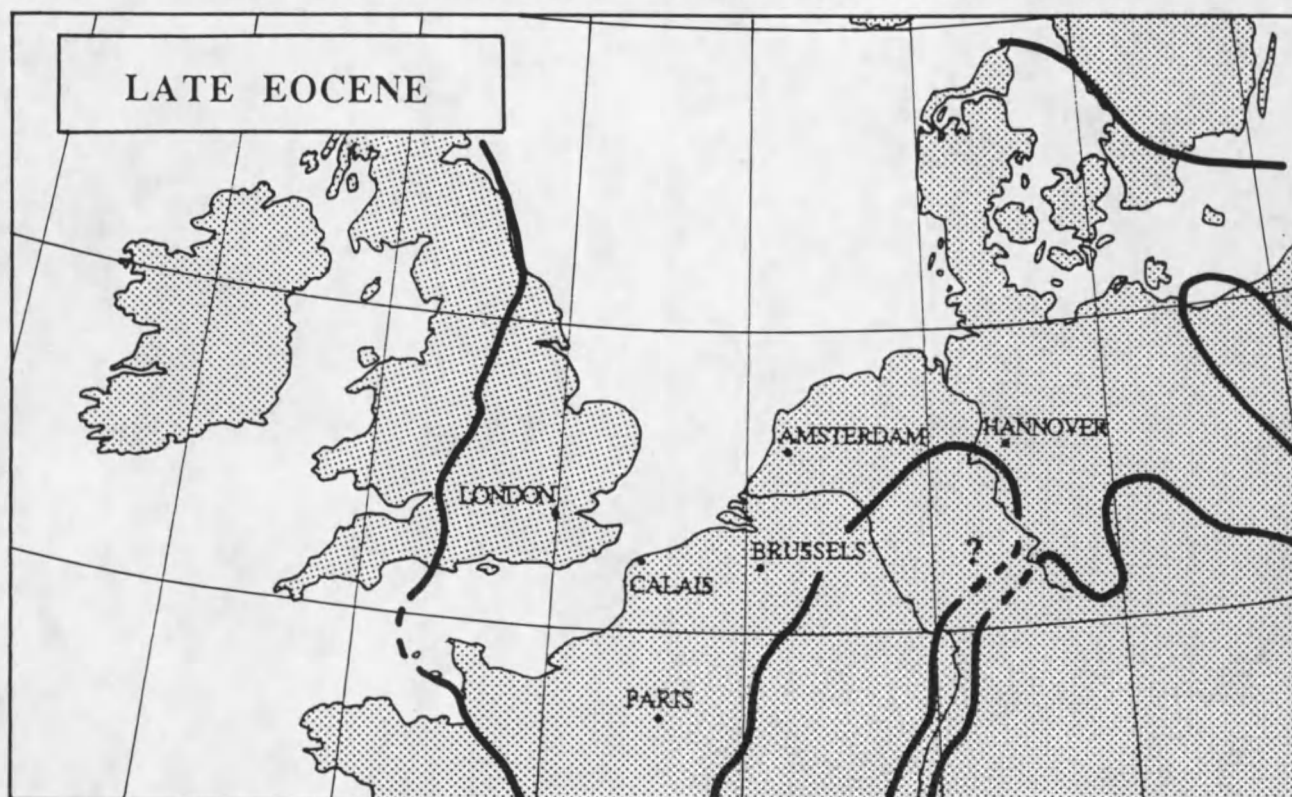


Figure 4.8 Paleography of the southern North Sea area during the Late Eocene (after P.Ziegler, 1982 and Kockel, 1988).

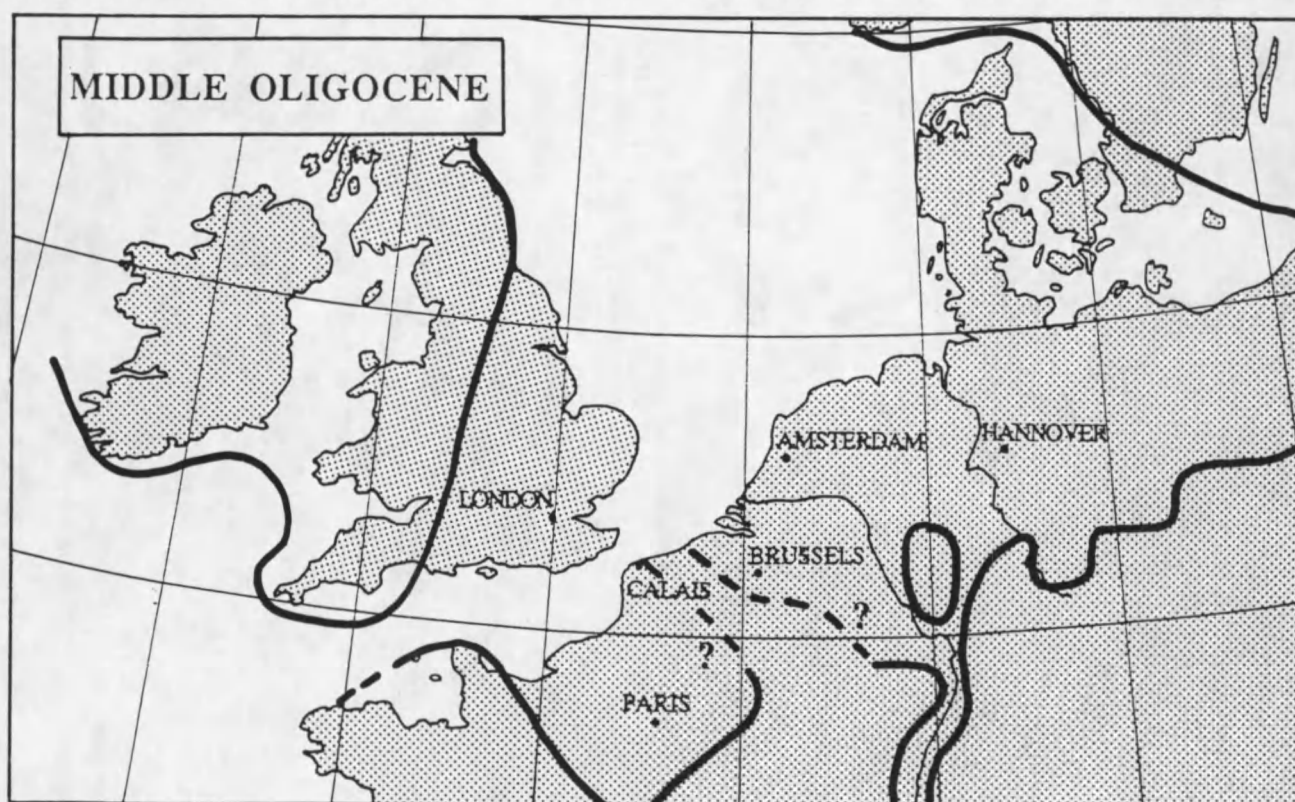


Figure 4.9 Paleography of the southern North Sea area during the Middle Oligocene (after P.Ziegler, 1982 and Kockel, 1988).

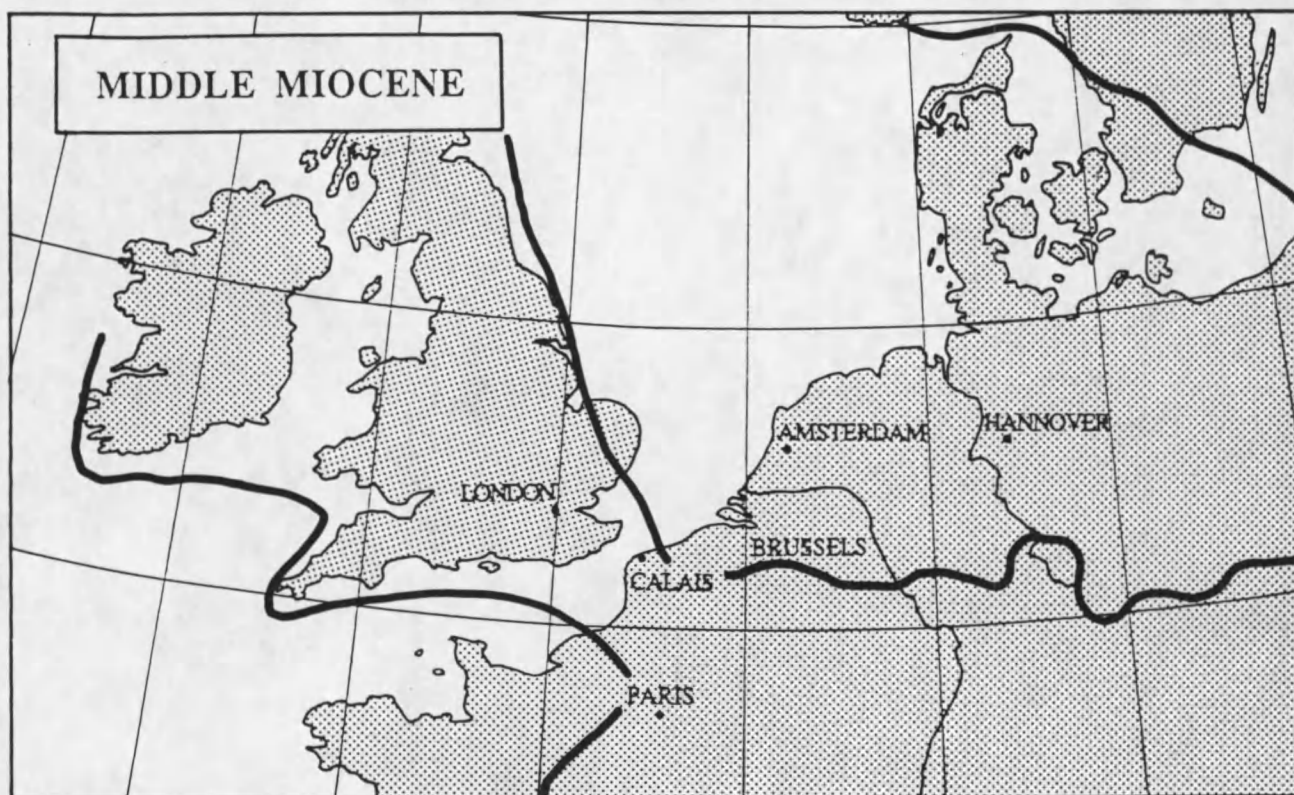


Figure 4.10 Paleography of the southern North Sea area during the Middle Miocene (after P.Ziegler, 1982 and Kockel, 1988).

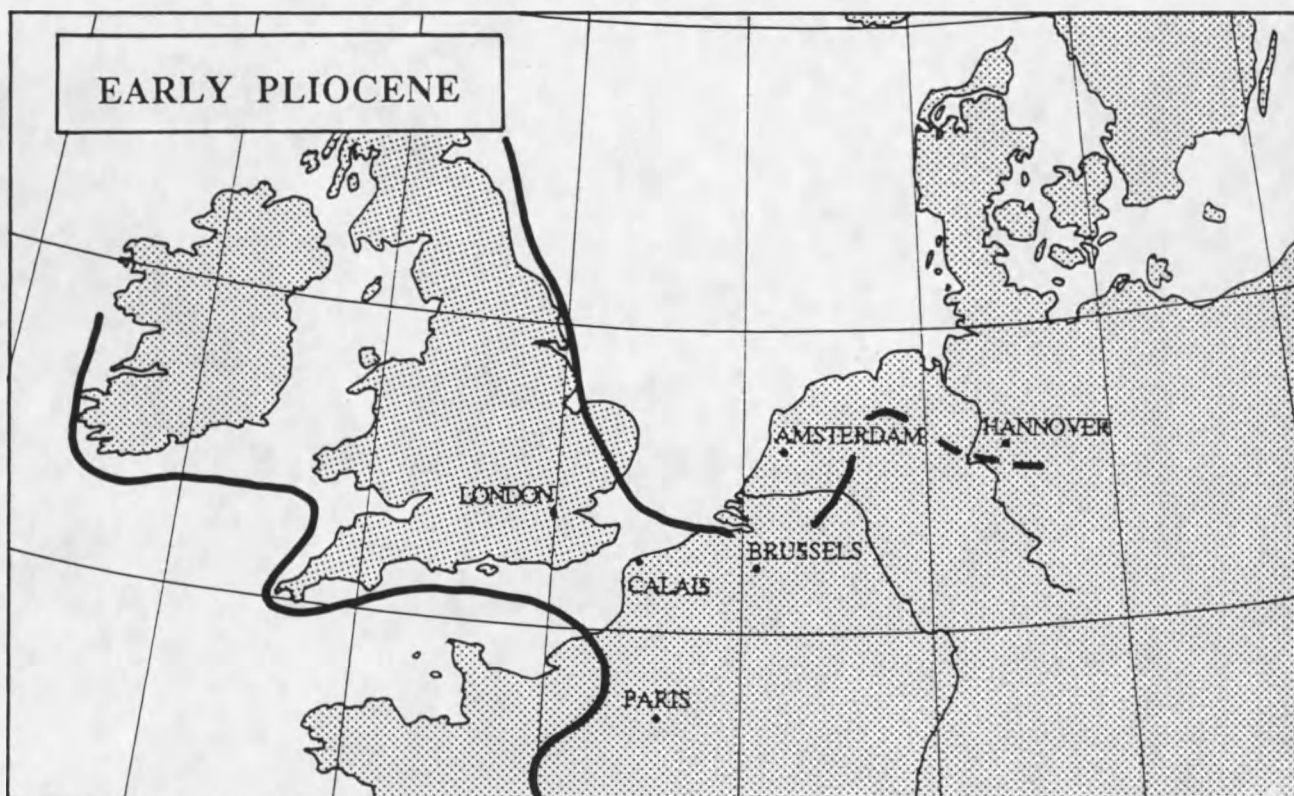


Figure 4.11 Paleography of the southern North Sea area during the Early Pliocene (after Zagwijn & Doppert, 1978 and P.Ziegler, 1982).

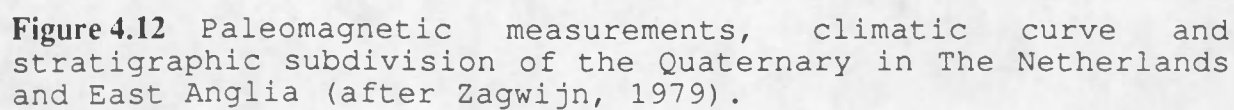


Figure 4.12 Paleomagnetic measurements, climatic curve and stratigraphic subdivision of the Quaternary in The Netherlands and East Anglia (after Zagwijn, 1979).

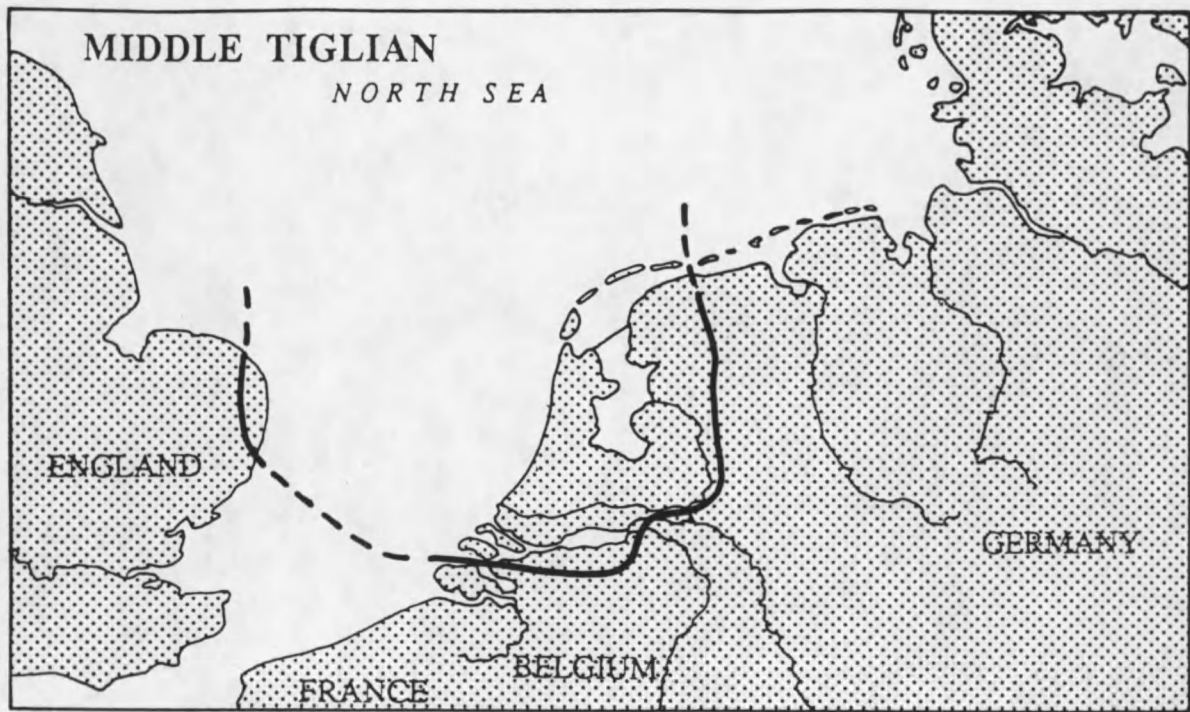


Figure 4.13 Paleography of the southern North Sea area during the Middle Tiglian (after Zagwijn, 1979).

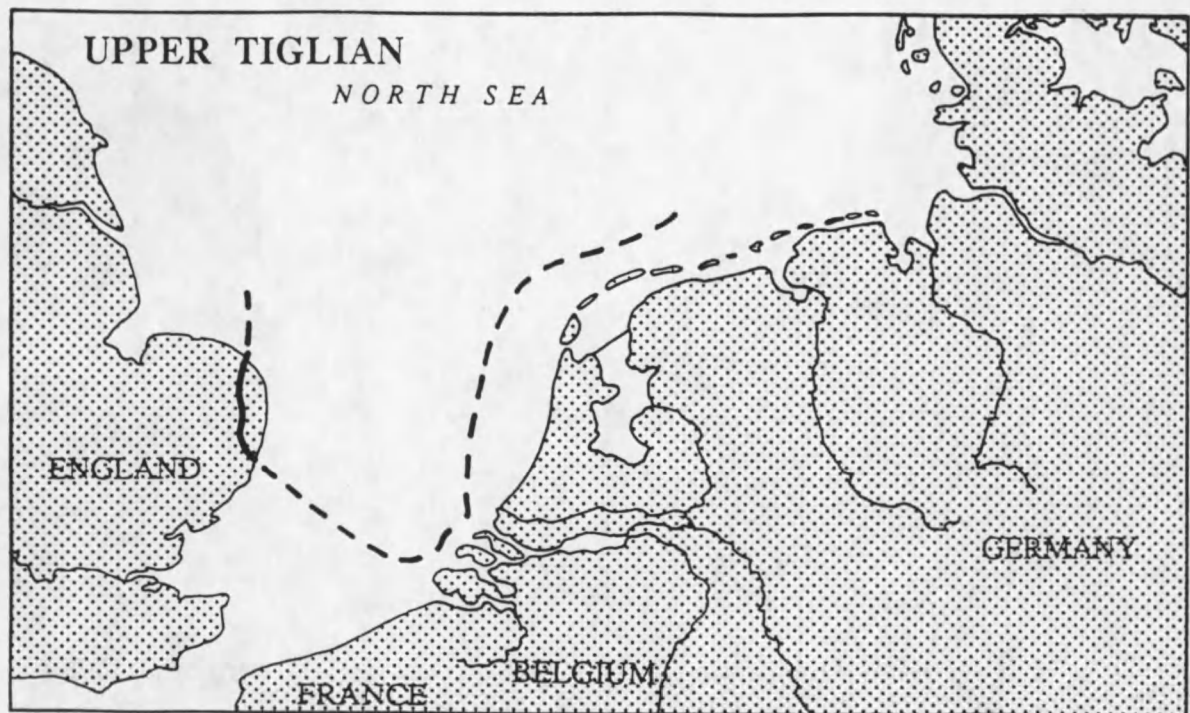


Figure 4.14 Paleography of the southern North Sea area during the Late Tiglian (after Zagwijn, 1979).

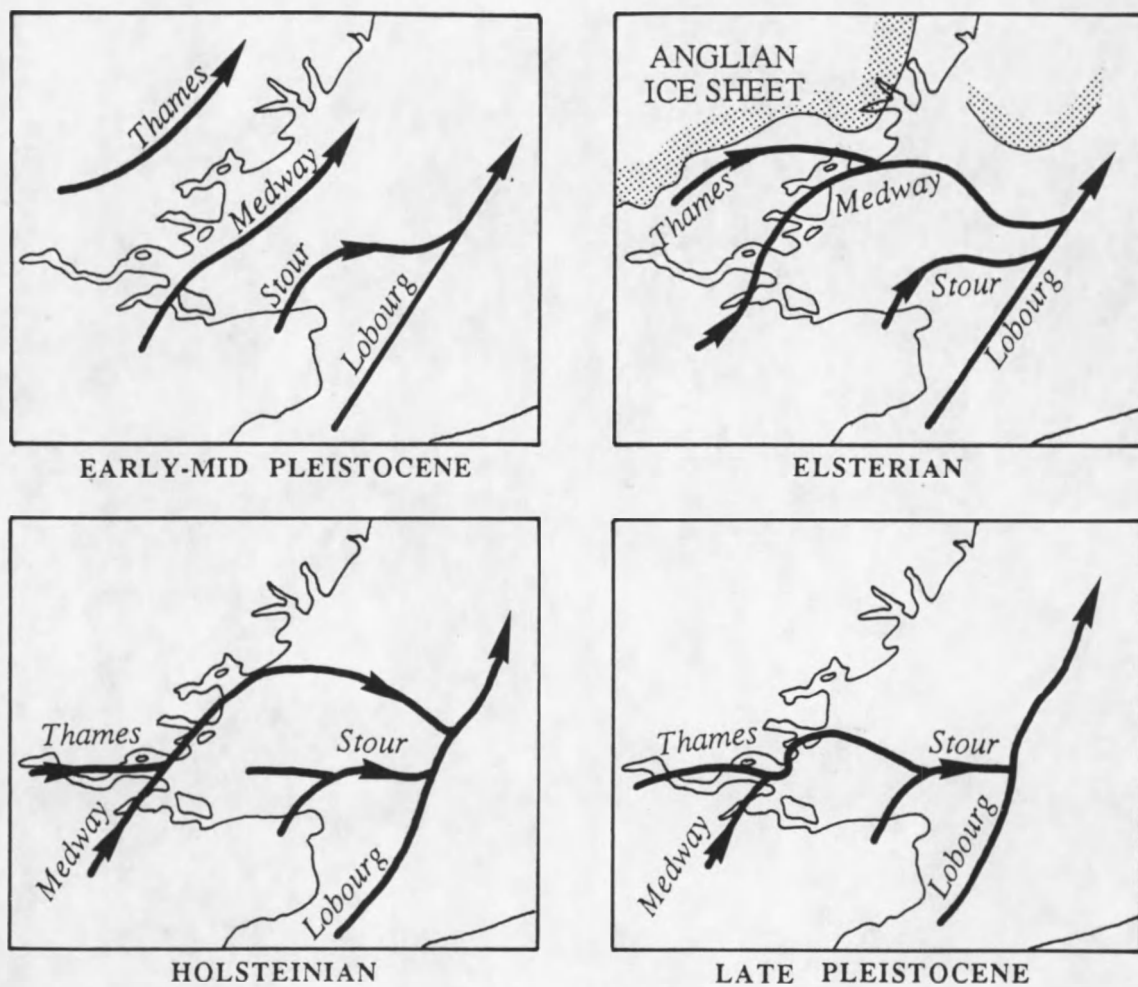


Figure 4.15 Development of the Thames-Lobourg river system during the Quaternary (after Balson & D'Olier, 1988).

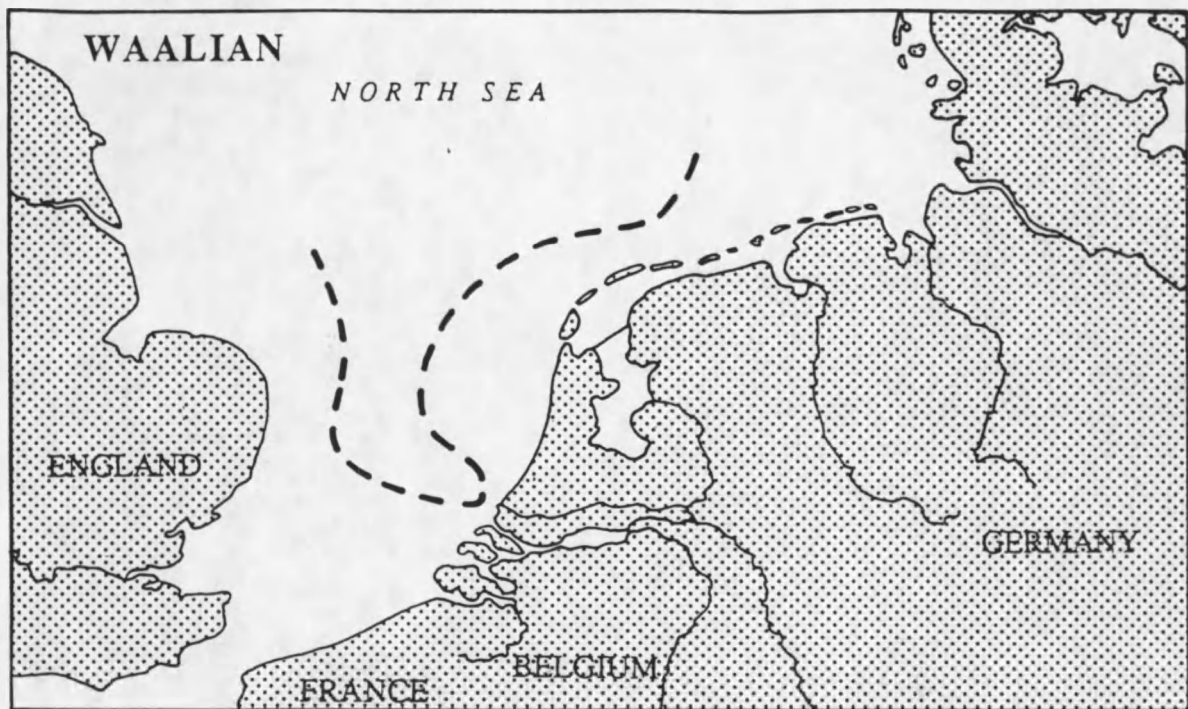


Figure 4.16 Paleography of the southern North Sea area during the Waalian (after Zagwijn, 1979).

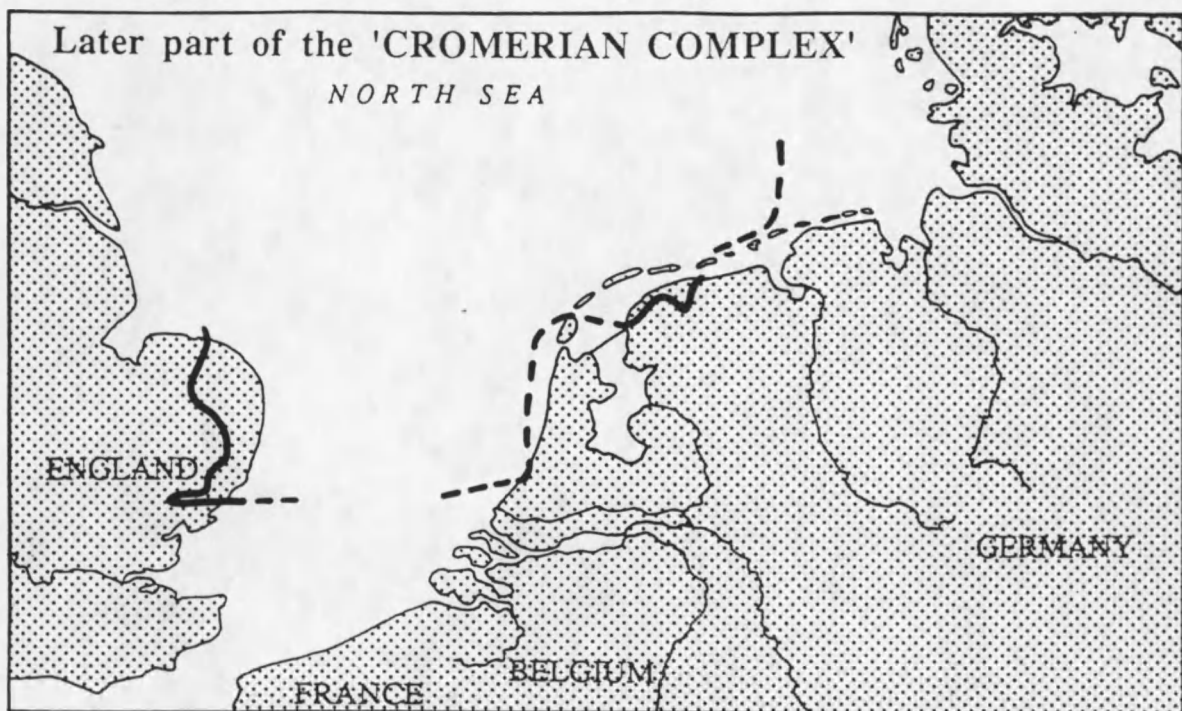


Figure 4.17 Paleography of the southern North Sea area during the later part of the Cromerian Complex (after Zagwijn, 1979).

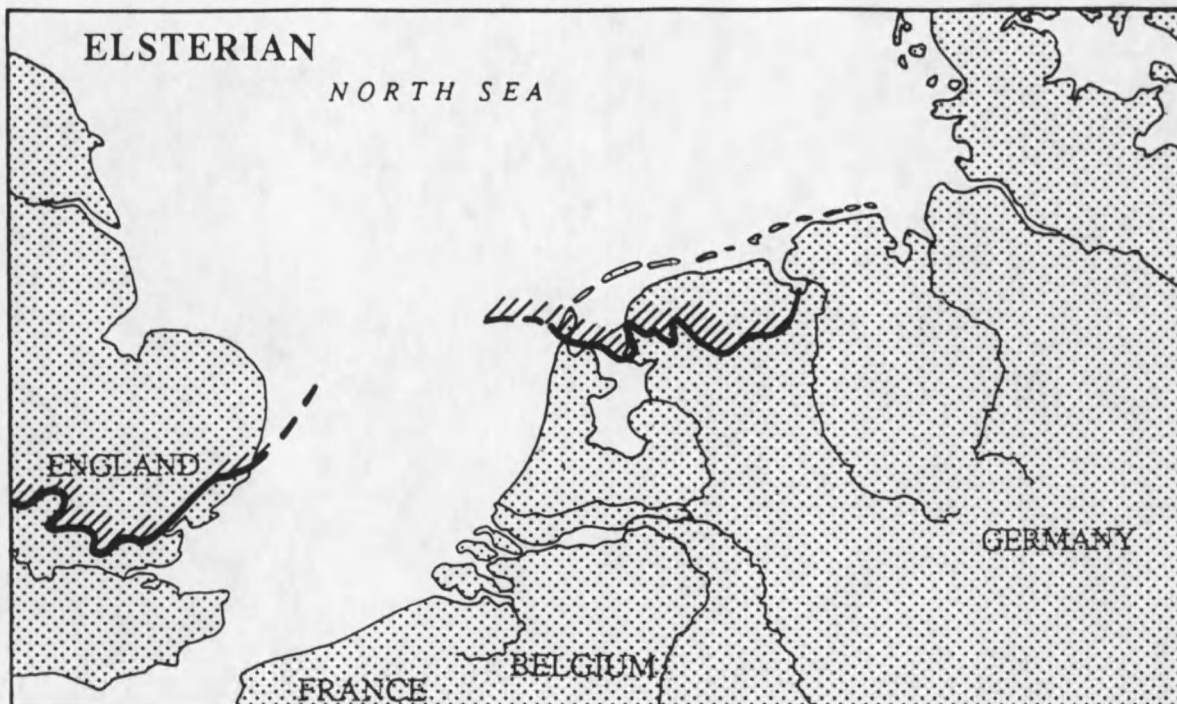


Figure 4.18 Paleography of the southern North Sea area during the Elsterian (after Zagwijn, 1979).

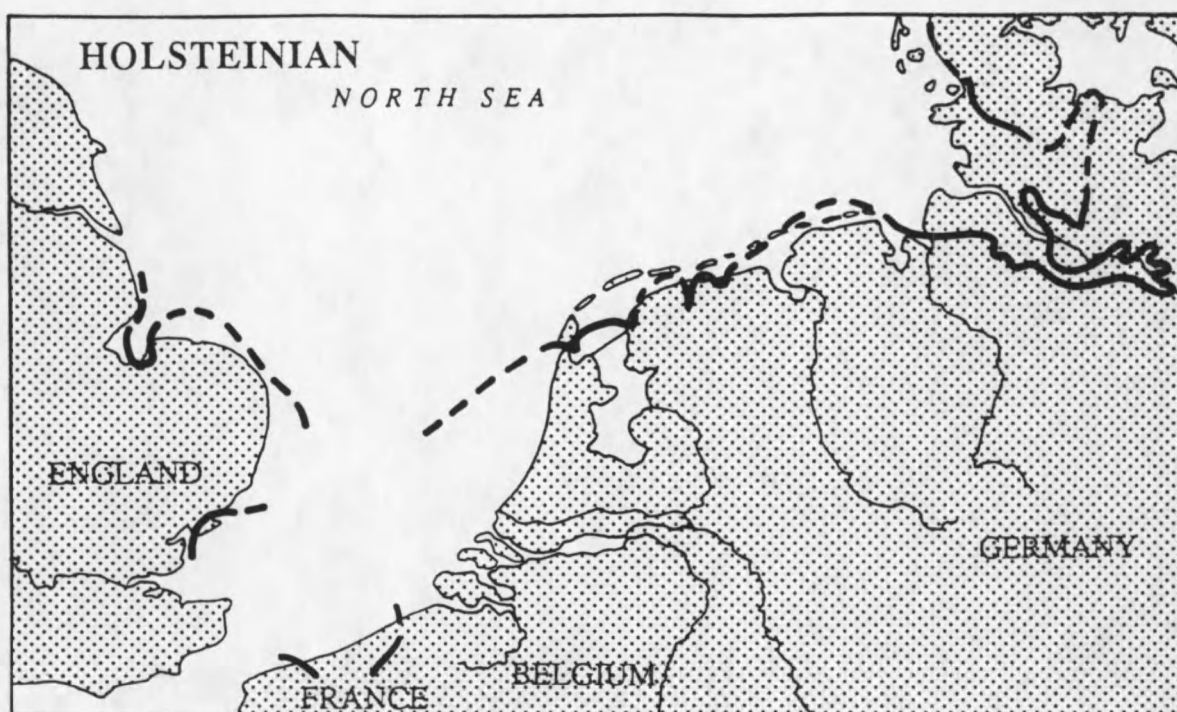


Figure 4.19 Paleography of the southern North Sea area during the Holsteinian (after Zagwijn, 1979).

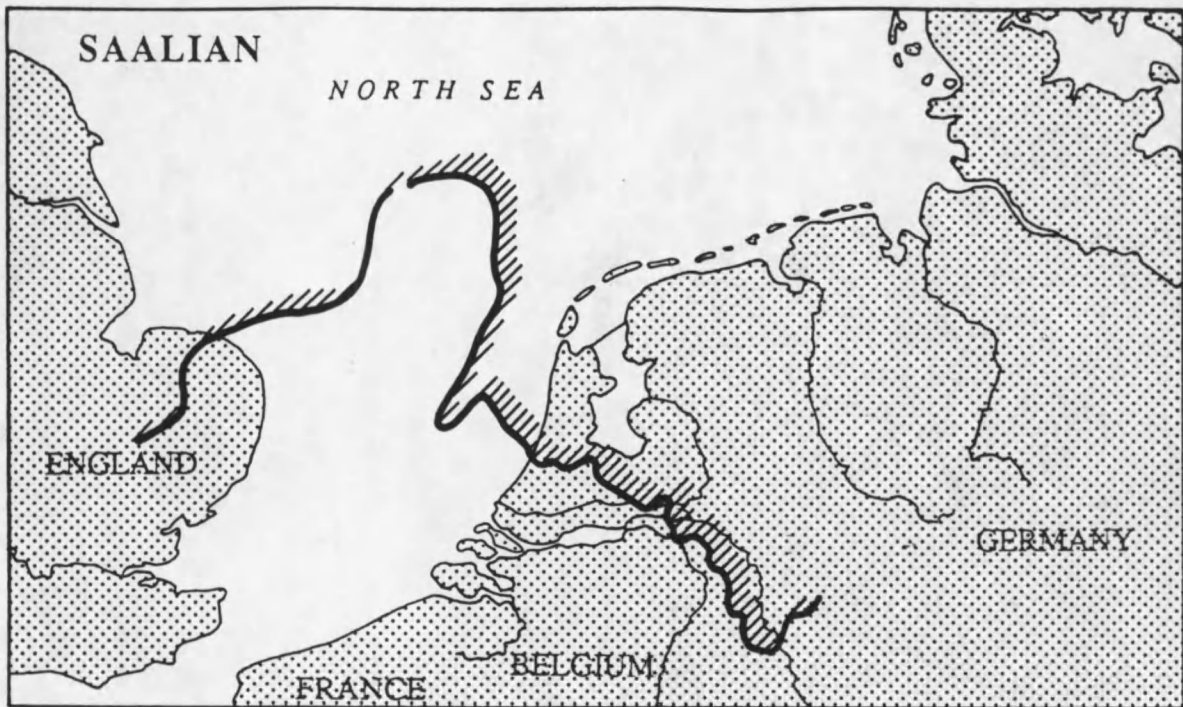


Figure 4.20 Paleography of the southern North Sea area during the Saalian (after Zagwijn, 1979). The extension of British land ice is after West (1977).

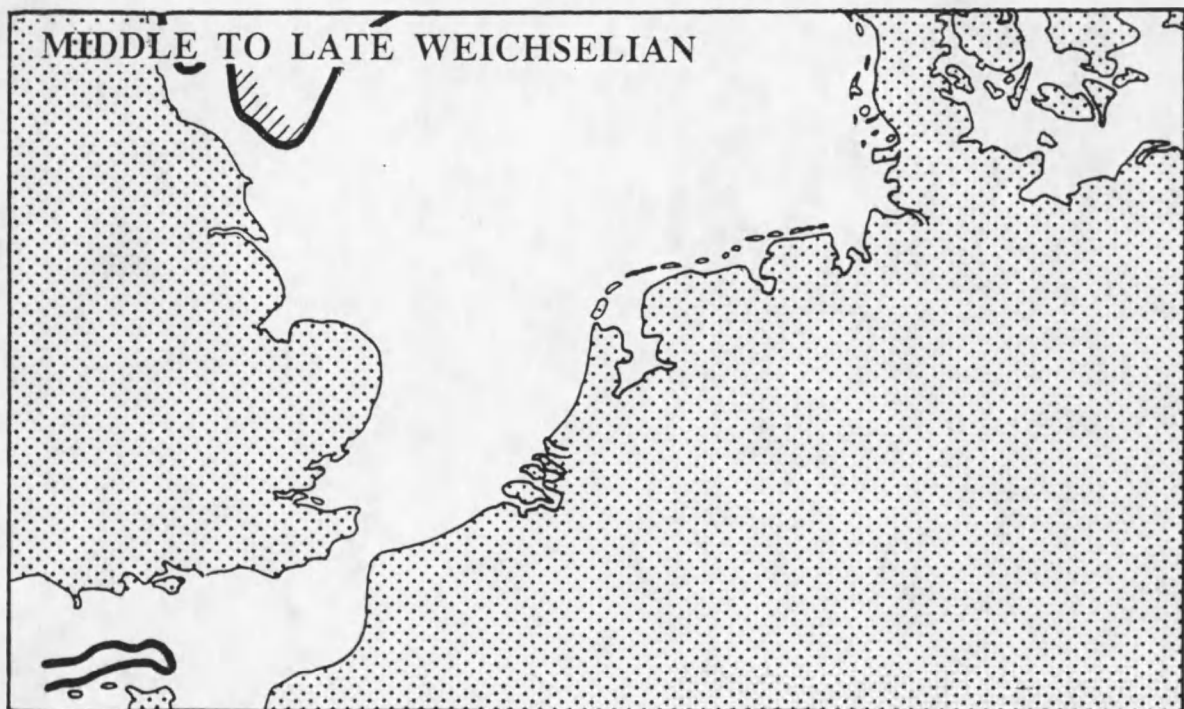


Figure 4.21 Paleography of the southern North Sea area during the Middle to Late Weichselian (after Jelgersma, 1979).

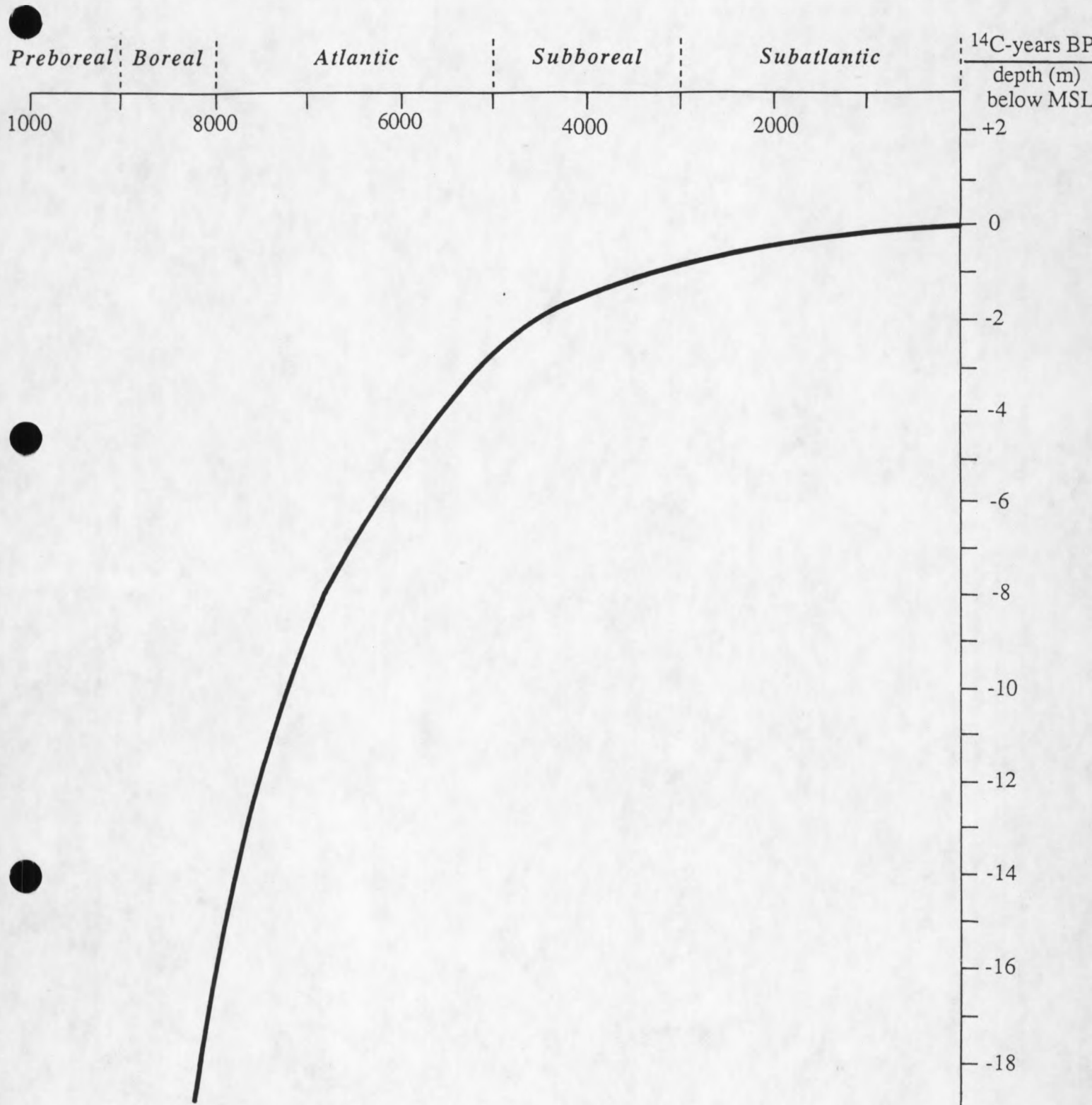


Figure 4.22 Curve for the relative sea-level rise during the Holocene, based on data from the Belgian coastal plain. MSL = mean lowest low water-level at spring-tide (after Köhn, 1988).

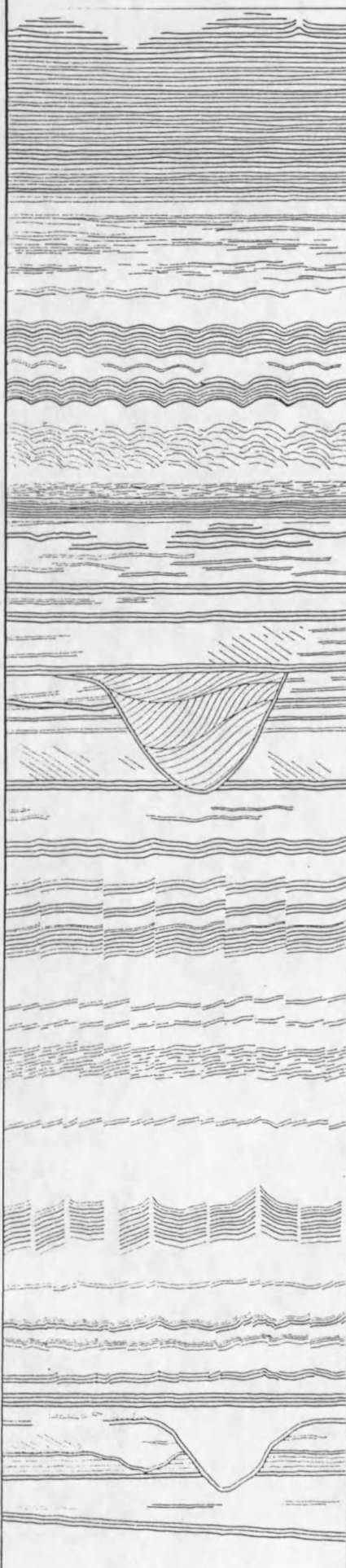
SCHEMATIC TYPE SECTION	DEPOSITIONAL SEQUENCES						LITHOSTRA - TIGRAPHIC CORRELATION	
	NAME	BOUNDARY			REFLECTOR DESCRIPTION			
		NAME	TYPE	AMPL CONT. FREQ.				
	R2	N1.1	onlap/truncation	low	cont.	low	Boom Member (B)	
	R1	R2.1	concordance	medium	cont.	low	Ruisbroek Member (B)	
		R1.1	onlap/truncation	low	cont.	low		
	P1						Watervliet Member (B)	
							Bassevelde Member (B)	
	B1	P1.1	concordance	medium	cont.	low	Meetjesland Formation (B)	
		B2.1	baselap	high	cont.	low		
	L1	B1.1	truncation	medium	cont.	high	Oedelem Member (B)	
	Y5	L1.1	toplap	high	cont.	low	Vlierzele Member (B)	
	Y4	Y5.1	downlap/truncation	medium	cont.	low	Merelbeke Member (B)	
		Y3.1	baselap/truncation	variable	cont.	low		
	Y2						Egcm Member (B)	
		Y2.1	downlap	high	cont.	low	Kortemark Member (B)	
	Y1						London Clay (U.K.) or Flanders Clay (B) (Ieper Clay)	
	T3	Y1.1	concordance	high	cont.	low	lagoonal to continental Landen Formation (B)	
	T2	T3.1	downlap/truncation	medium	discont.	low		
	T1	T2.1	downlap/truncation	medium	cont.	medium	marine Landen Formation (B)	
			T1.1	onlap	high	cont.	low	

Figure 5.1 Schematic seismic-stratigraphic sequence chart and correlation table of the Paleogene deposits in the Southern Bight (after De Batist, 1989).

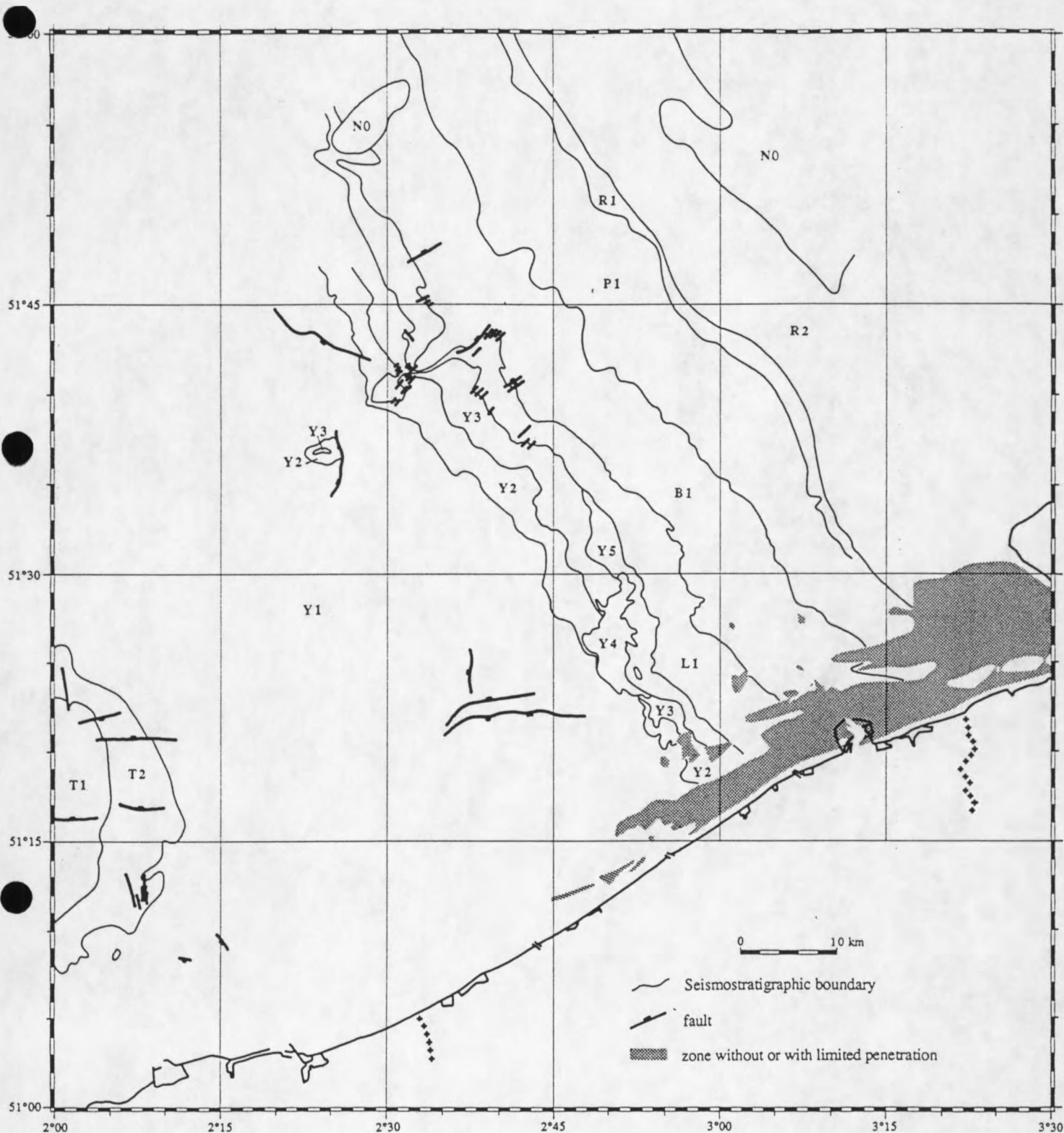


Figure 5.2 Seismic-stratigraphic solid map of the Paleogene deposits in the Southern Bight (after De Batist, 1989).

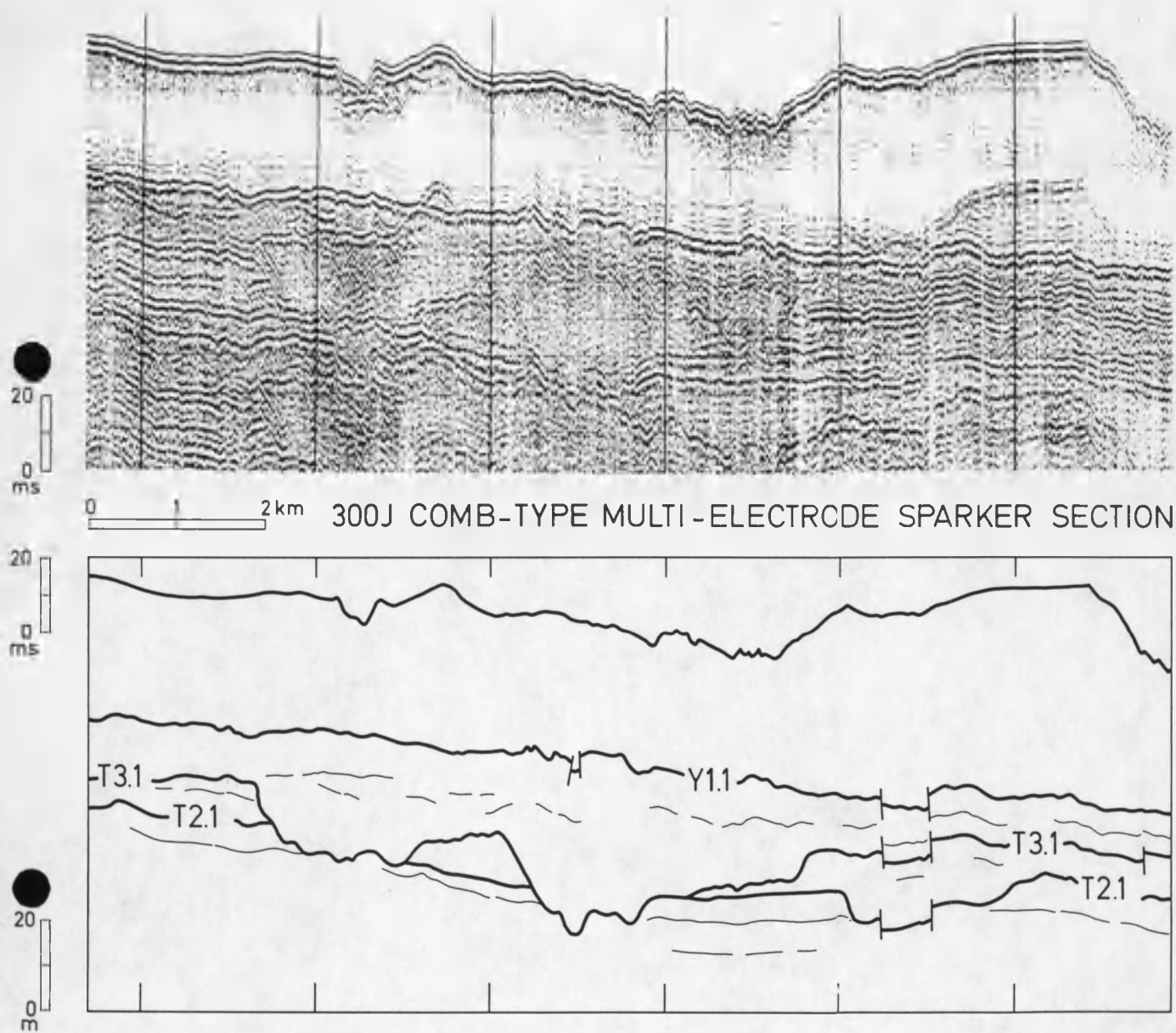


Figure 5.3 Analog record of a sparker section and interpreted line-drawing showing Thanetian gully erosion features (after Henriët et al., 1989).

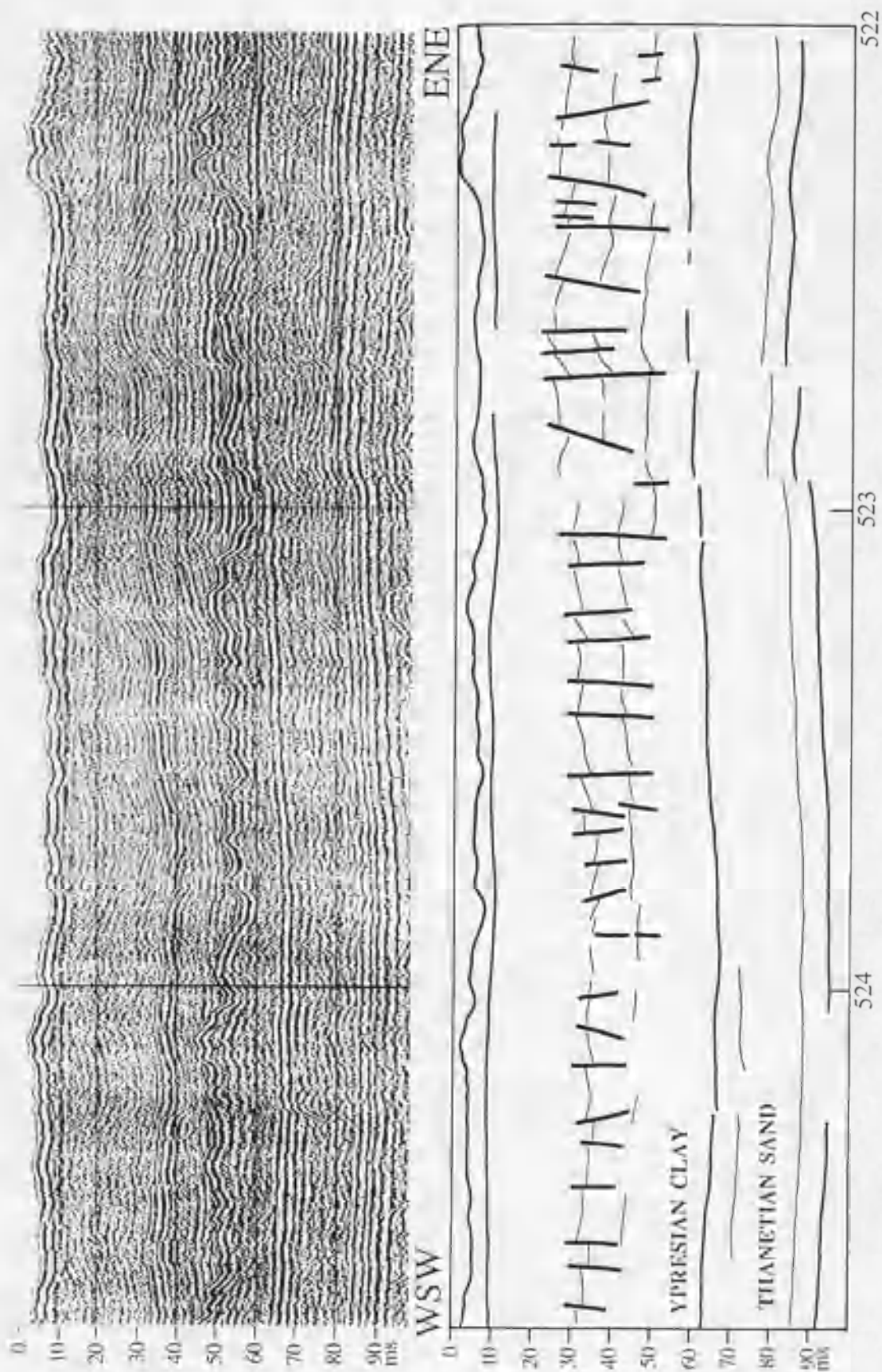


Figure 5.4 Analog record of a sparker section and interpreted line-drawing showing the lower interval of Ypresian clay-tectonic deformations (after De Batist et al., 1989). Depth calculated with an interval velocity of 1620 m/s.

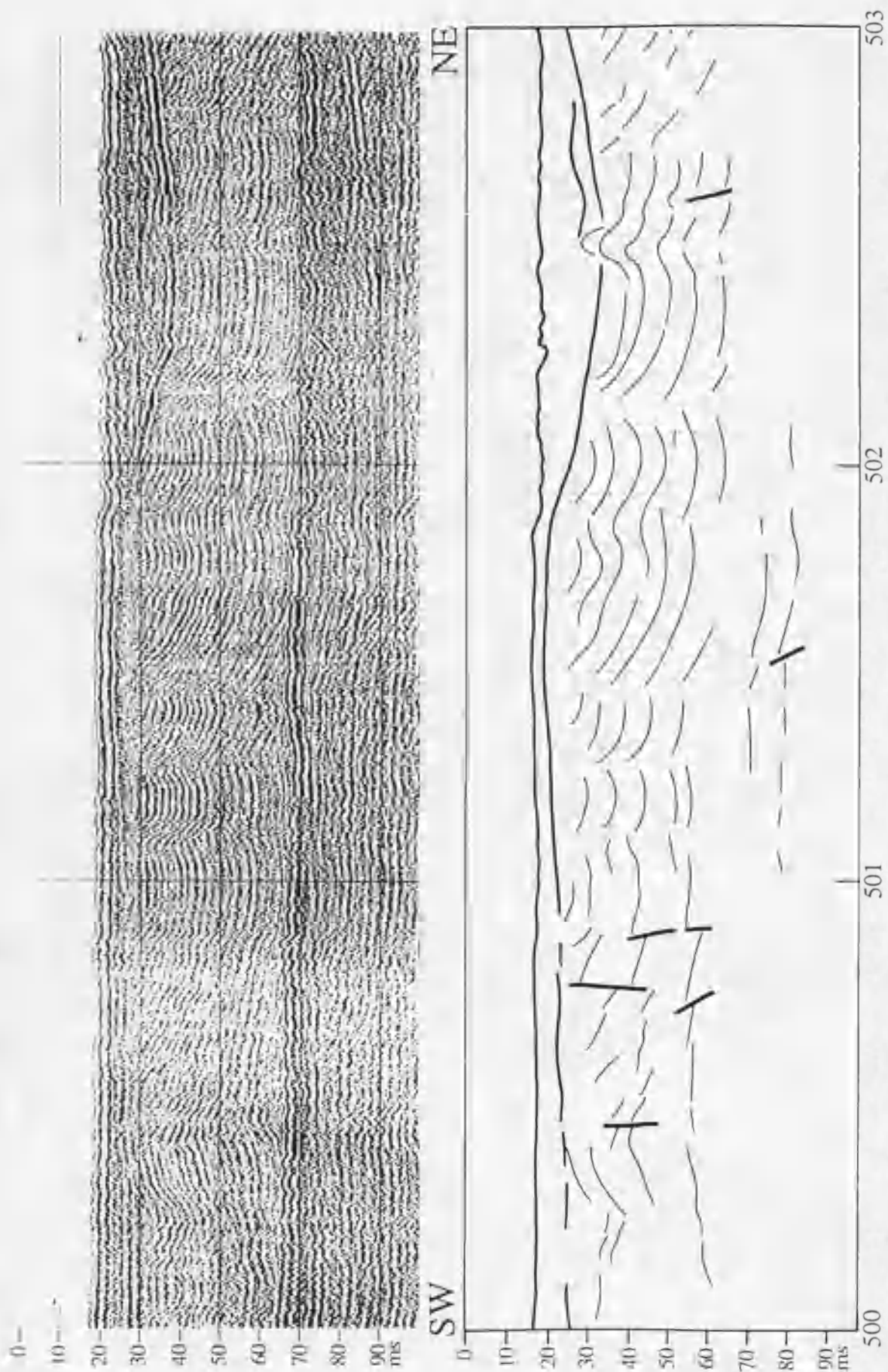


Figure 5.5 Analog record of a sparker section and interpreted line-drawing showing the middle interval of Ypresian clay-tectonic deformations (after De Batist et al., 1989). Depth calculated with an interval velocity of 1620 m/s.

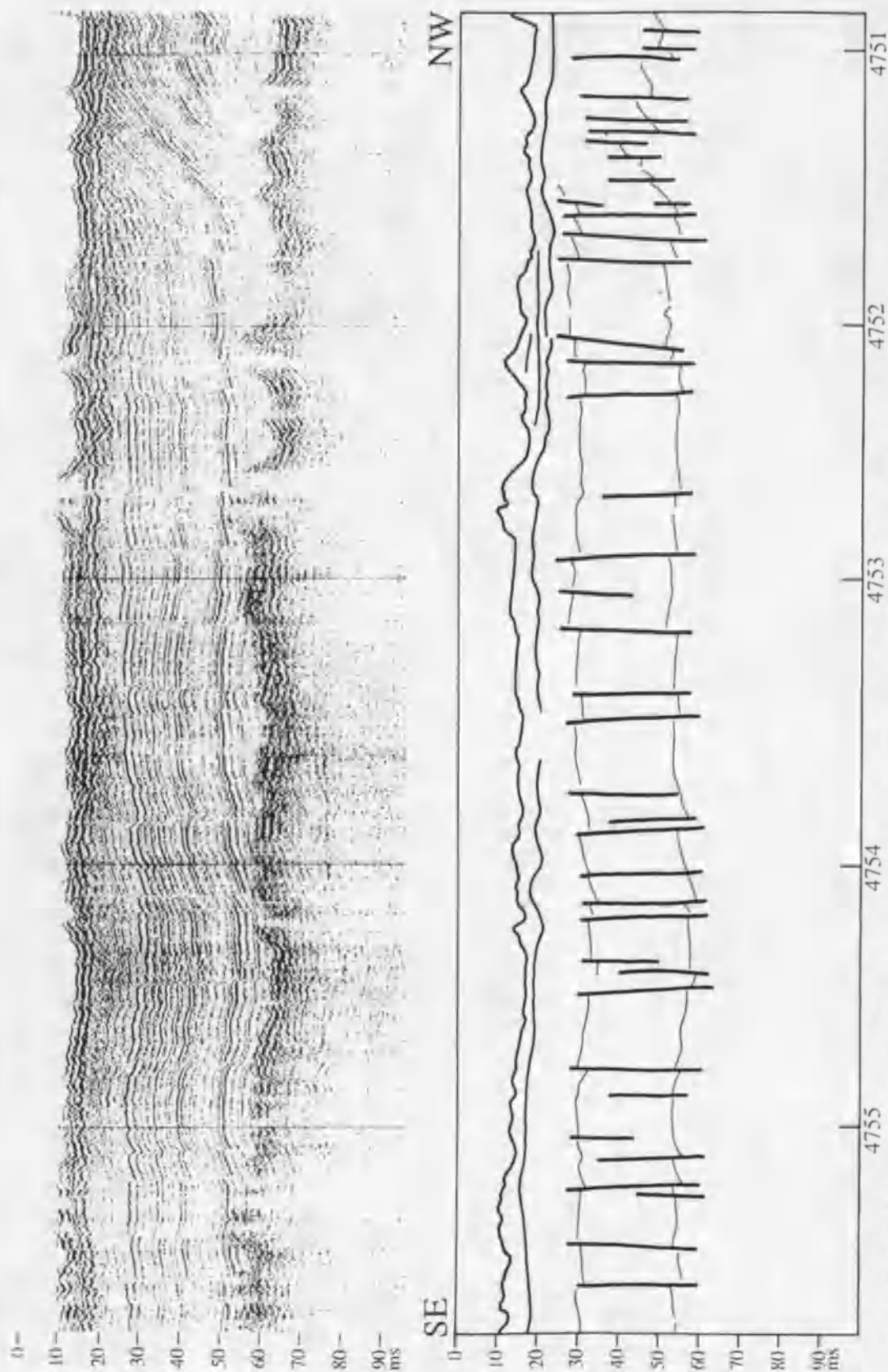


Figure 5.6 Analog record of a sparker section and interpreted line-drawing showing the upper interval of Ypresian clay-tectonic deformations (after De Batist et al., 1989). Depth calculated with an interval velocity of 1620 m/s.

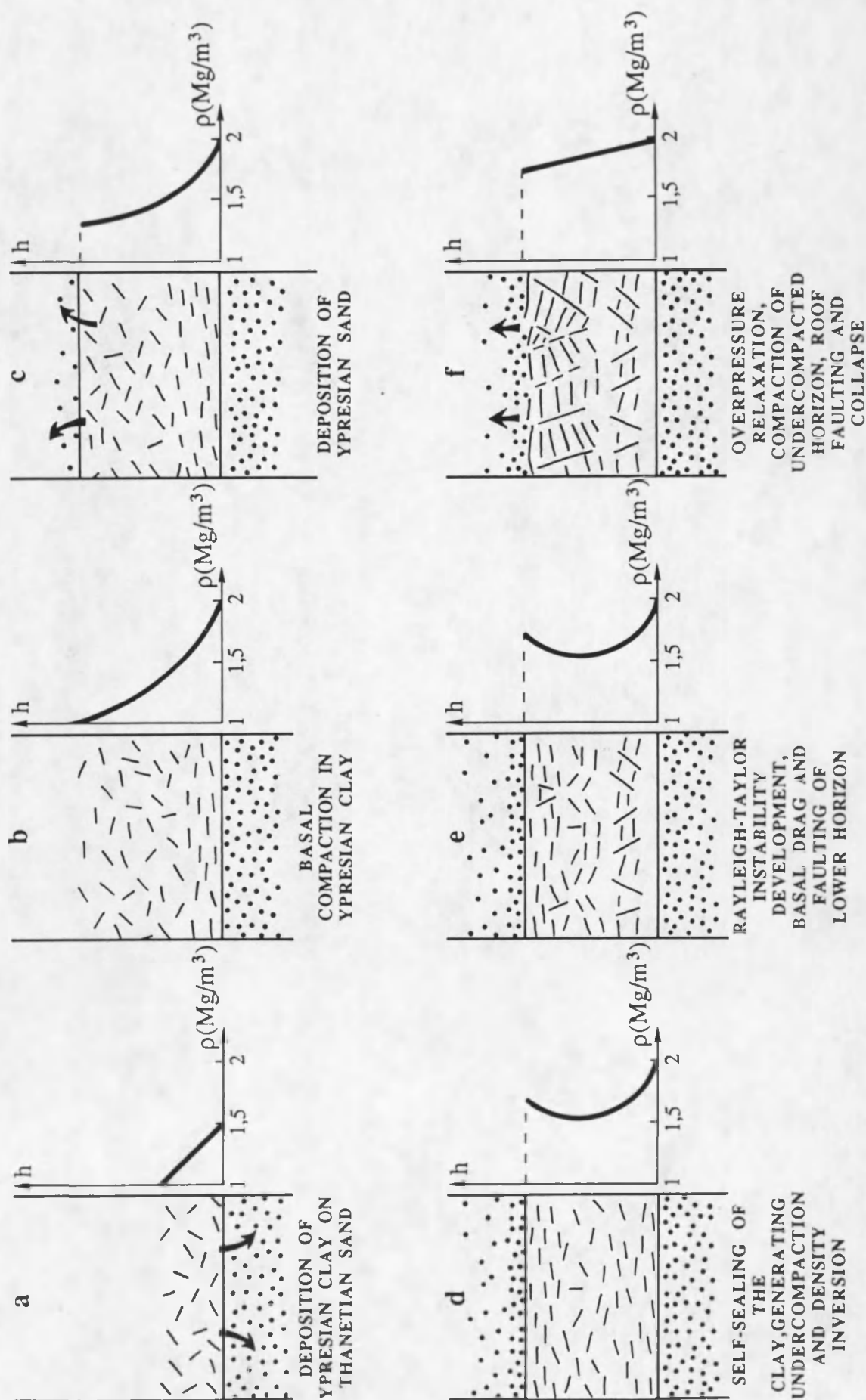


Figure 5.7 Genetic model of the clay-tectonic deformations in the Ypresian Clay (after Henriët et al., 1988).

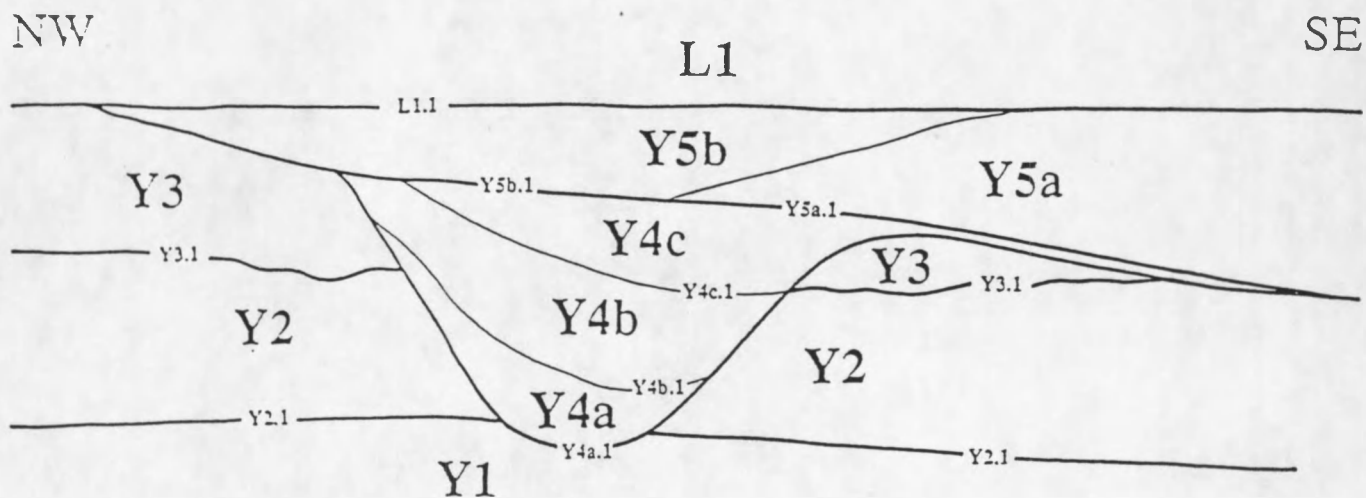


Figure 5.8 Schematic representation of the Ypresian basin-fill sequences offshore Ostend (after De Batist, 1989).

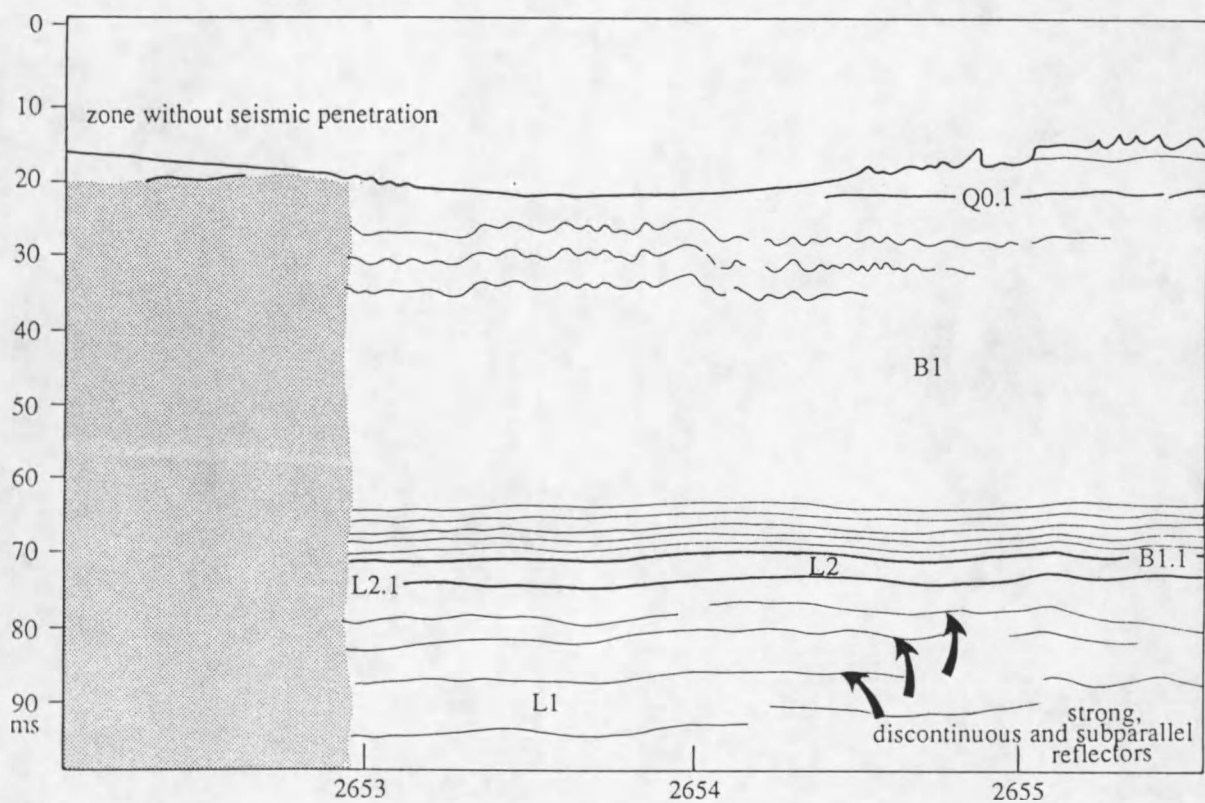
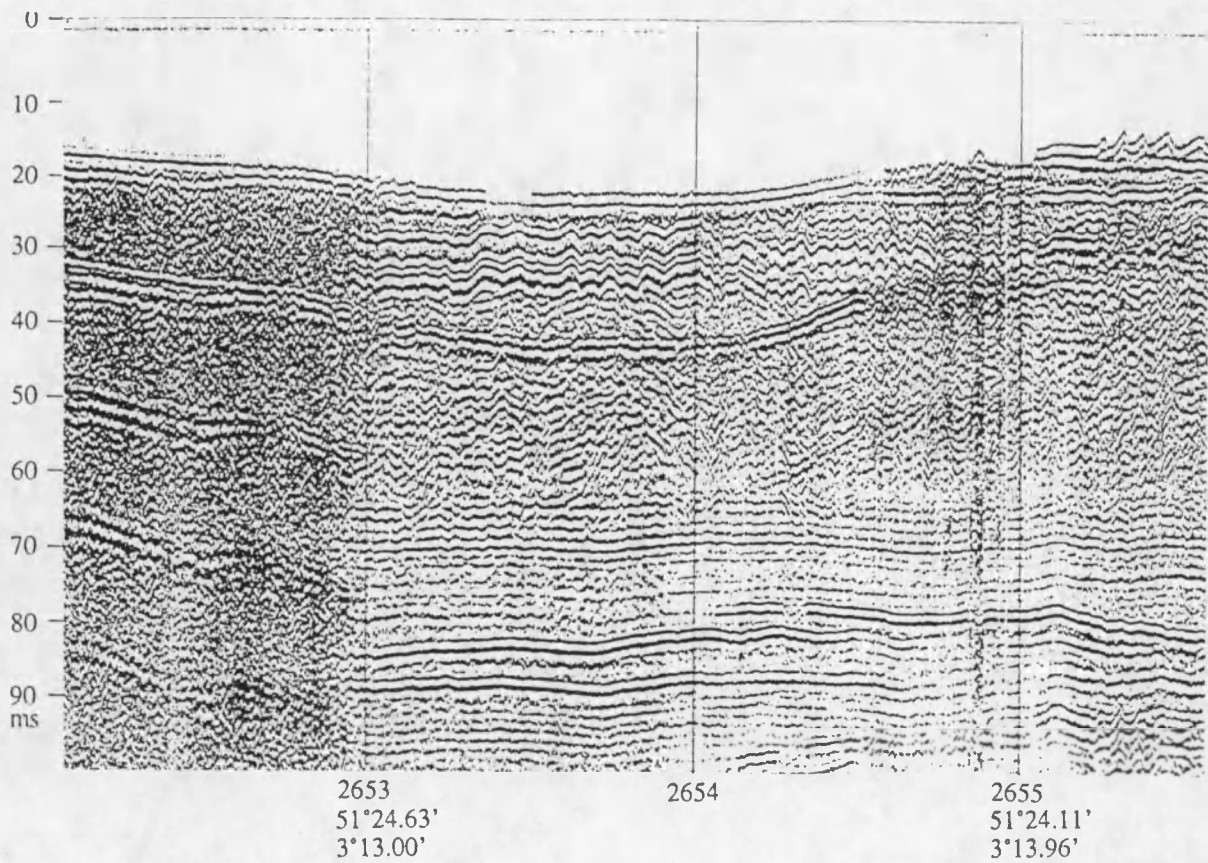


Figure 5.9 Analog record of a sparker section and interpreted line-drawing showing the L1 sequence (after De Batist, 1989).

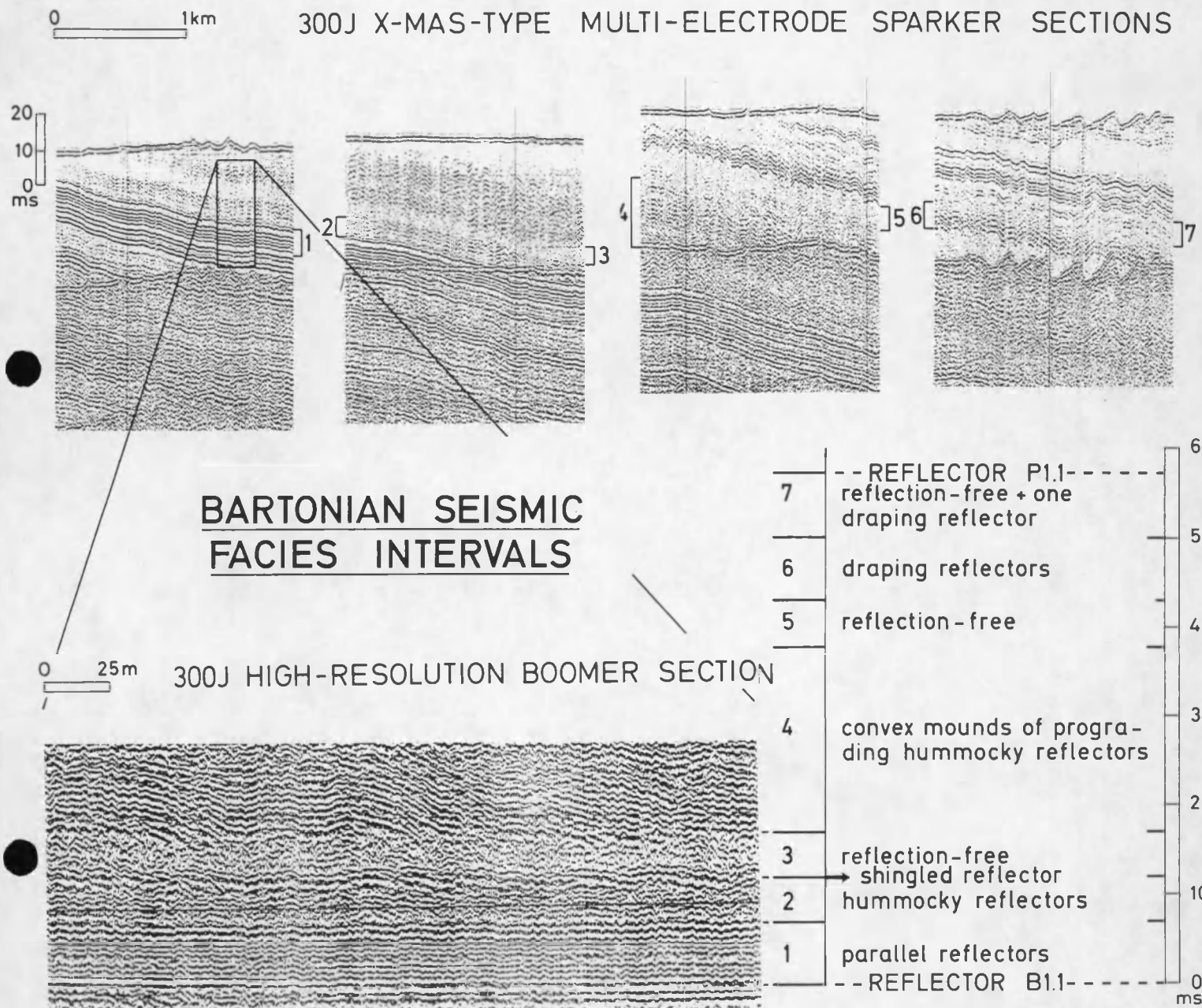


Figure 5.10 Analog record of a boomer section and interpreted line-drawing showing the different seismic facies units in the B1 sequence (after Henri et al., 1989).

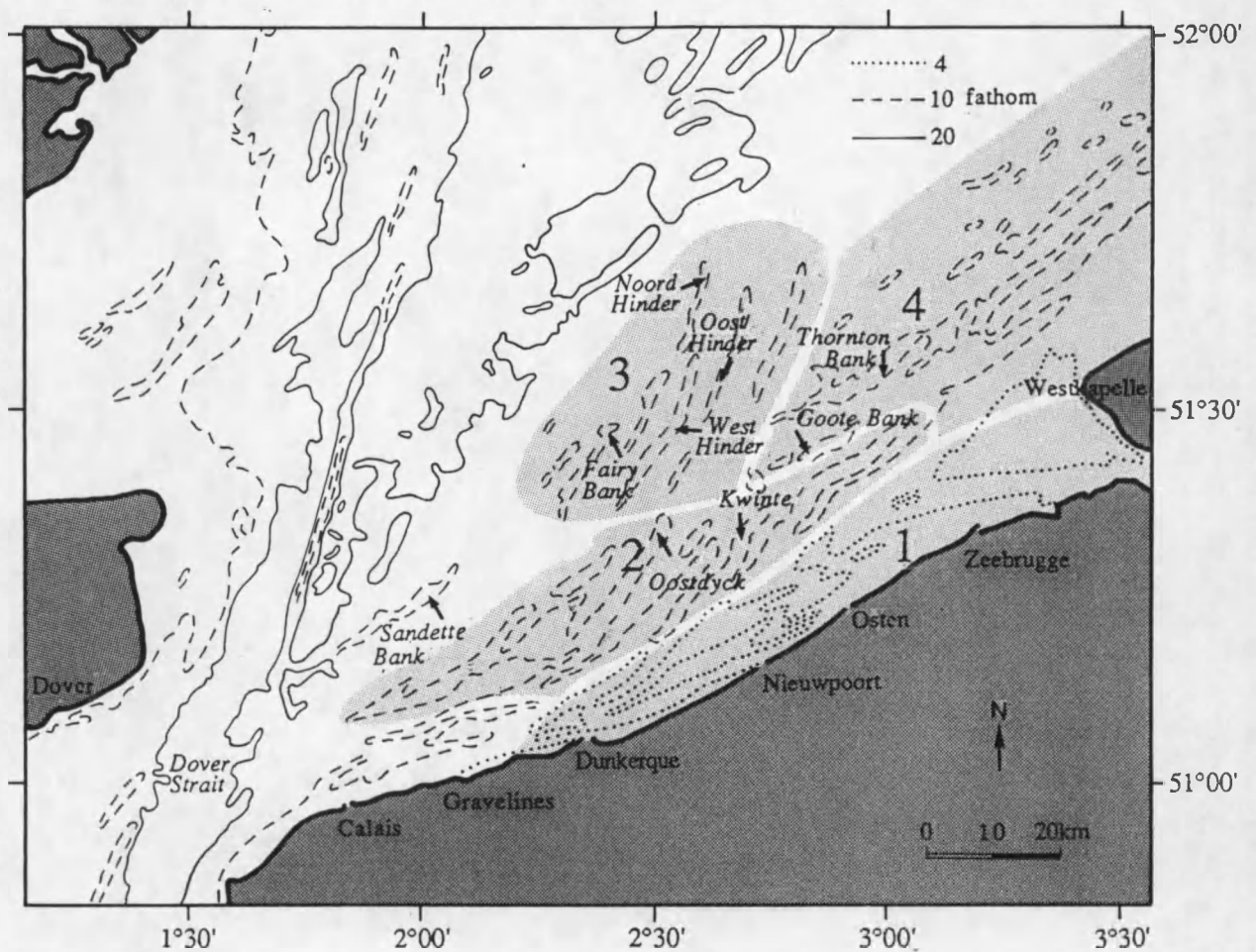


Figure 5.11 Location of tidal sand banks in the study area
 1. The Coastal Banks and mouth of the river Scheldt
 2. The Flemish Banks
 3. The Hinder group
 4. The Zeeland ridges (after Bastin, 1974).

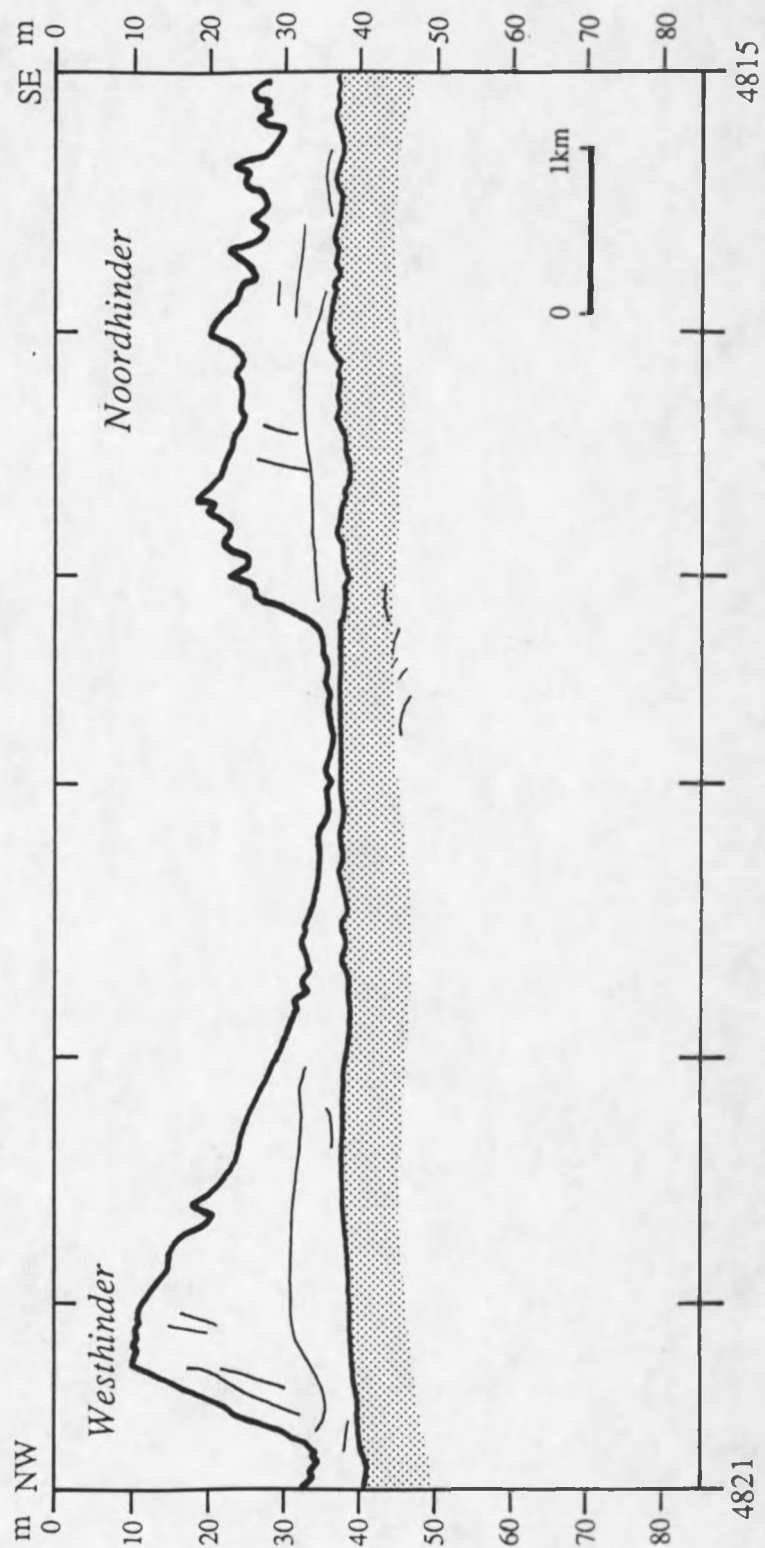
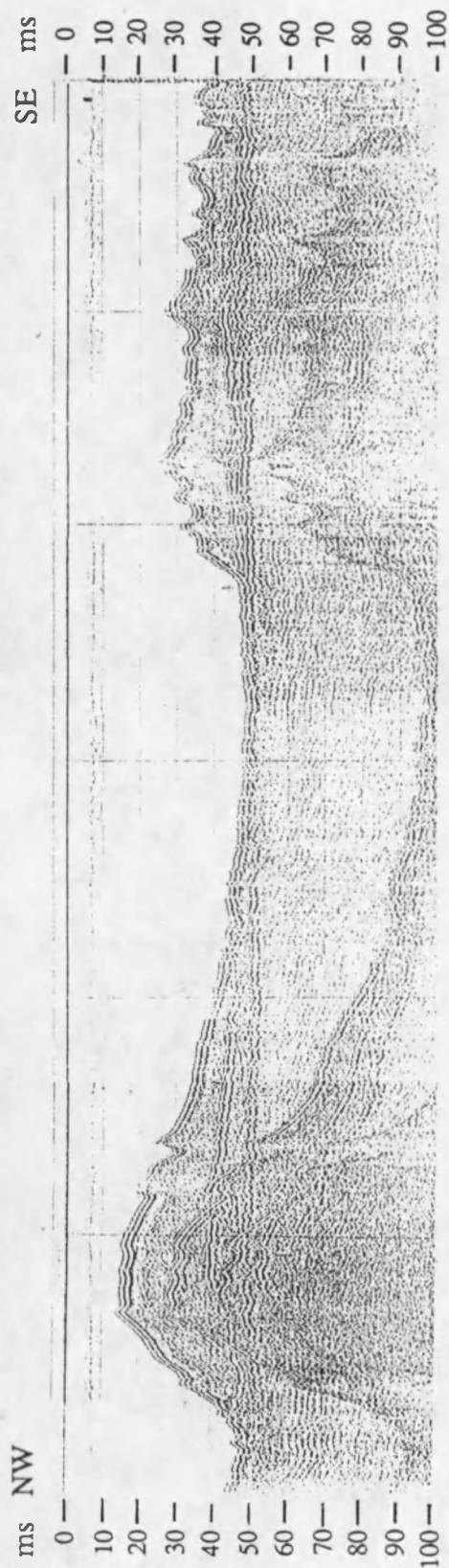


Figure 5.12 Analog record of a sparker section and interpreted line-drawing showing the seismic facies of a tidal sand bank.

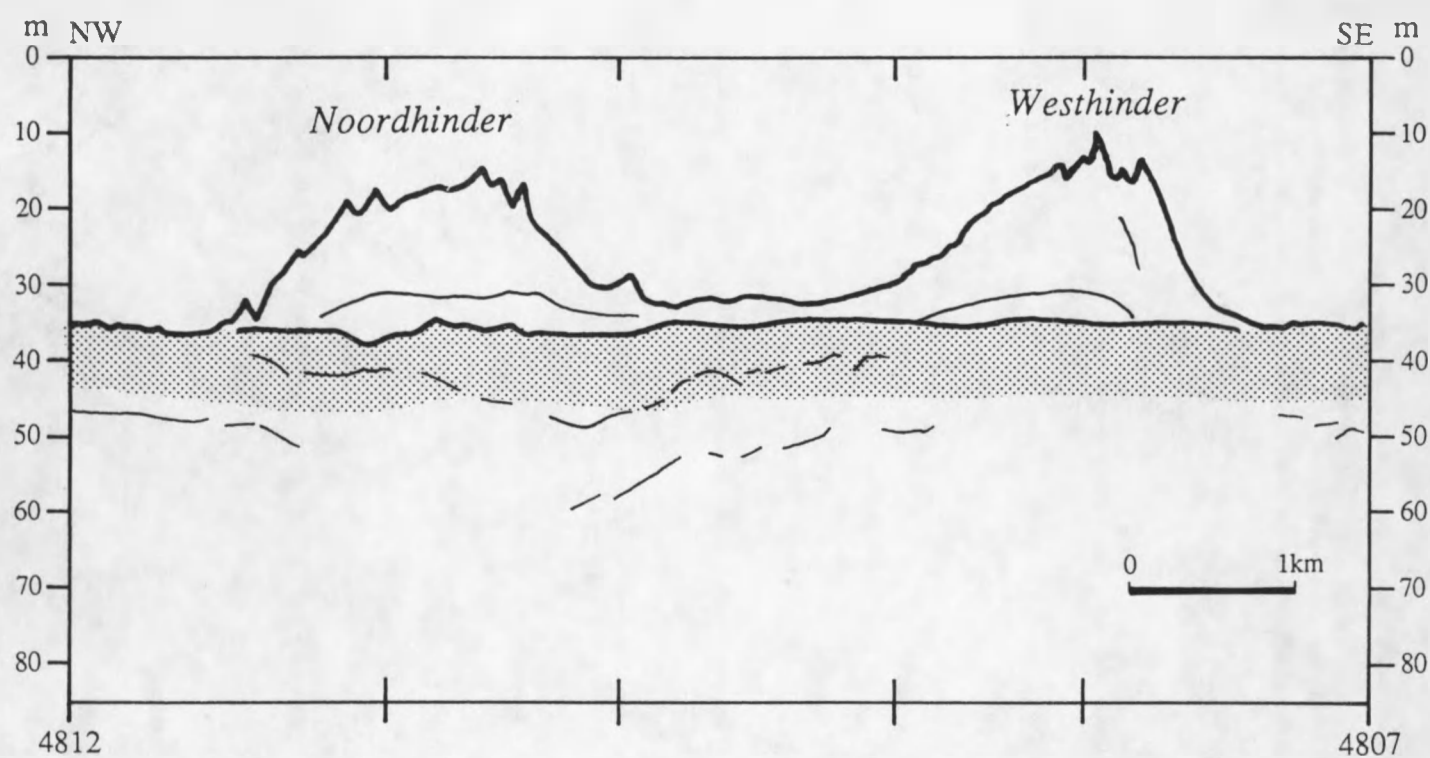
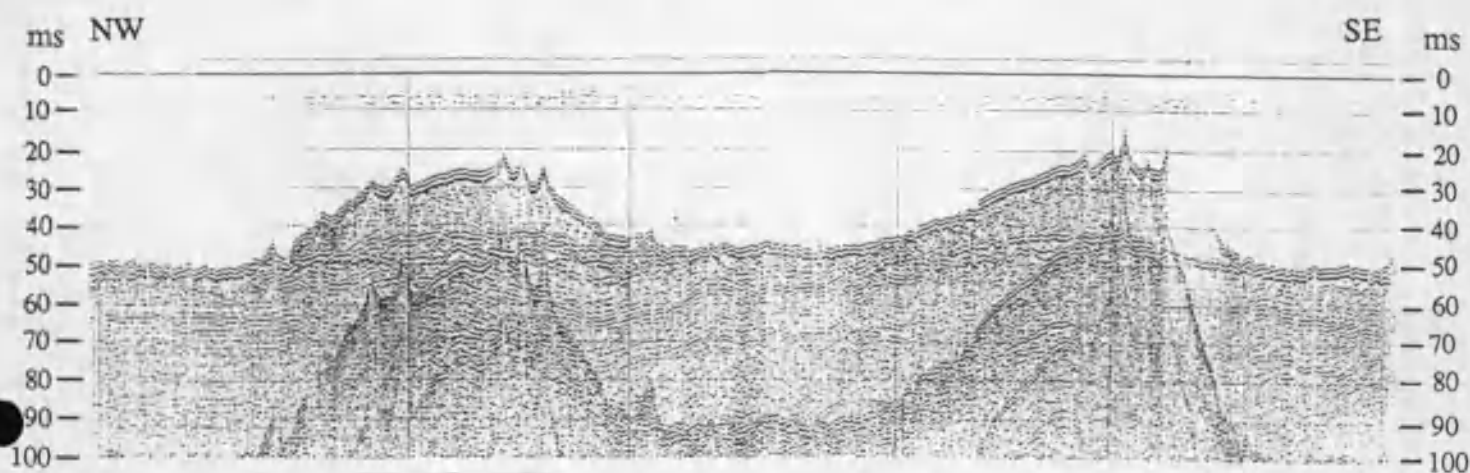


Figure 5.13 Analog record of a sparker section and interpreted line-drawing showing sand banks of the Hinder group, containing sedimentary nuclei.

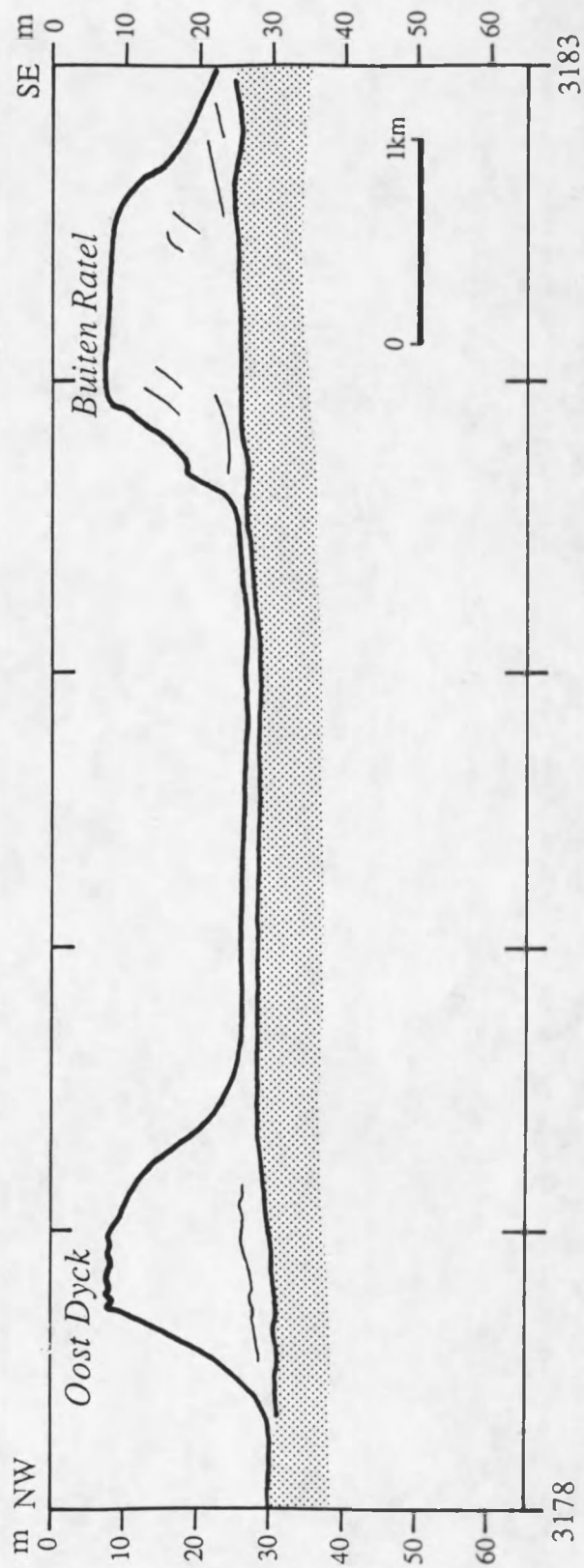
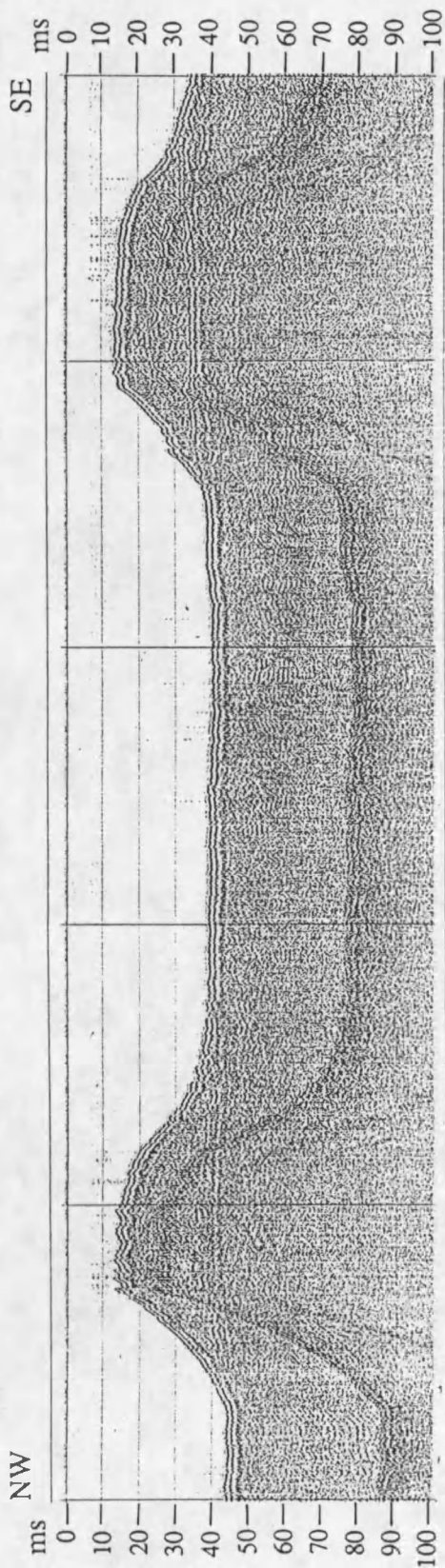


Figure 5.14 Analog record of a sparker section and interpreted line-drawing showing the Flemish Banks.

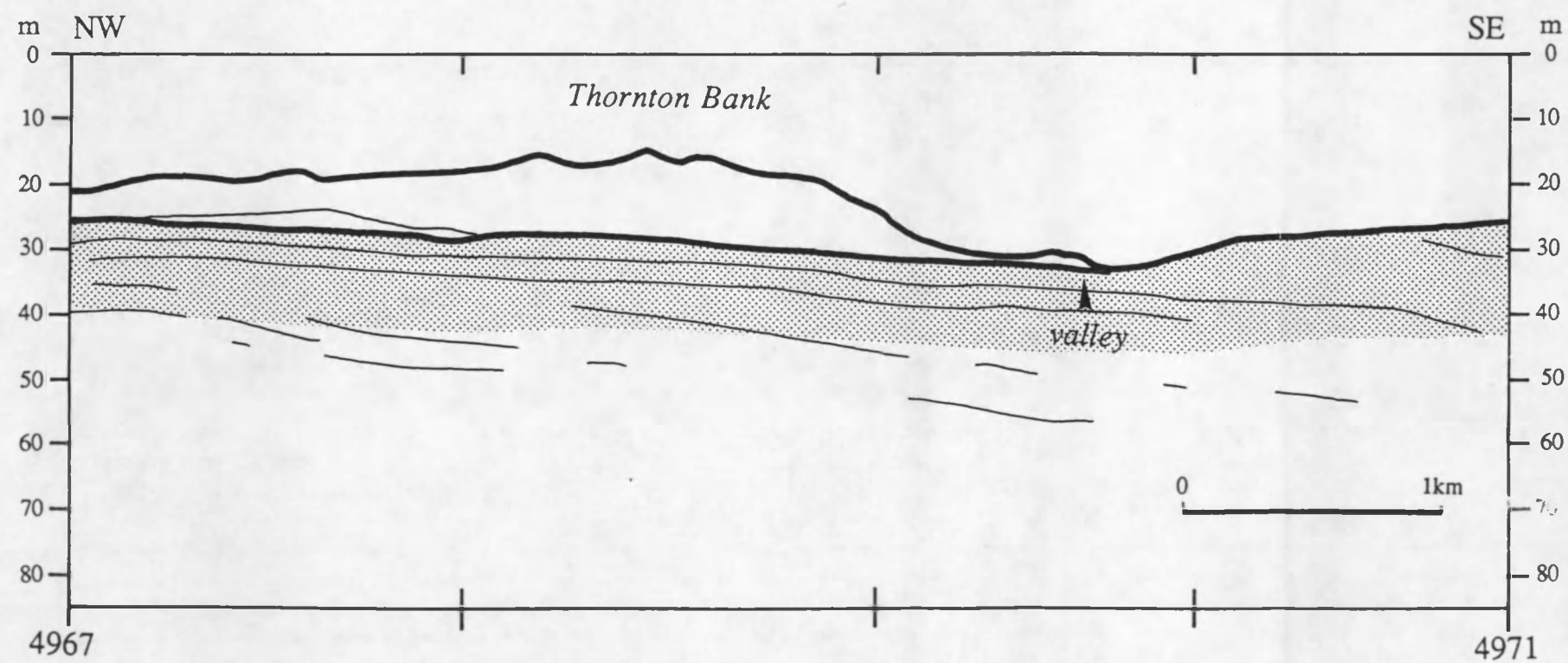
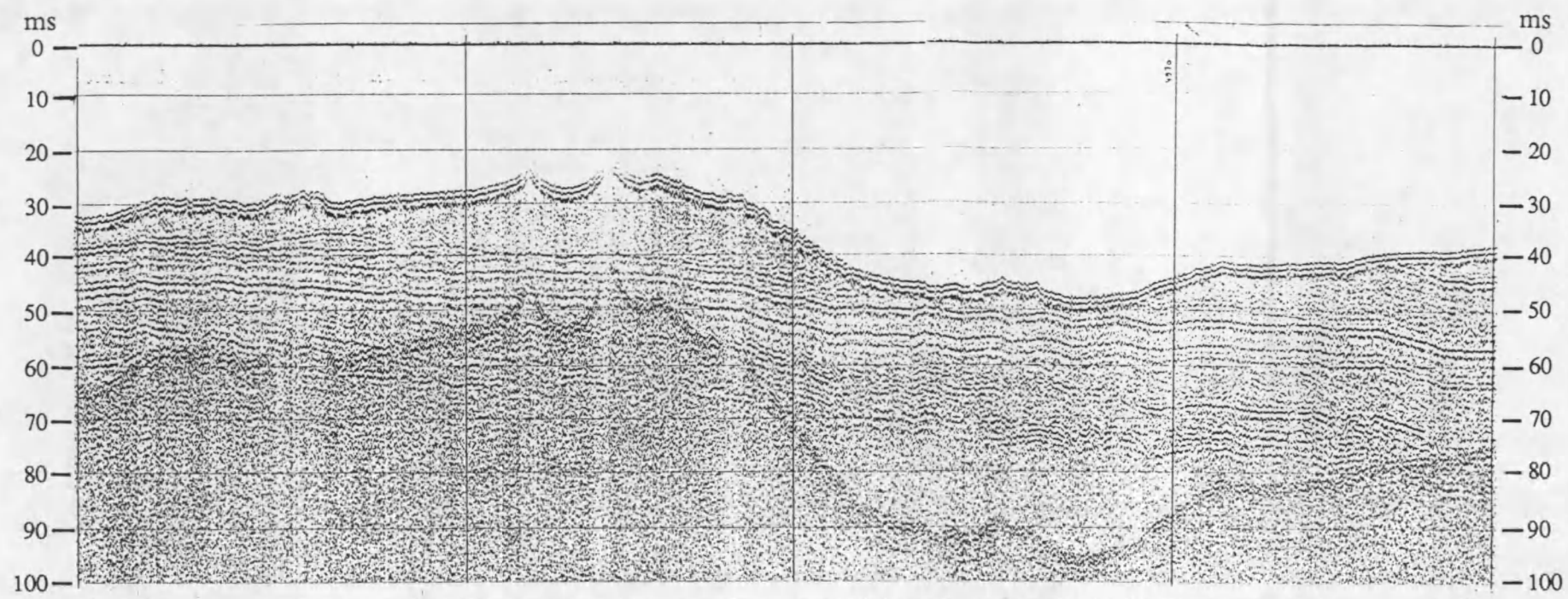


Figure 5.15 Analog record of a sparker section and interpreted line-drawing showing a valley bounding the Thornton Bank.

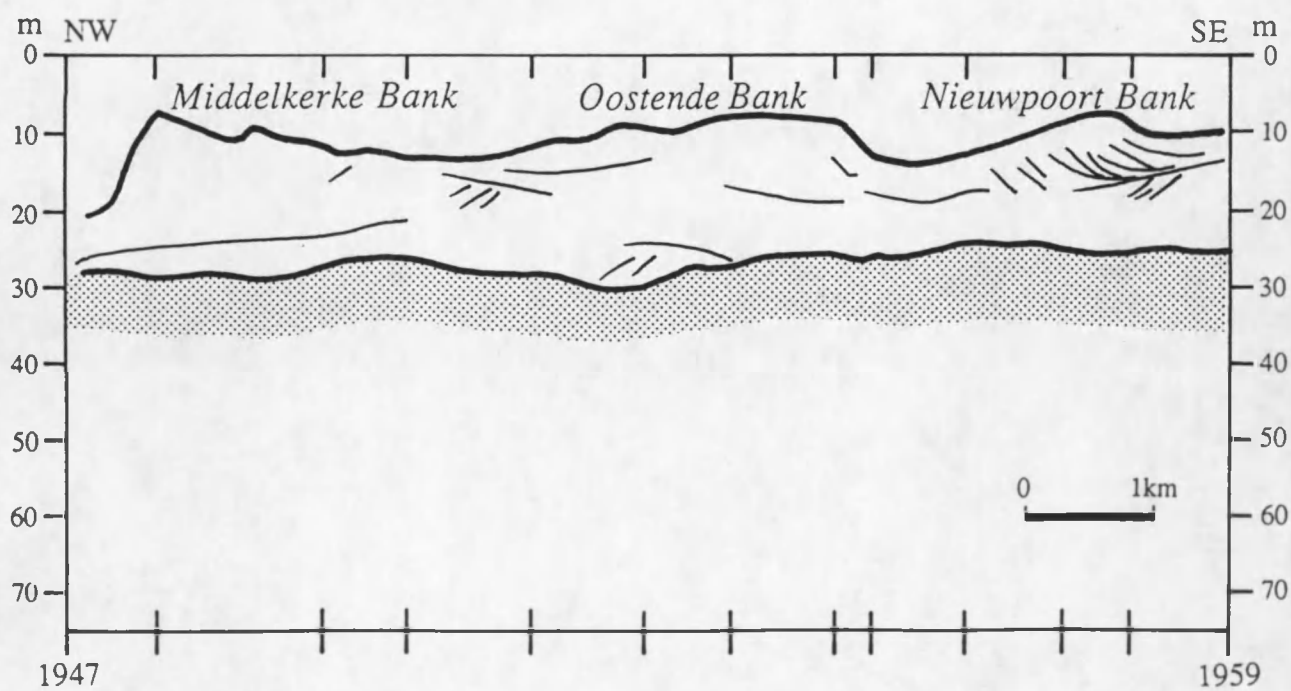
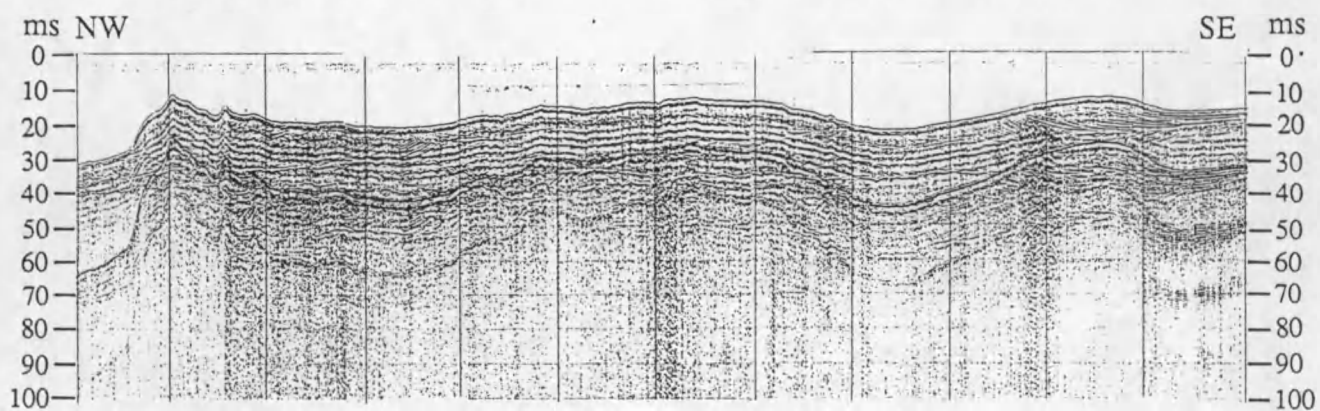
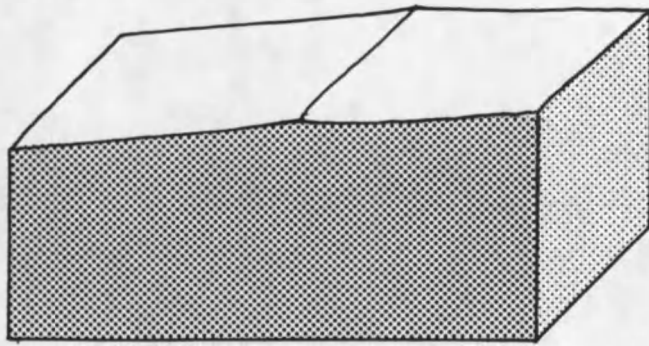
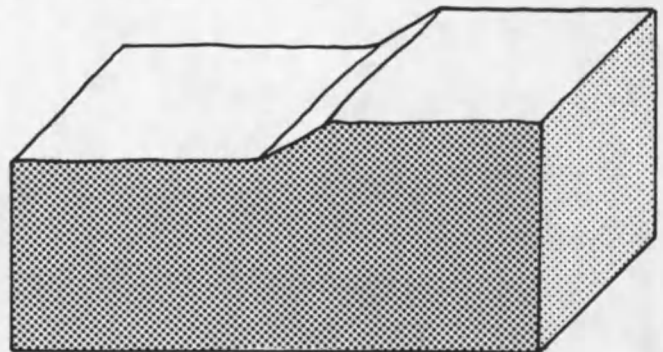


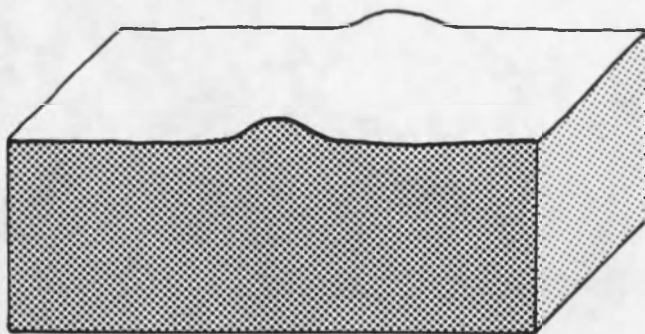
Figure 5.16 Analog record of a sparker section and interpreted line-drawing showing the Coastal Banks.



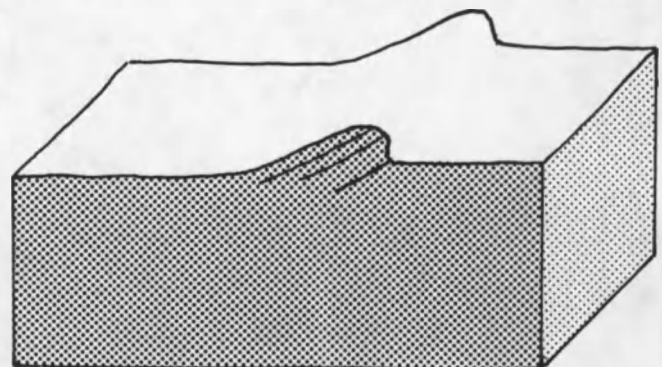
(a)



(b)



(c)



(d)

Figure 6.2 Schematic 3D representation of different types of planation surface boundaries
 a. slope break
 b. scarp
 c. ridge
 d. cuesta

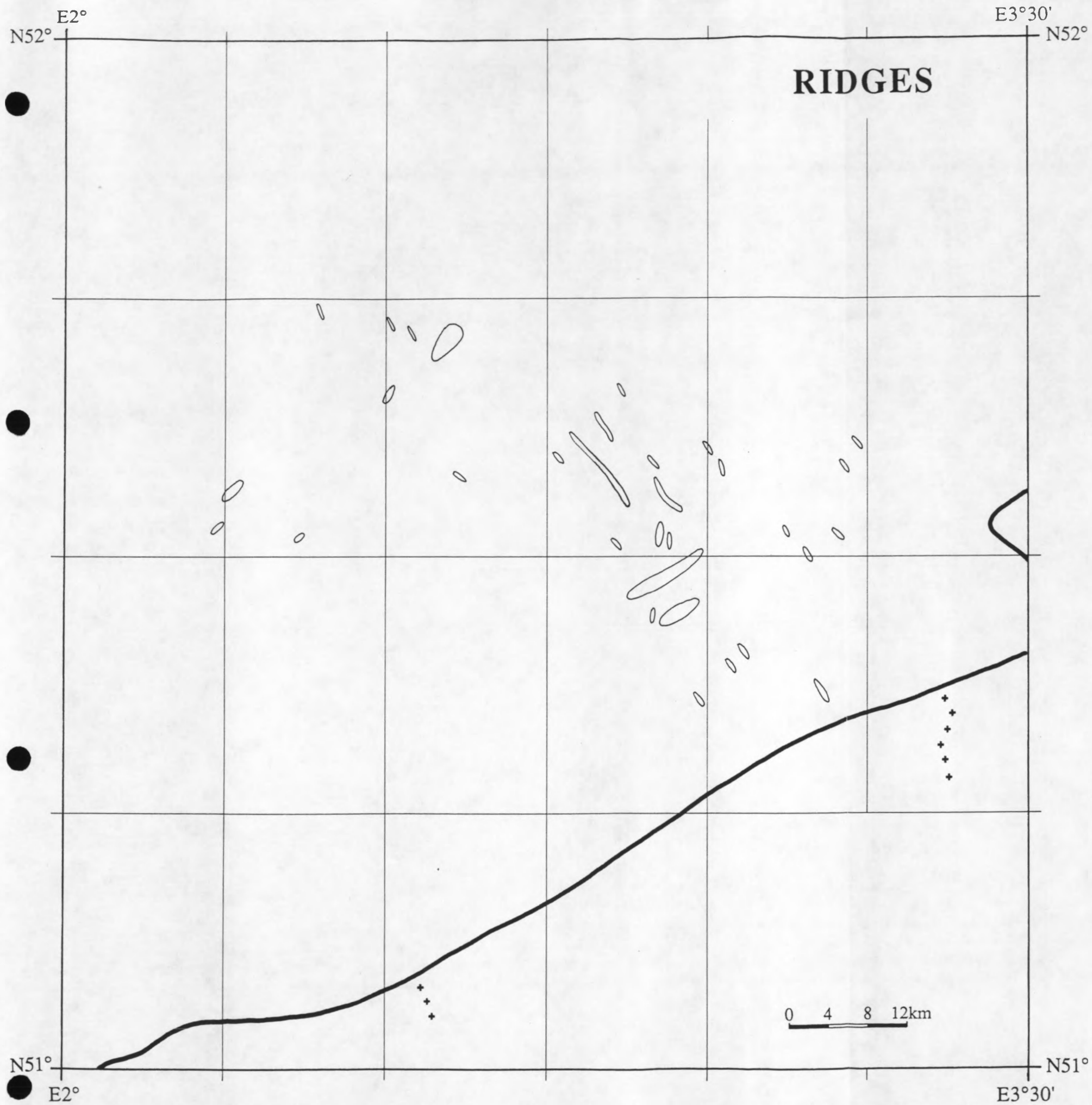


Figure 6.3 Distribution of ridges in the study area.

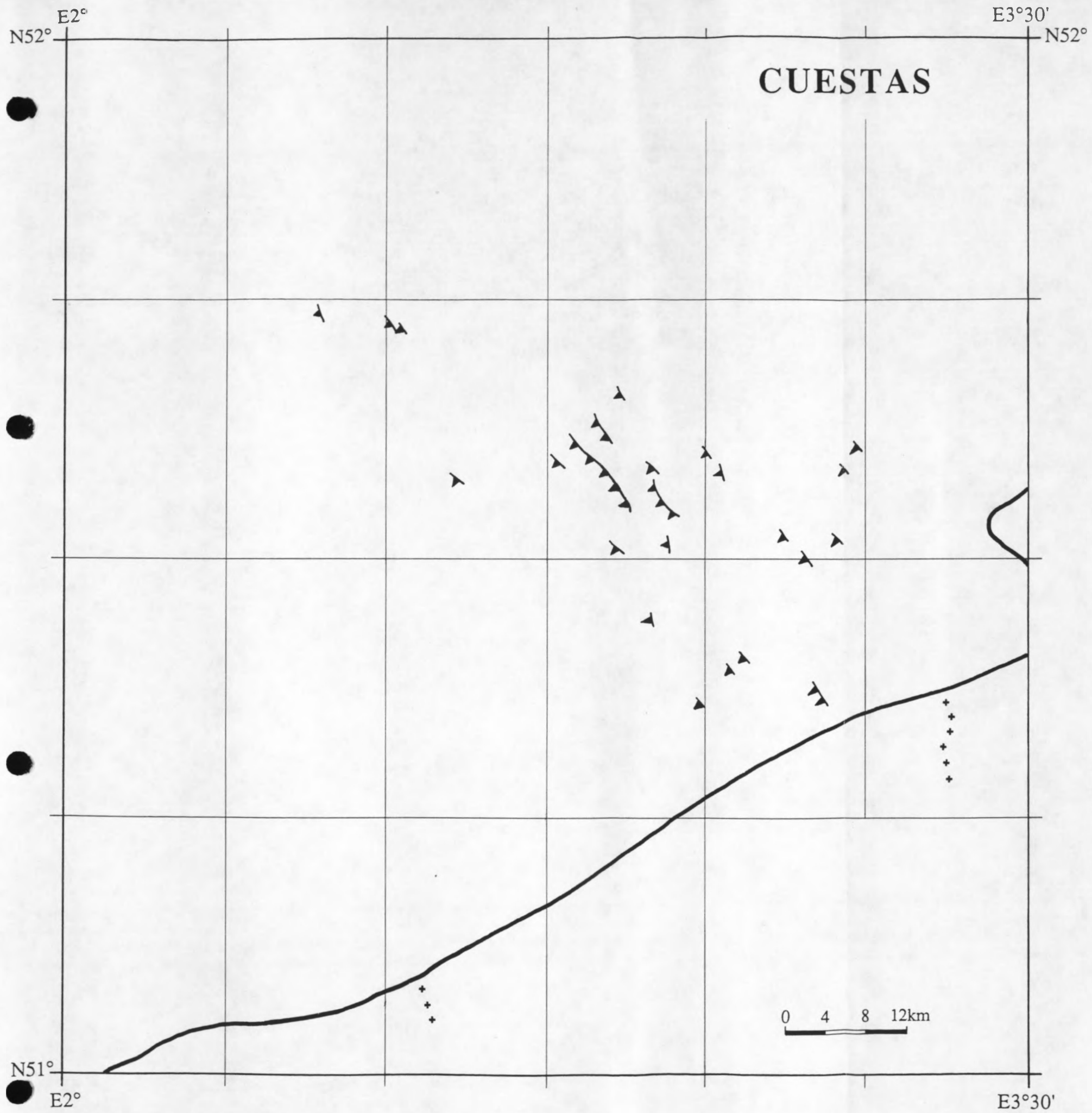


Figure 6.4 Distribution of cuestas in the study area.

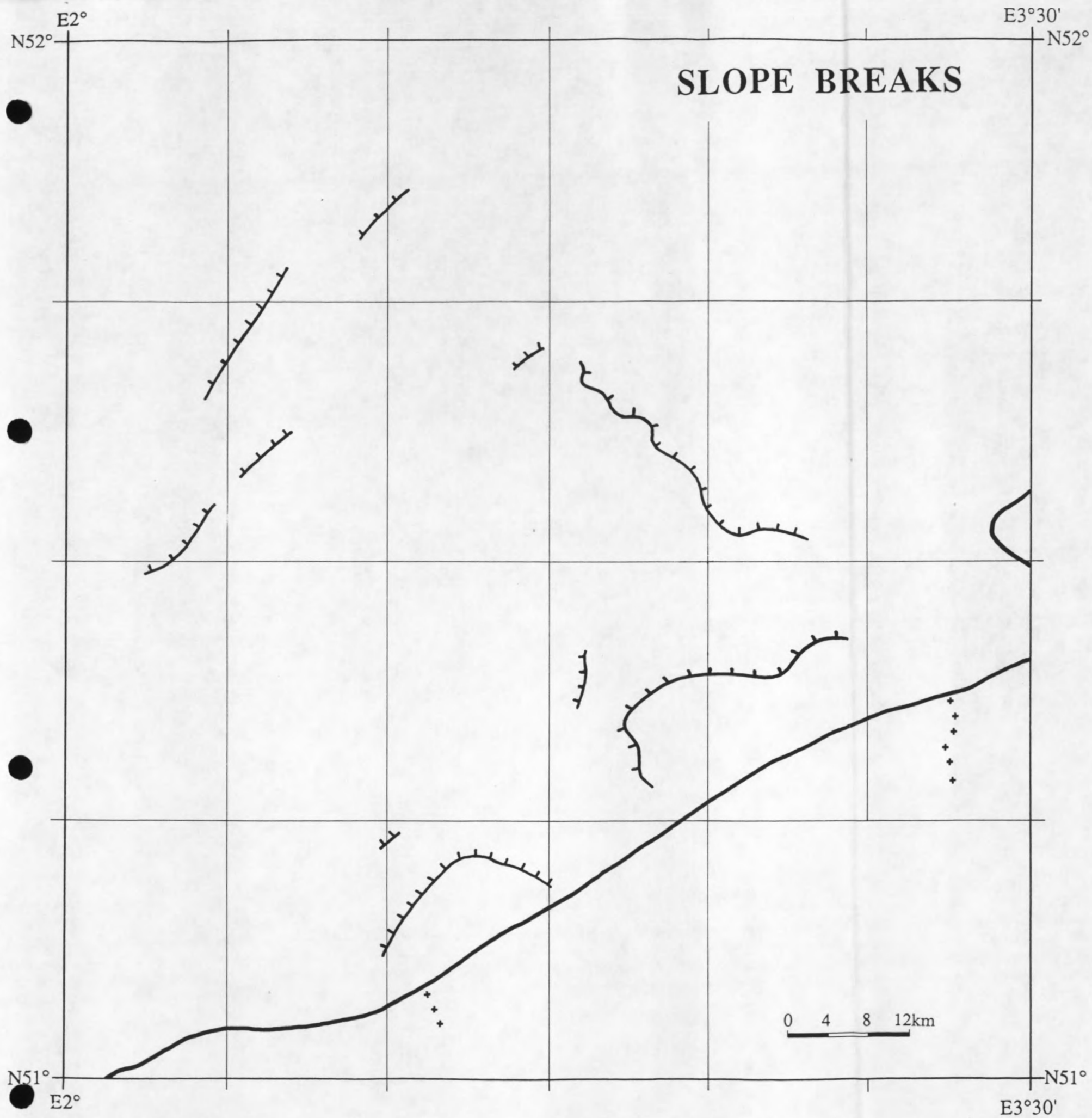


Figure 6.5 Distribution of slope breaks in the study area.

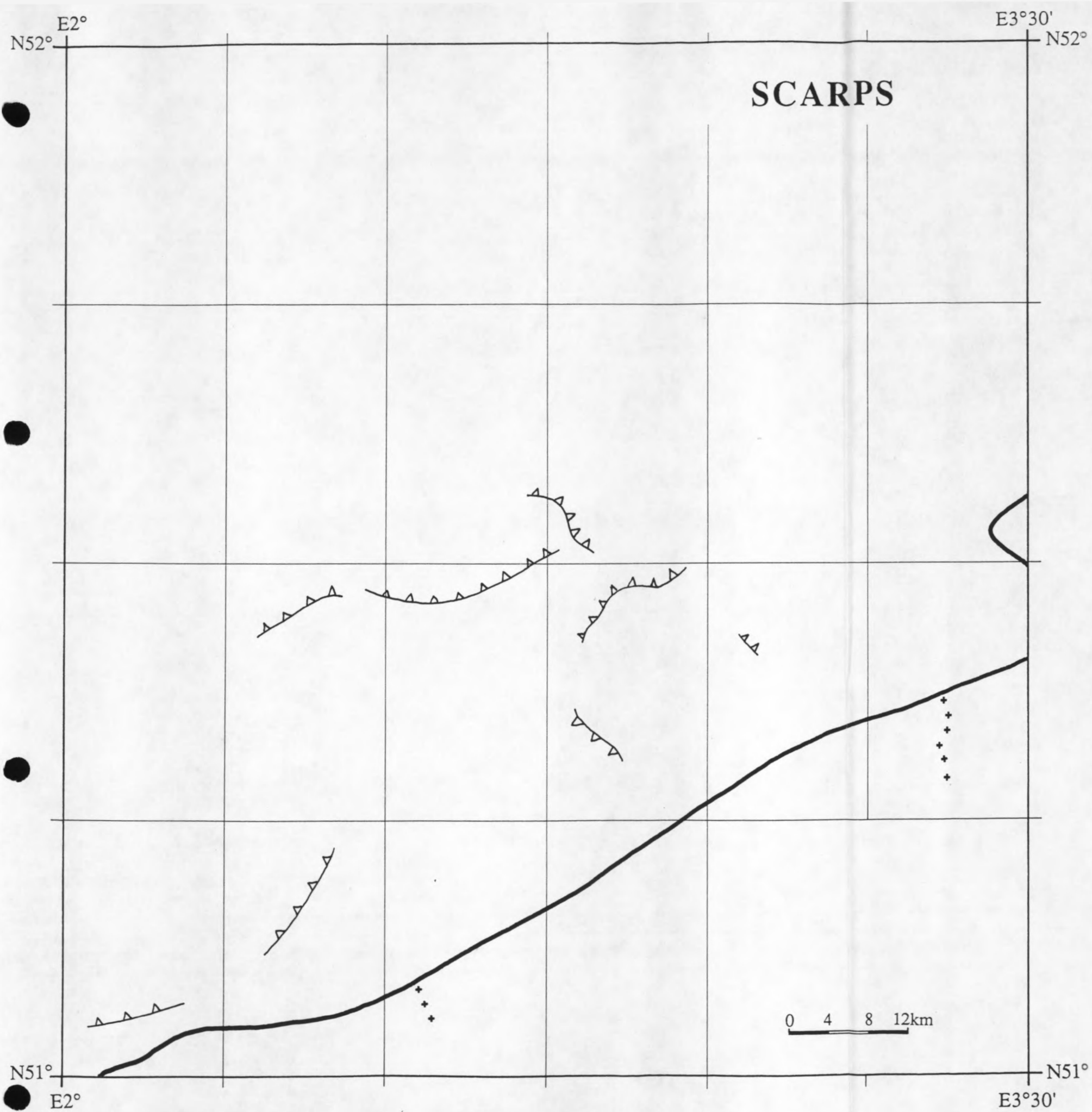


Figure 6.6 Distribution of scarps in the study area.

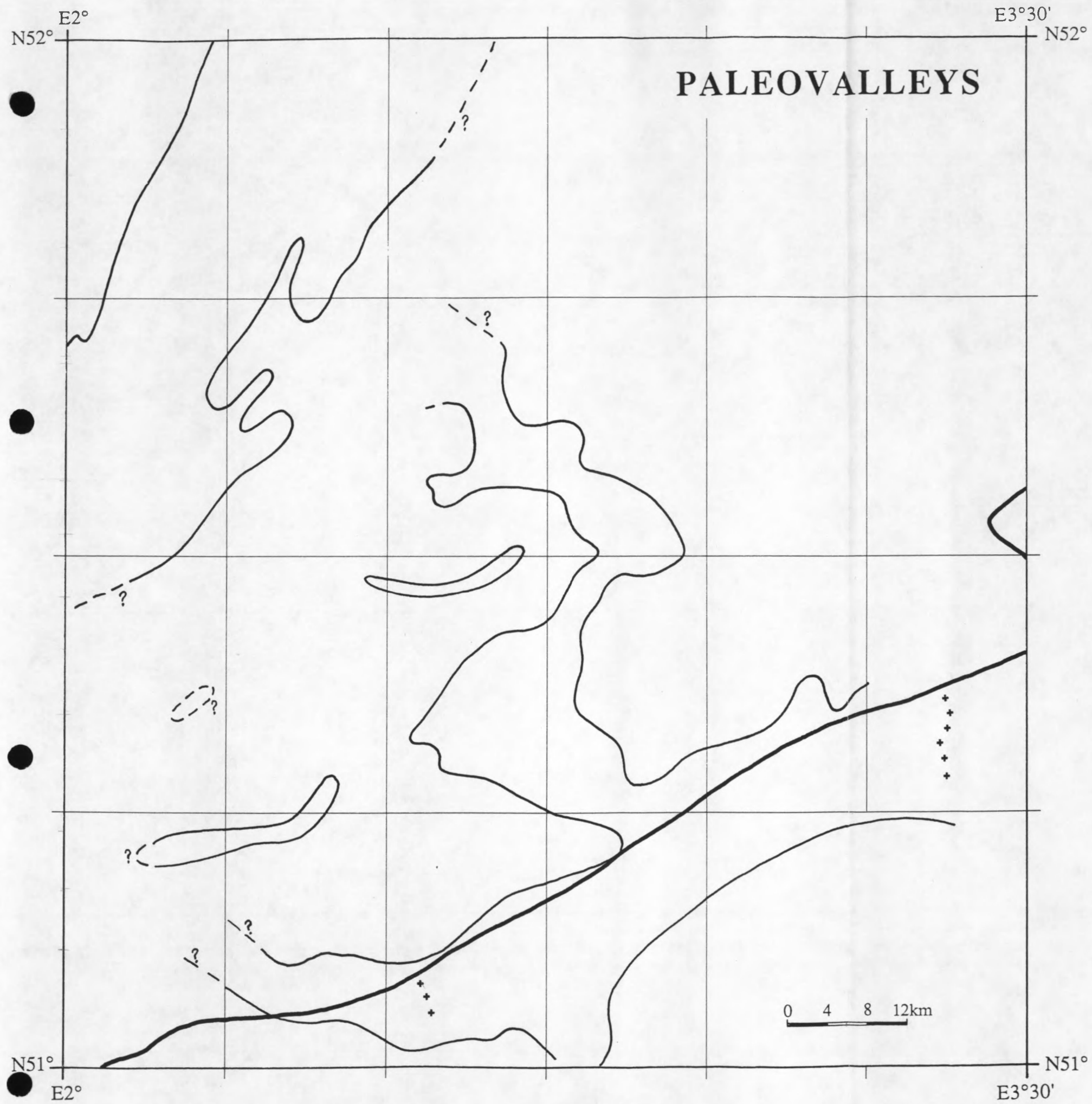


Figure 6.7 Distribution of paleovalleys in the study area.

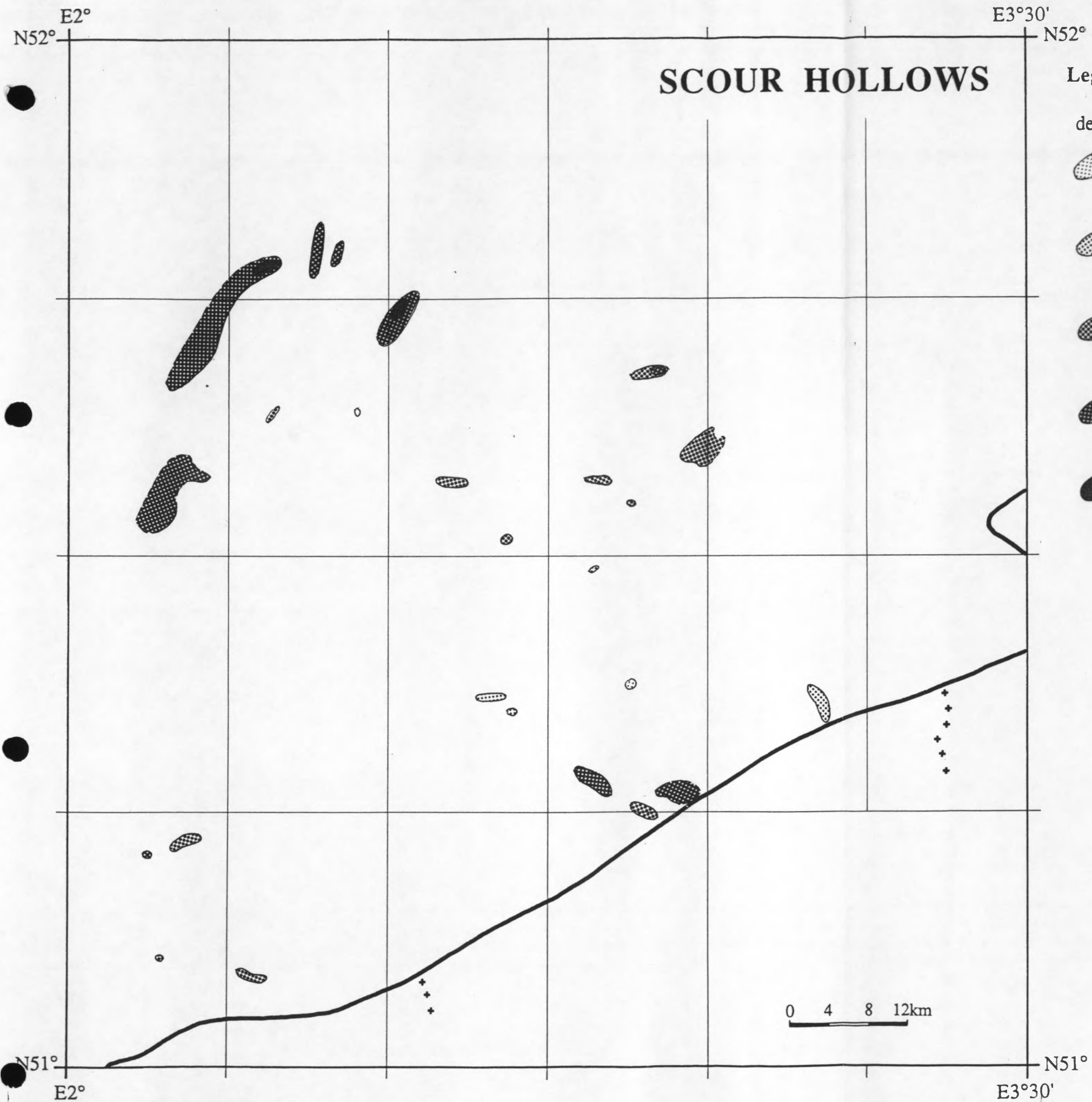


Figure 6.8 Distribution of pits in the study area.

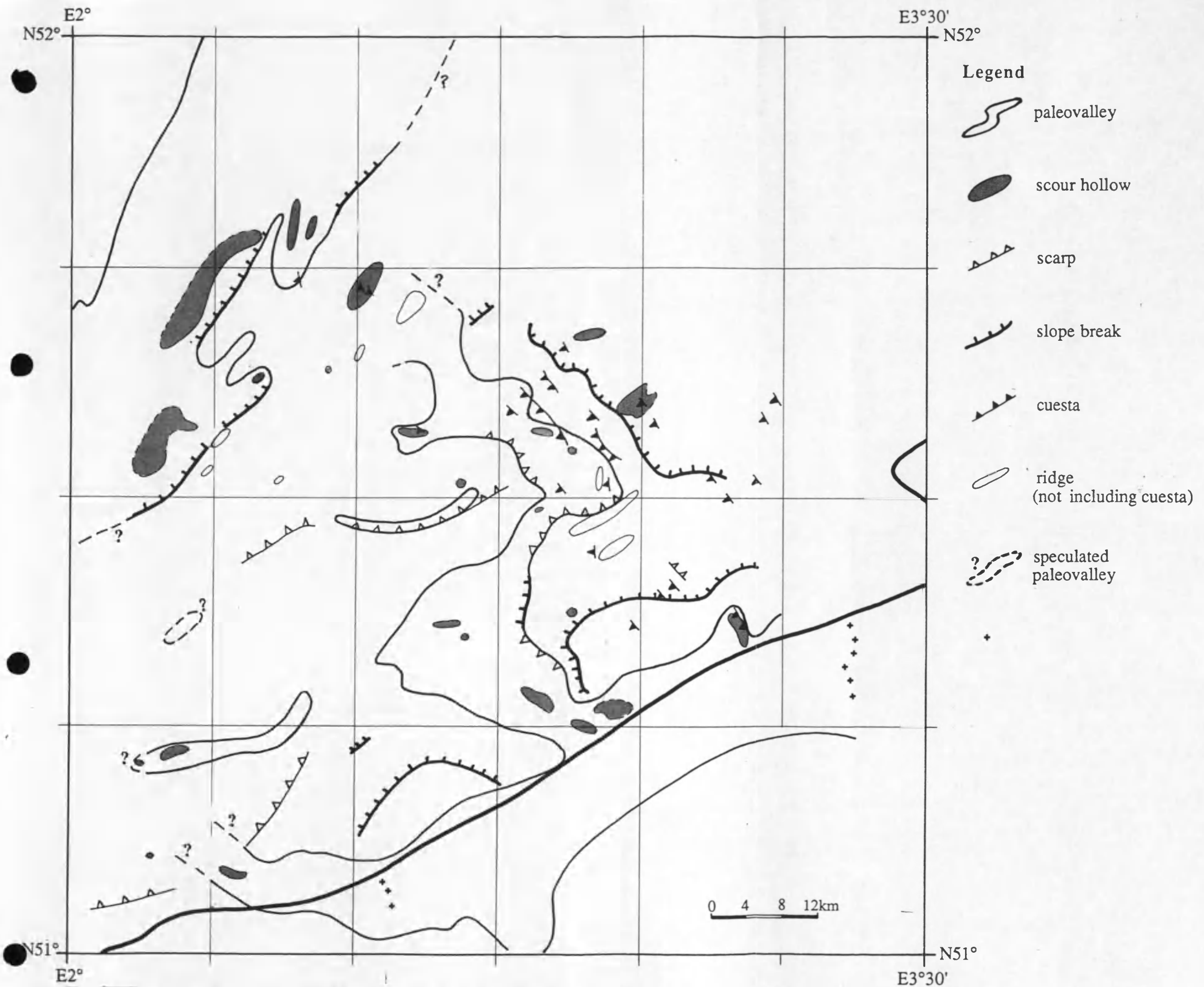


Figure 6.9 Distribution of different morphological features in the study area.

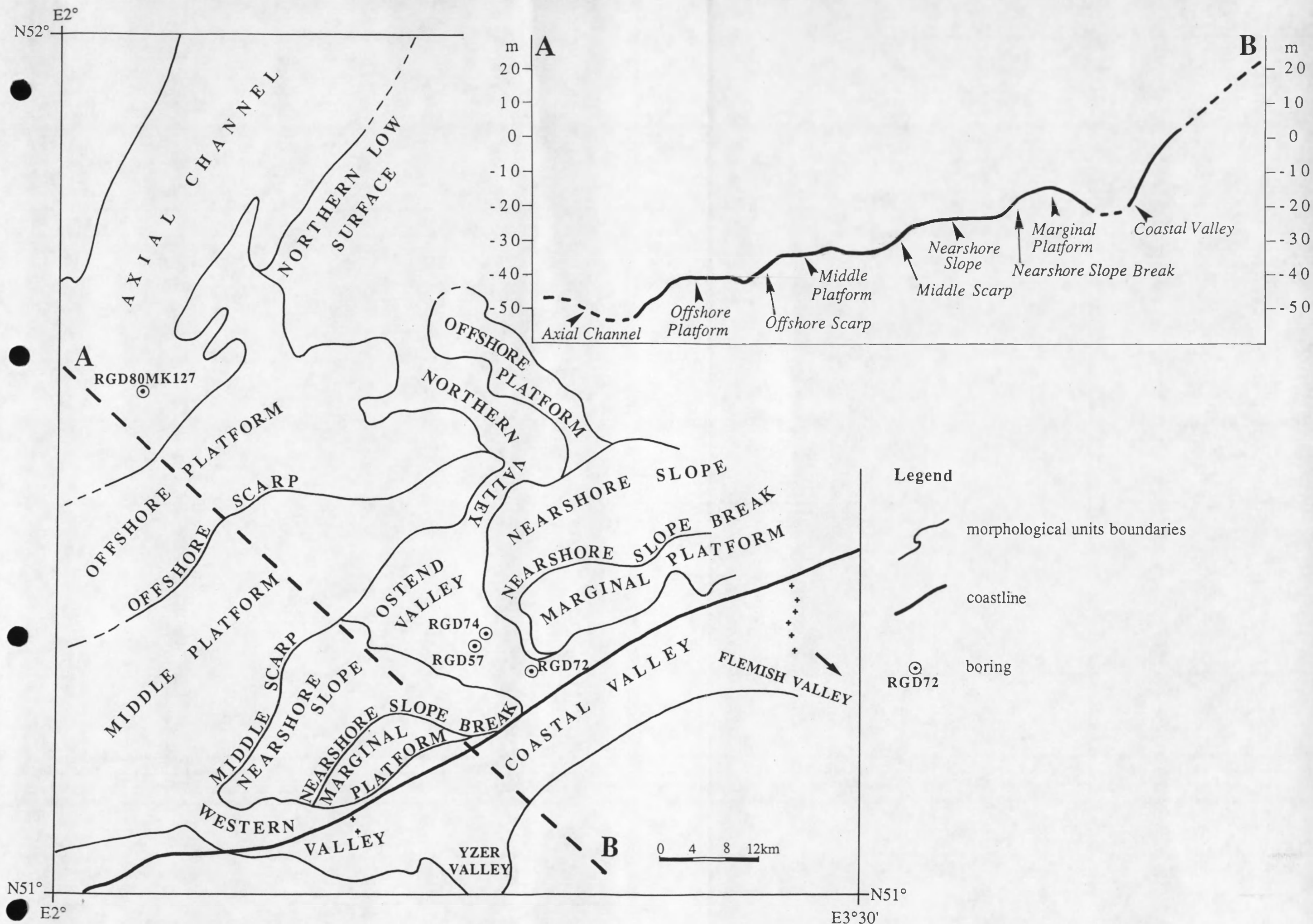


Figure 6.10 Distribution of morphological units in the study area.

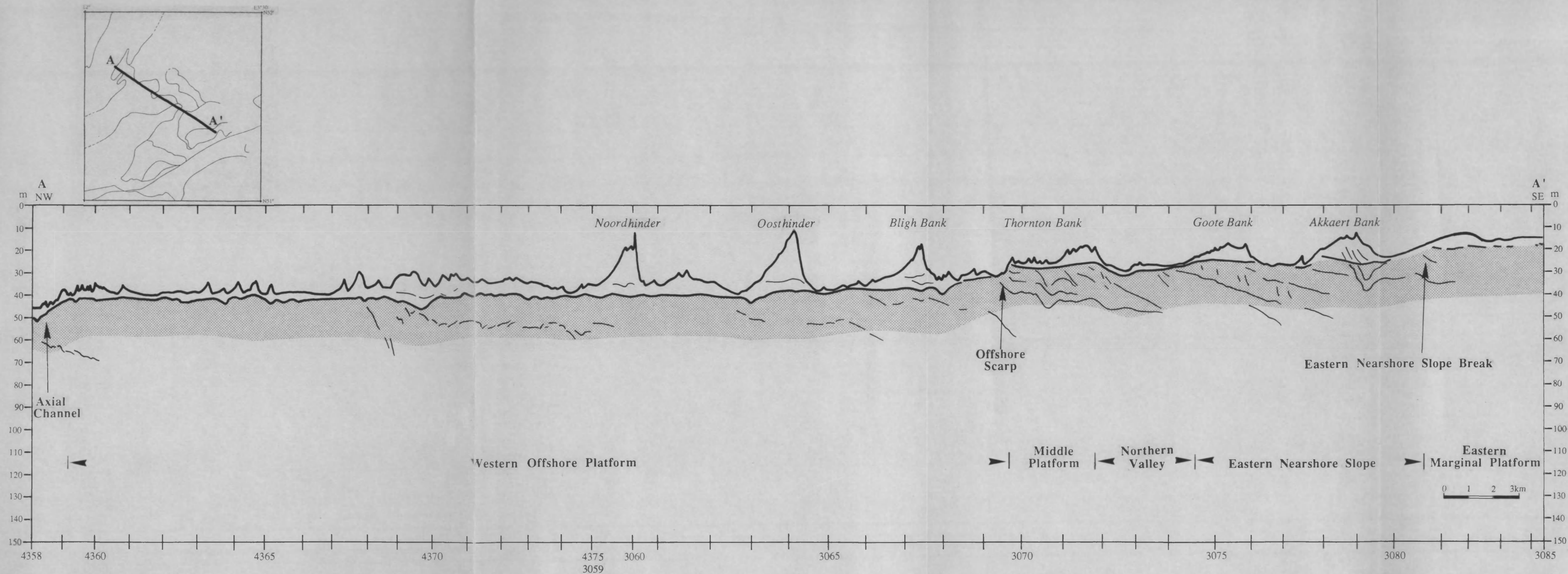


Fig. 3

Figure 6.11a Interpreted line-drawing of cross-section A-A'.

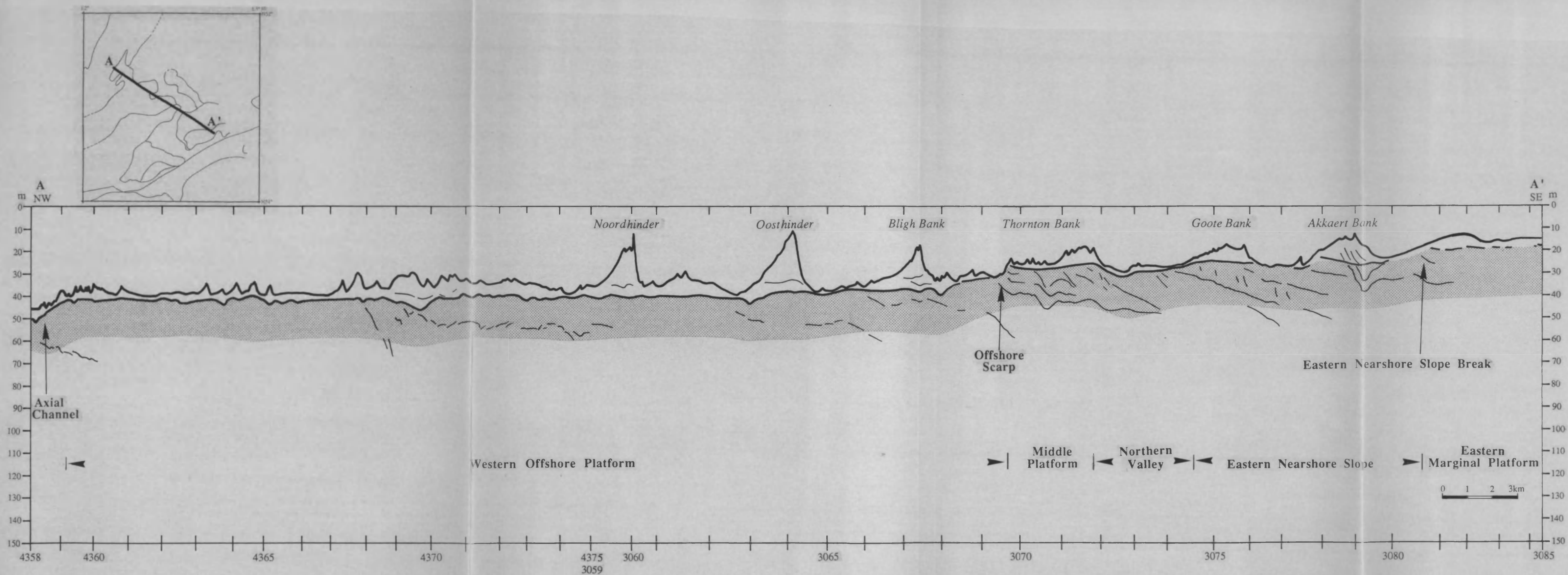


Figure 6.11a Interpreted line-drawing of cross-section A-A'.

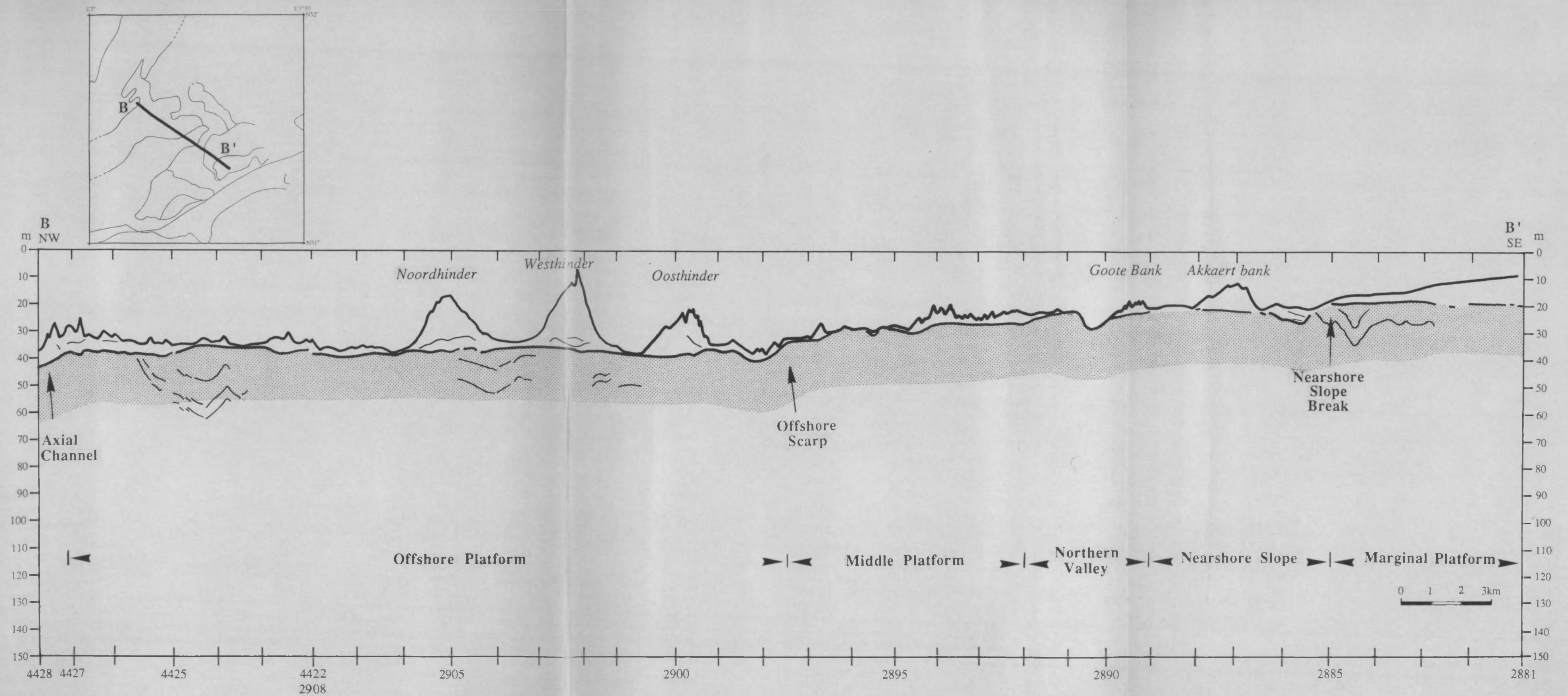


Figure 6.11b Interpreted line-drawing of cross-section B-B'.

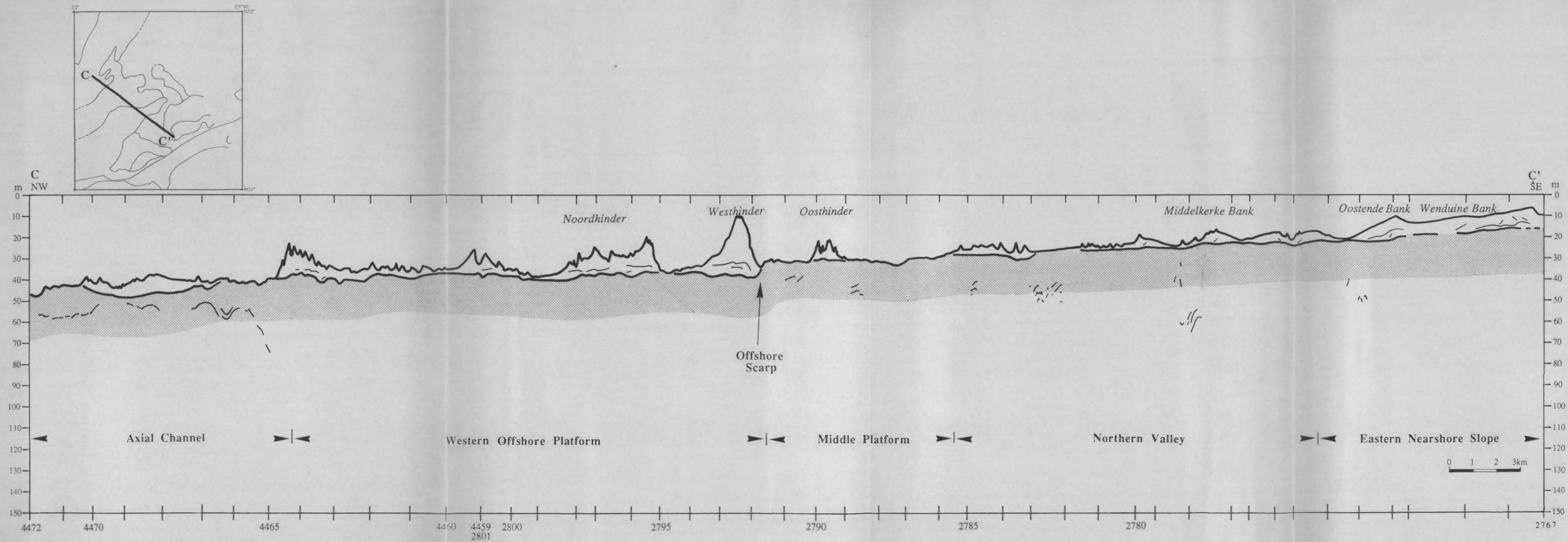


Figure 6.11c Interpreted line-drawing of cross-section C-C'.

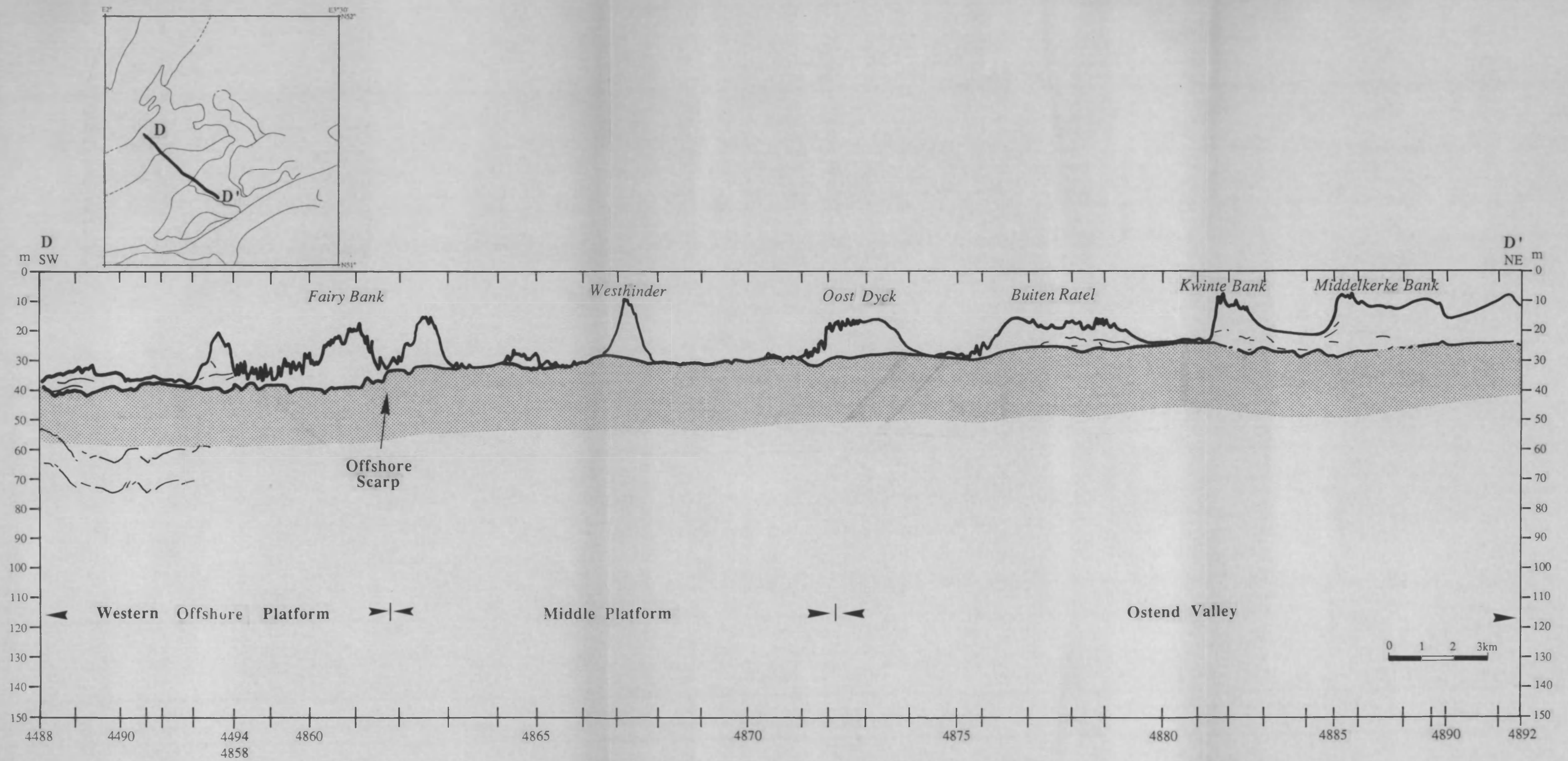


Figure 6.11d Interpreted line-drawing of cross-section D-D'.

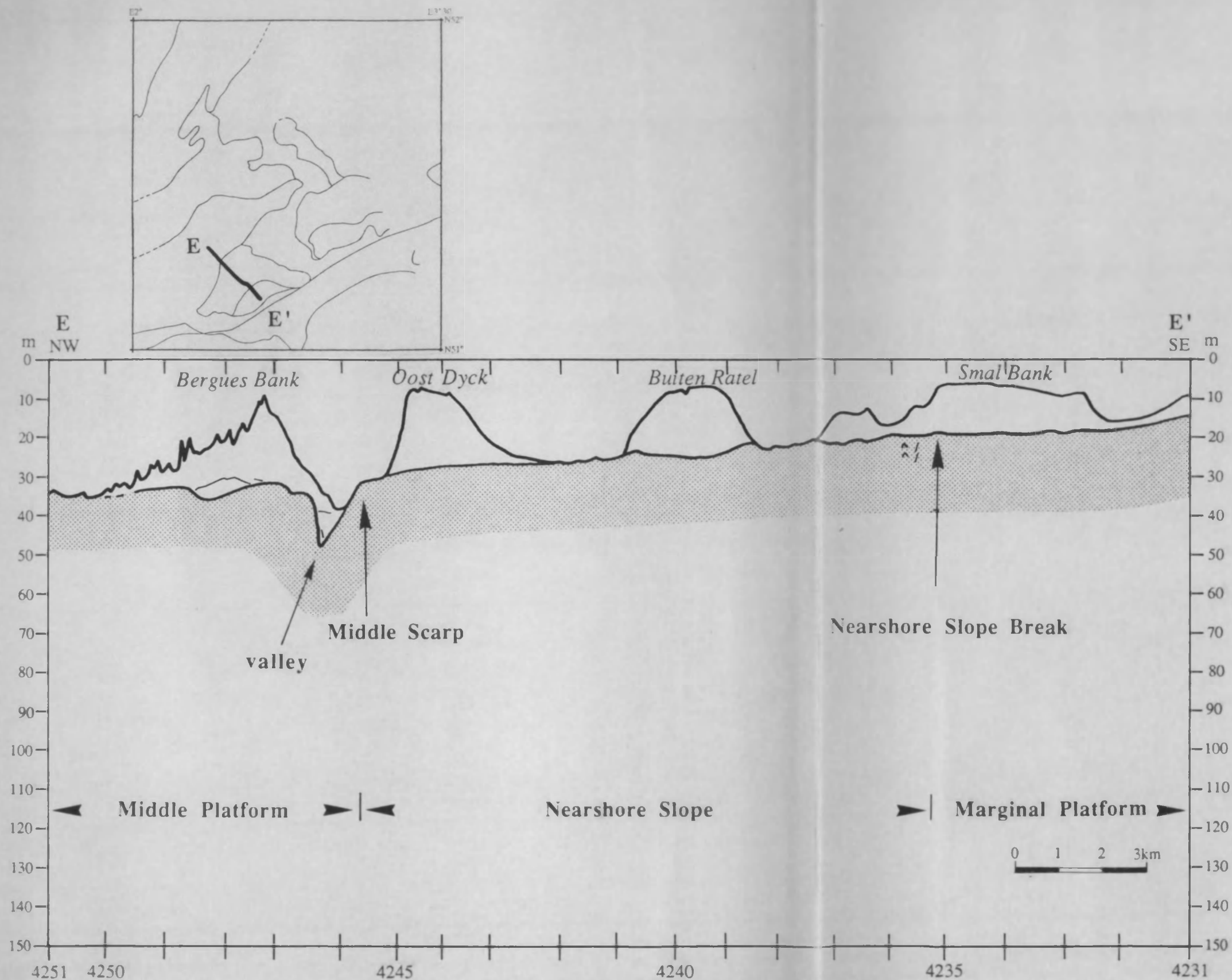


Figure 6.11e Interpreted line-drawing of cross-section E-E'.

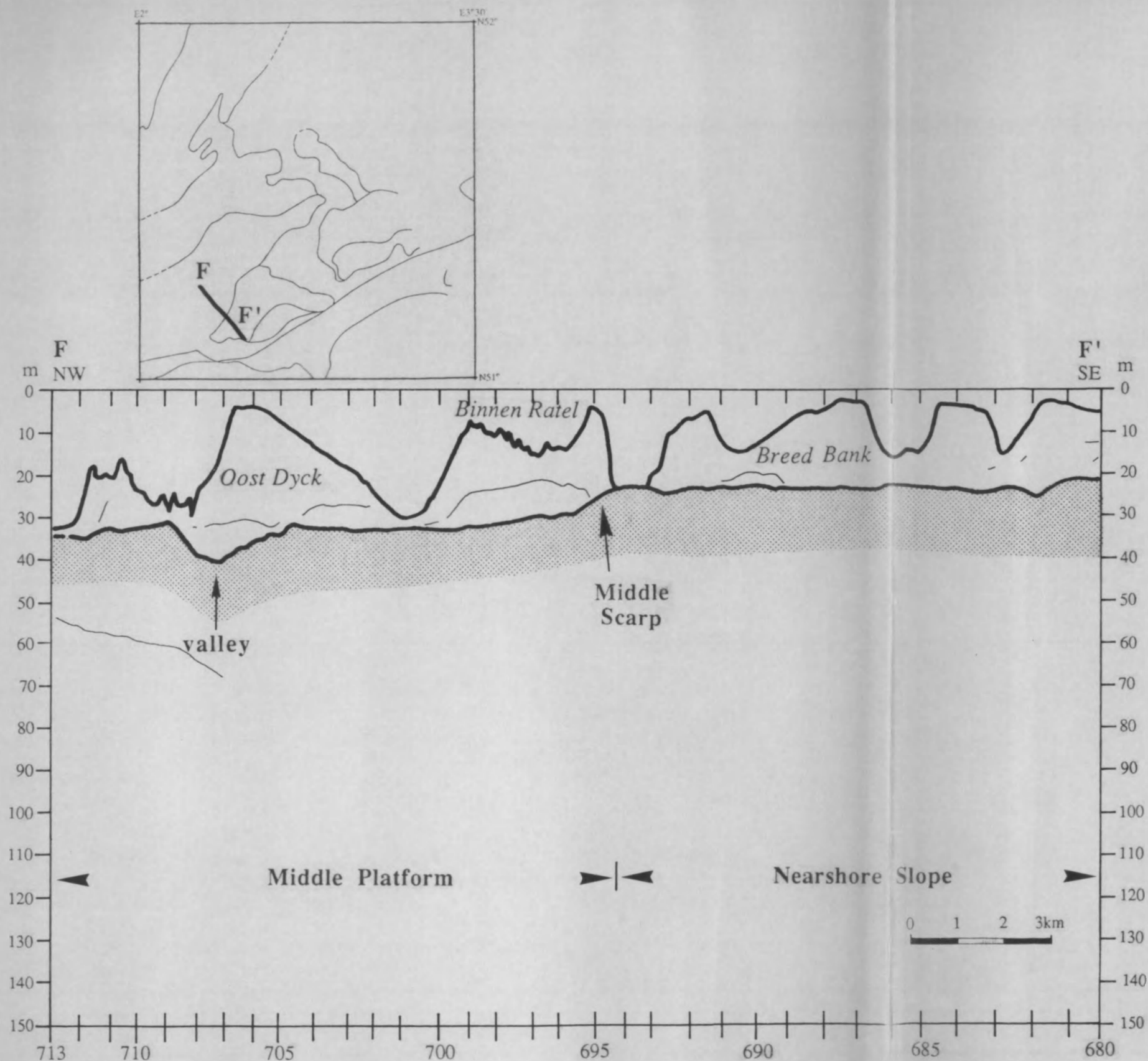


Figure 6.11f Interpreted line-drawing of cross-section F-F'.

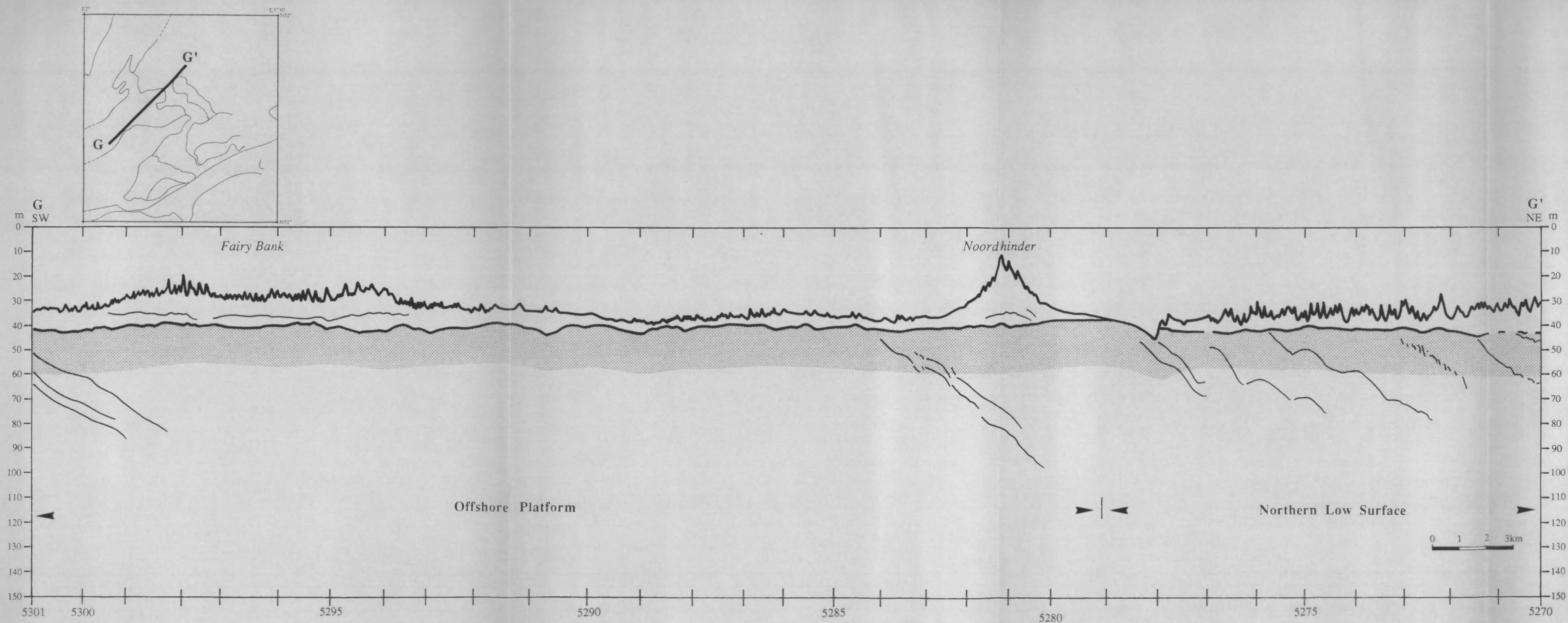


Figure 6 11g Interpreted line-drawing of cross-section G-G'.

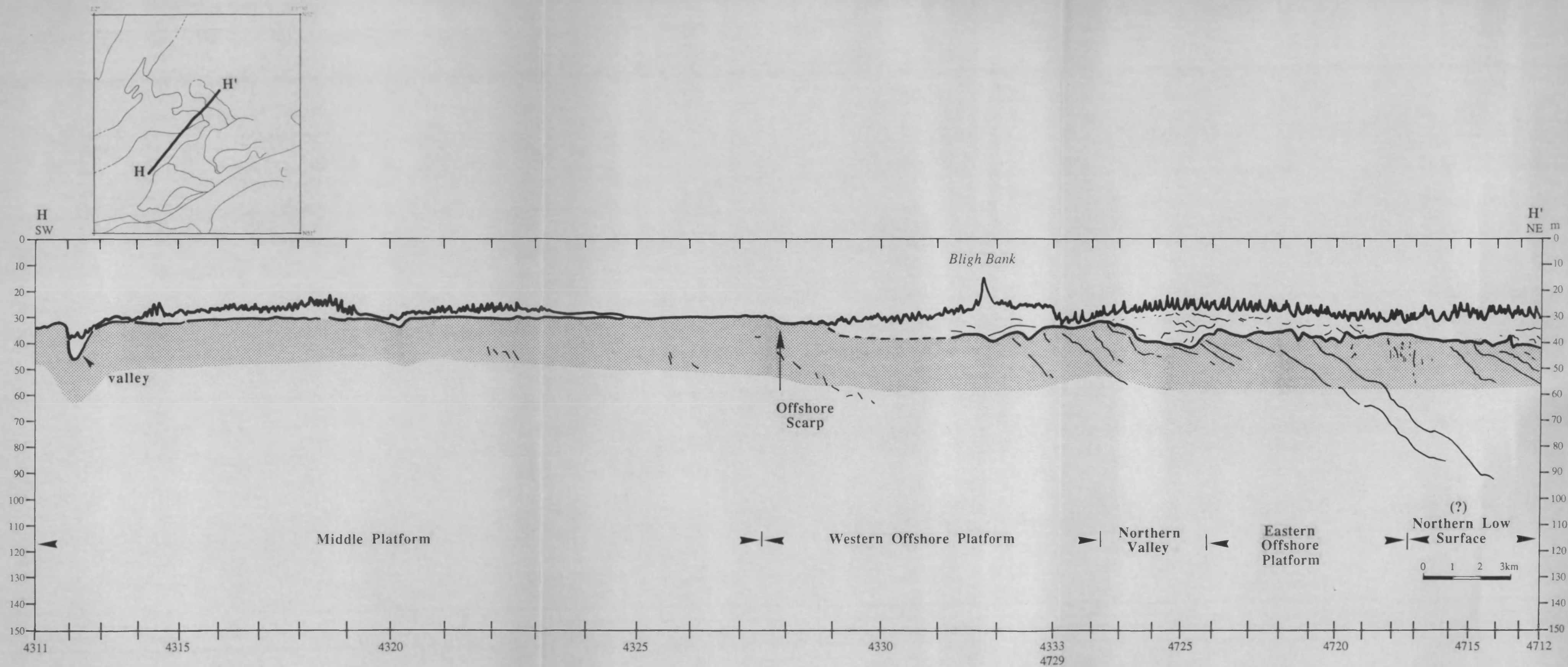


Figure 6.11h Interpreted line-drawing of cross-section H-H'.

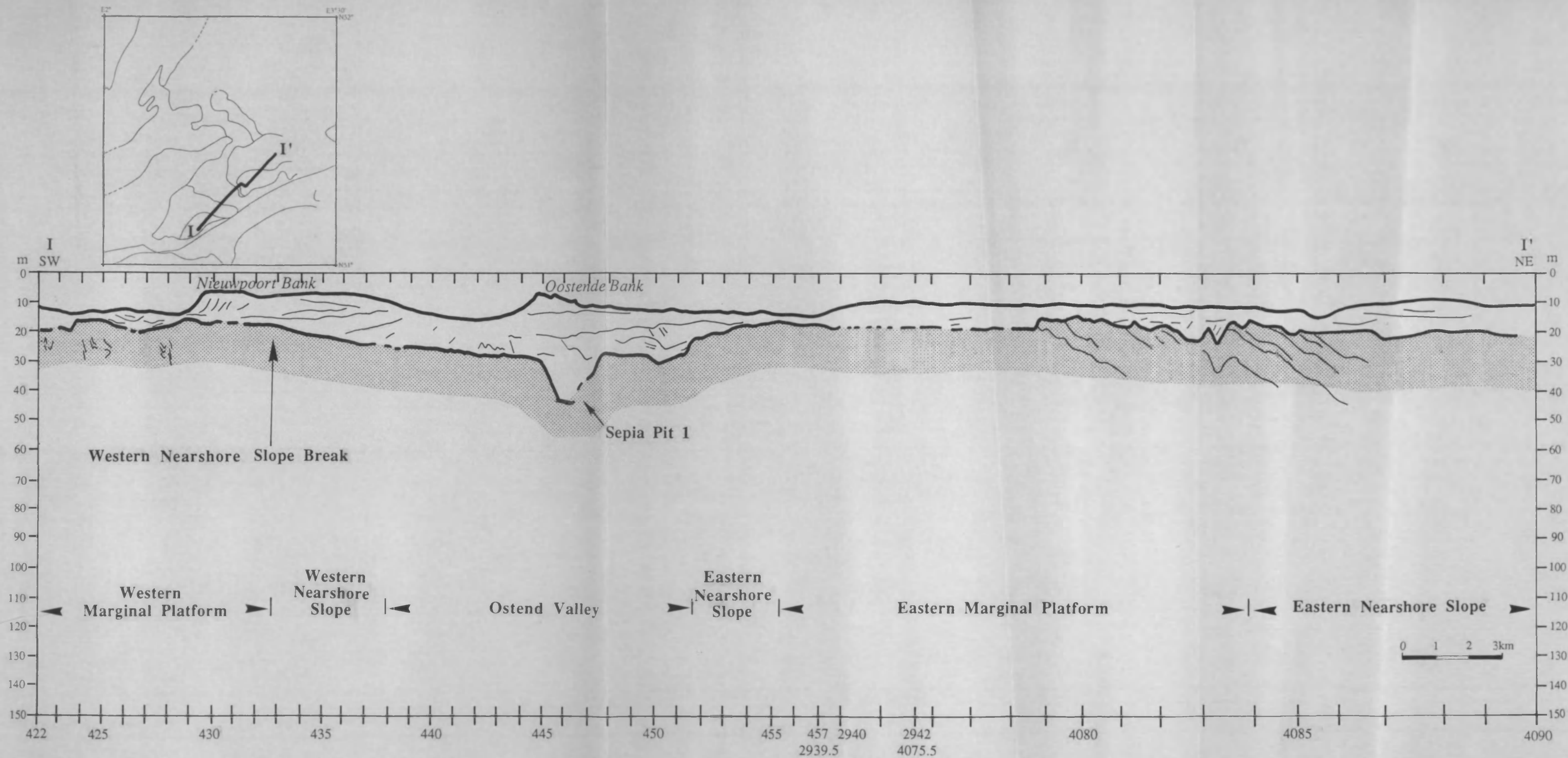


Figure 6.11i Interpreted line-drawing of cross-section I-I'.

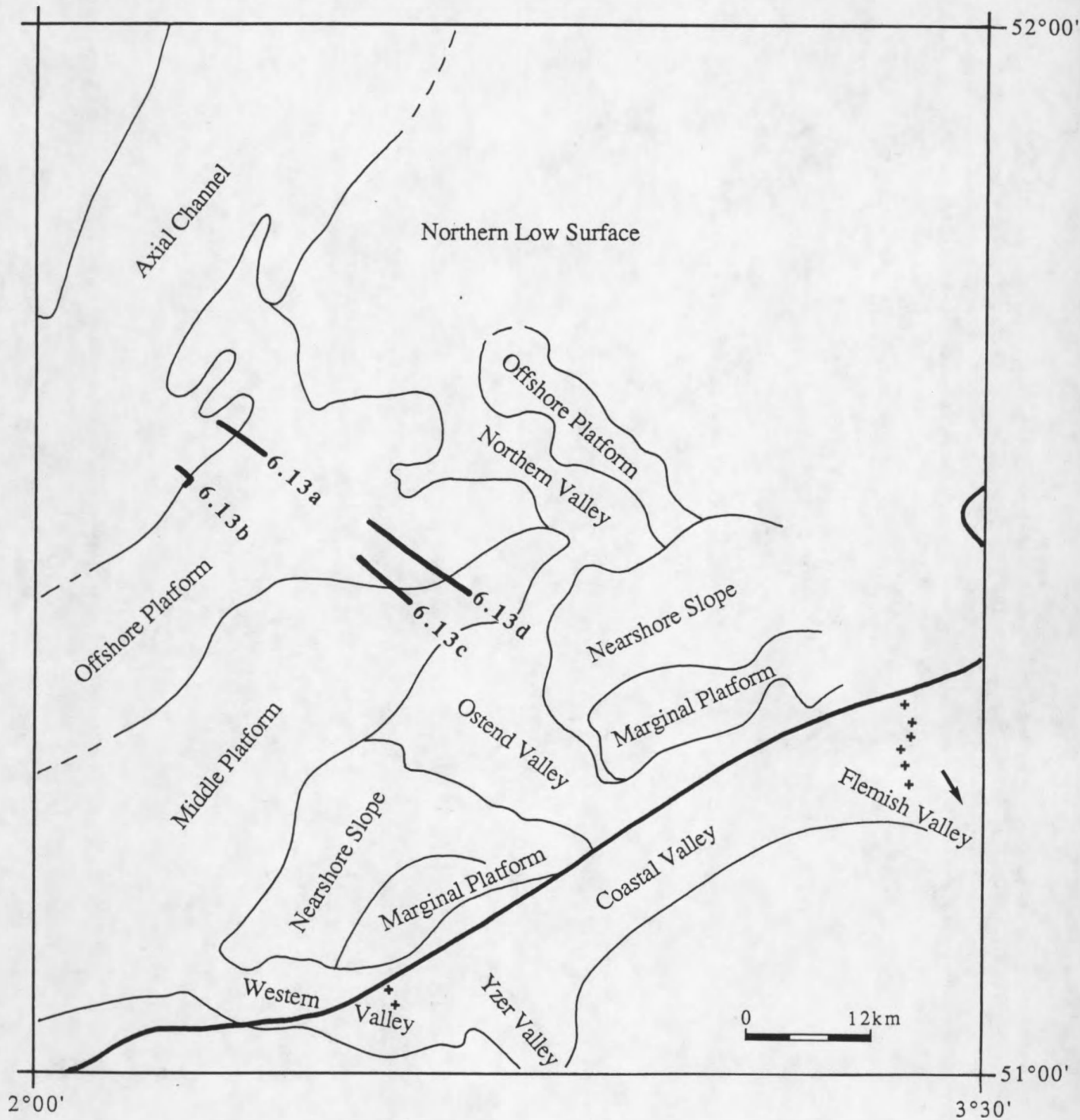


Figure 6.12 Location of profiles across the Offshore Platform and the Offshore Scarp.

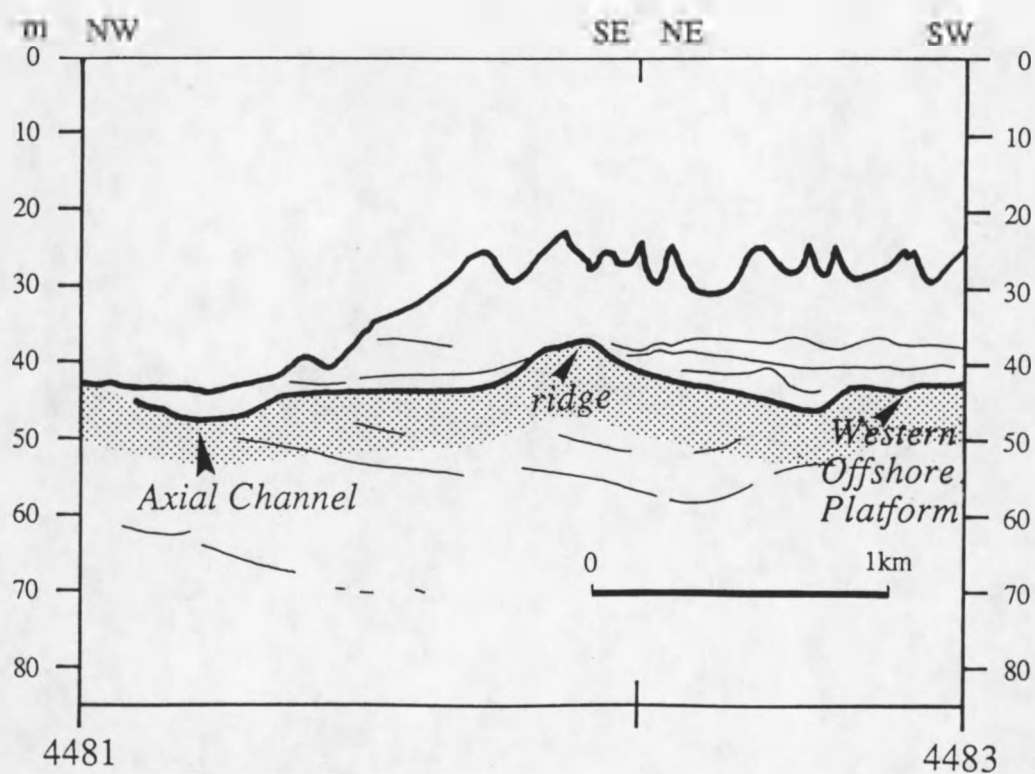
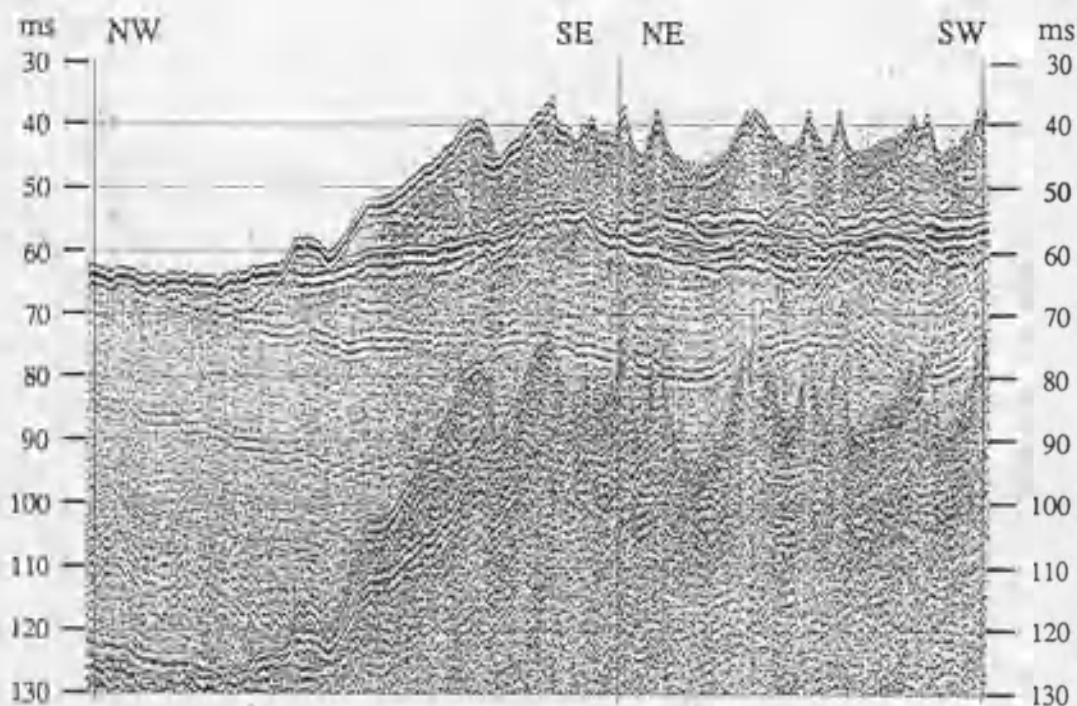


Figure 6.13a Analog record of a sparker section and interpreted line-drawing showing the seaward part of the Offshore Platform. For location of the profile see fig. 6.12.

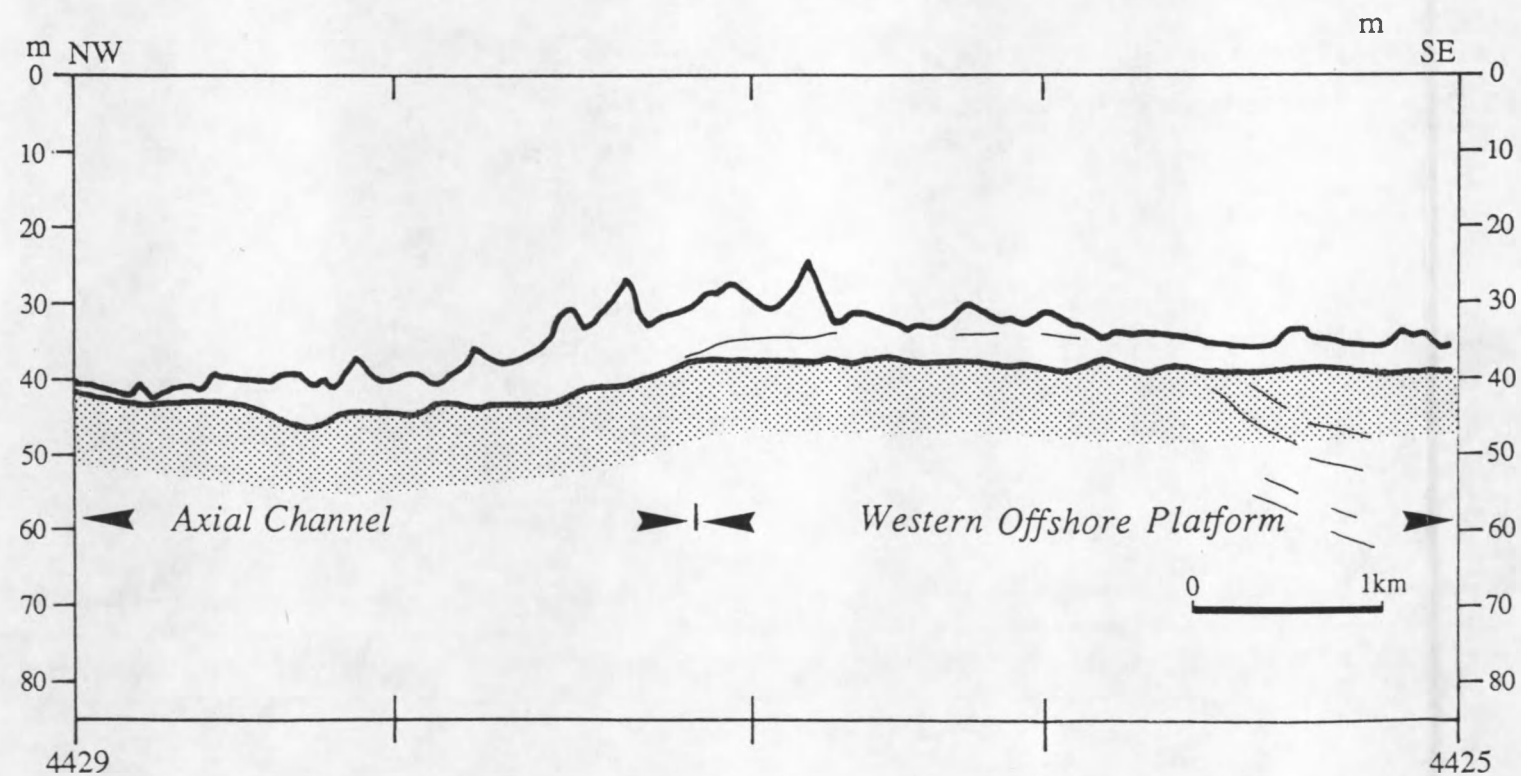
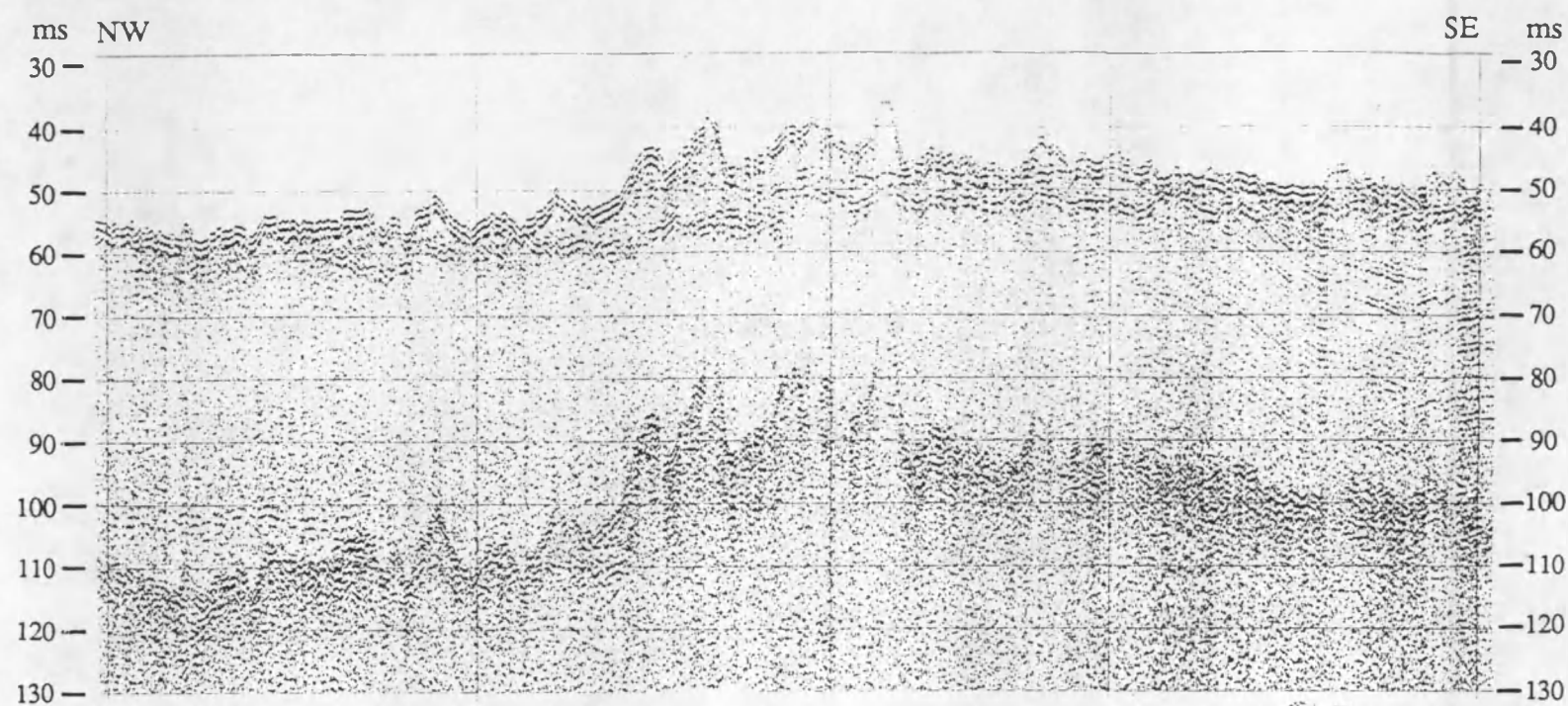


Figure 6.13b Analog record of a sparker section and interpreted line-drawing showing the seaward part of the Offshore Platform. For location of the profile see fig. 6.12.

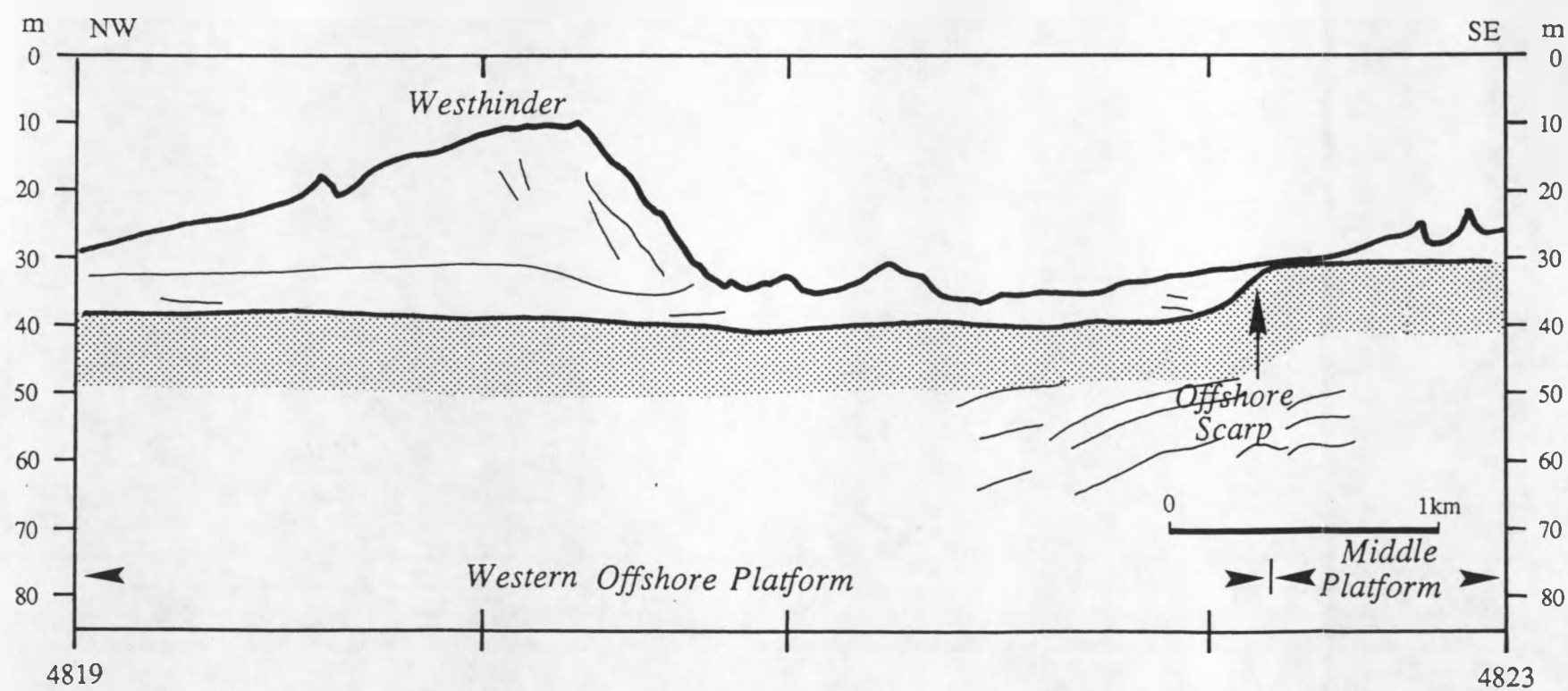
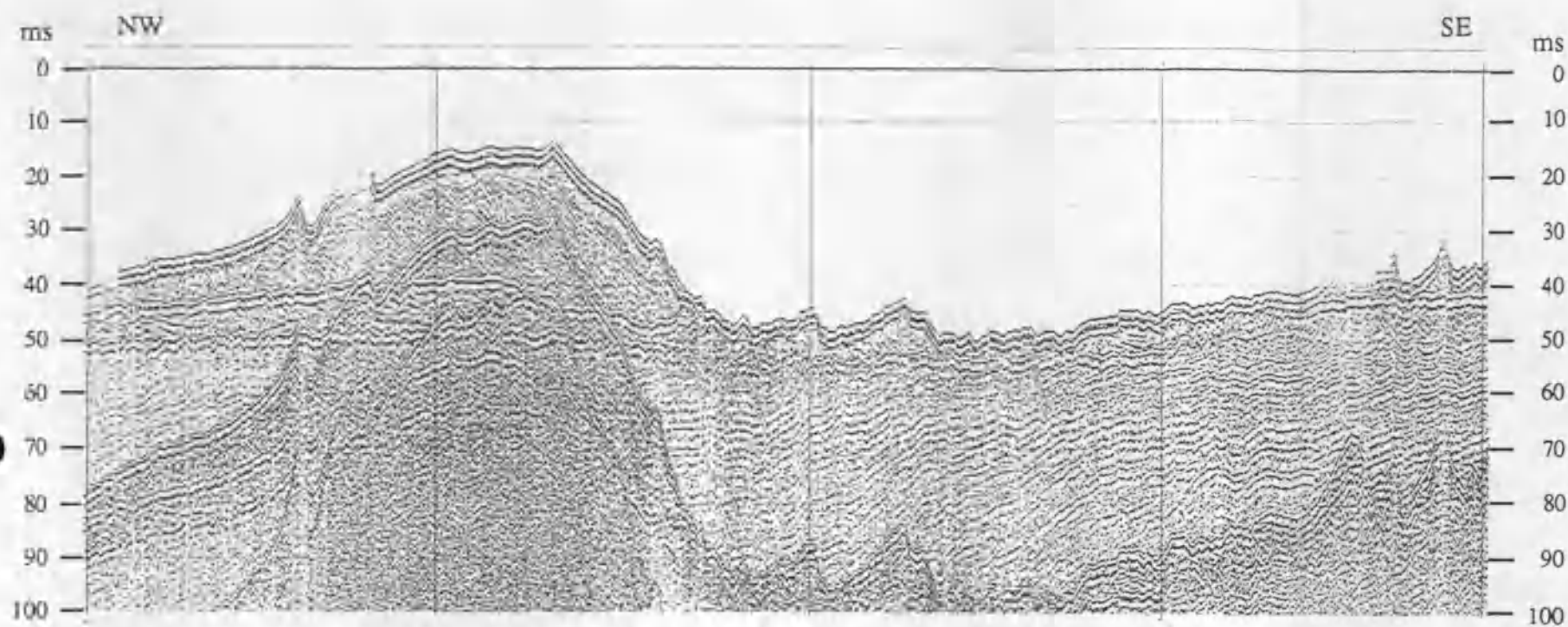


Figure 6.13c Analog record of a sparker section and interpreted line-drawing showing the landward part of the Offshore Platform and the Offshore Scarp. For location of the profile see fig. 6.12.

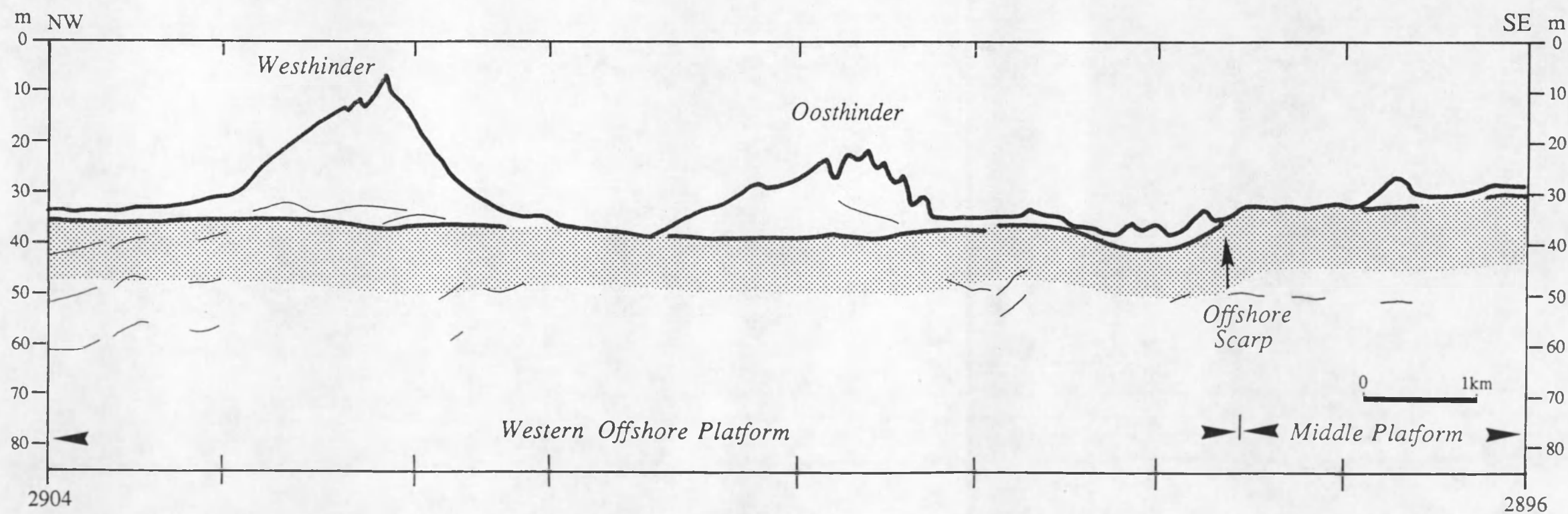
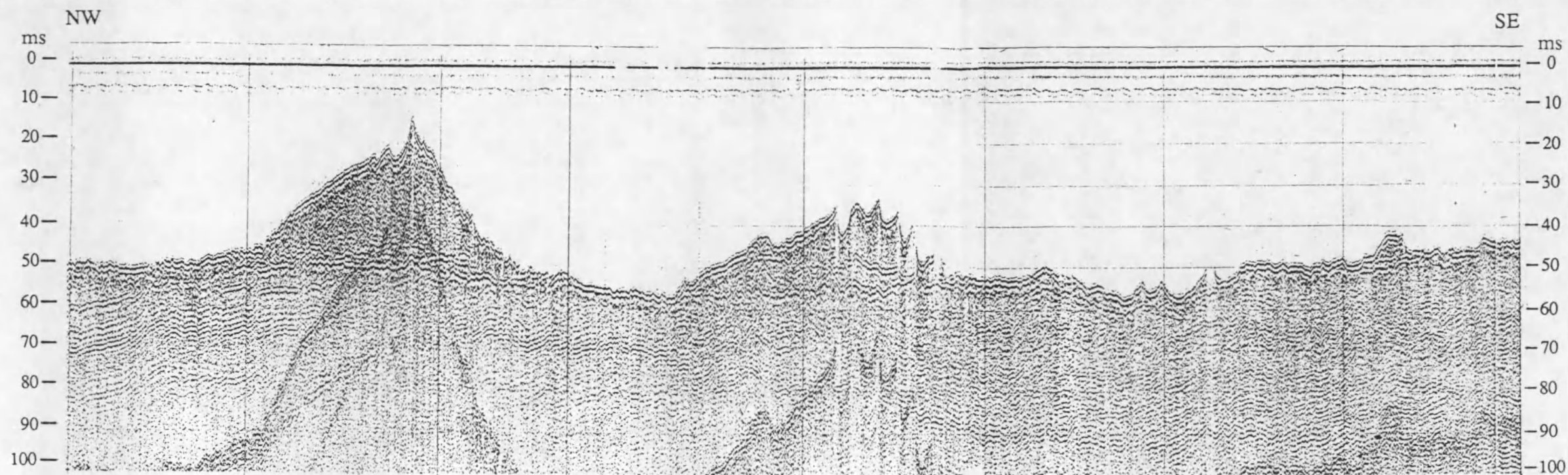


Figure 6.13d Analog record of a sparker section and interpreted line-drawing showing the landward part of the Offshore Platform. For location of the profile see fig. 6.12.



Figure 6.14 Location of profiles across the Middle Platform and the Middle Scarp.

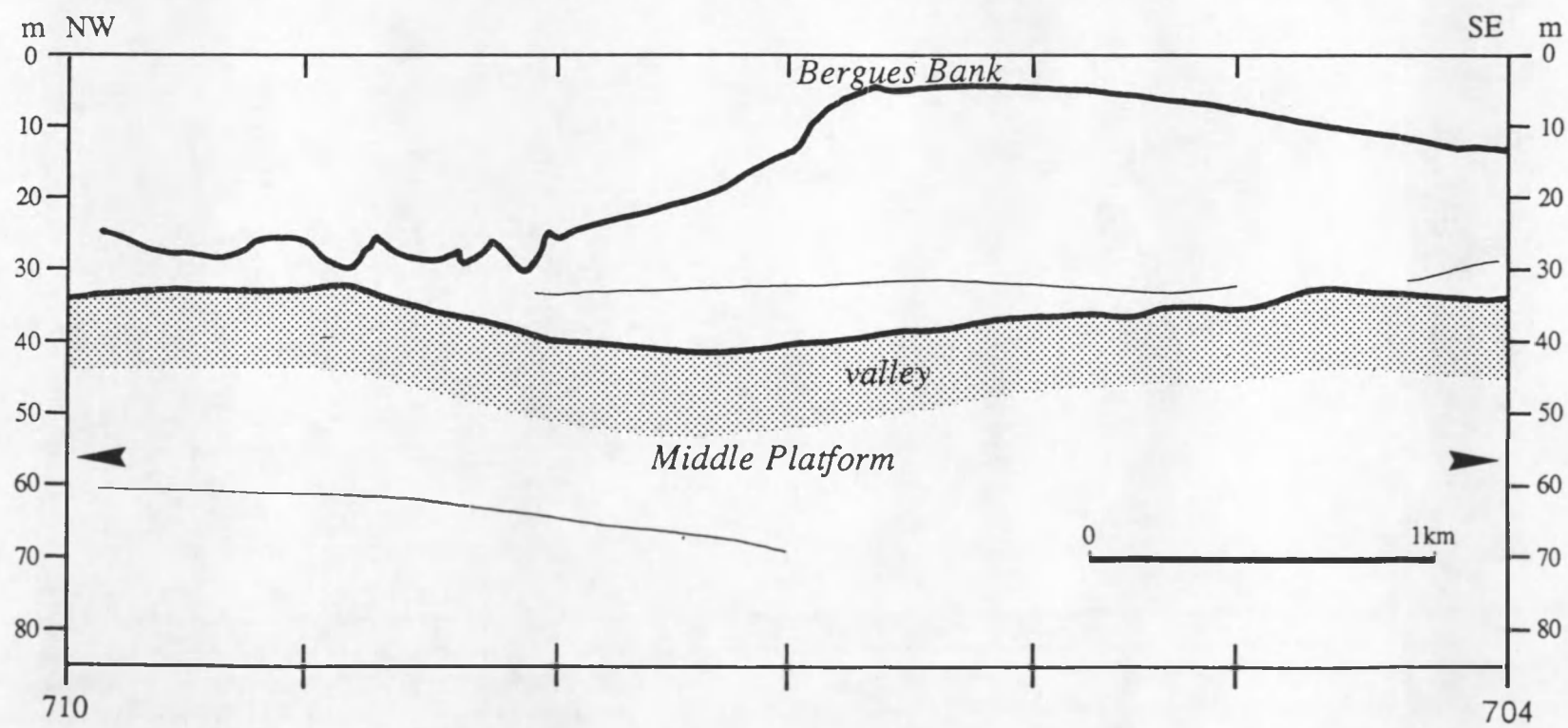
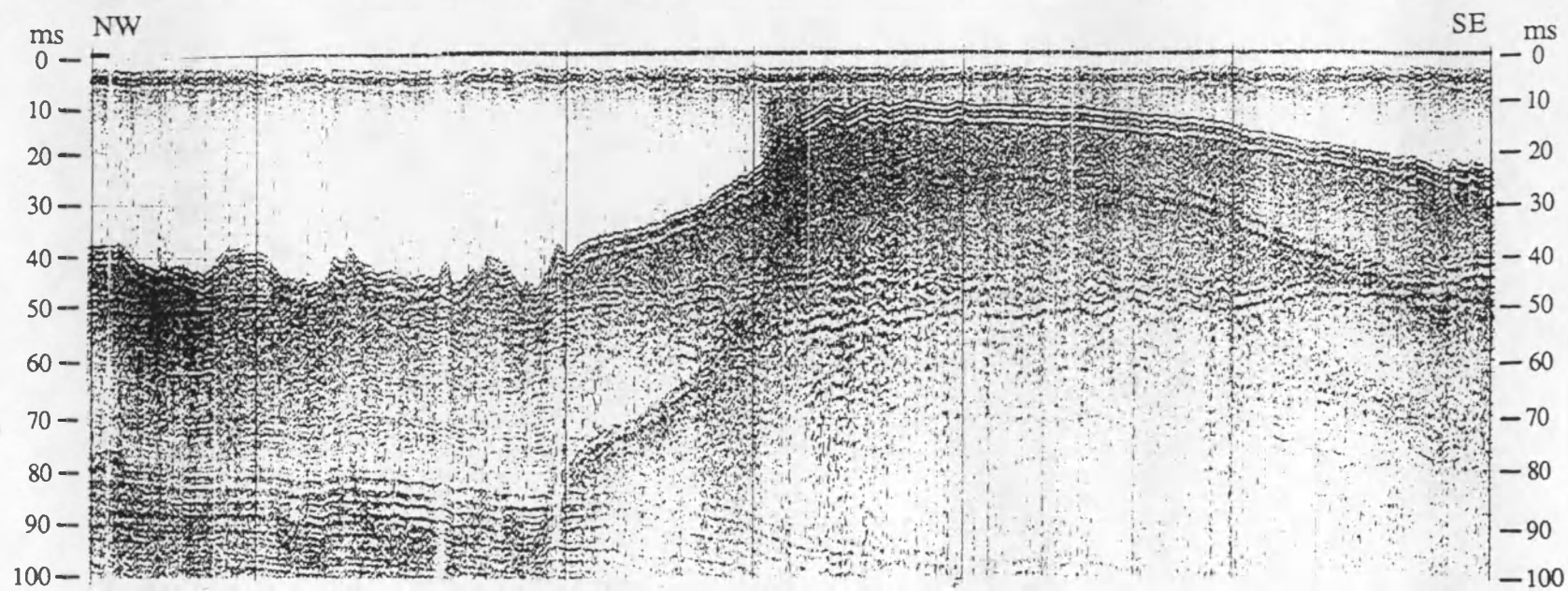


Figure 6.15a Analog record of a sparker section and interpreted line-drawing showing the southwestern part of the Middle Platform. For location of the profile see fig. 6.14.

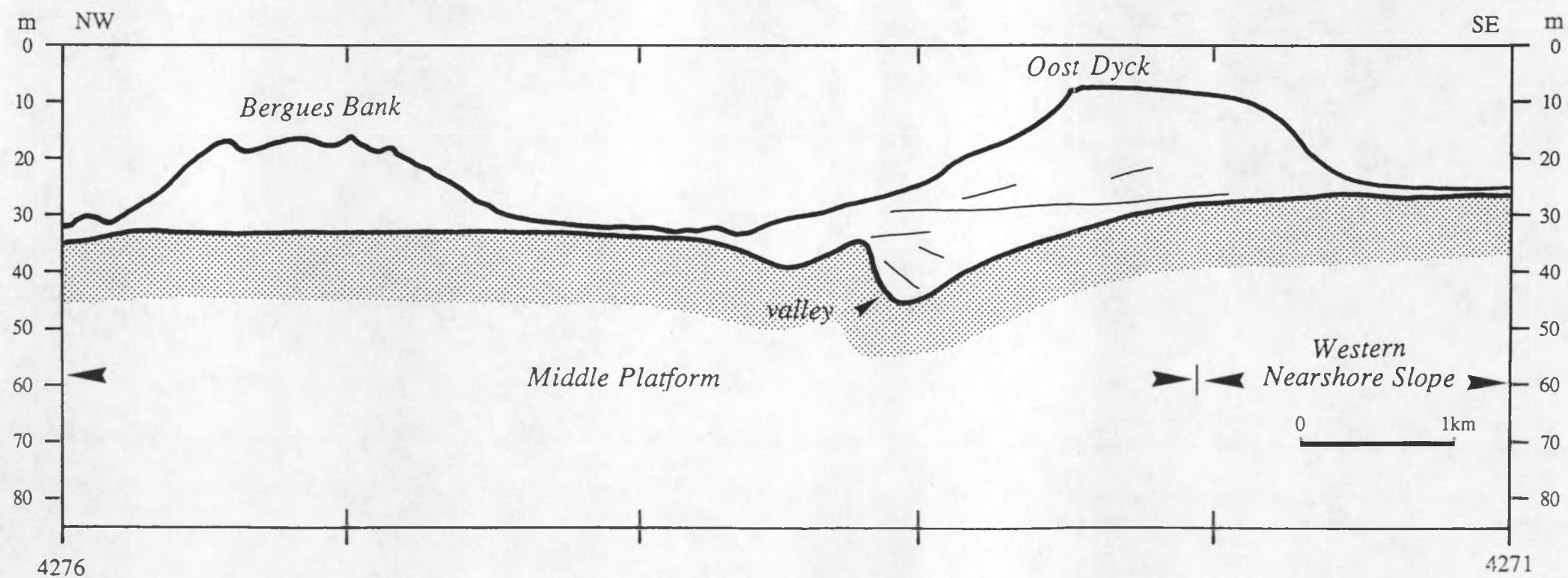
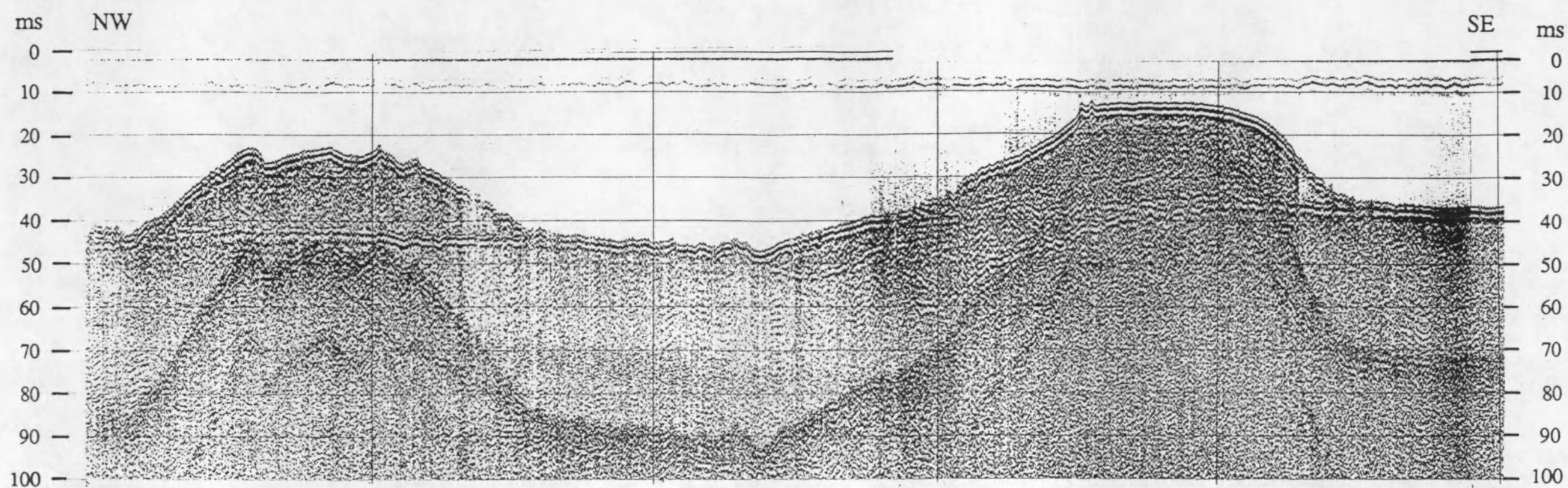


Figure 6.15b Analog record of a sparker section and interpreted line-drawing showing the southwestern part of the Middle Platform. For location of the profile see fig. 6.14.

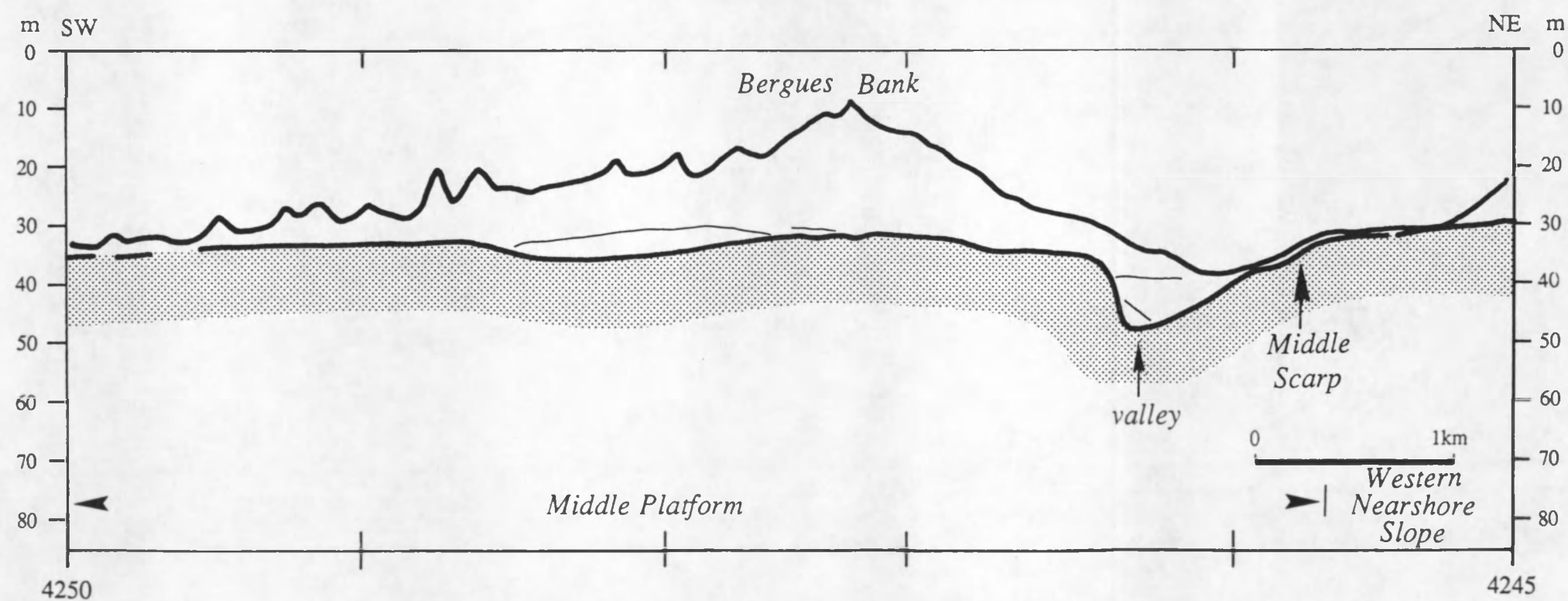
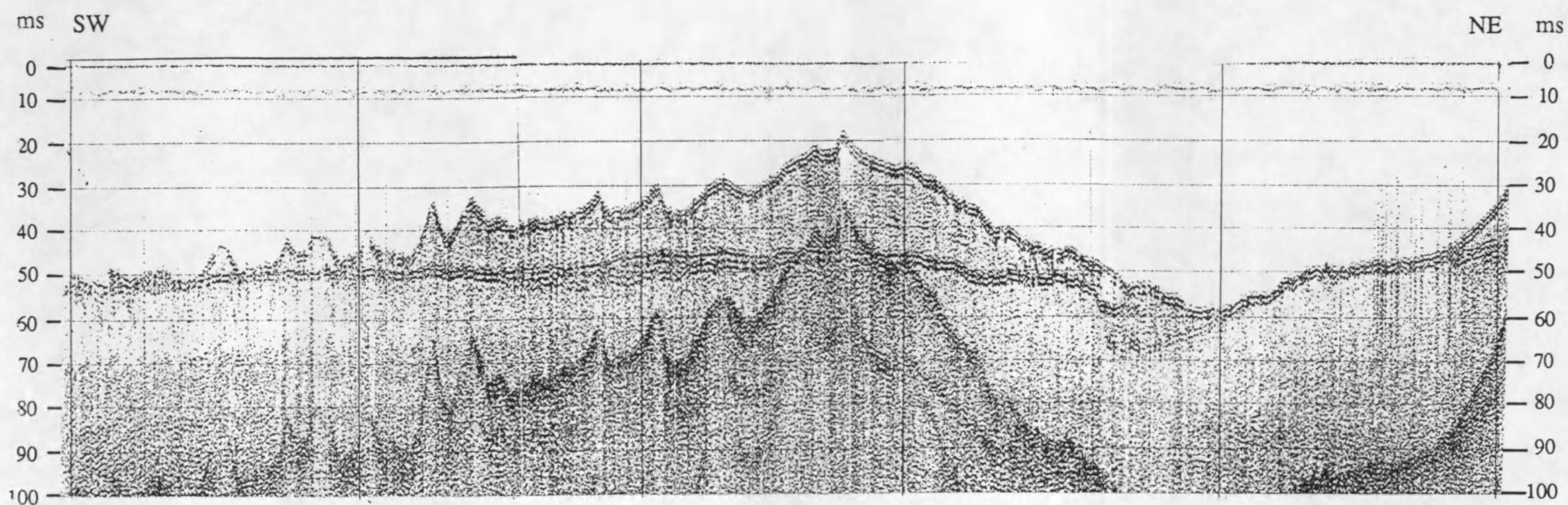


Figure 6.15c Analog record of a sparker section and interpreted line-drawing showing the northwestern part of the Middle Platform. For location of the profile see fig. 6.14.

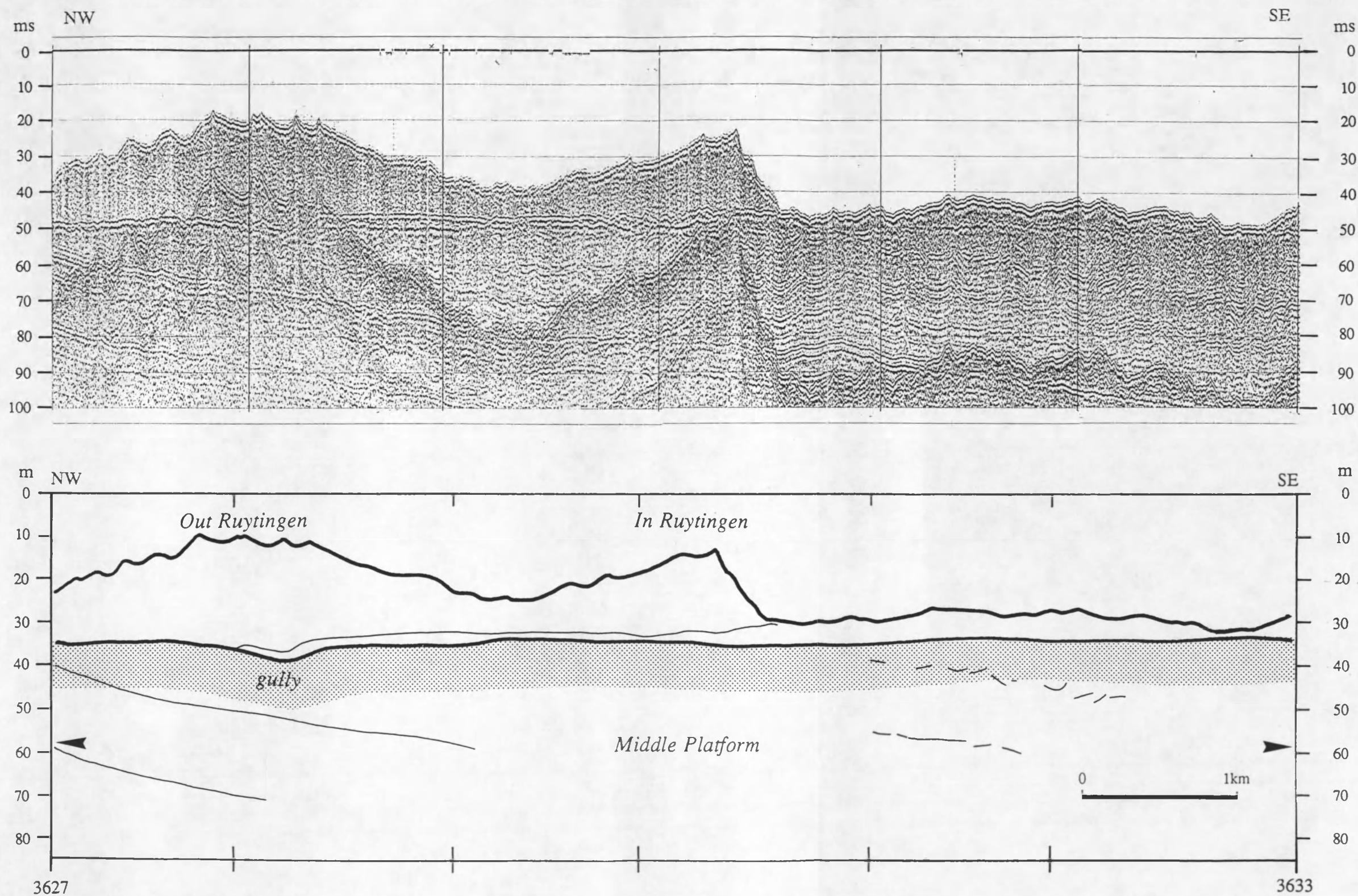


Figure 6.15d Analog record of a sparker section and interpreted line-drawing showing the northwestern part of the Middle Platform. For location of the profile see fig. 6.14.

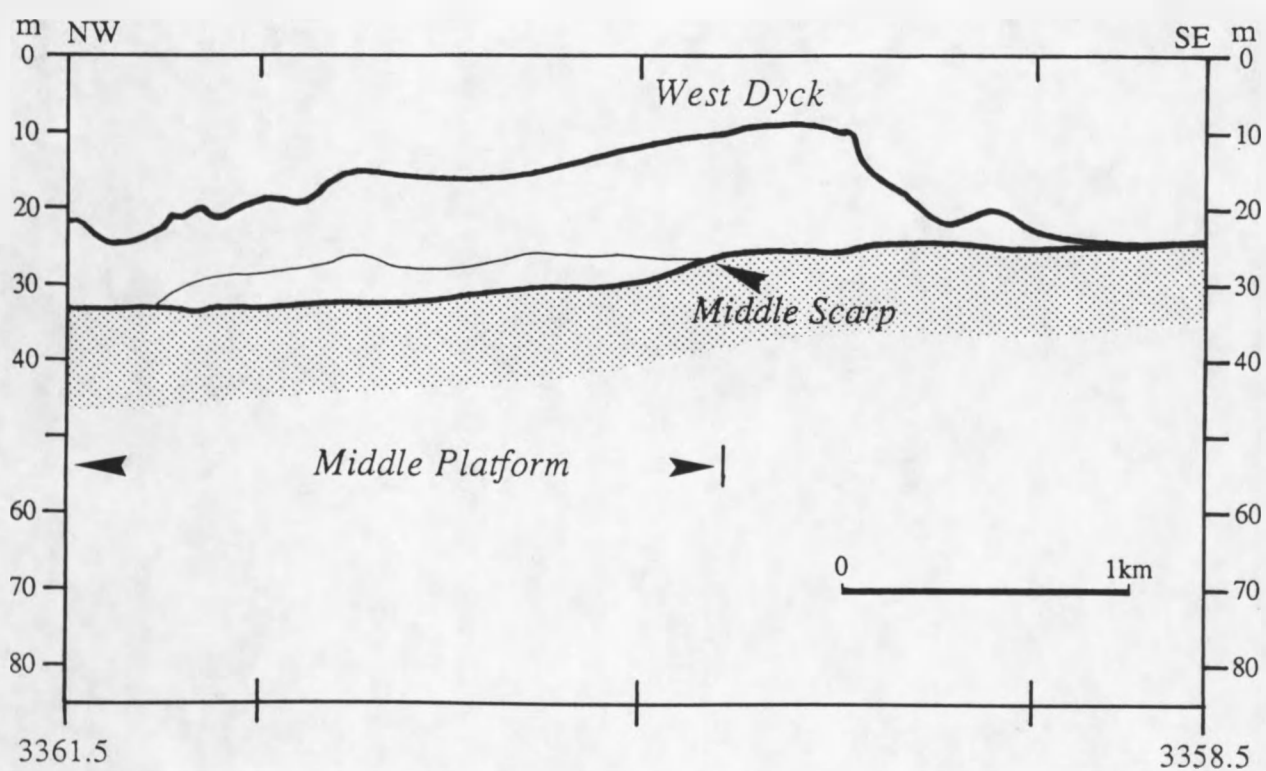
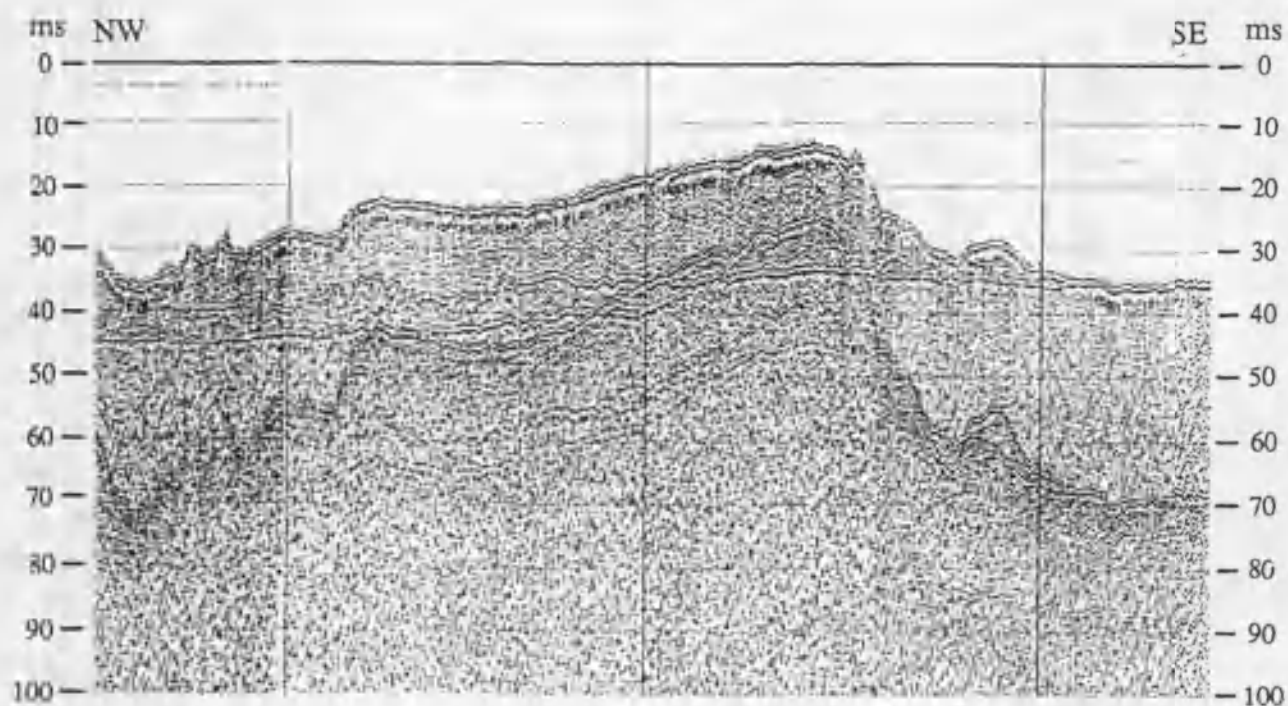


Figure 6.15e Analog record of a sparker section and interpreted line-drawing showing the western part of the Middle Scarp. For location of the profile see fig. 6.14.

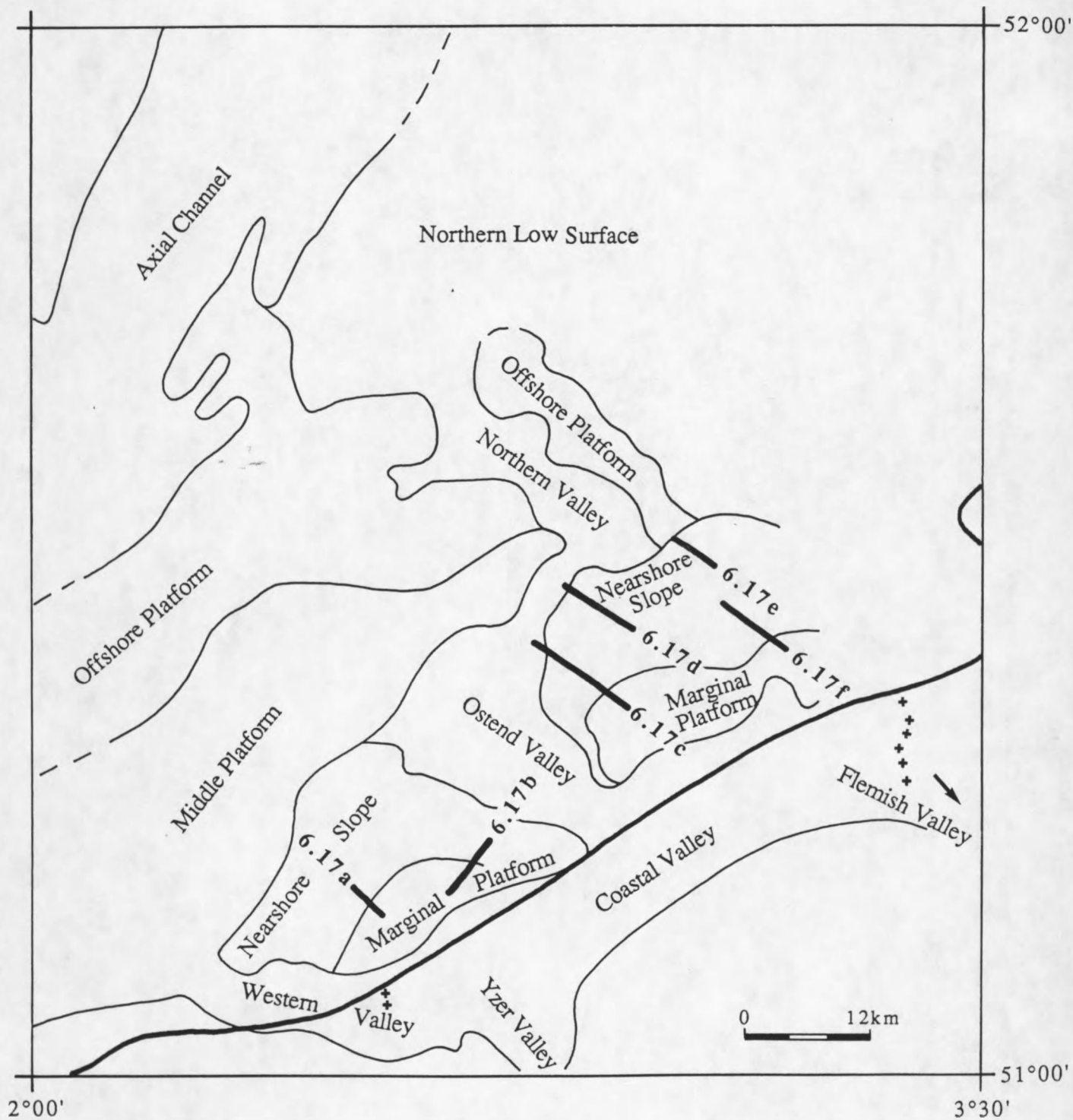


Figure 6.16 Location of profiles across the Nearshore Slope, the Nearshore Slope Break and the Marginal Platform.

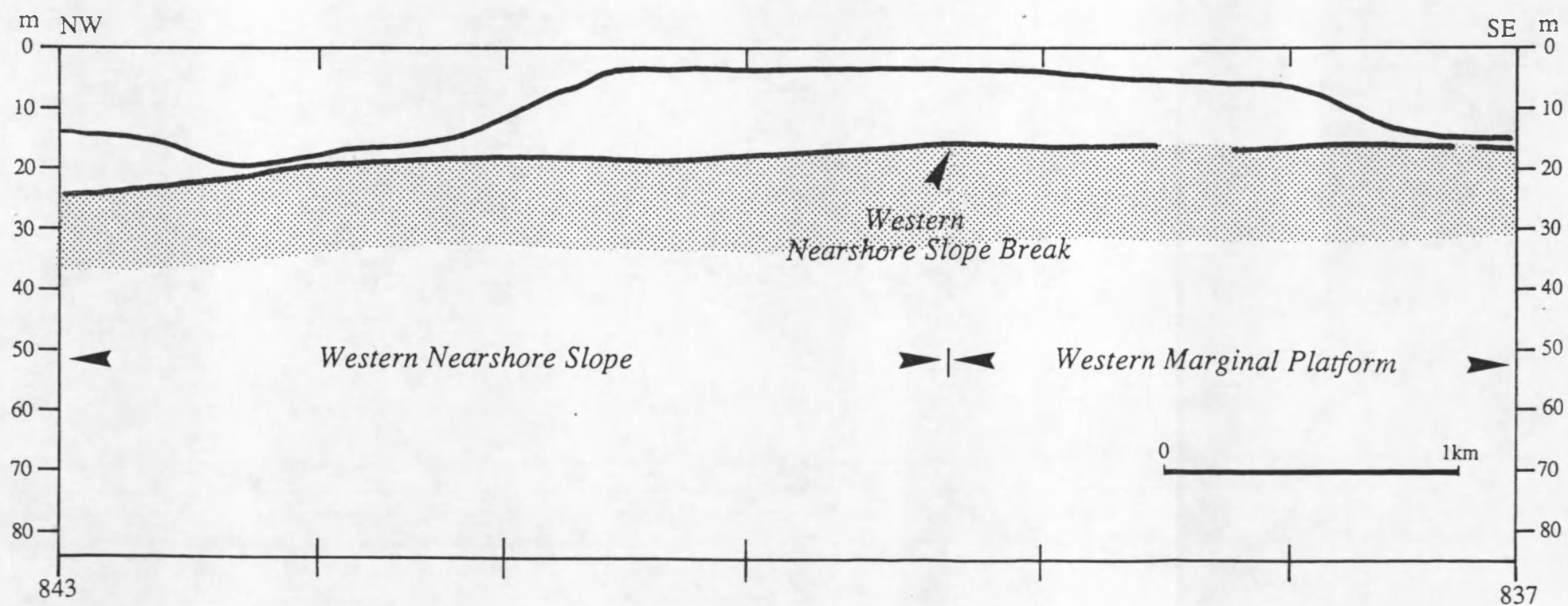
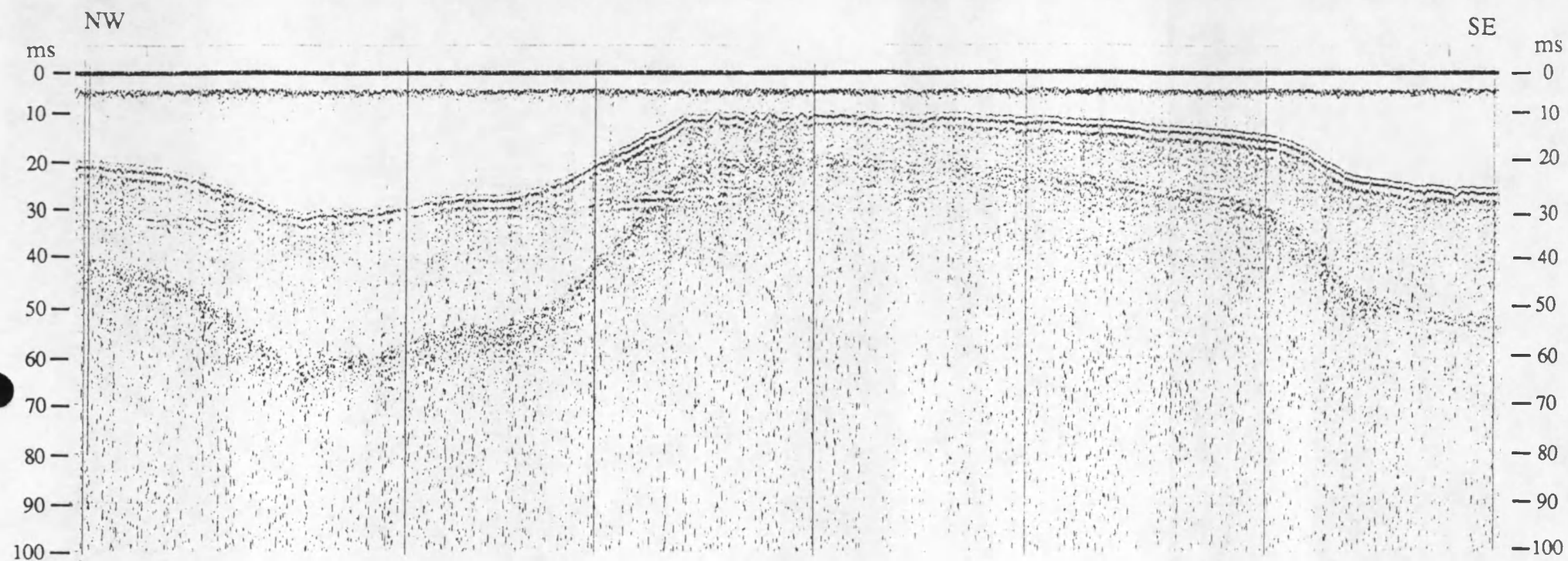


Figure 6.17a Analog record of a sparker section and interpreted line-drawing showing the Western Nearshore Slope Break. For location of the profile see fig. 6.16.

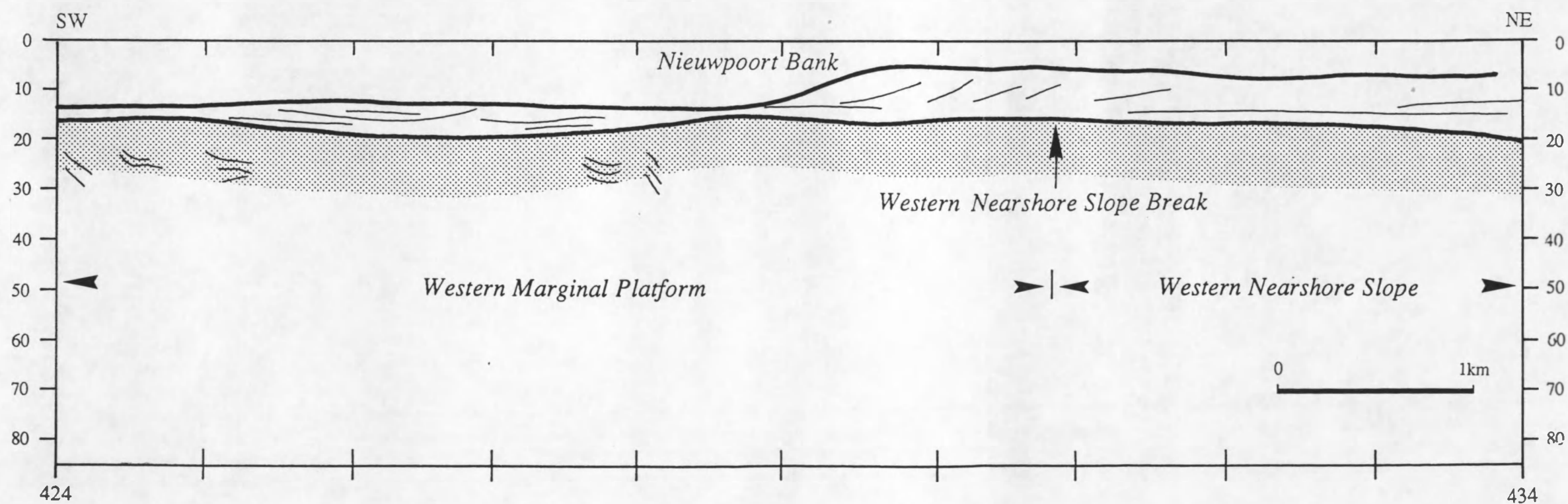
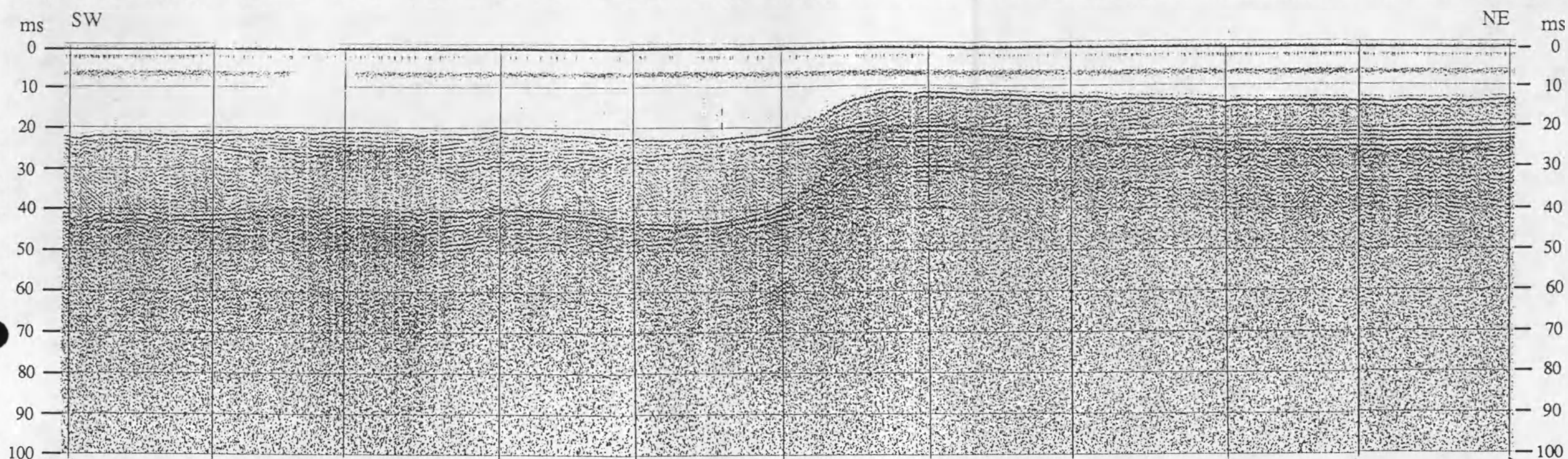


Figure 6.17b Analog record of a sparker section and interpreted line-drawing showing the Western Nearshore Slope Break. For location of the profile see fig. 6.16.

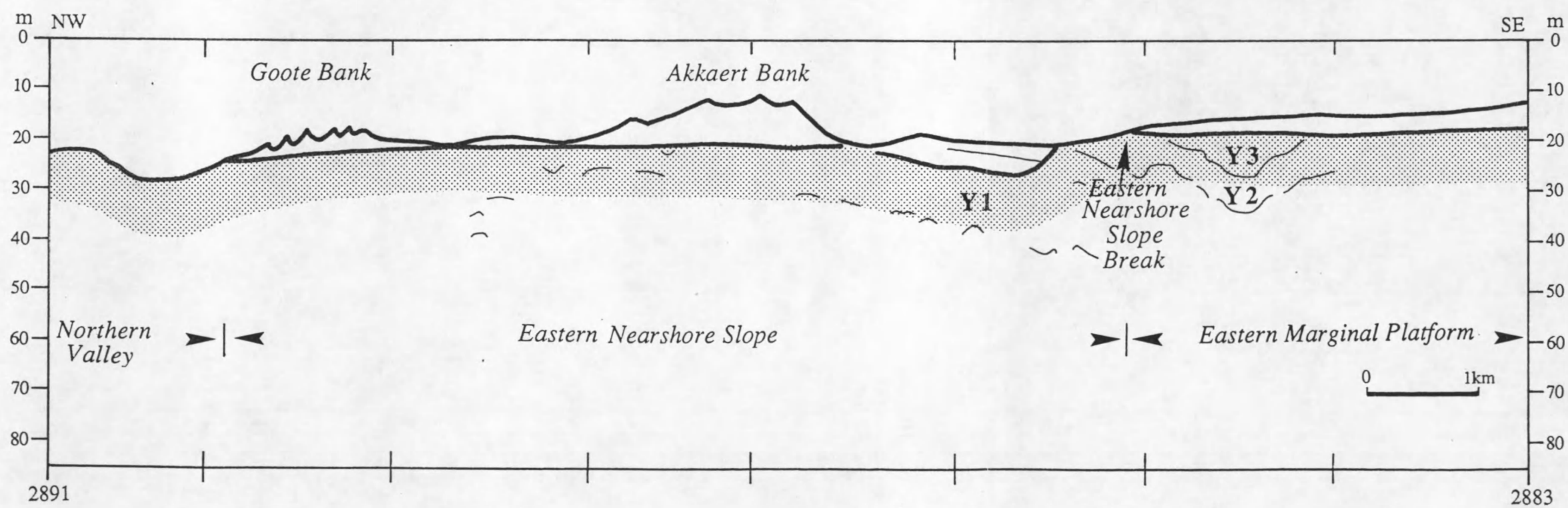
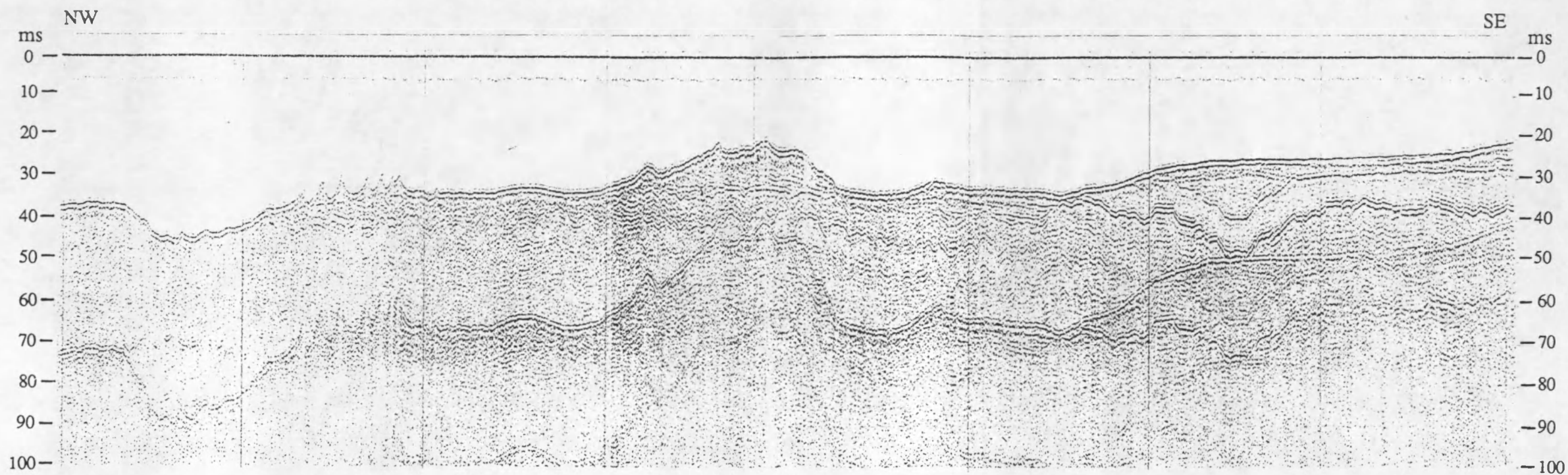


Figure 6.17c Analog record of a sparker section and interpreted line-drawing showing the western depression in the Eastern Nearshore Slope. For location of the profile see fig. 6.16.

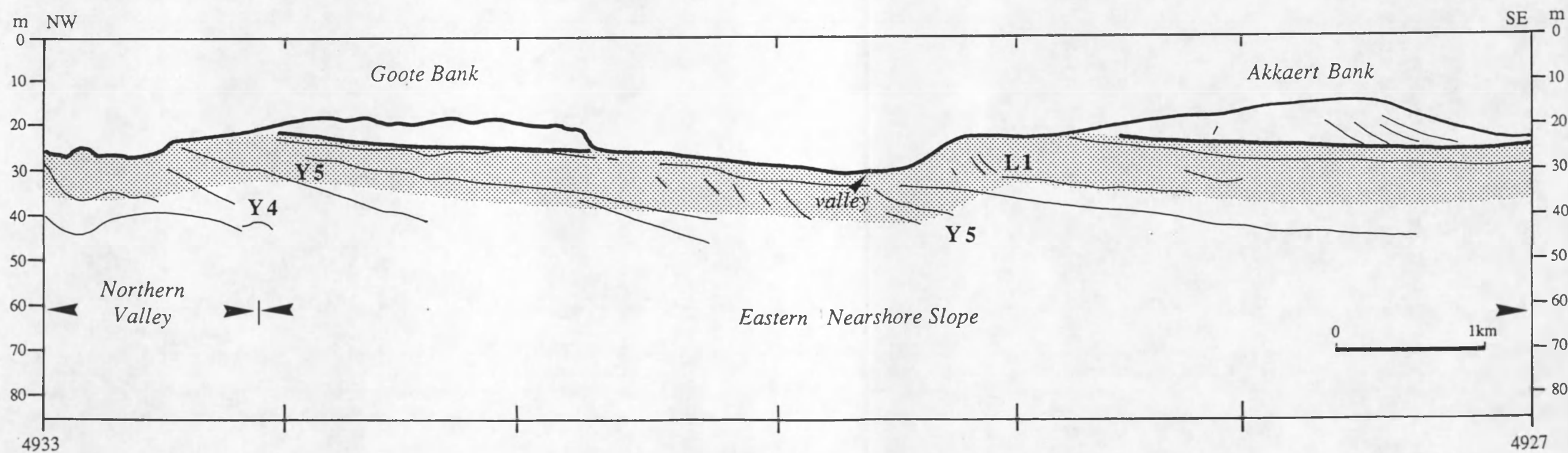
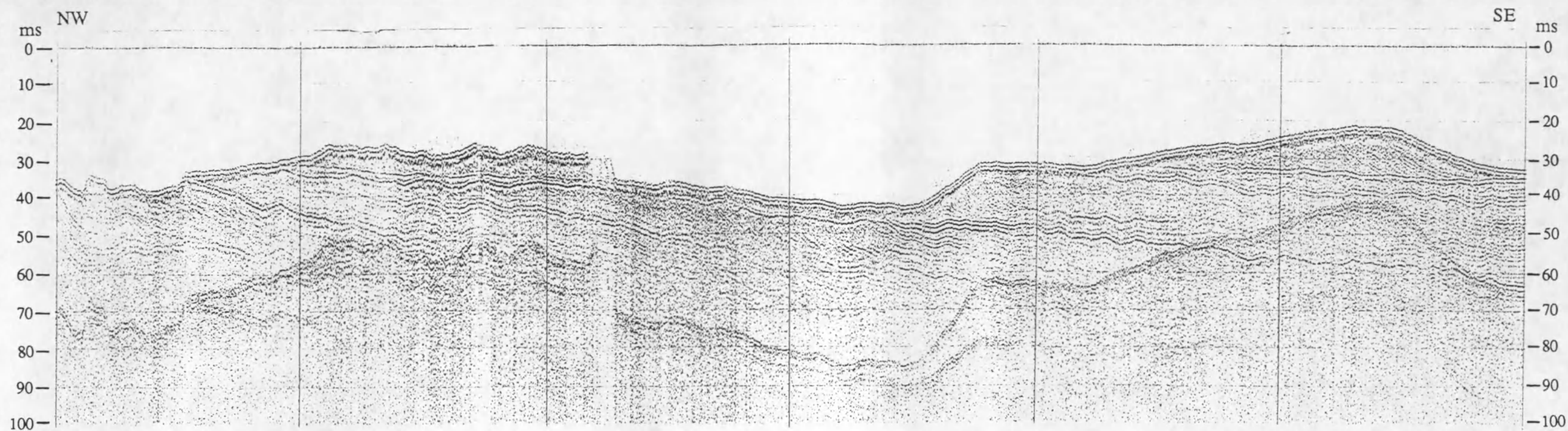


Figure 6.17d Analog record of a sparker section and interpreted line-drawing showing the western part of the valley in the Nearshore Slope. For location of the profile see fig. 6.16.

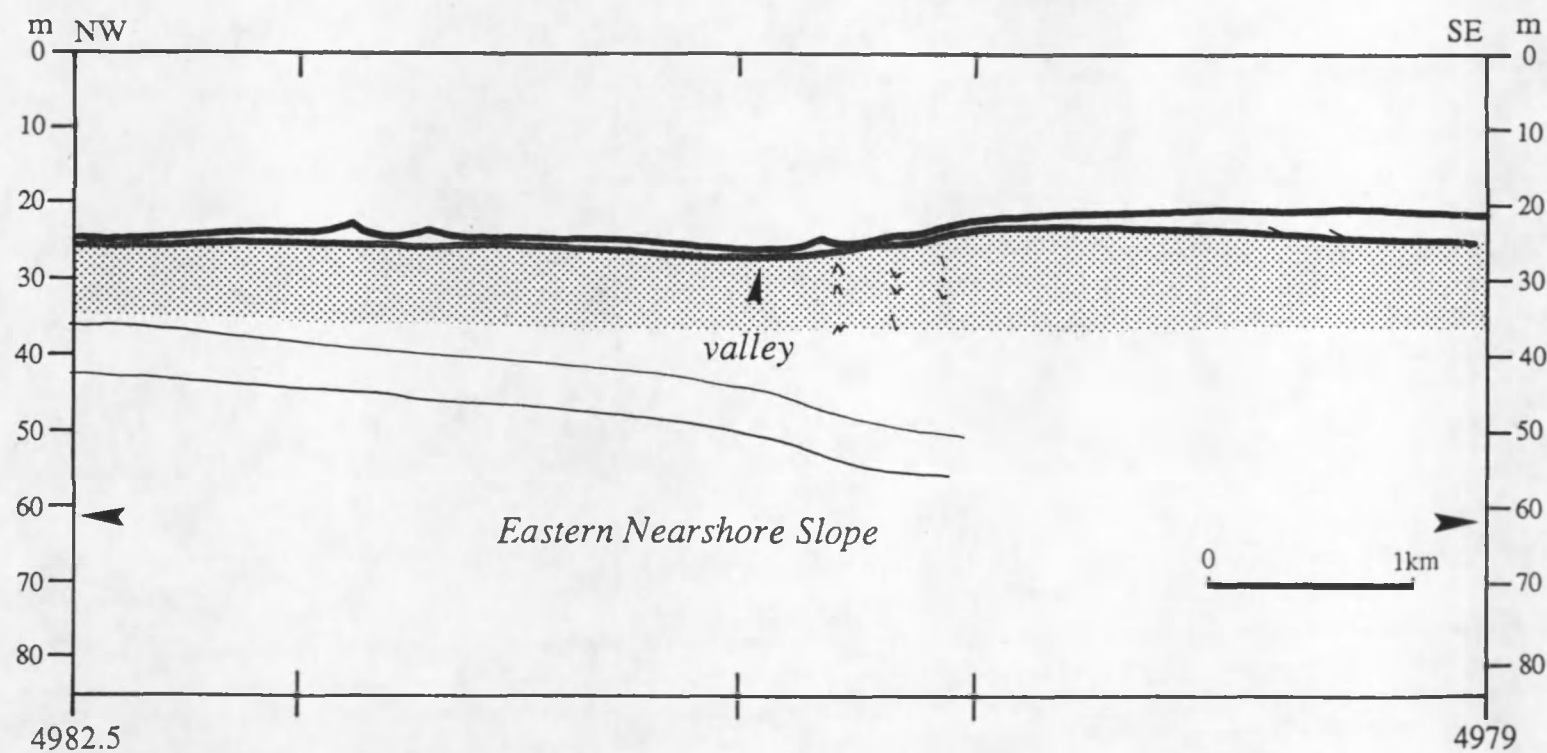
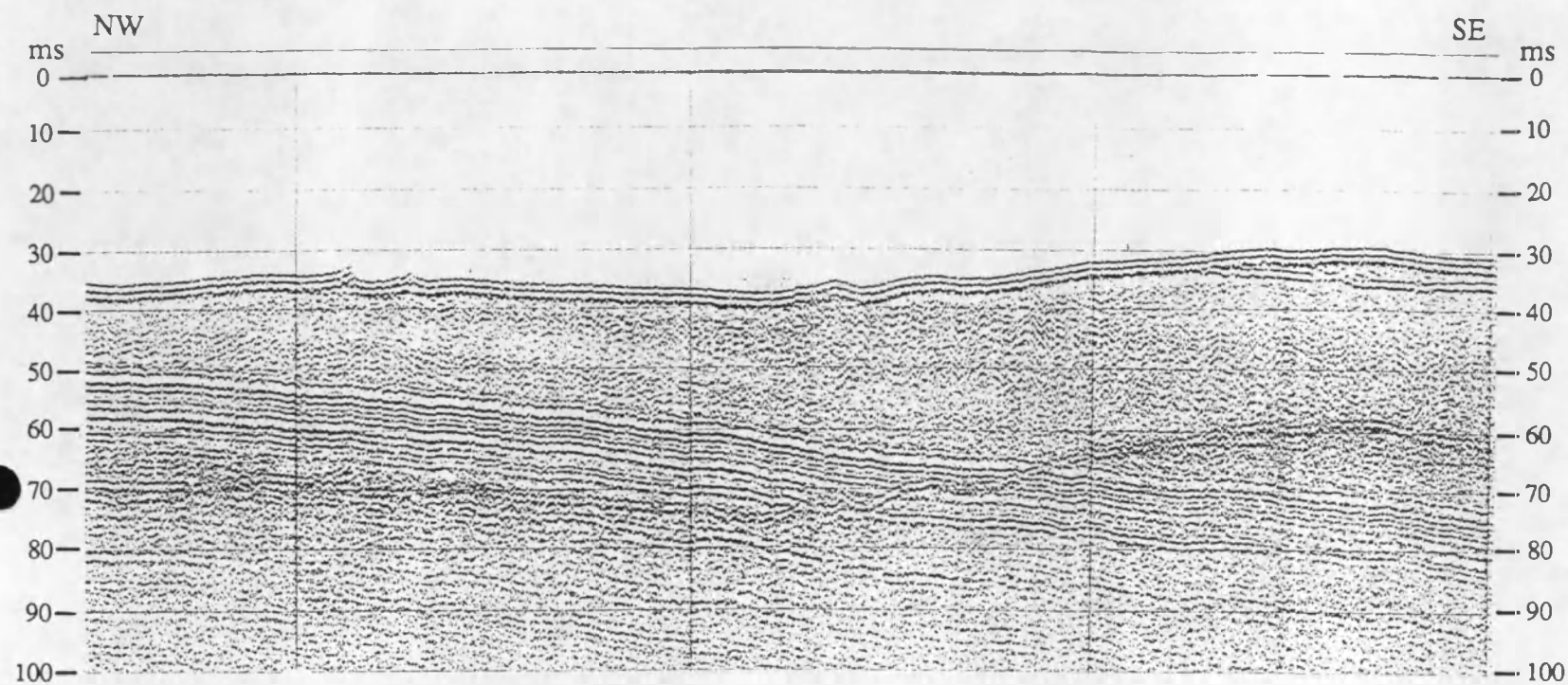


Figure 6.17e Analog record of a sparker section and interpreted line-drawing showing the eastern part of the valley in the Nearshore Slope. For location of the profile see fig. 6.16.

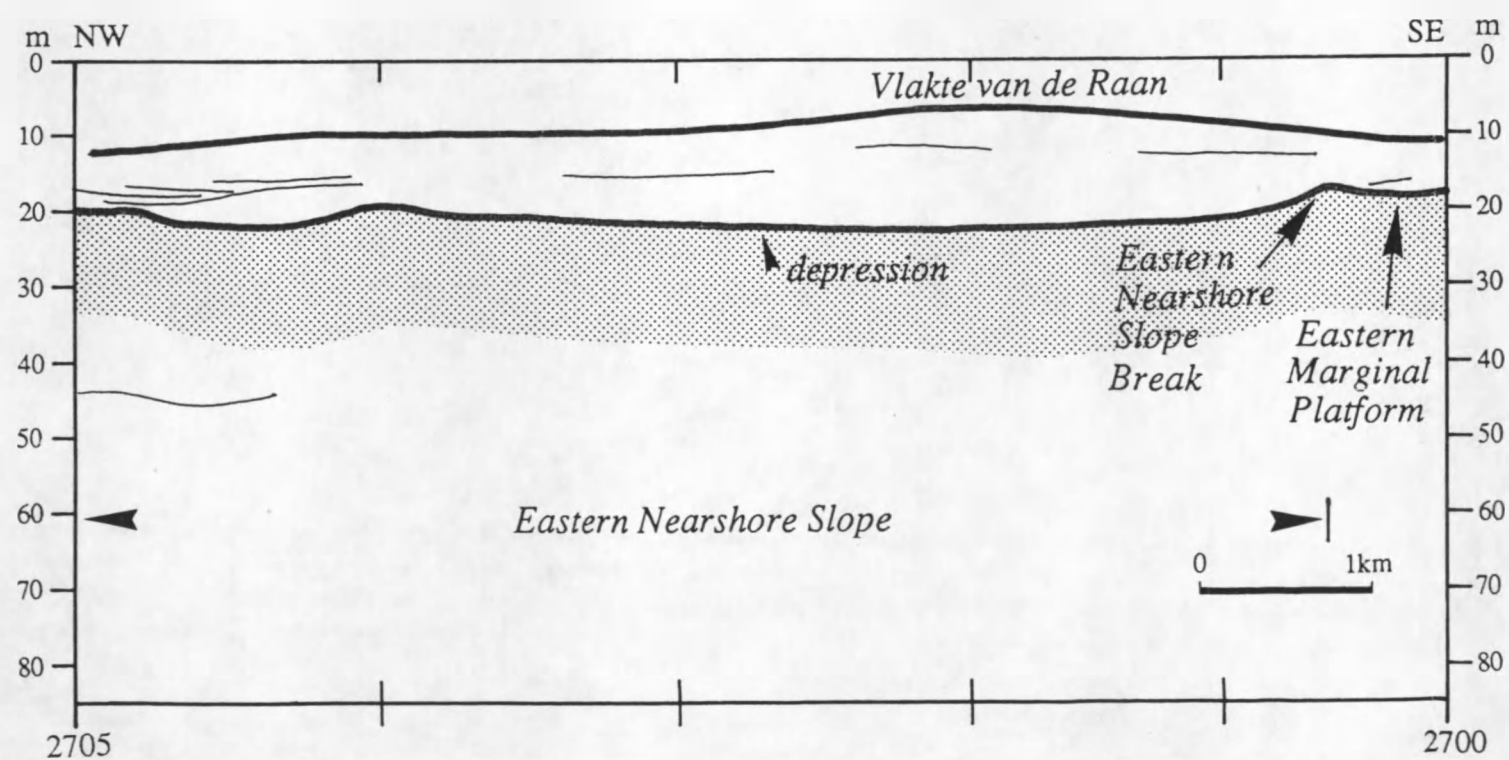
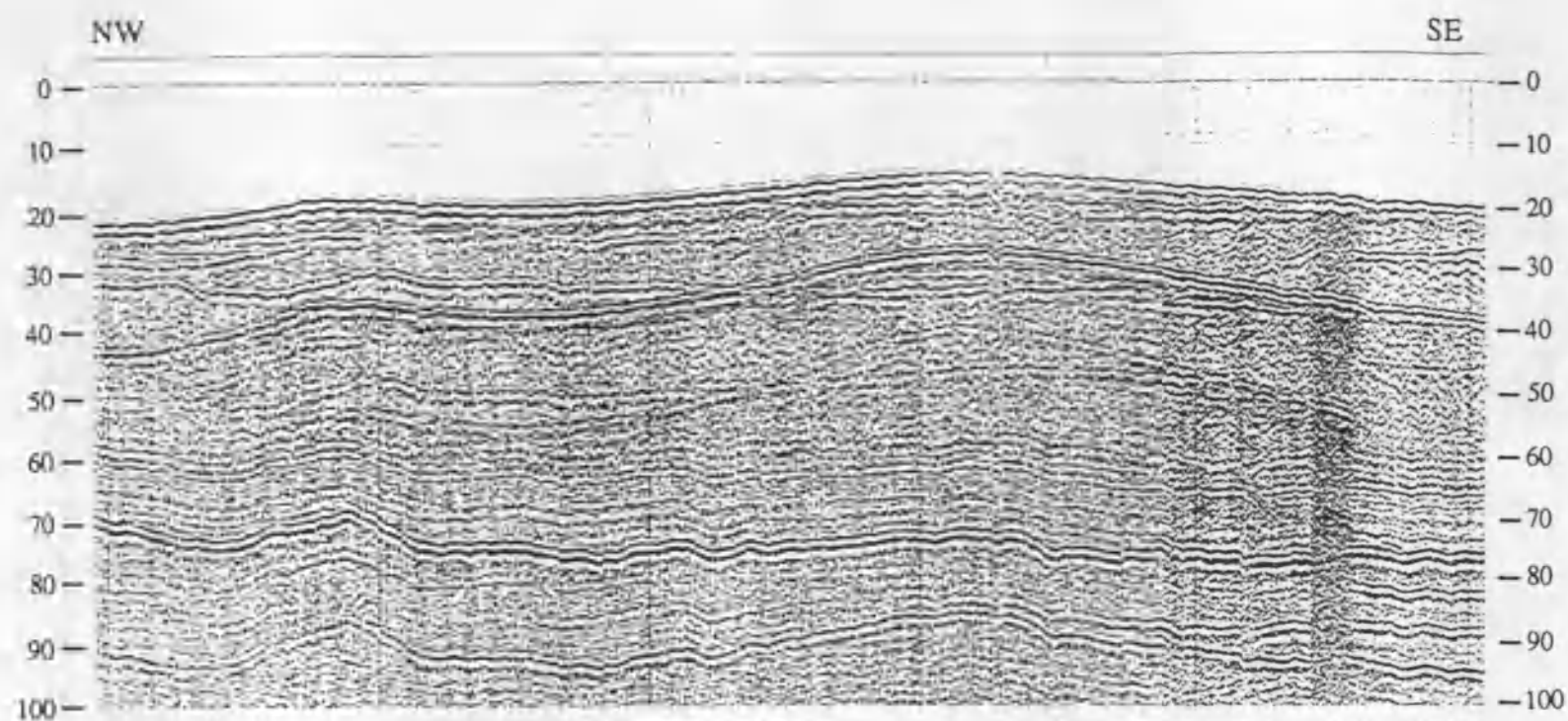


Figure 6.17f Analog record of a sparker section and interpreted line-drawing showing the eastern depression in the Eastern Nearshore Slope. For location of the profile see fig. 6.16.

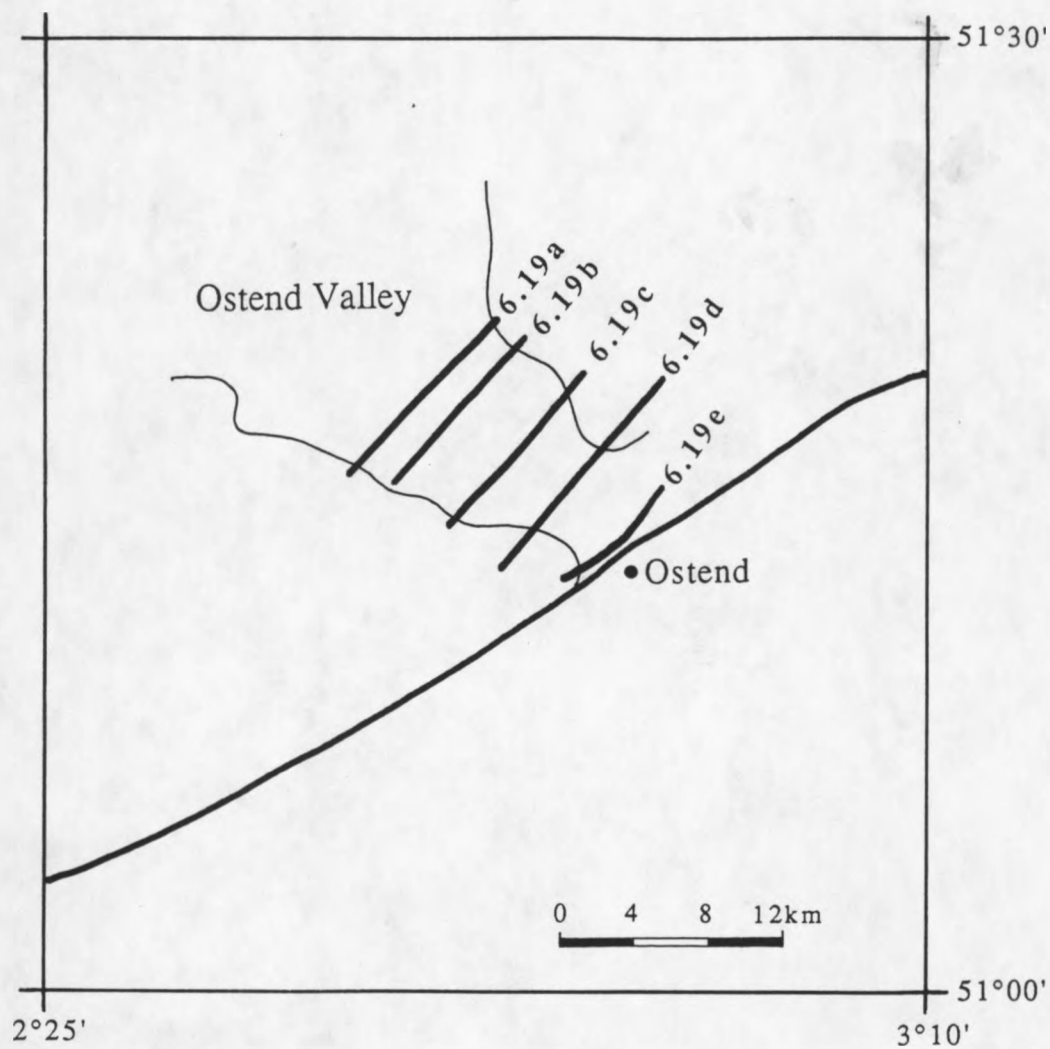


Figure 6.18 Location of profiles across the Ostend Valley.

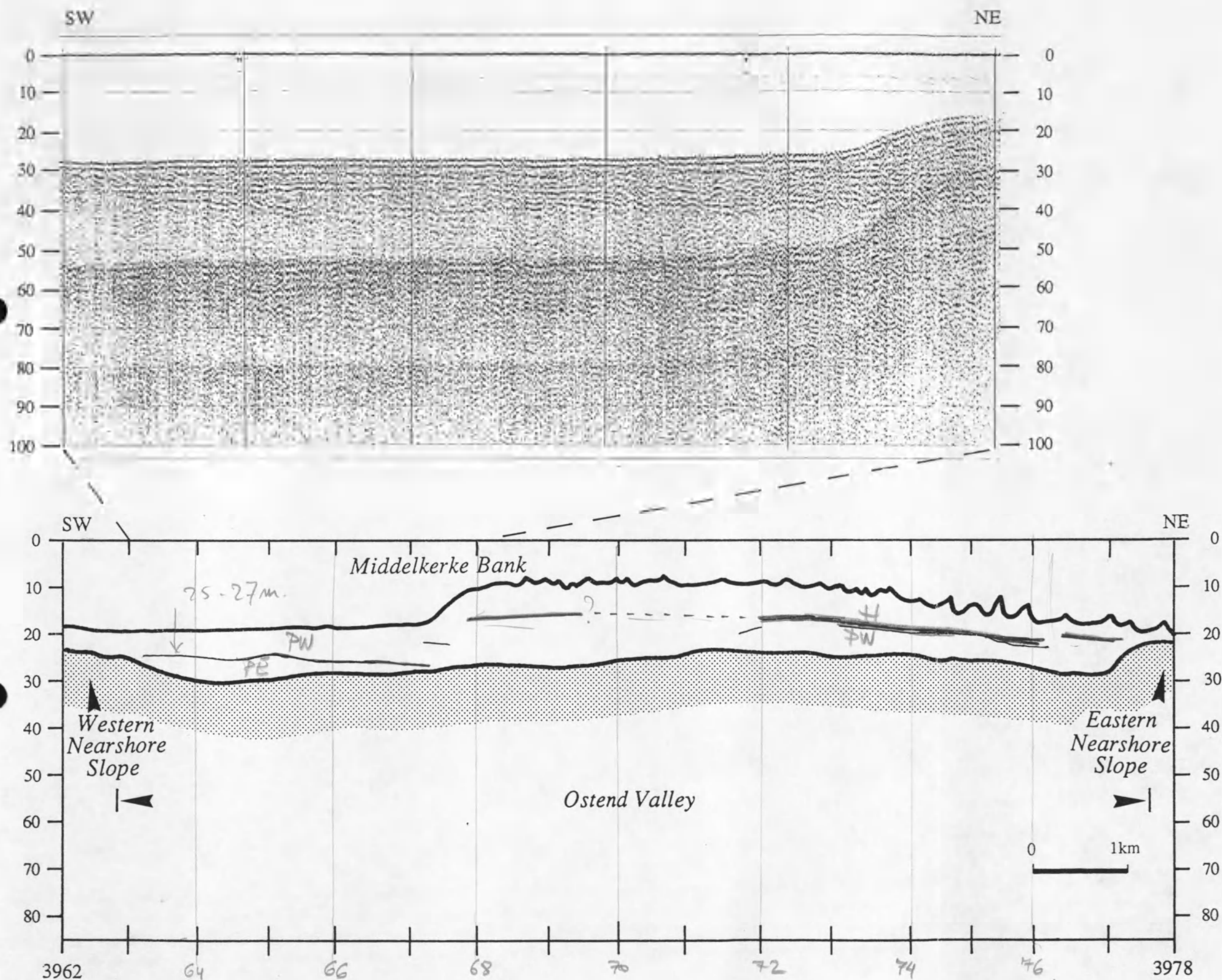


Figure 6.19a Analog record of a sparker section and interpreted line-drawing showing the seaward part of the Ostend Valley. For location of the profile see fig. 6.18.

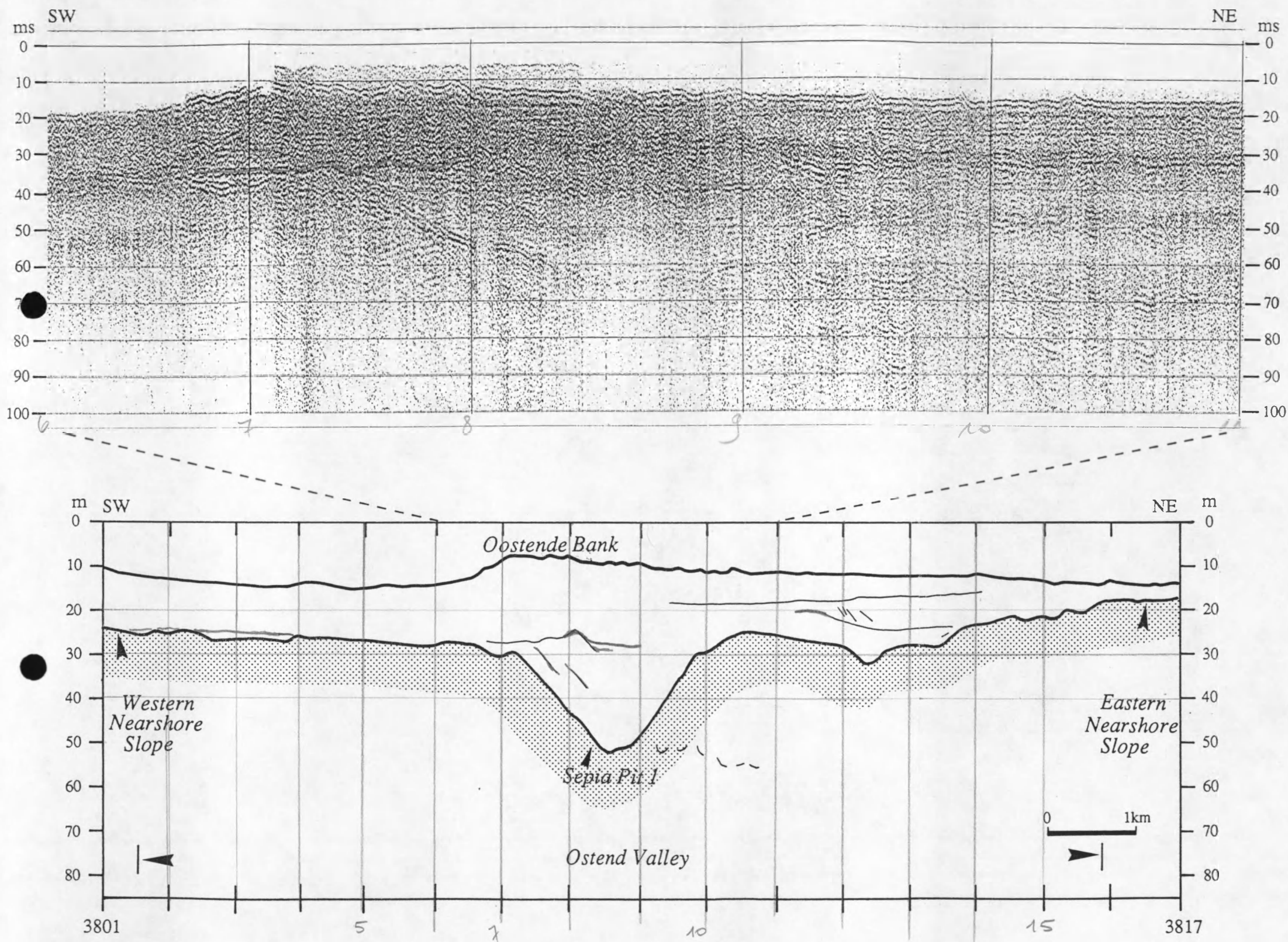


Figure 6.19c Analog record of a sparker section and interpreted line-drawing showing the middle part of the Ostend Valley. For location of the profile see fig. 6.18.

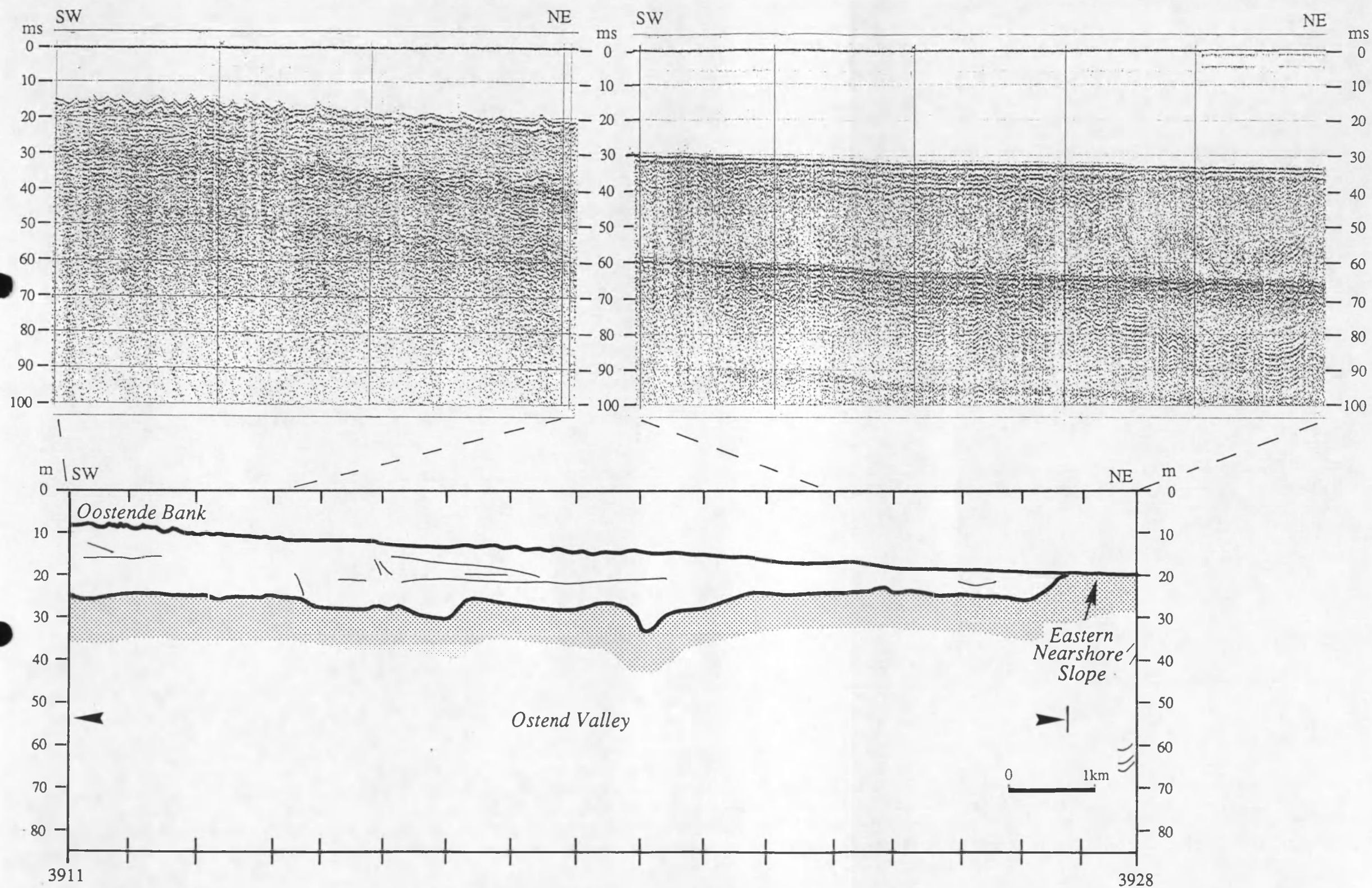


Figure 6.19b Analog record of a sparker section and interpreted line-drawing showing the seaward part of the Ostend Valley. For location of the profile see fig. 6.18.

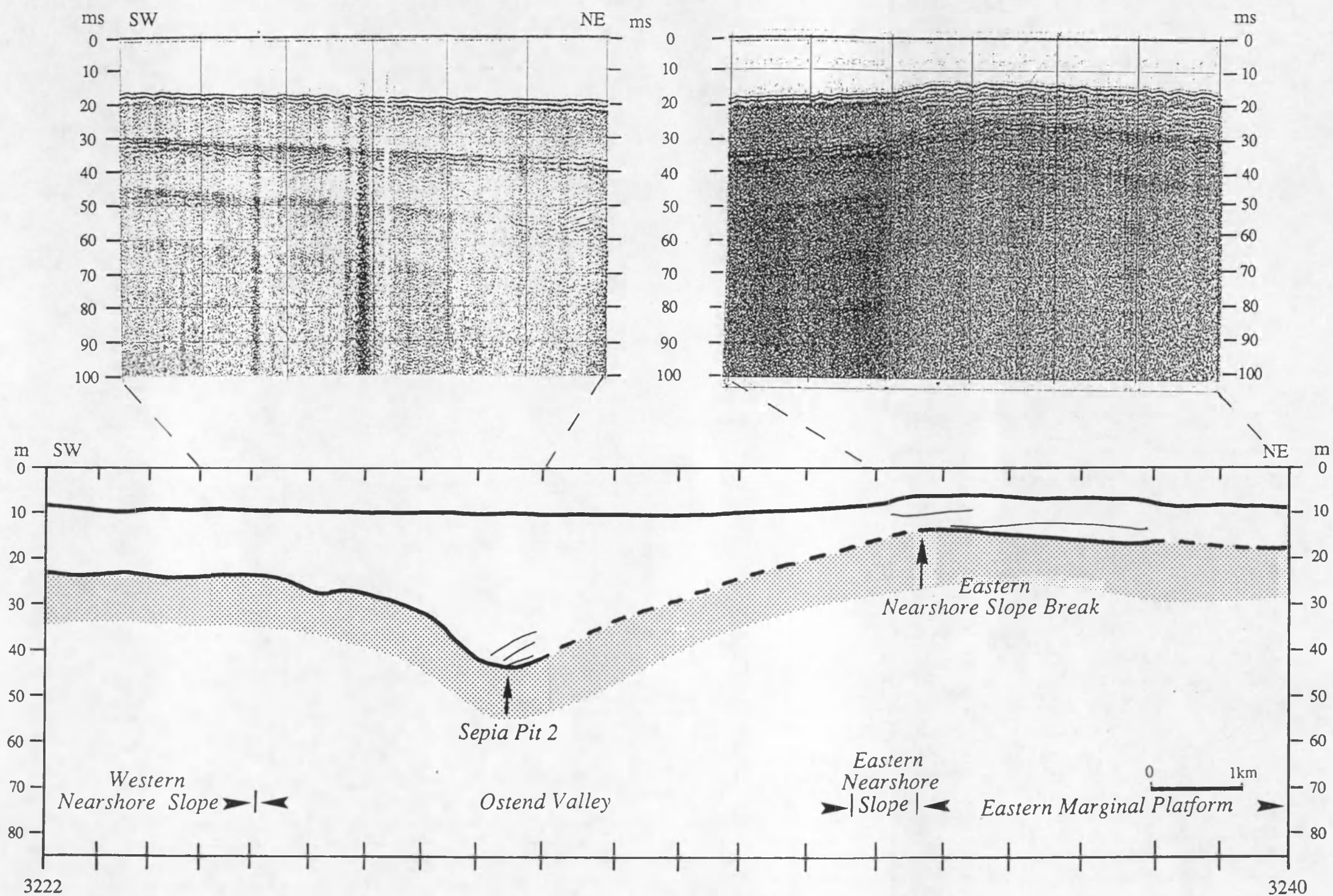


Figure 6.19d Analog record of a sparker section and interpreted line-drawing showing the landward part of the Ostend Valley. For location of the profile see fig. 6.18.

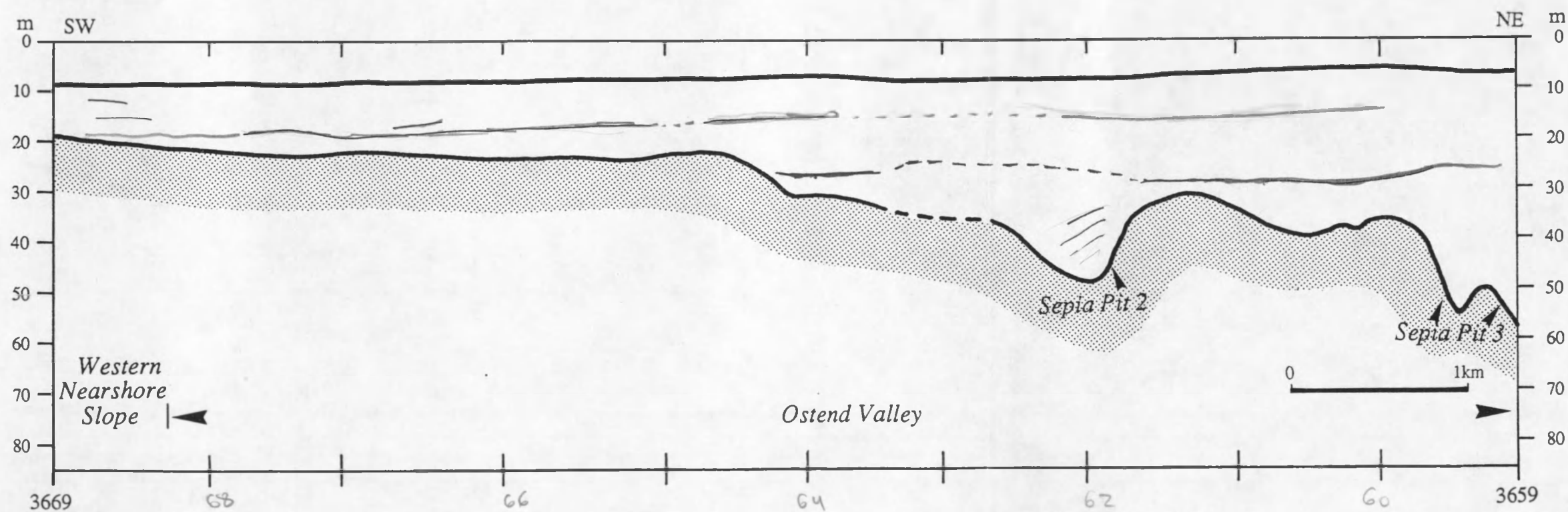
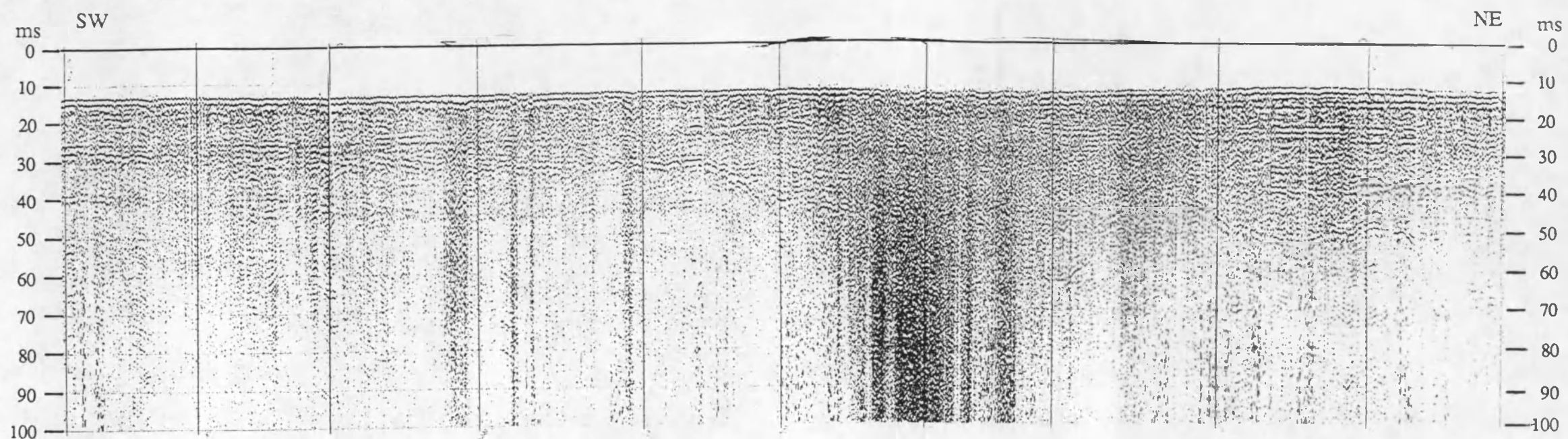


Figure 6.19e Analog record of a sparker section and interpreted line-drawing showing the landward part of the Ostend Valley. For location of the profile see fig. 6.18.

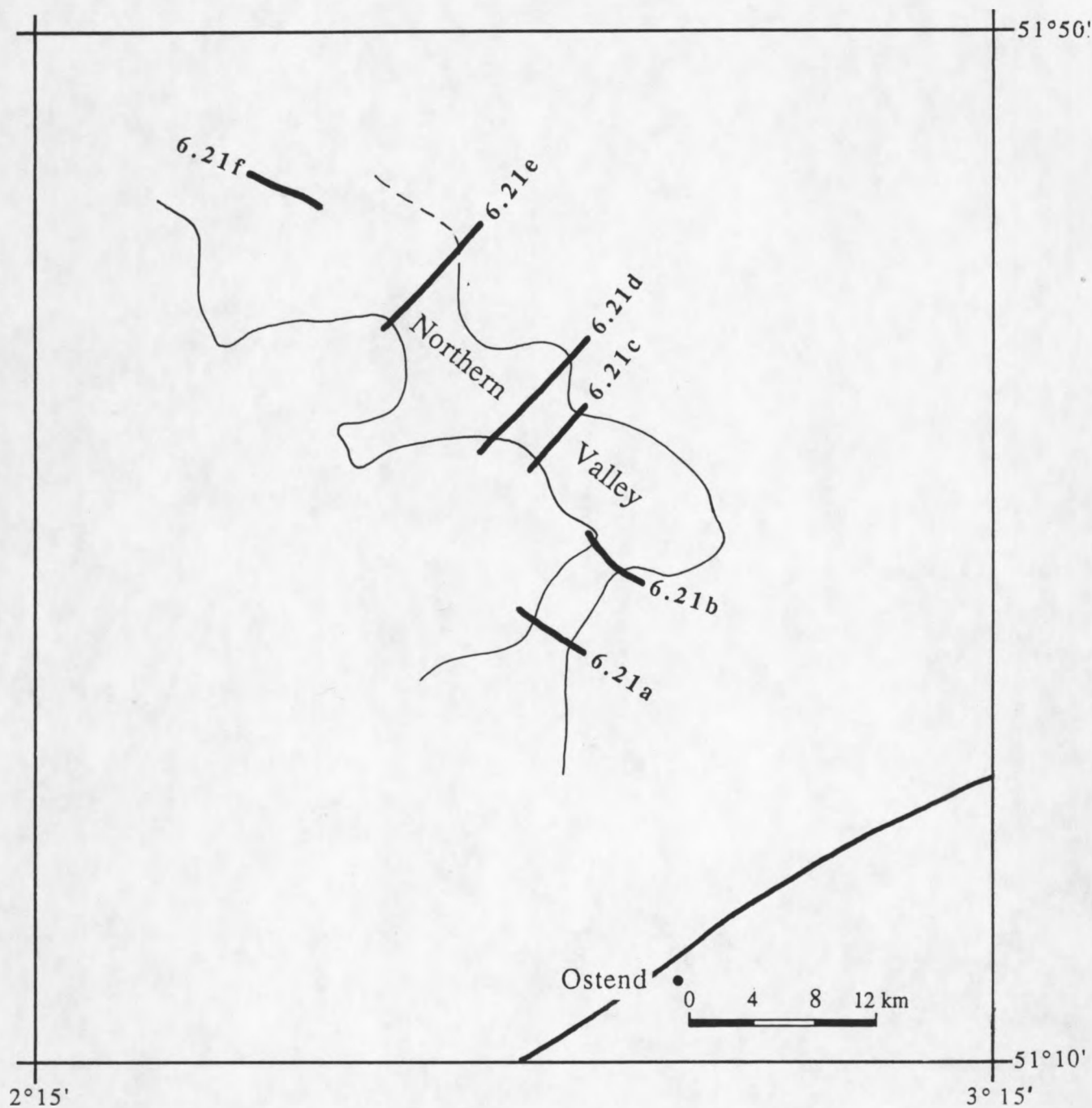


Figure 6.20 Location of profiles across the Northern Valley and the Northern Low Surface.

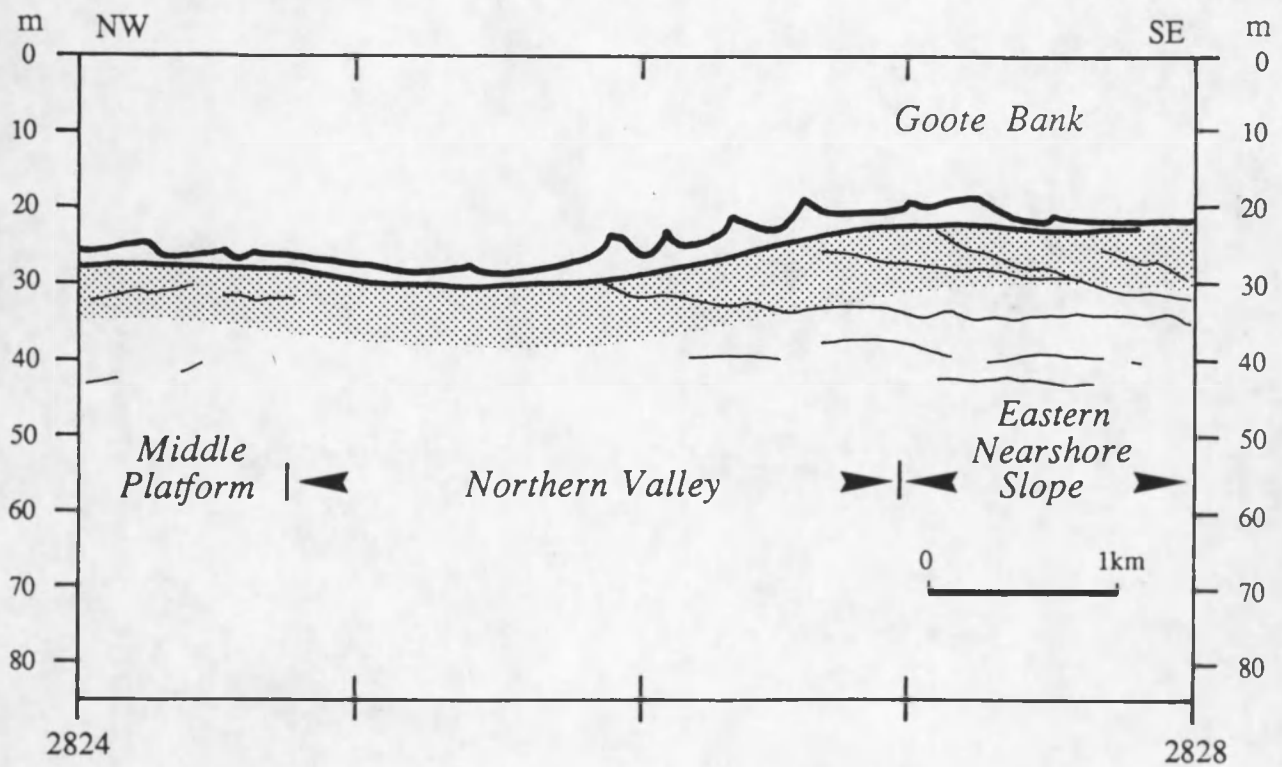
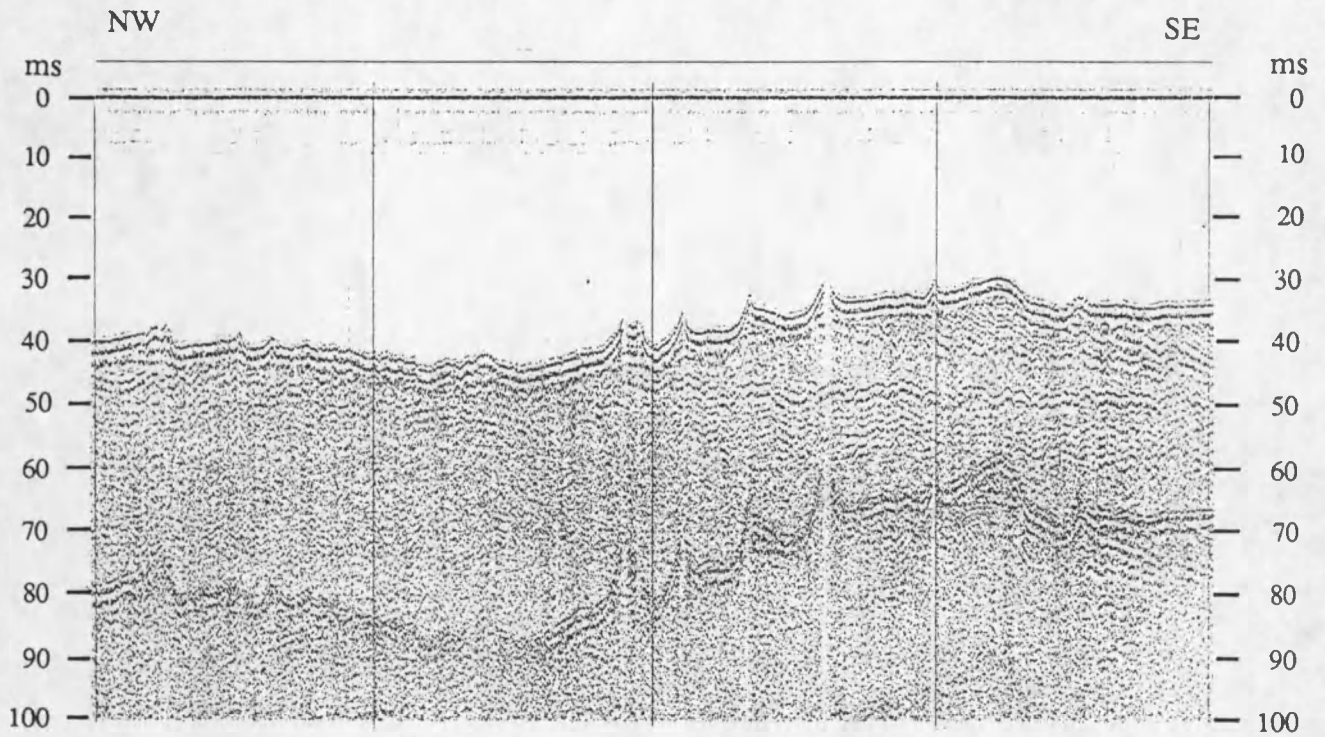


Figure 6.21a Analog record of a sparker section and interpreted line-drawing showing the NE trending Northern Valley. For location of the profile see fig. 6.20.

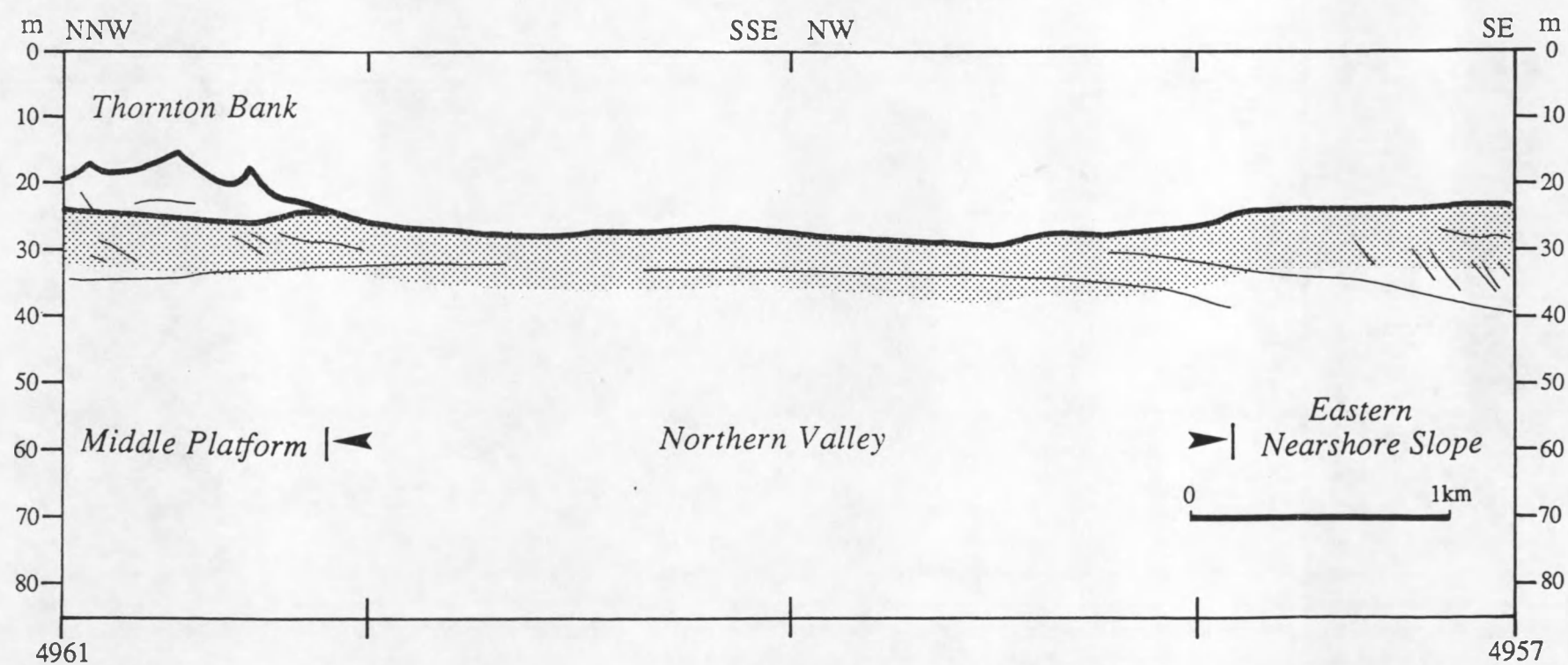
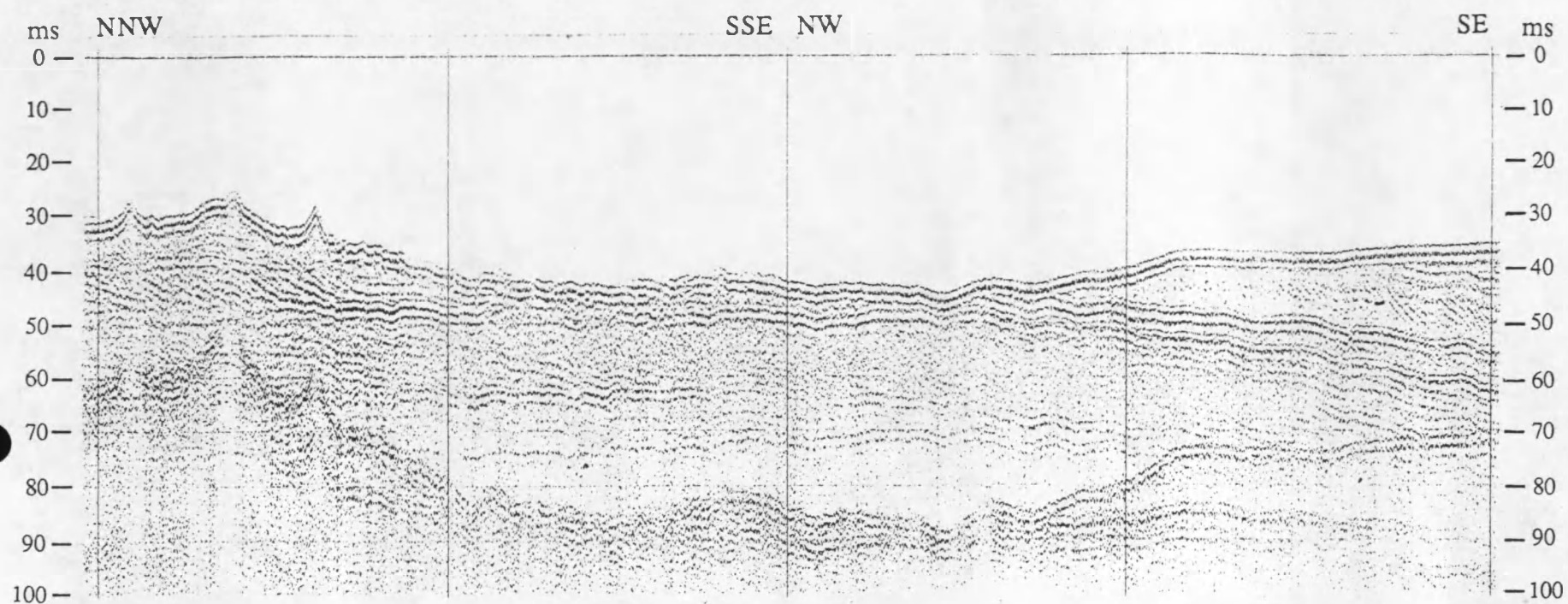


Figure 6.21b Analog record of a sparker section and interpreted line-drawing showing the NE trending Northern Valley. For location of the profile see fig. 6.20.

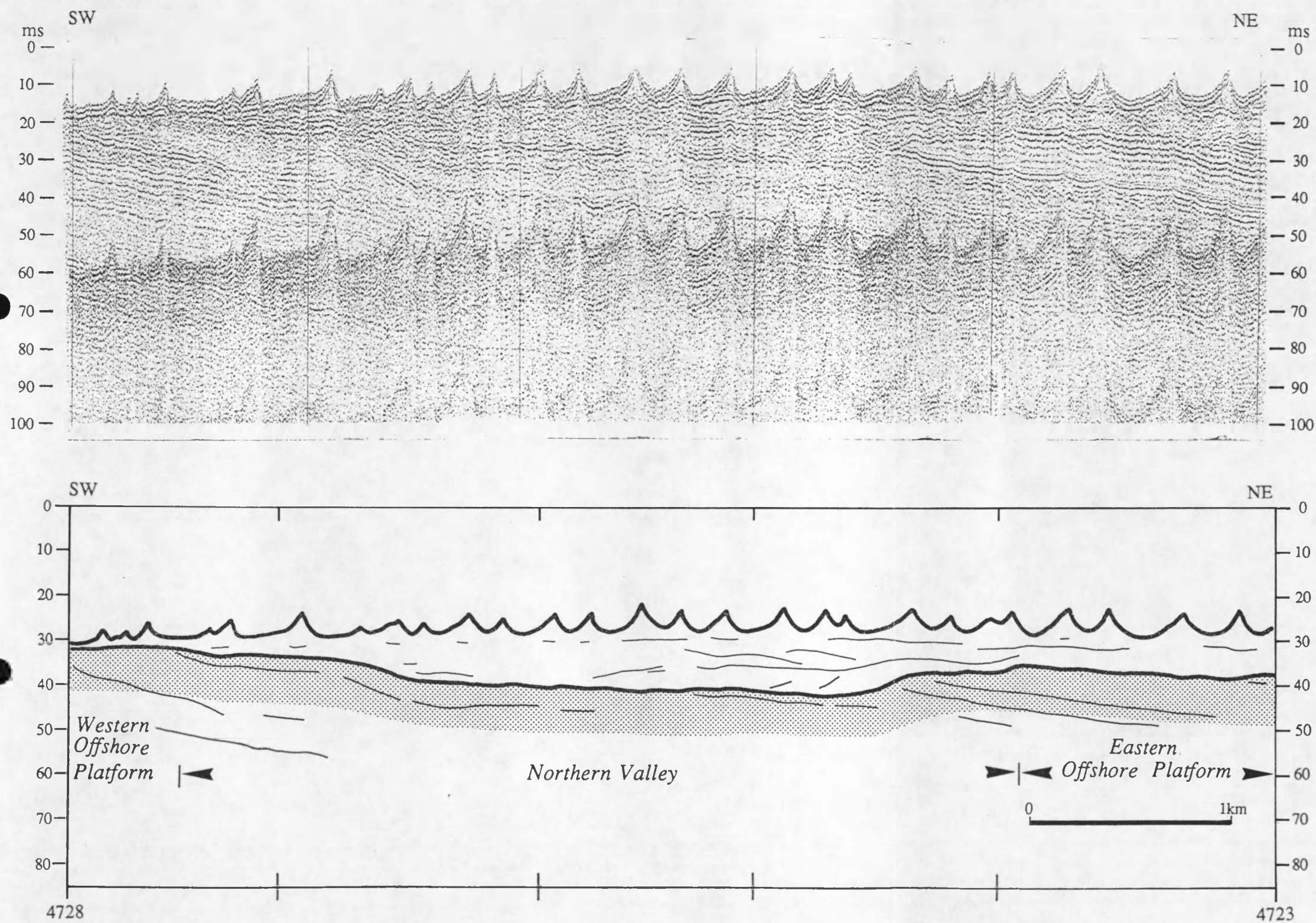


Figure 6.21c Analog record of a sparker section and interpreted line-drawing showing the NW trending Northern Valley. For location of the profile see fig. 6.20.

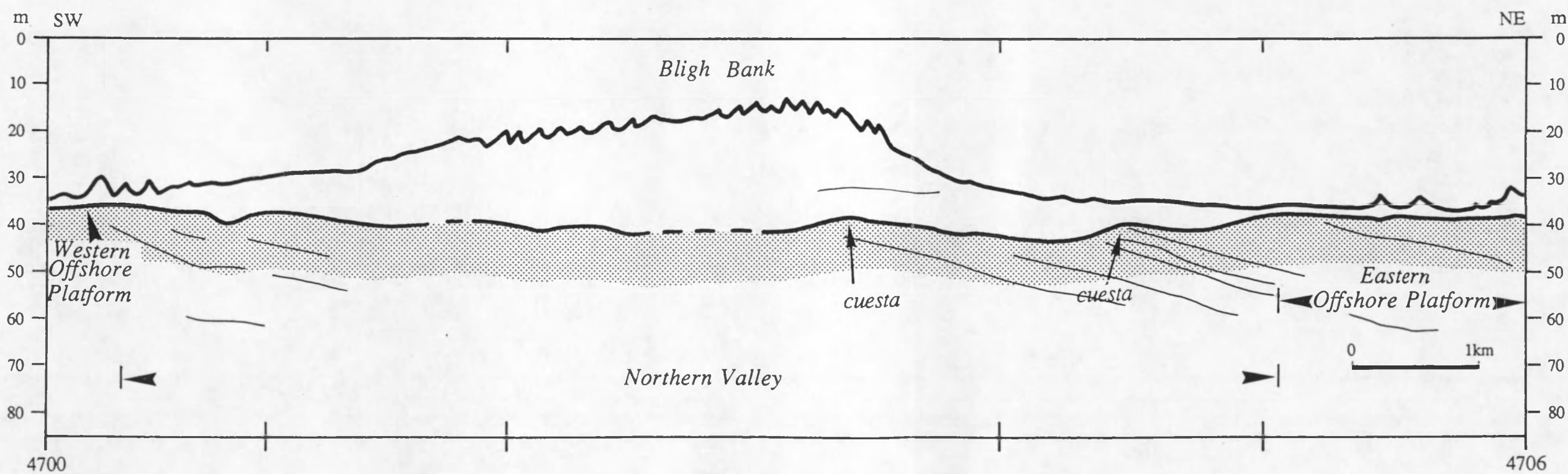
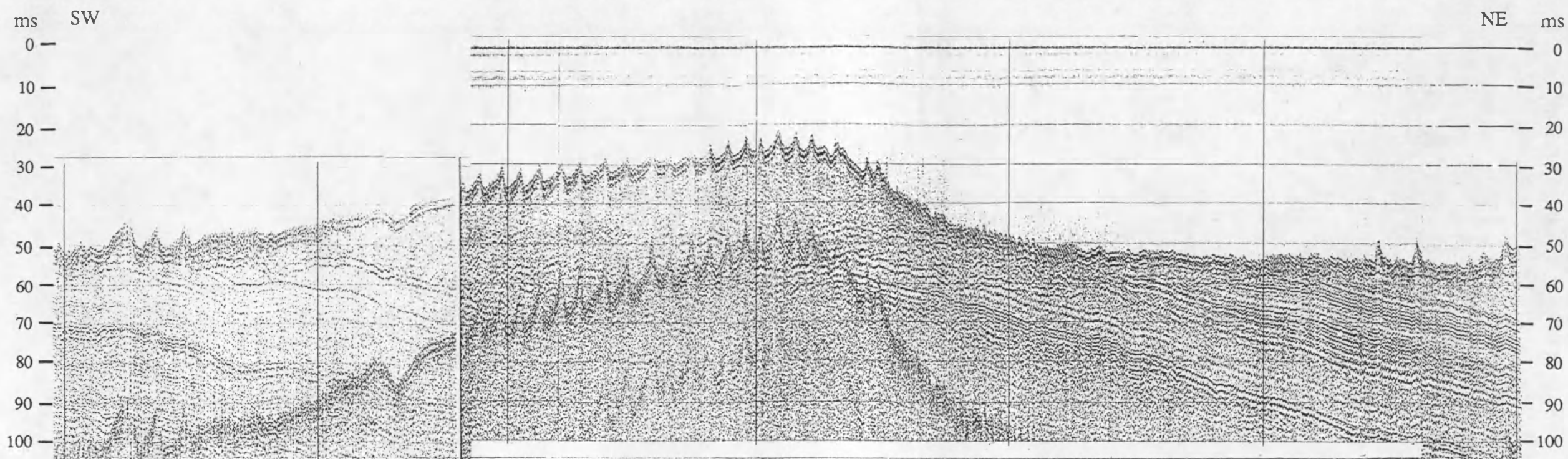


Figure 6.21d Analog record of a sparker section and interpreted line-drawing showing the NW trending Northern Valley. For location of the profile see fig. 6.20.

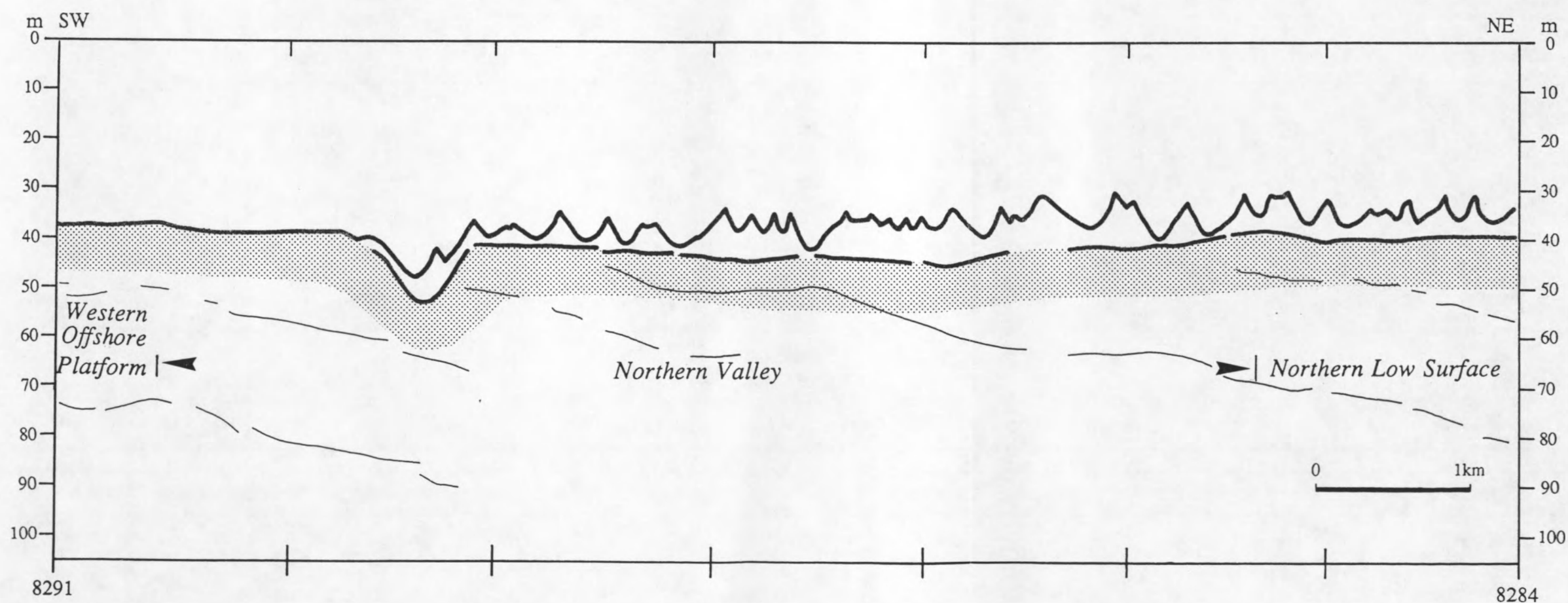
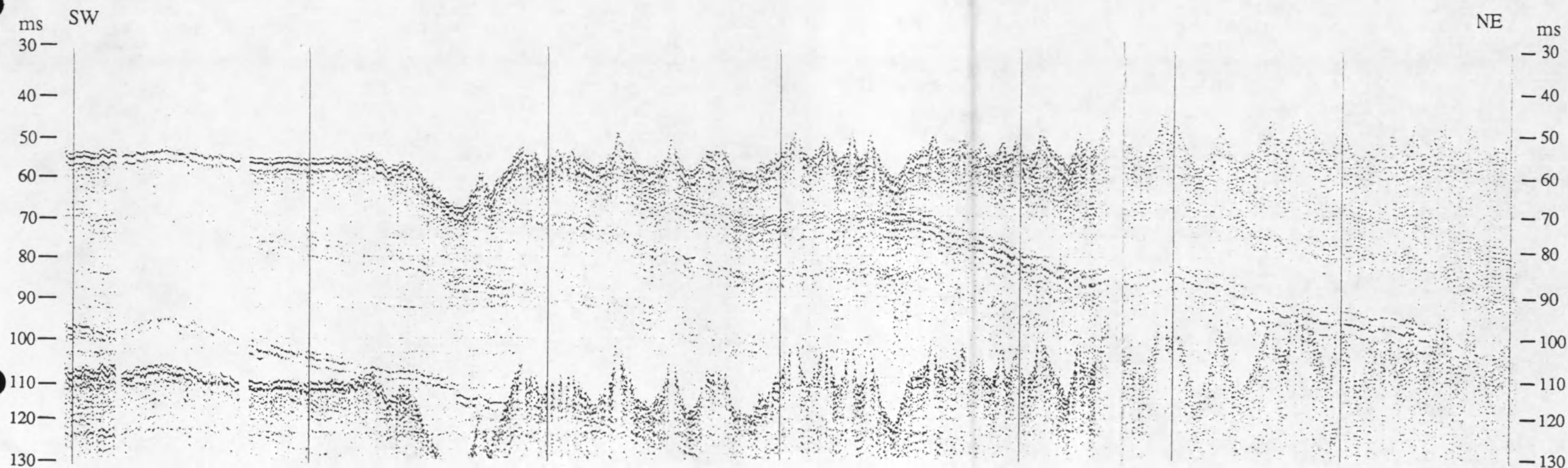


Figure 6.21e Analog record of a sparker section and interpreted line-drawing showing the NW trending Northern Valley. For location of the profile see fig. 6.20.

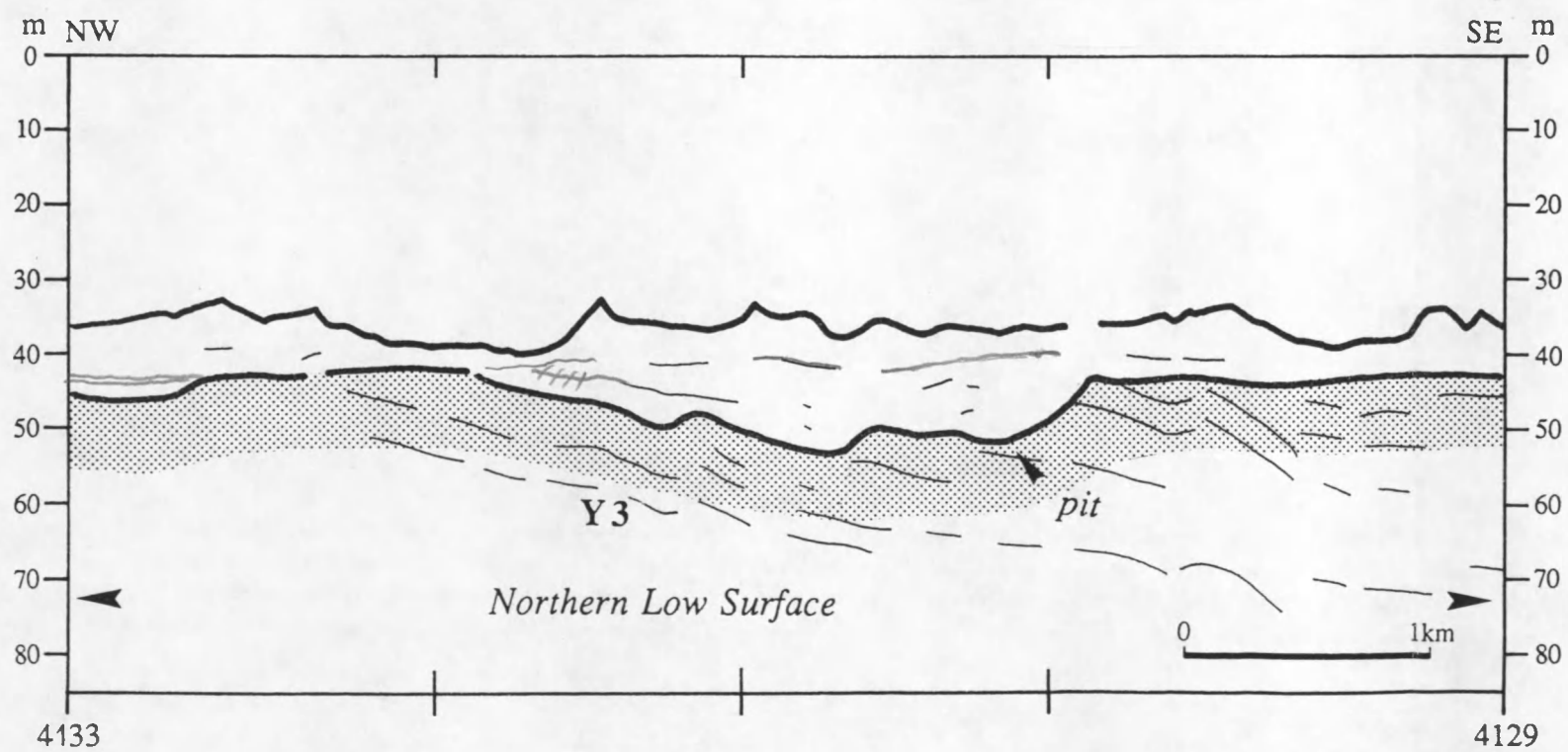
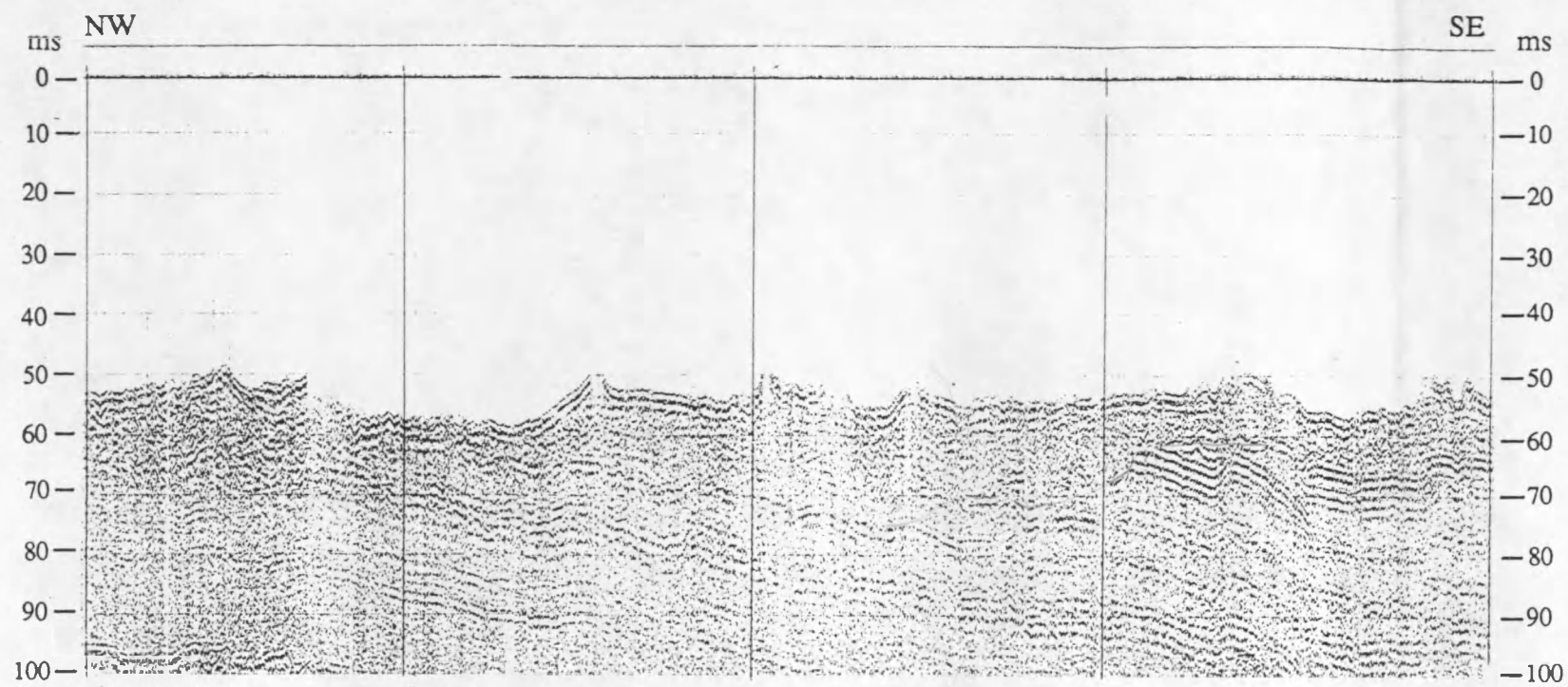


Figure 6.21f Analog record of a sparker section and interpreted line-drawing showing the Northern Low Surface. For location of the profile see fig. 6.20.

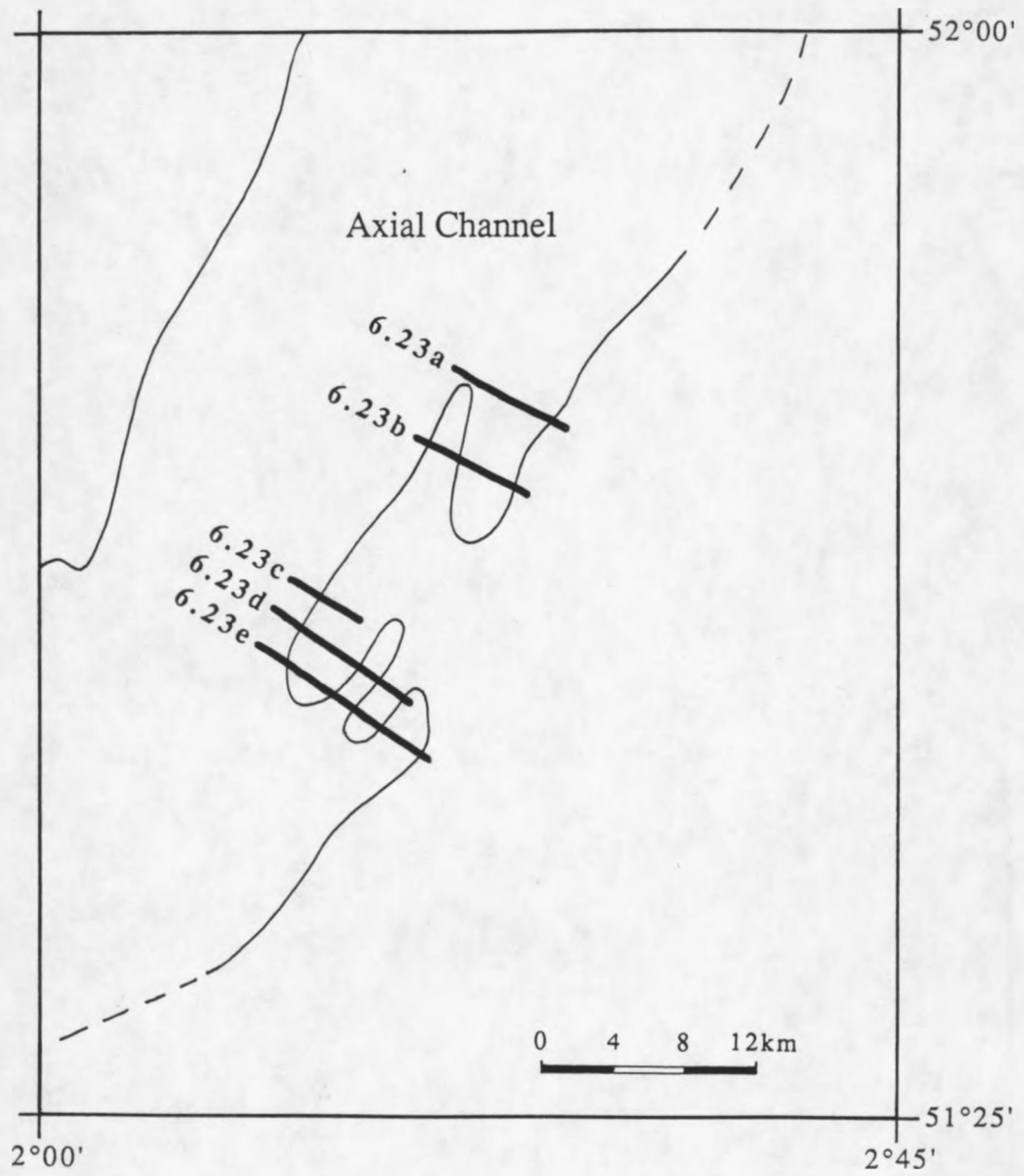


Figure 6.22 Location of profiles across the Axial Channel.

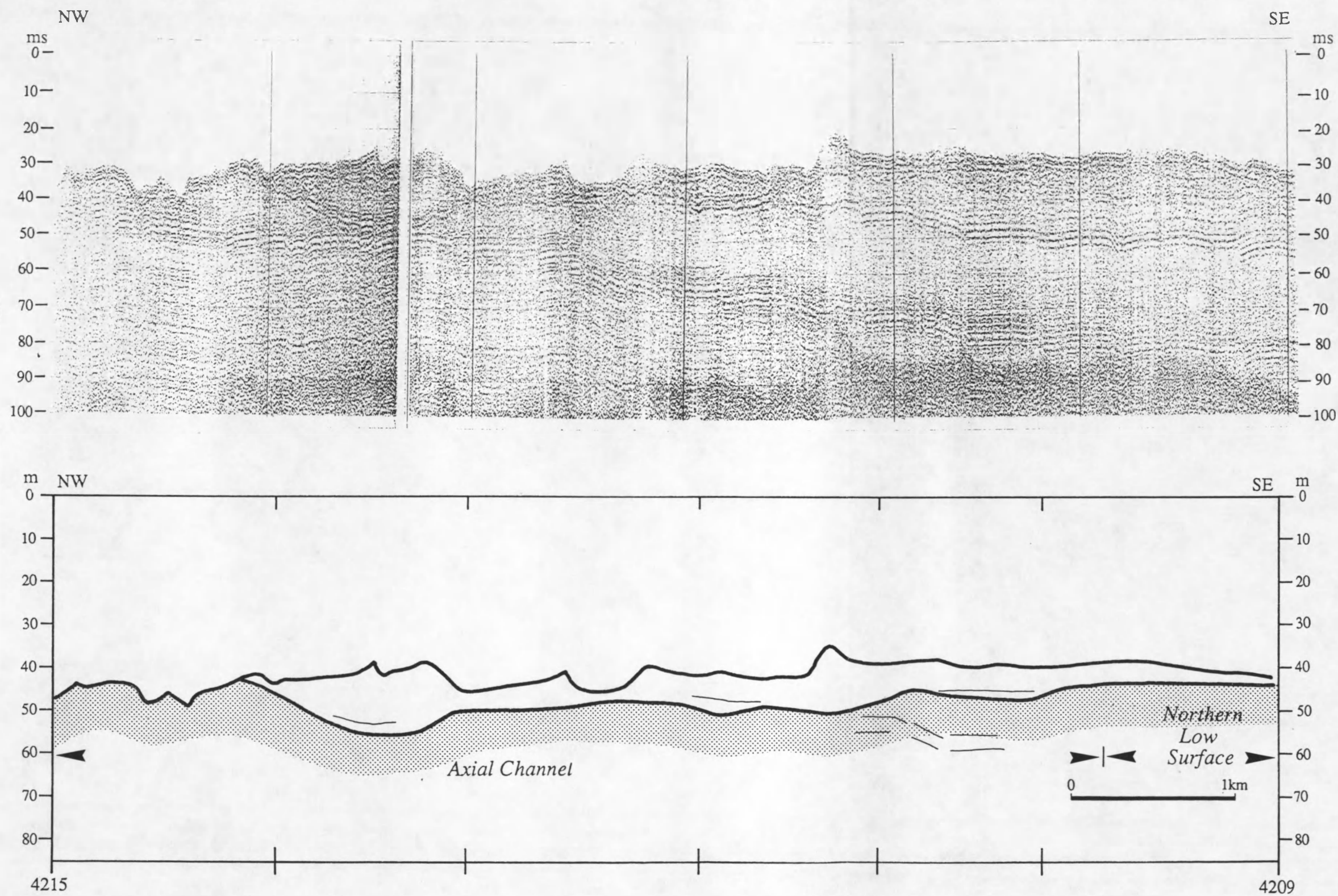


Figure 6.23a Analog record of a sparker section and interpreted line-drawing showing the southeastern part of the Axial Channel. For location of the profile see fig. 6.22.

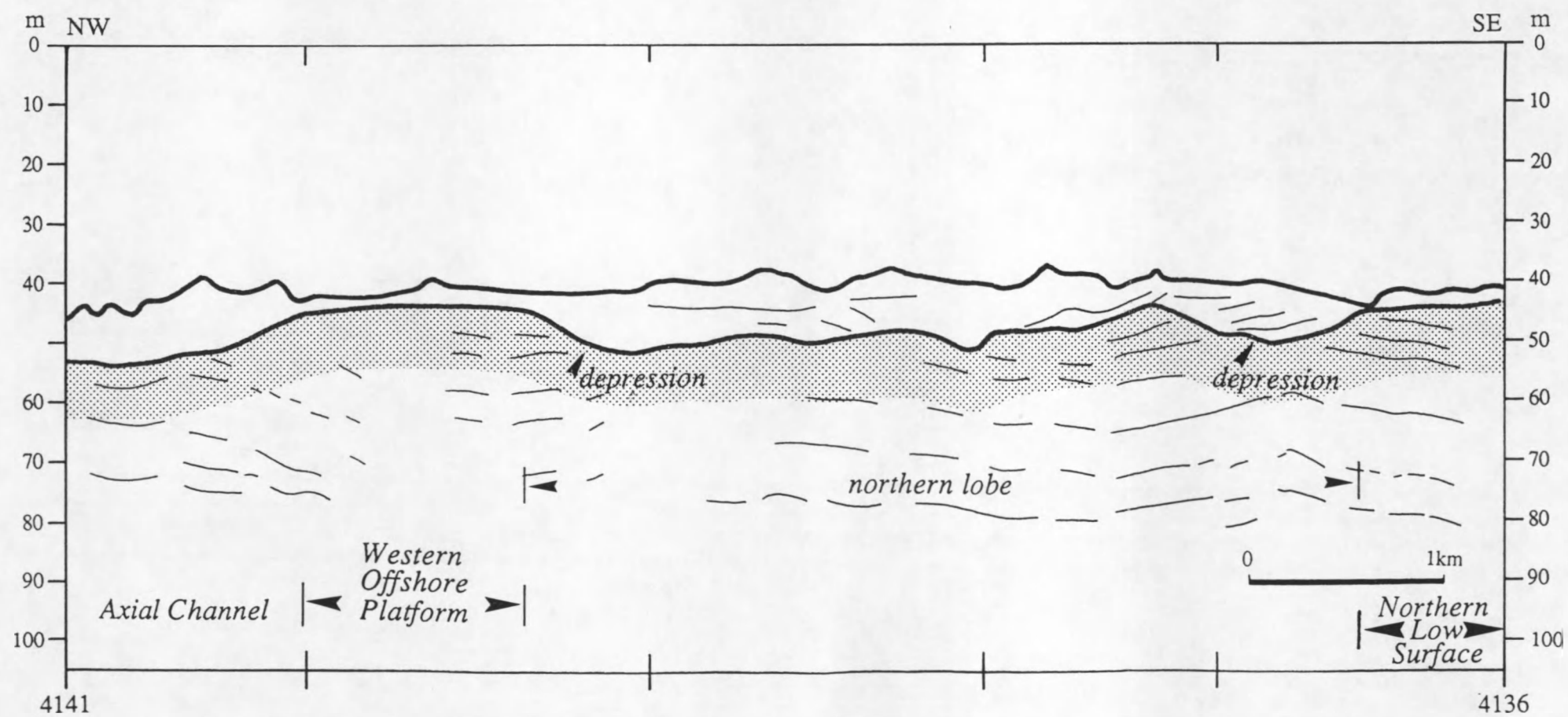
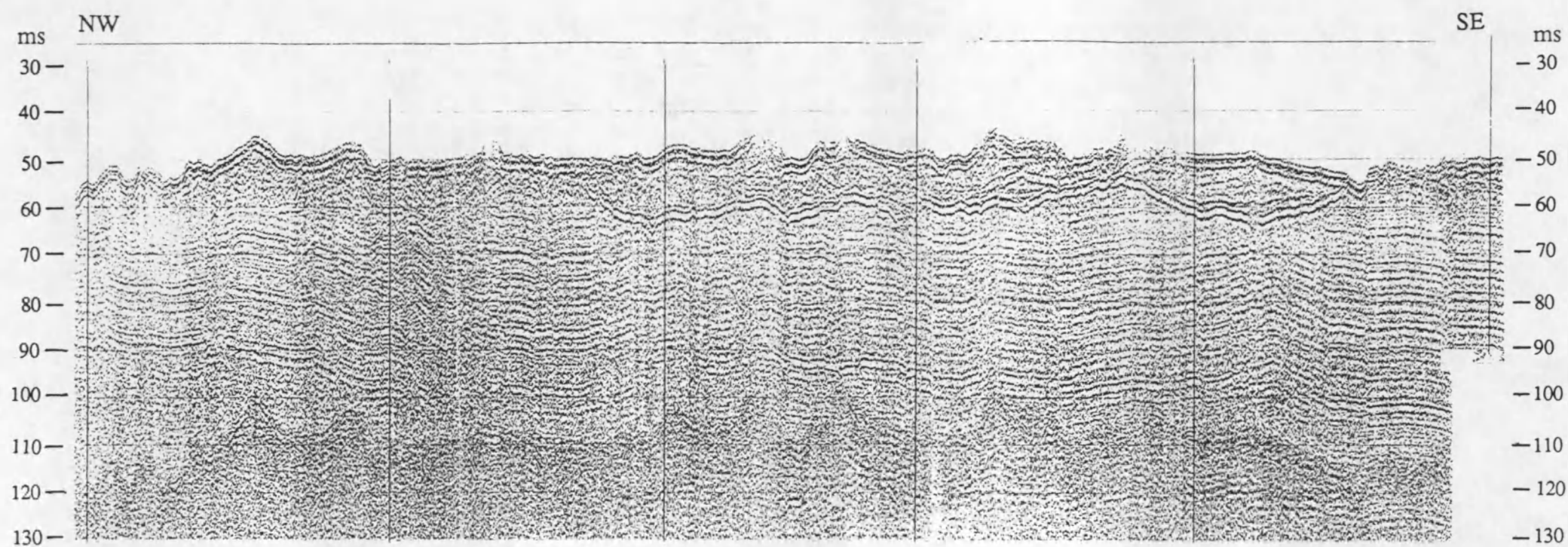


Figure 6.23b Analog record of a sparker section and interpreted line-drawing showing the northern lobe in the Axial Channel. For location of the profile see fig. 6.22.

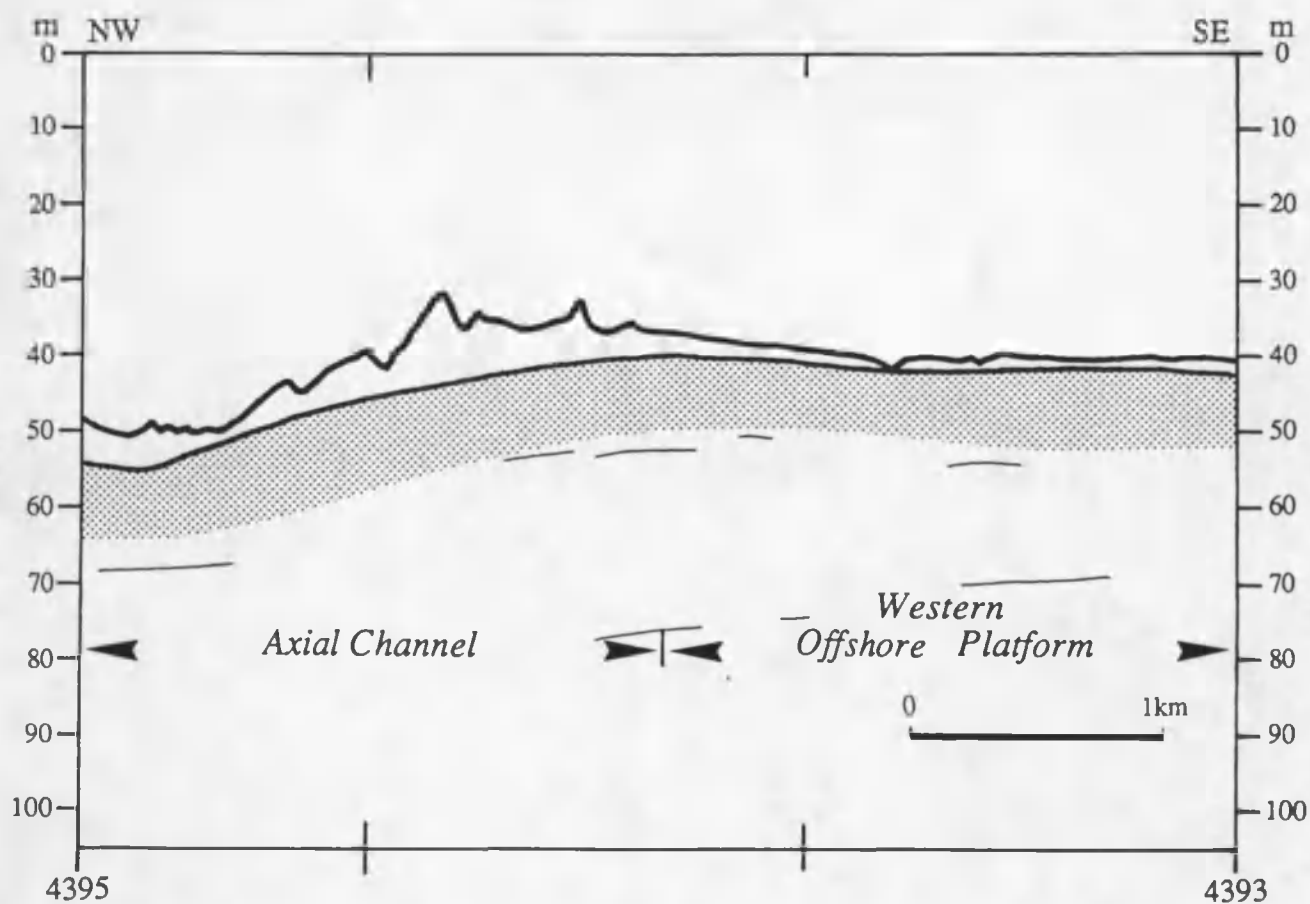
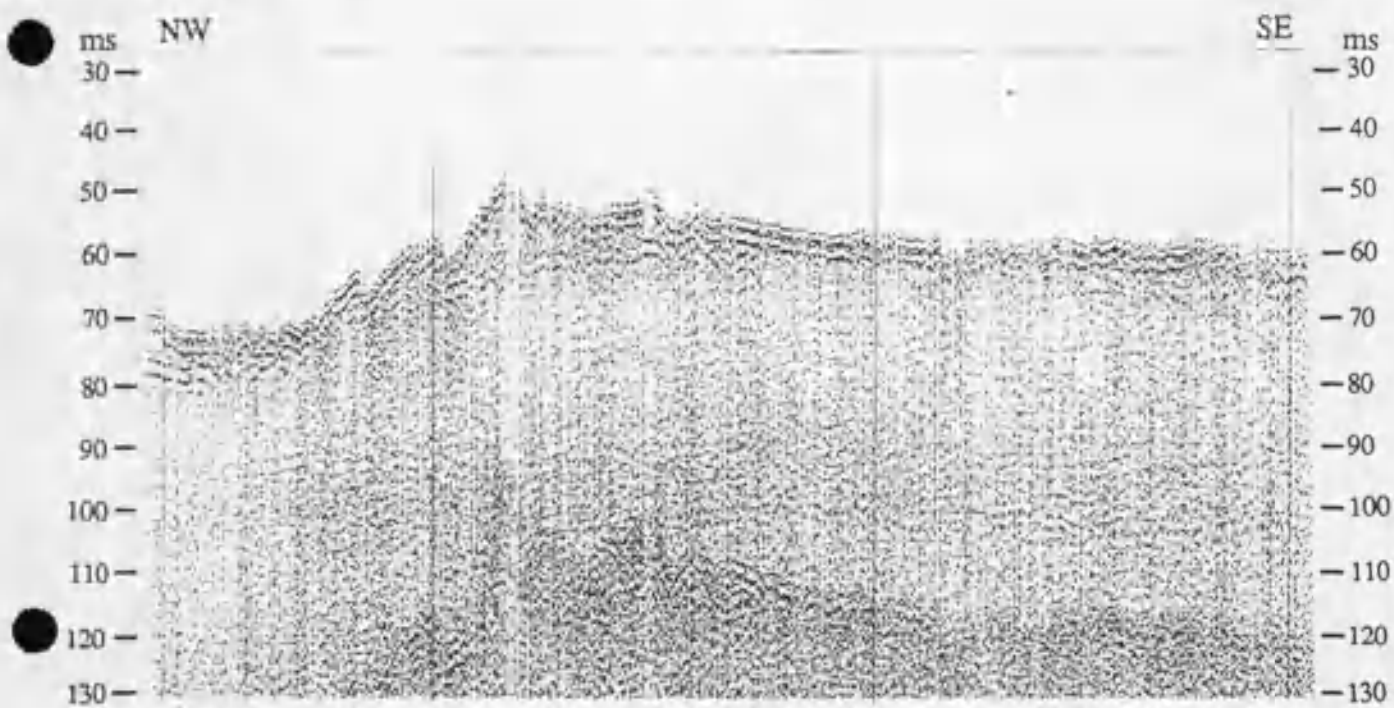


Figure 6.23c Analog record of a sparker section and interpreted line-drawing showing the part of the Axial Channel between the northern and southern lobes. For location of the profile see fig. 6.22.

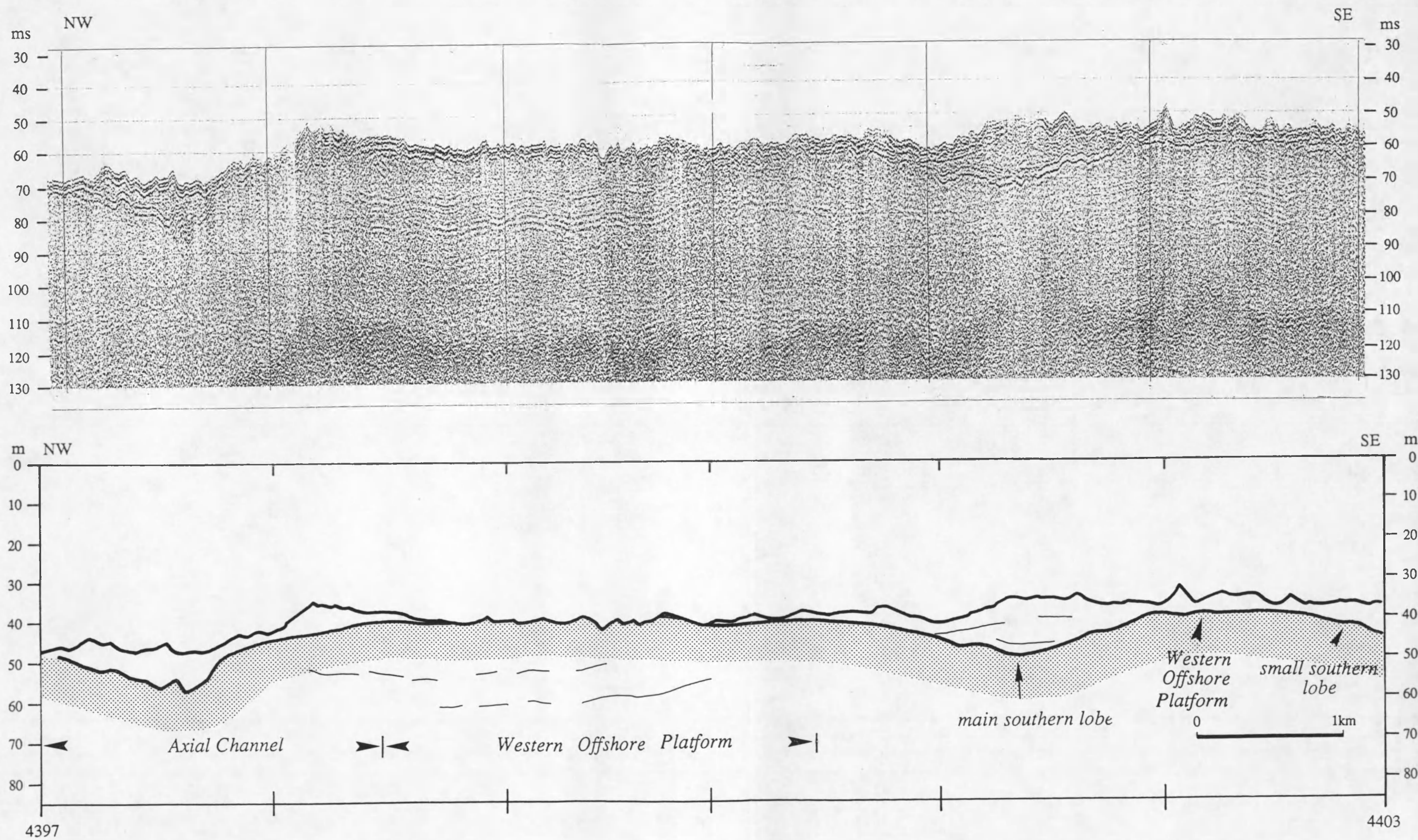


Figure 6.23d Analog record of a sparker section and interpreted line-drawing showing the southern lobe in the Axial Channel. For location of the profile see fig. 6.22.

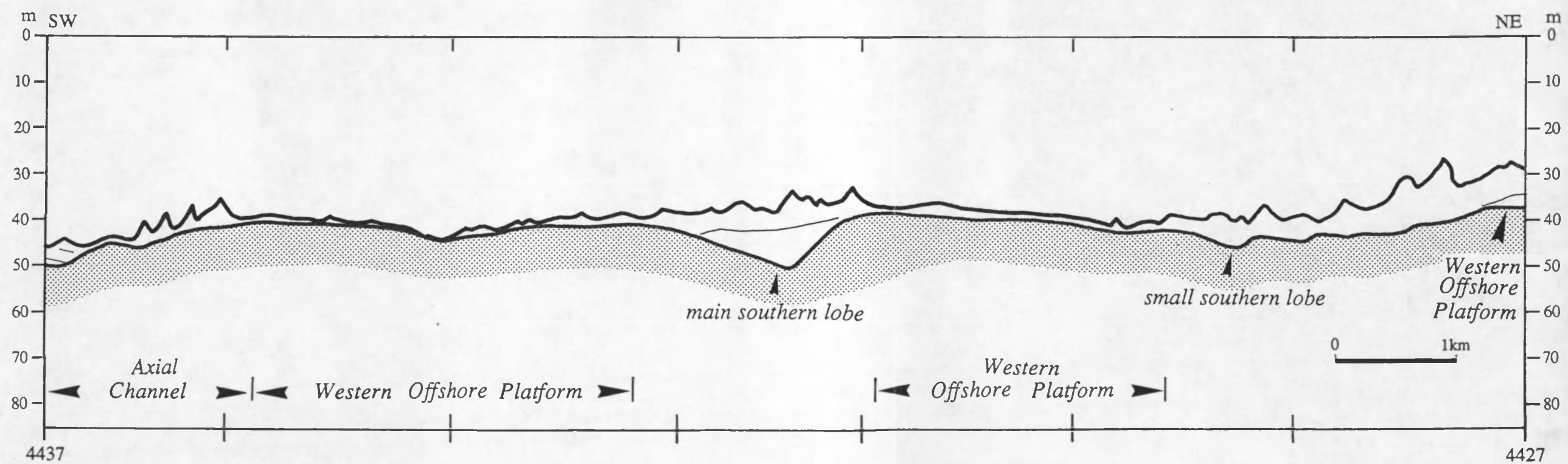
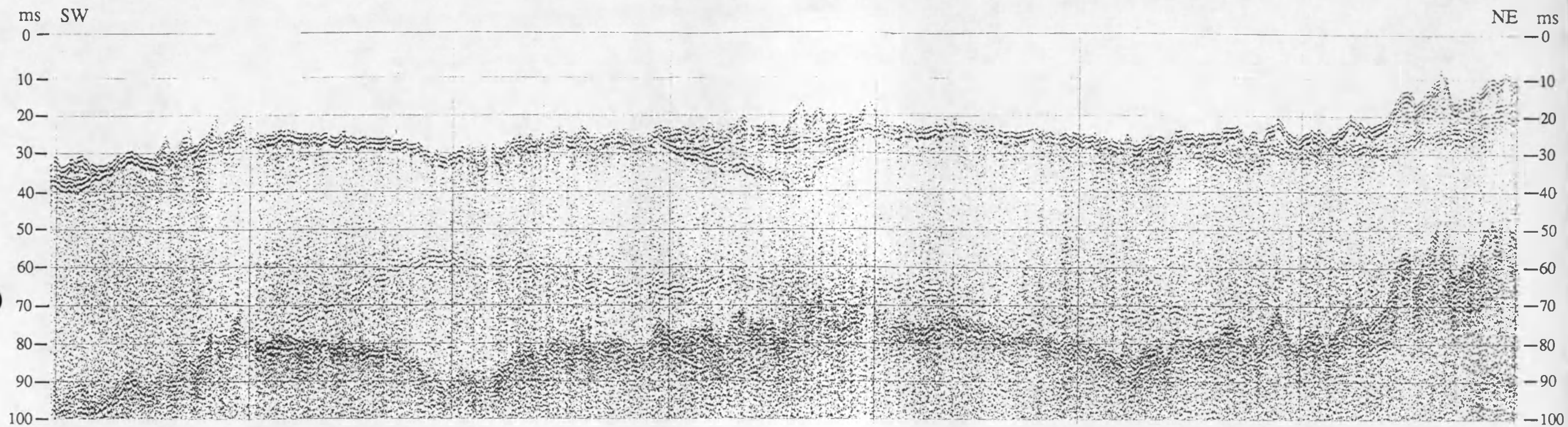


Figure 6.23e Analog record of a sparker section and interpreted line-drawing showing the southern lobe in the Axial Channel. For location of the profile see fig. 6.22.

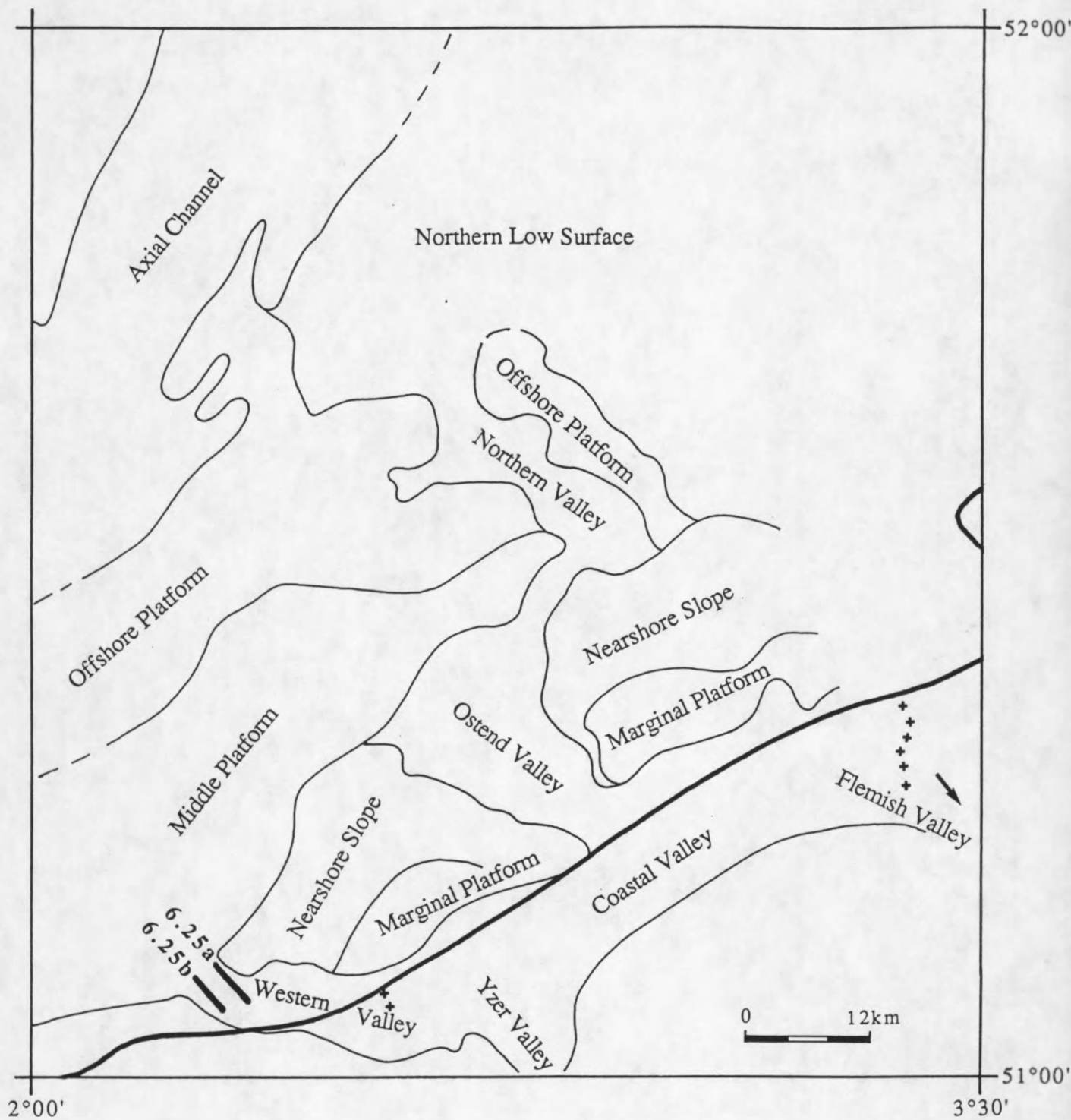


Figure 6.24 Location of profiles across the Dunkerque Pit.

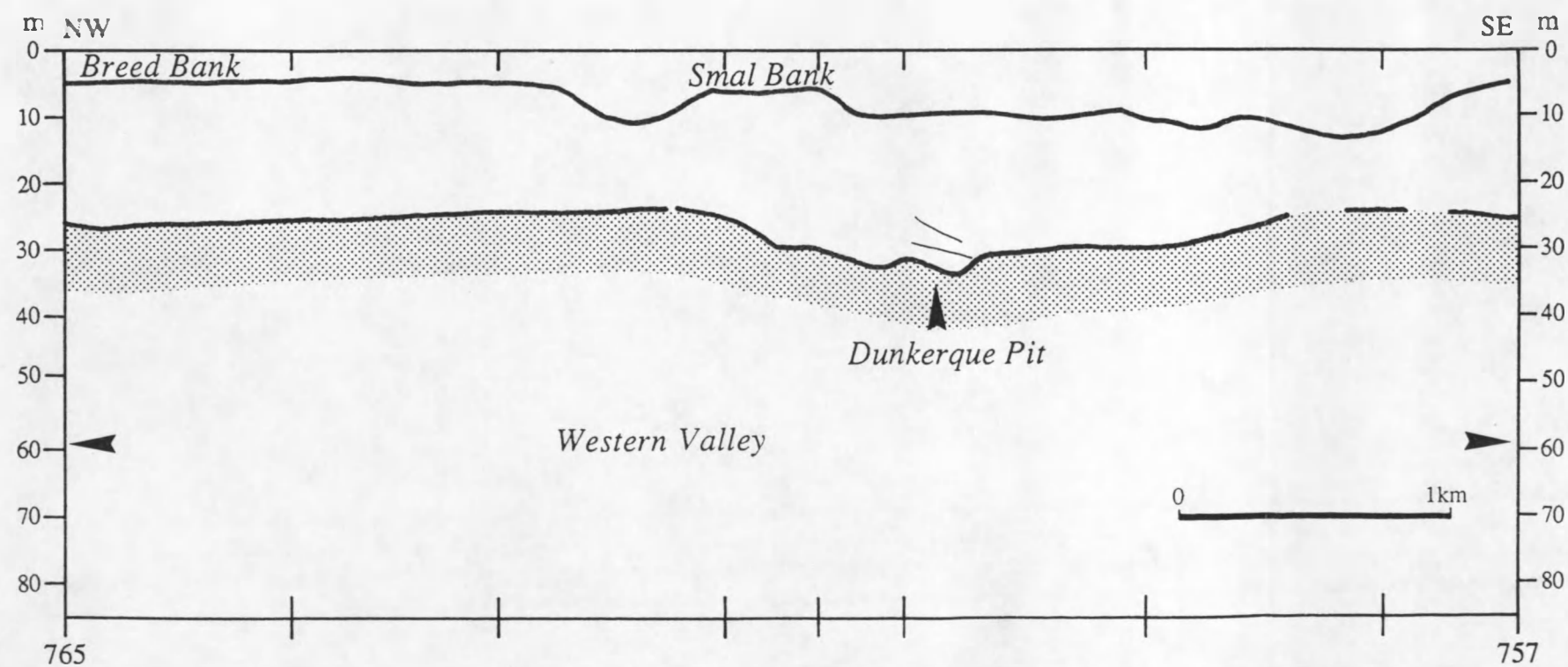
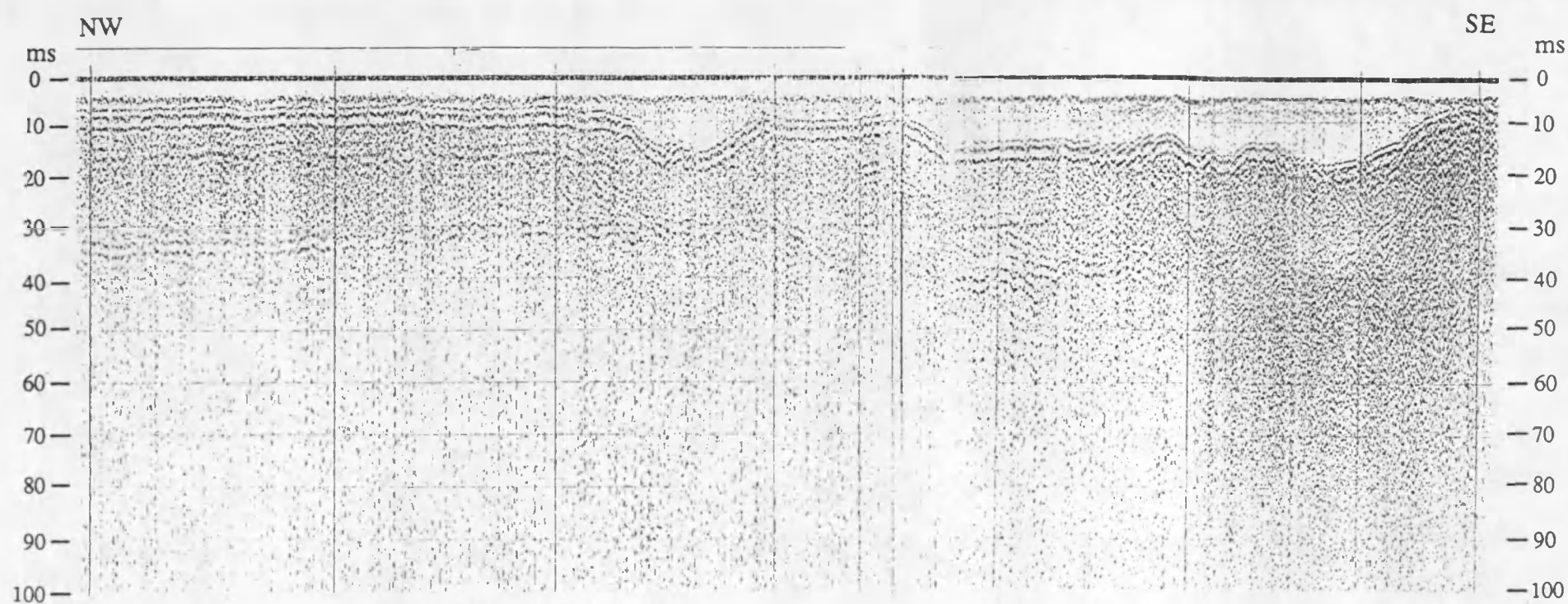


Figure 6.25a Analog record of a sparker section and interpreted line-drawing showing the Dunkerque Pit in the Western Valley. For location of the profile see fig. 6.24.

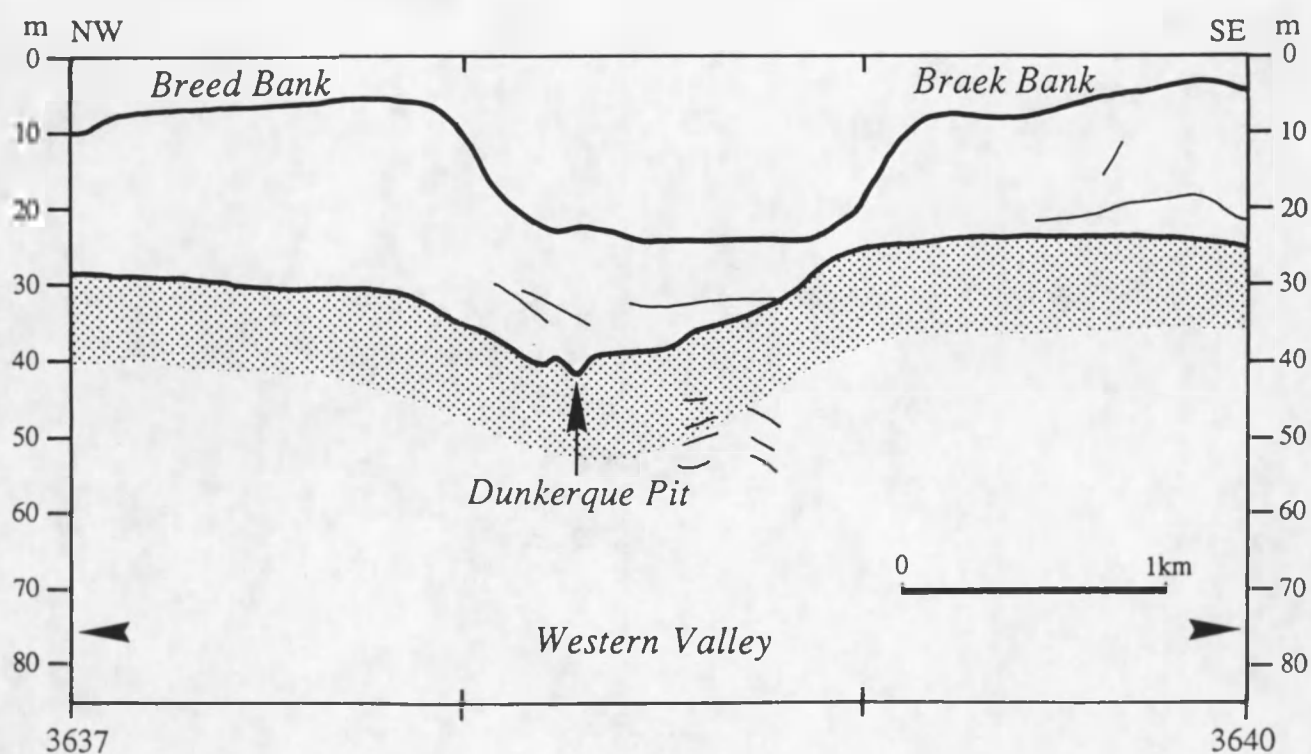
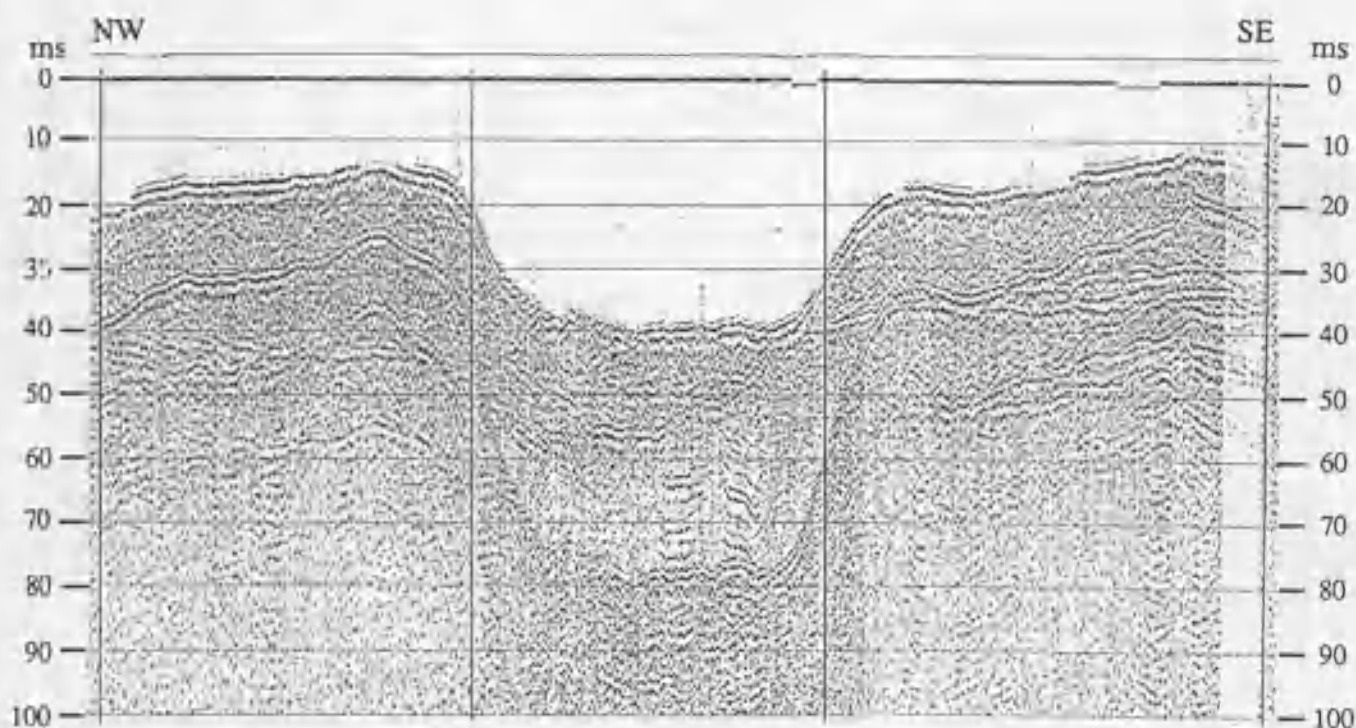


Figure 6.25b Analog record of a sparker section and interpreted line-drawing showing the Dunkerque Pit in the Western Valley. For location of the profile see fig. 6.24.

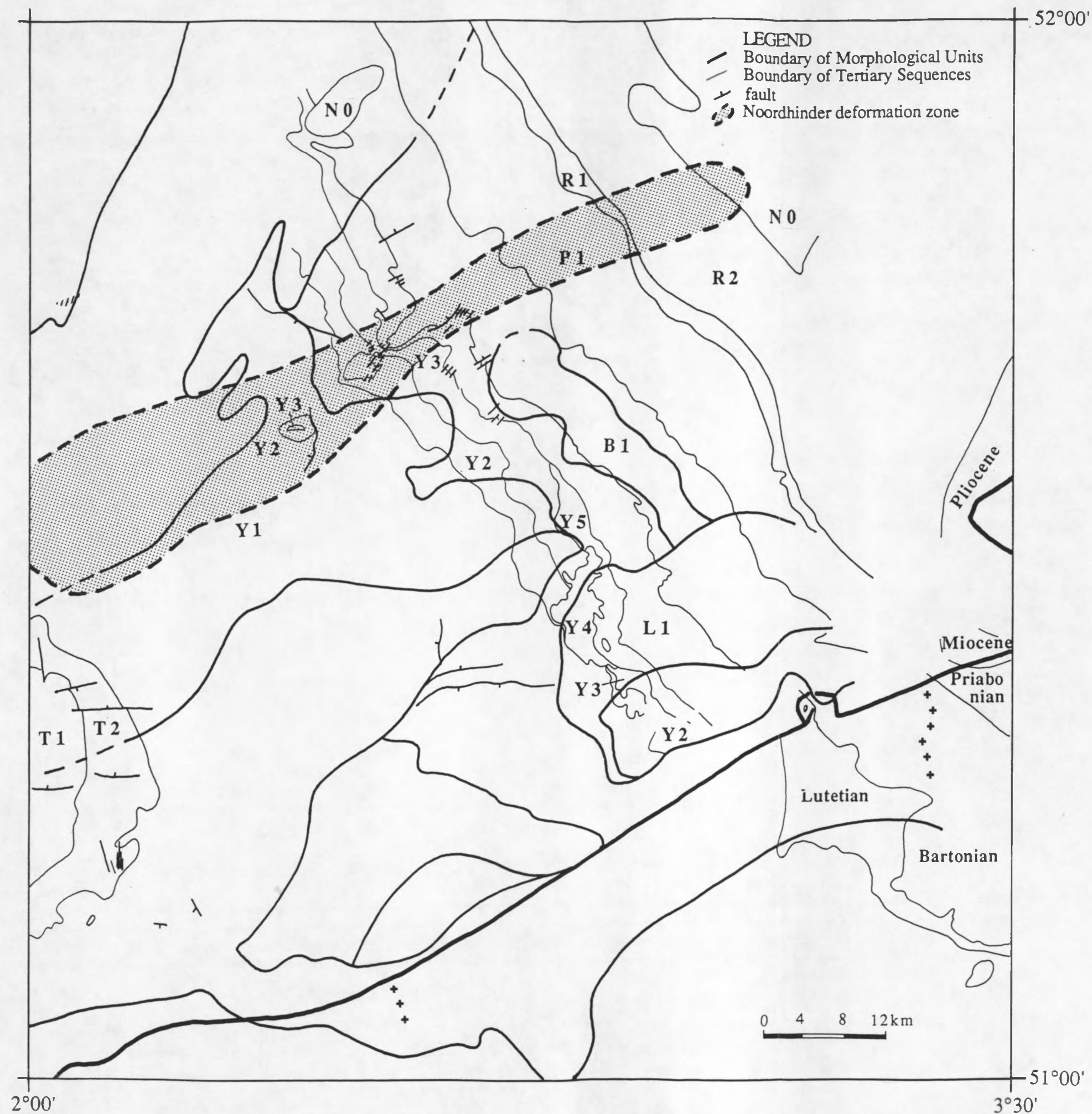


Figure 7.1 Paleogene sequences subcropping against the top-Tertiary erosion surface of the different morphological units (partly after De Batist, 1989).

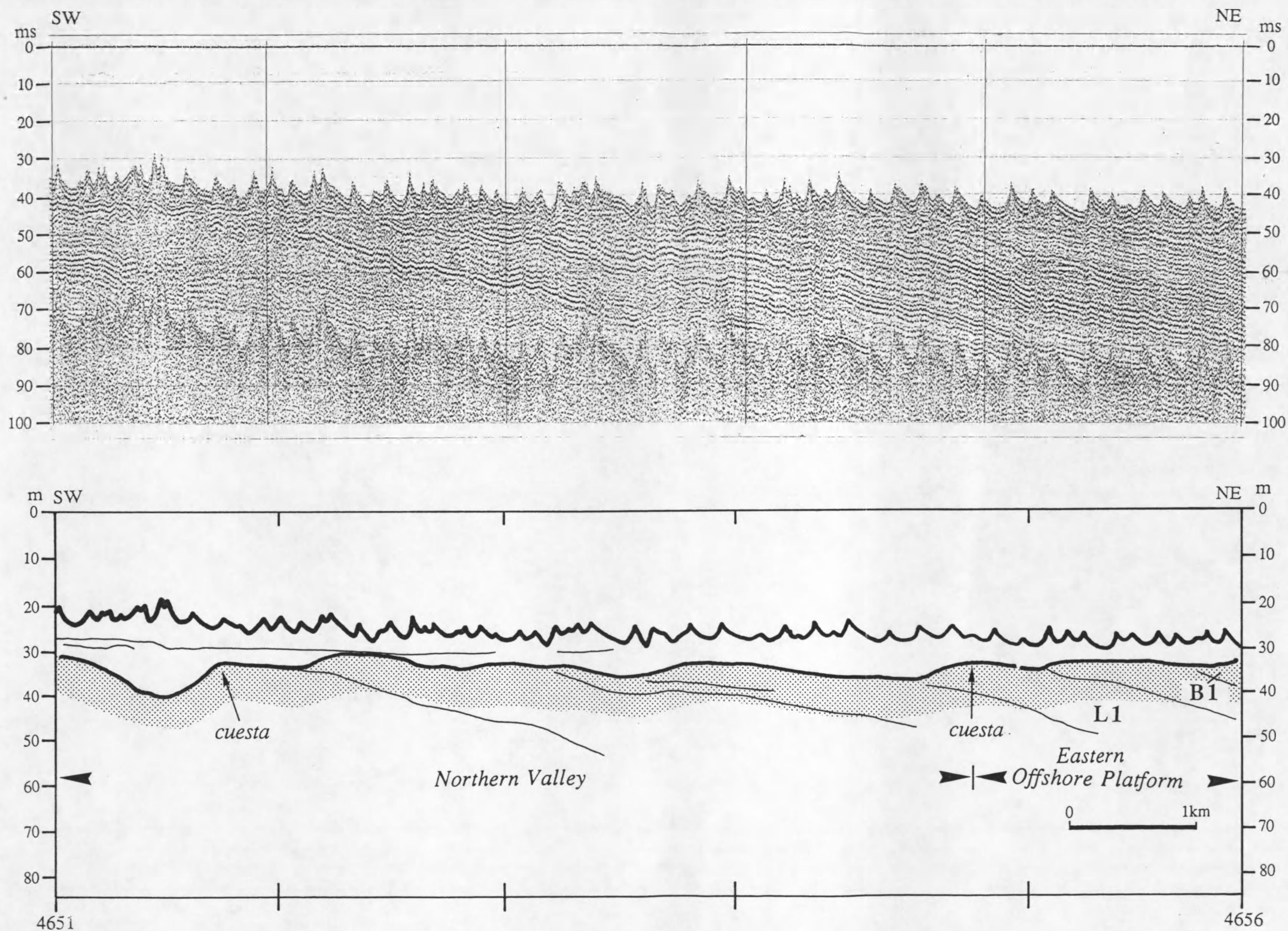


Figure 7.2 Analog record of a sparker section and interpreted line-drawing showing cuestas in the L1 sequence.

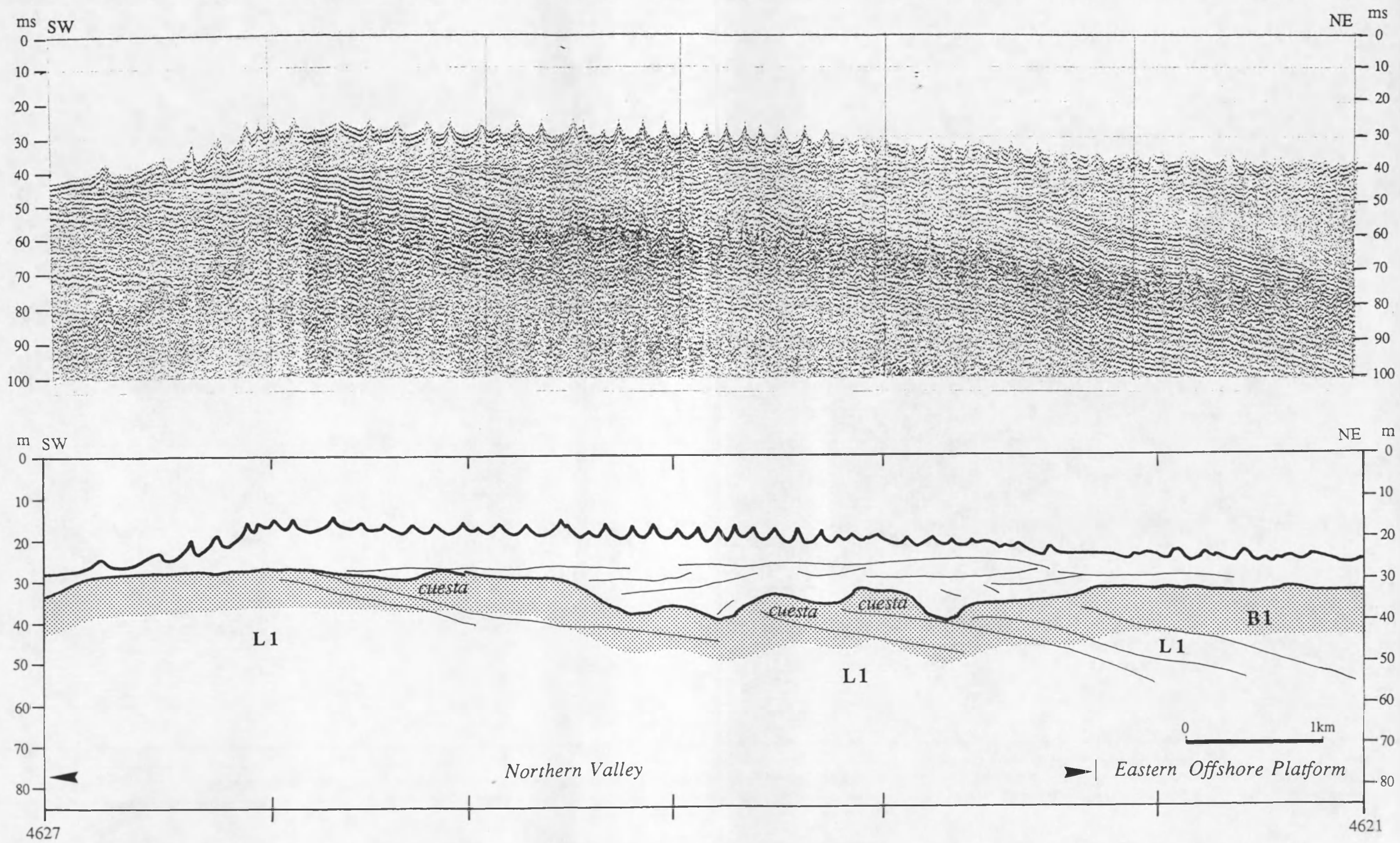


Figure 7.3 Analog record of a sparker section and interpreted line-drawing showing cuestas in the L1 sequence.

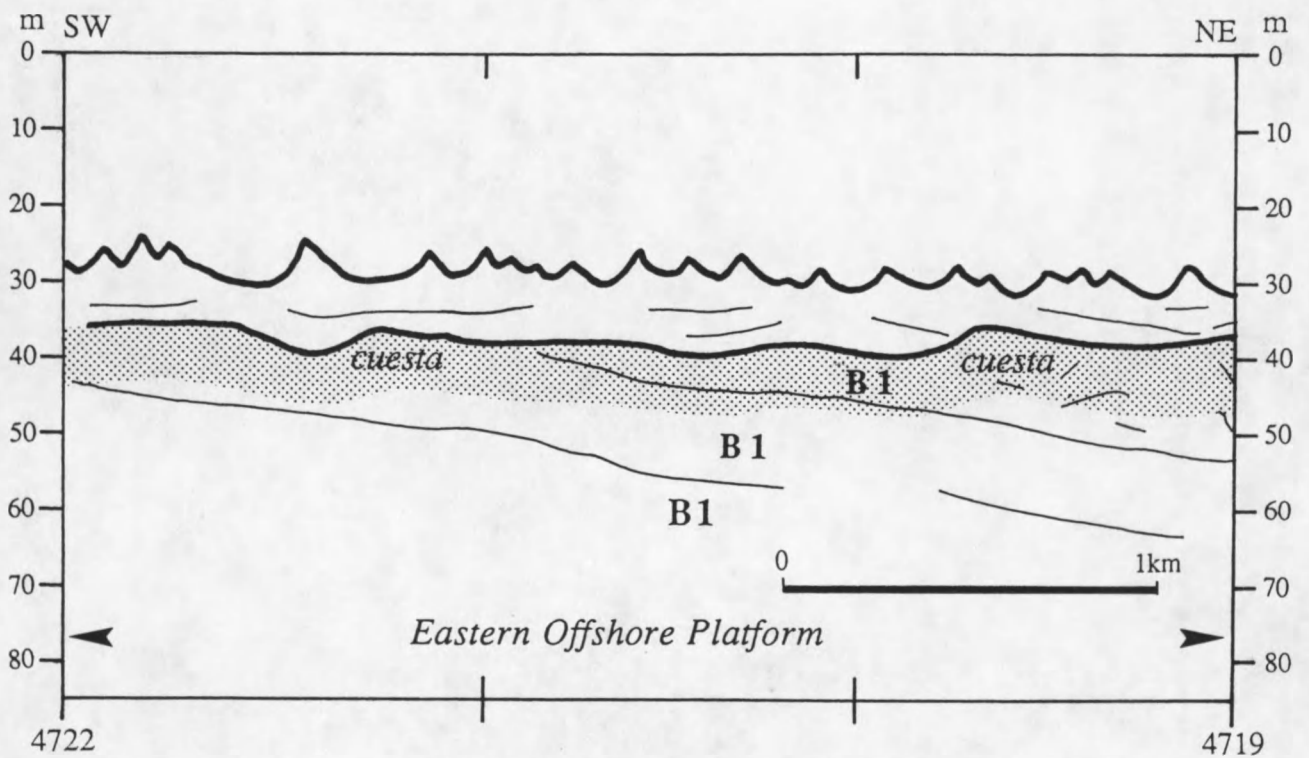
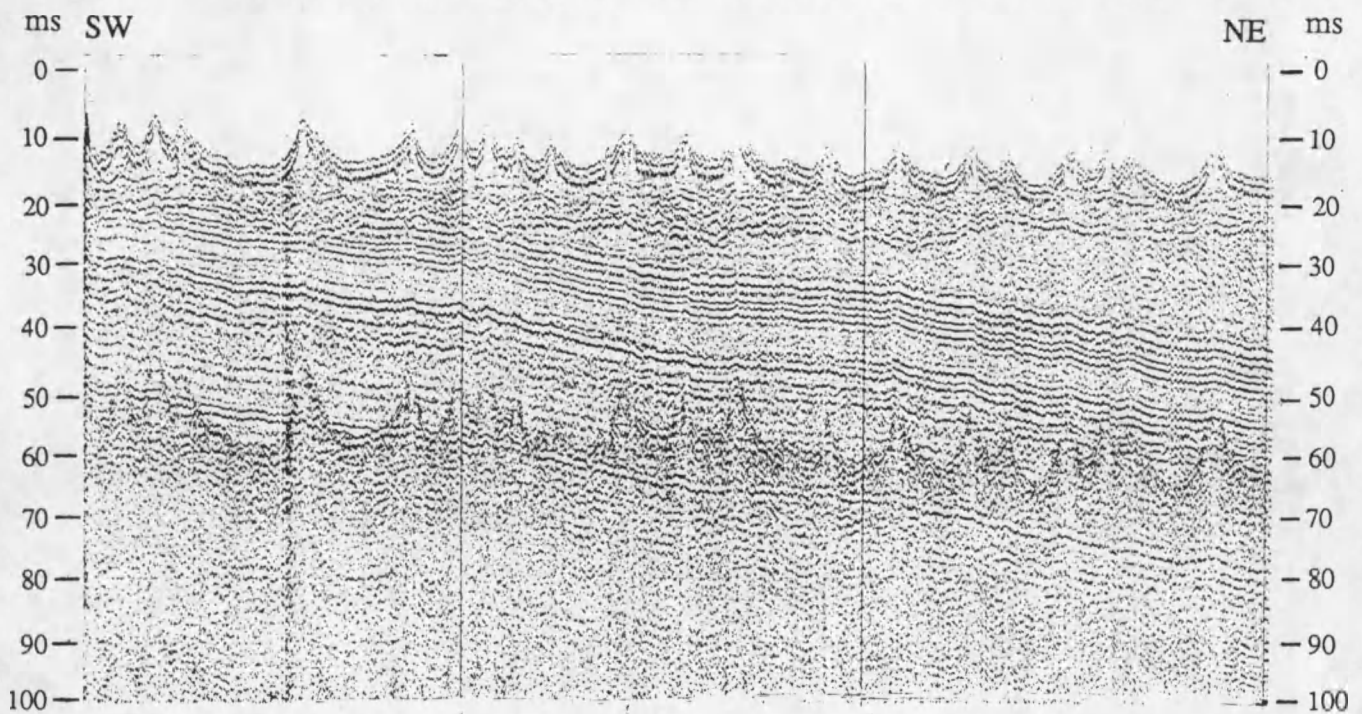


Figure 7.4 Analog record of a sparker section and interpreted line-drawing showing cuestas at different levels in the B1 sequence.

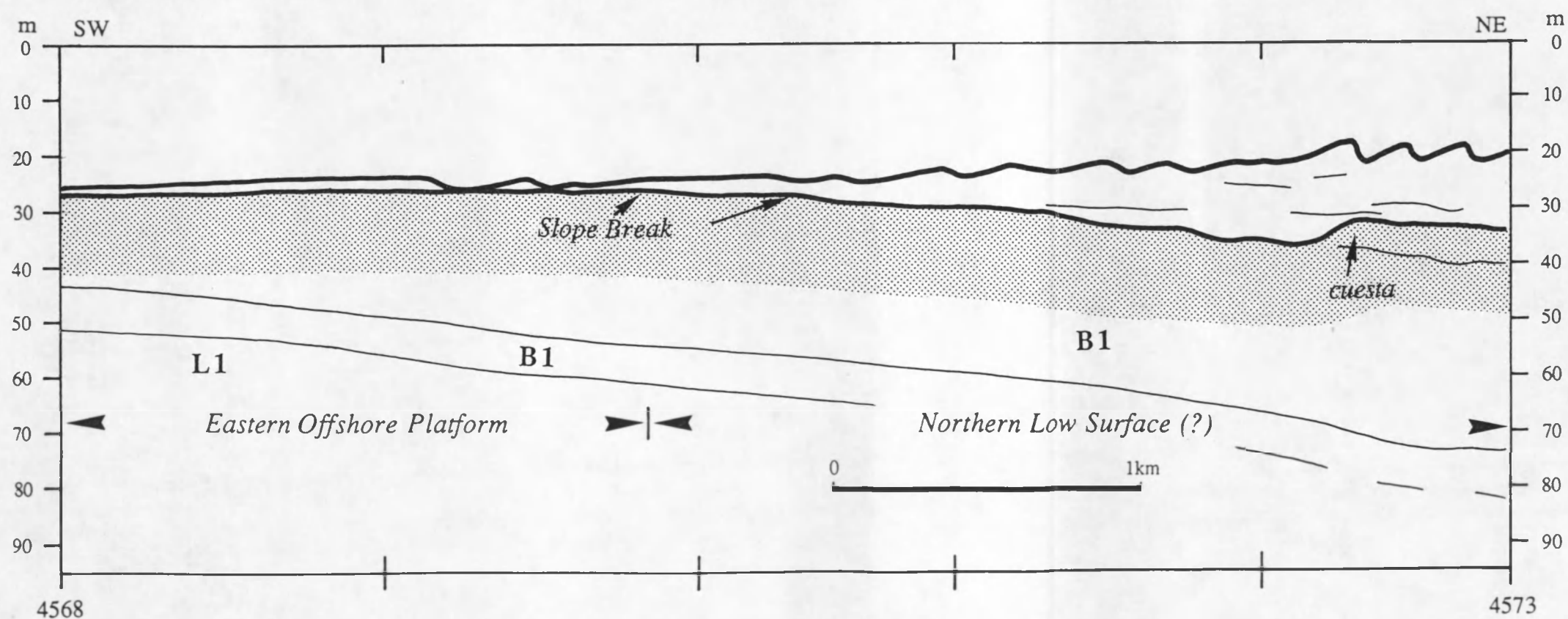
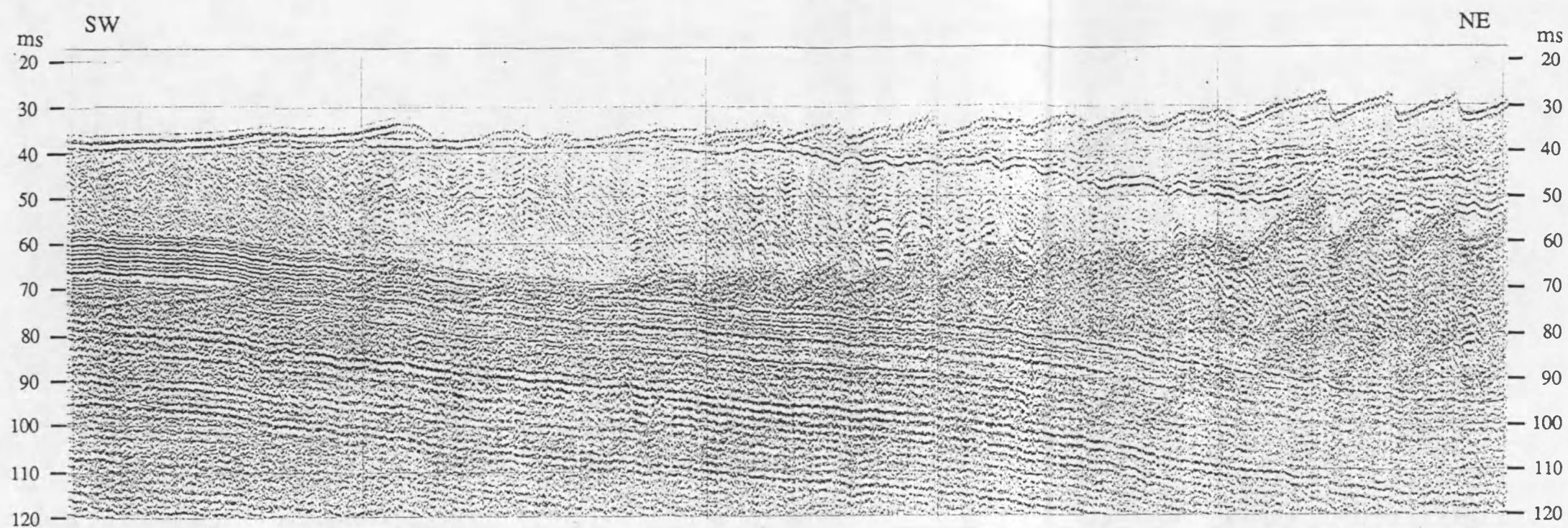


Figure 7.5 Analog record of a sparker section and interpreted line-drawing showing a cuesta and a slope break in the upper part of the B1 sequence.

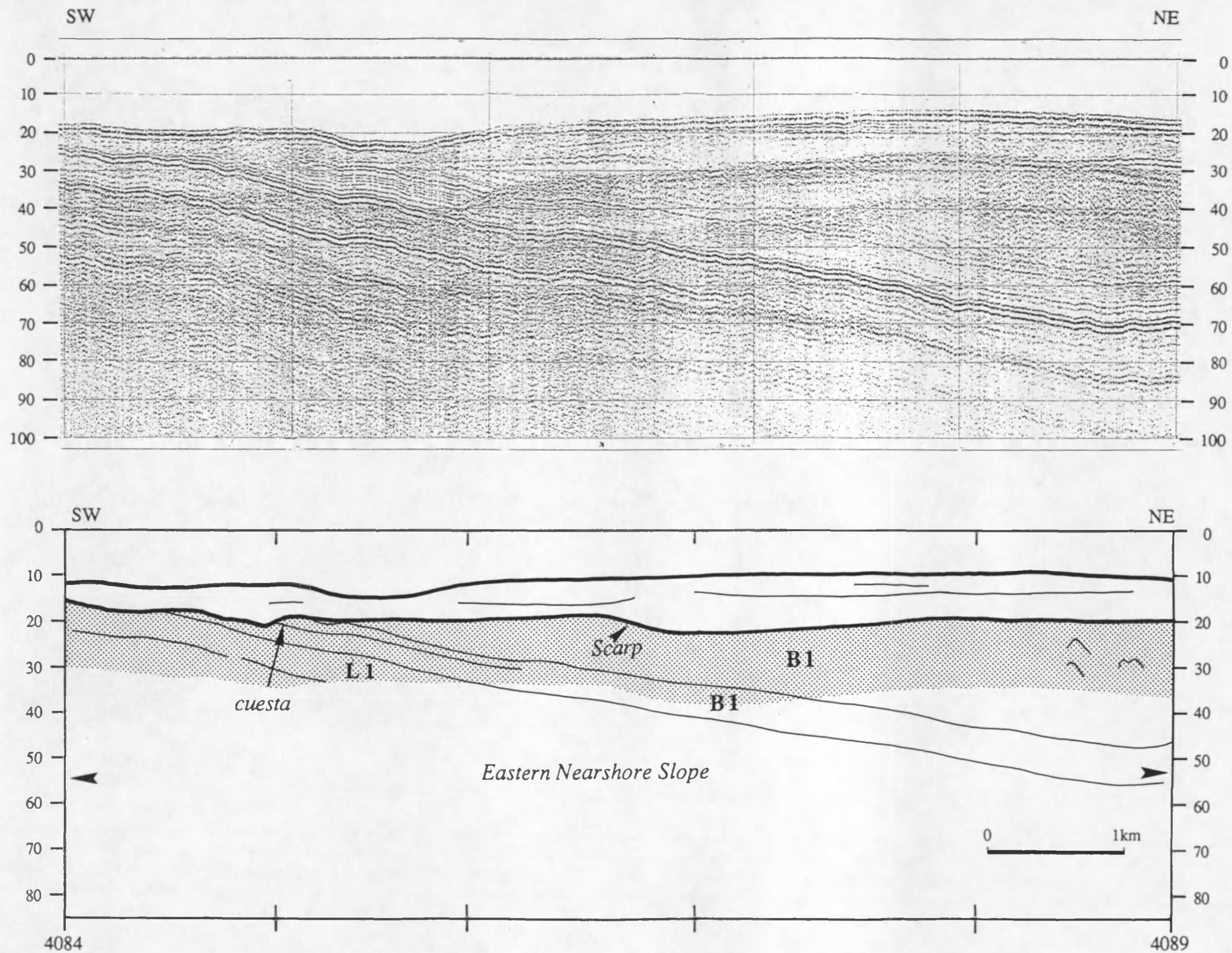


Figure 7.6 Analog record of a sparker section and interpreted line-drawing showing a cuesta and a scarp in the lower part of the B1 sequence.

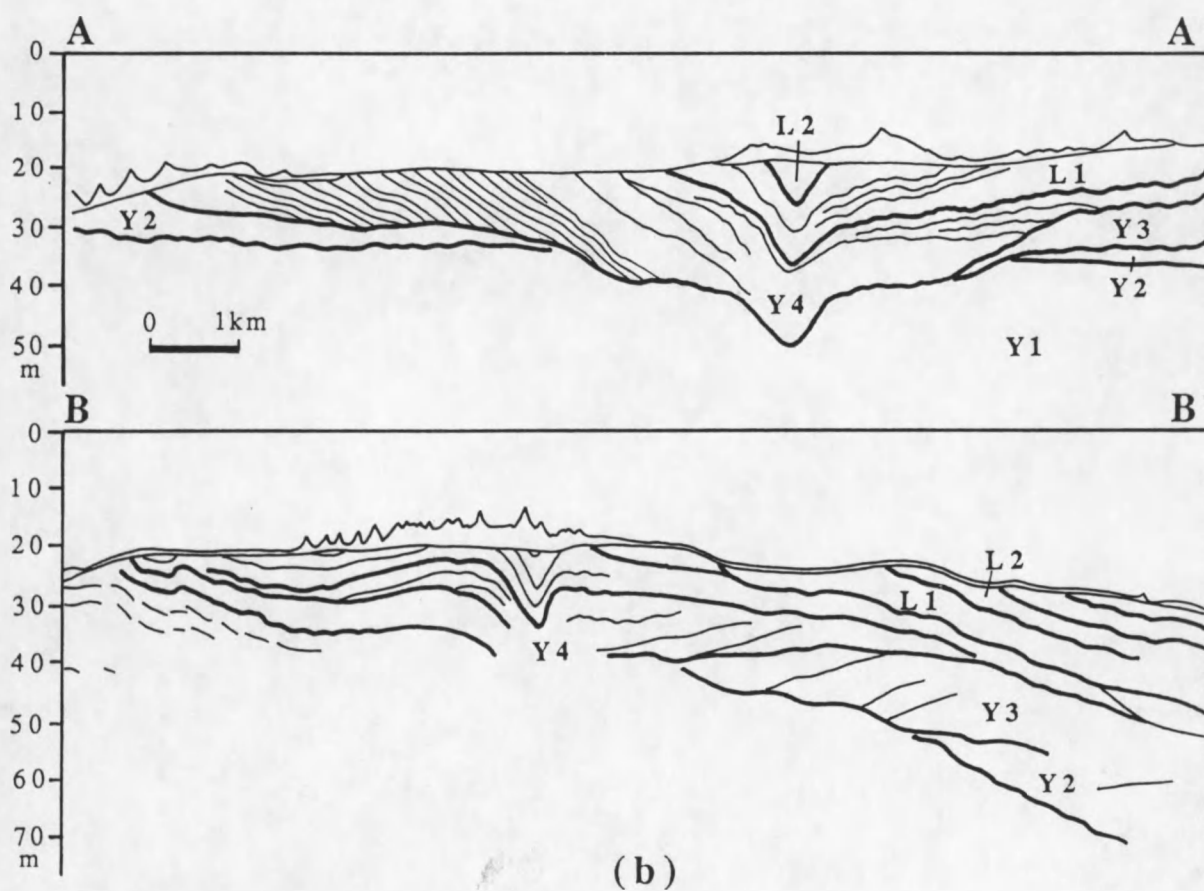
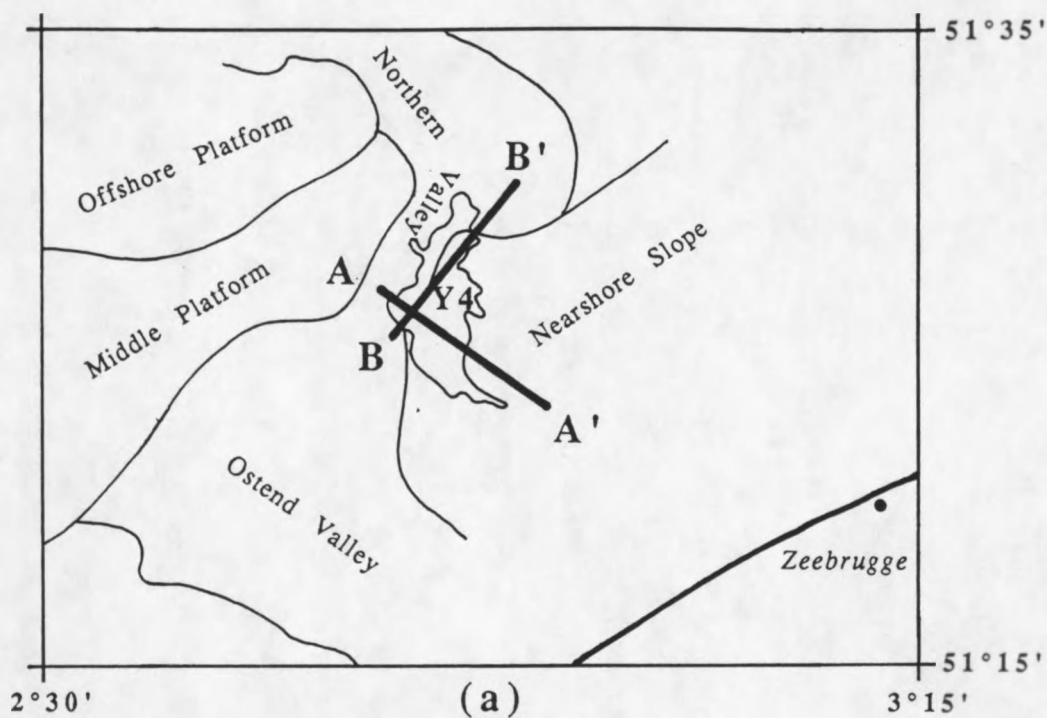


Figure 7.7 Analog record of a sparker section and interpreted line-drawing showing the high overlying the basin fill offshore Ostend.

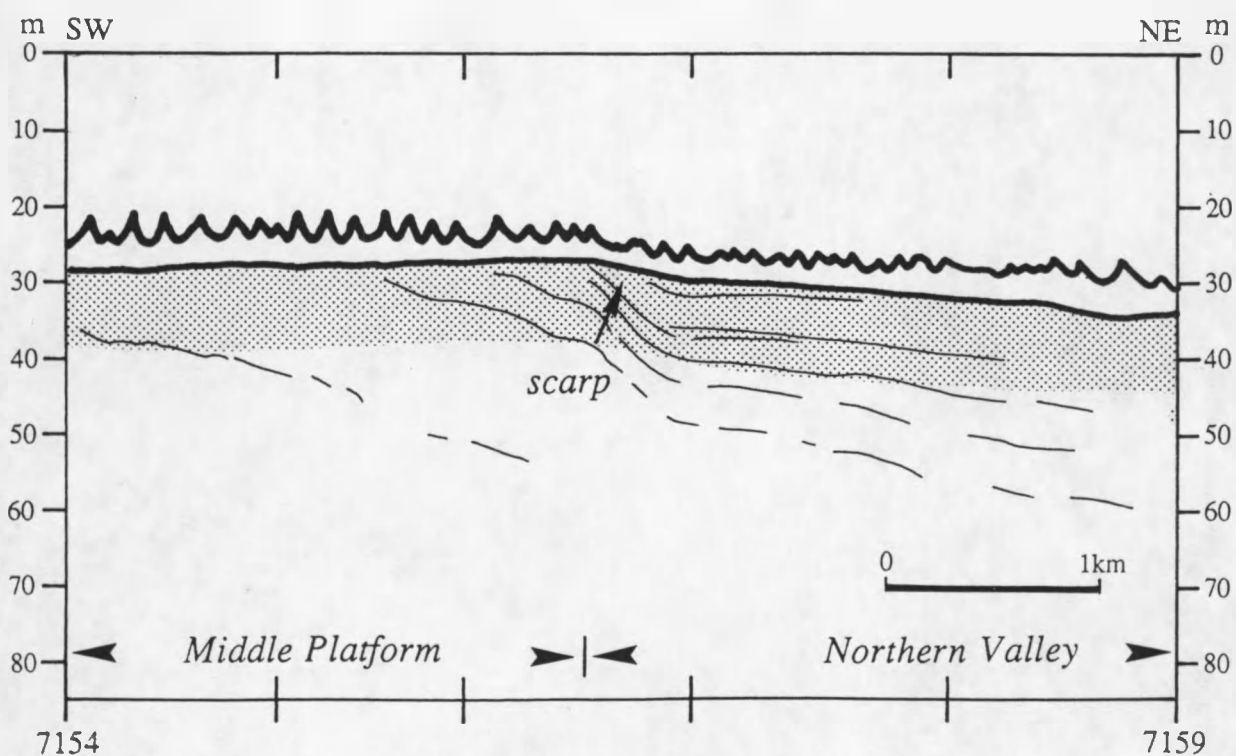
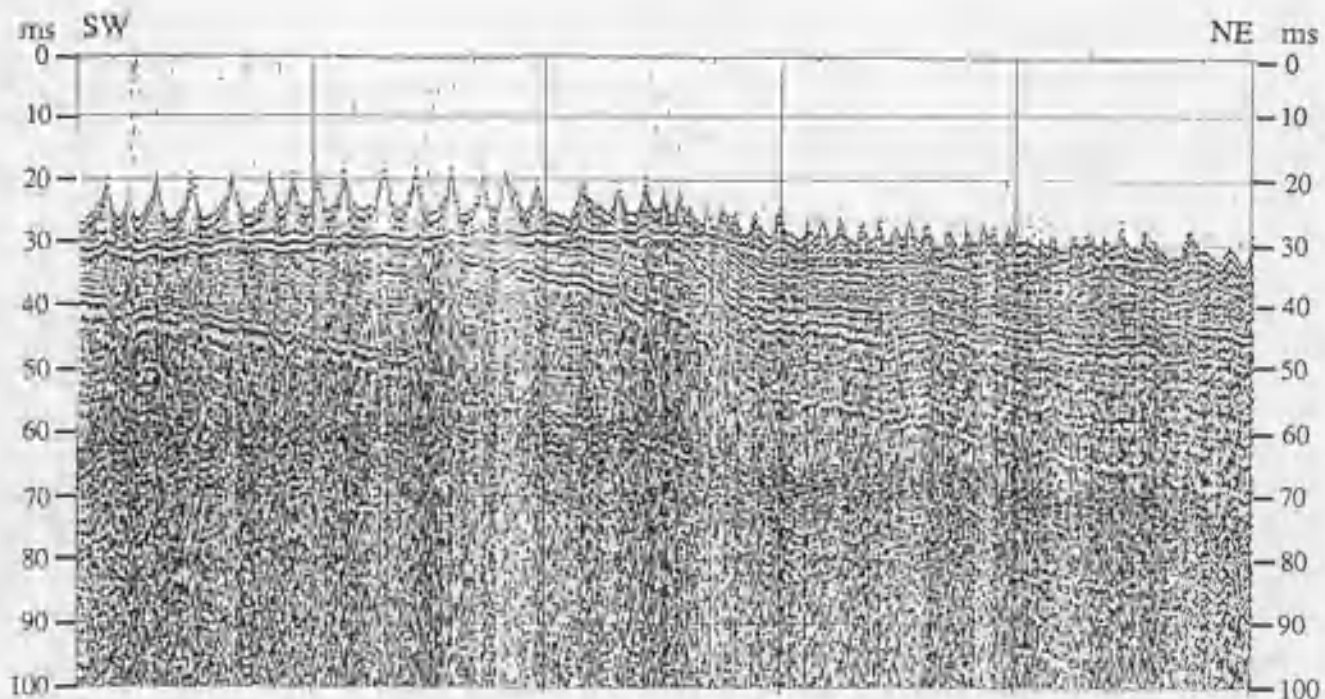


Figure 7.8 Analog record of a sparker section and interpreted line-drawing showing a scarp in the NW trending Northern Valley.

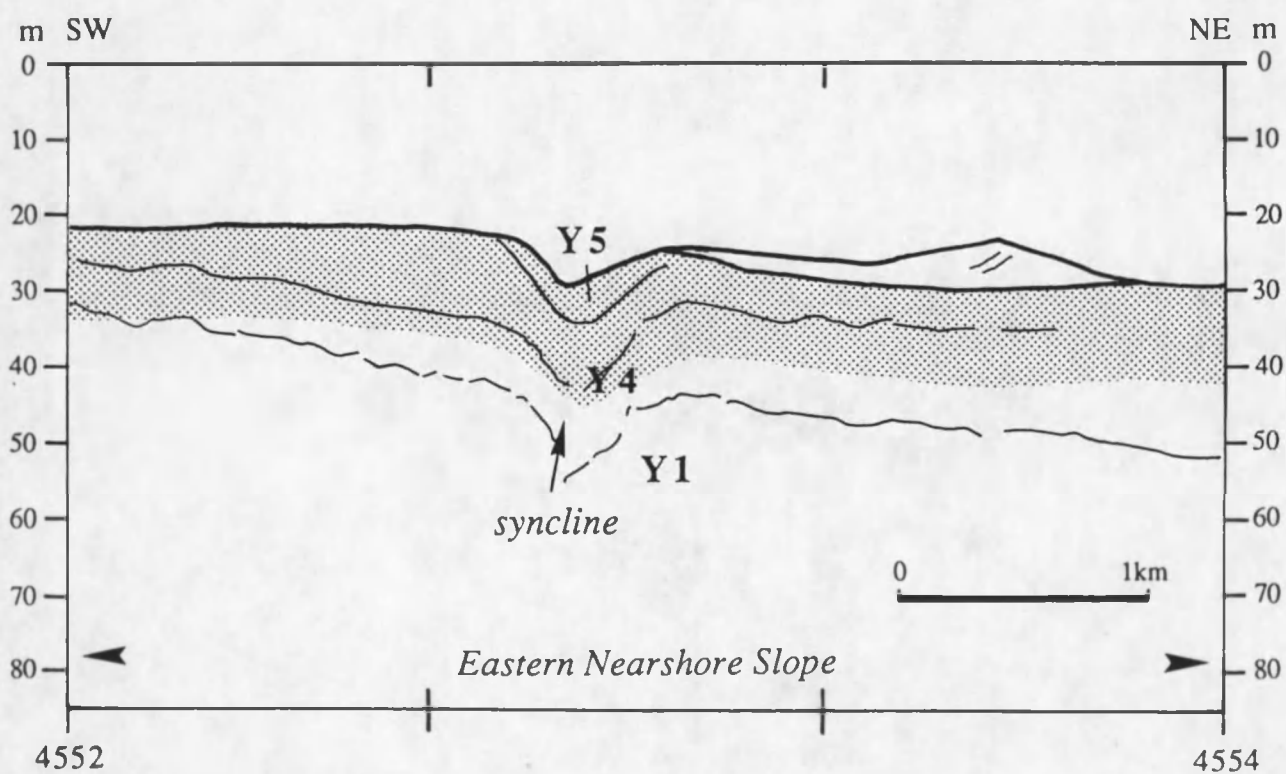
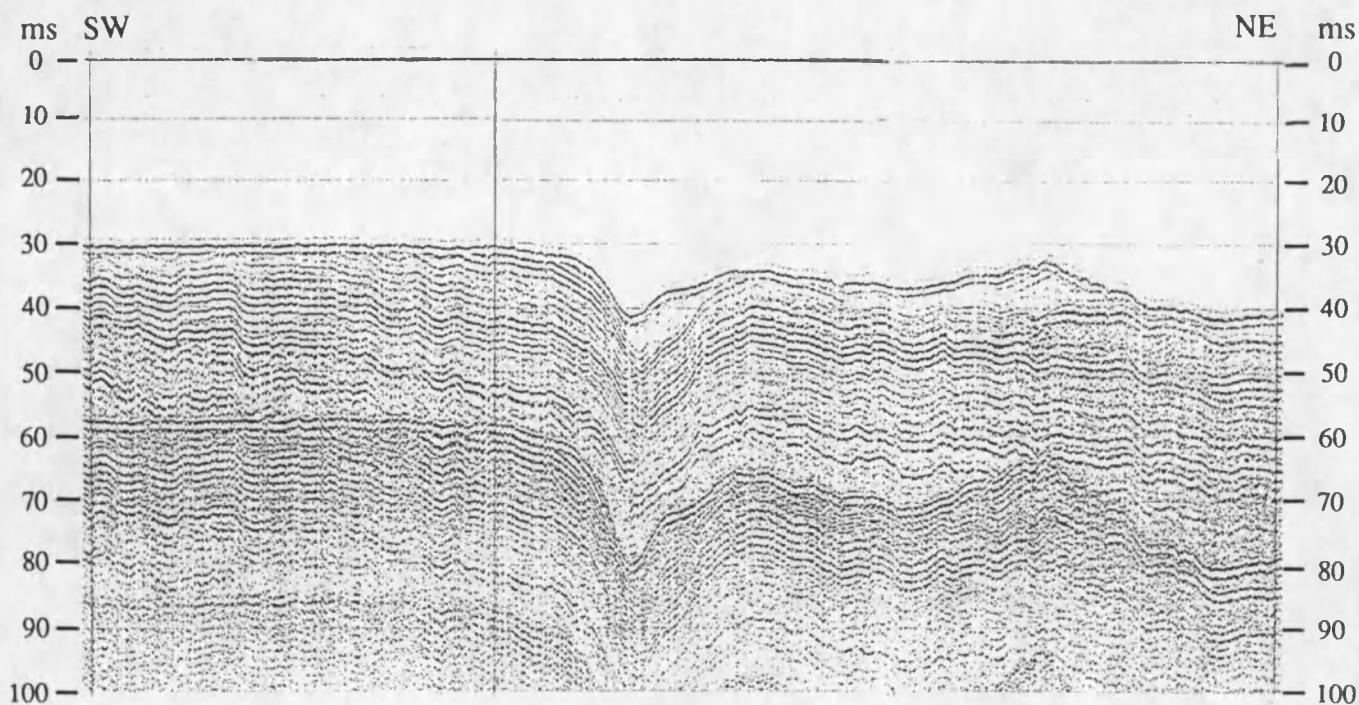


Figure 7.9 Analog record of a sparker section and interpreted line-drawing showing a syncline overlain by a depression.

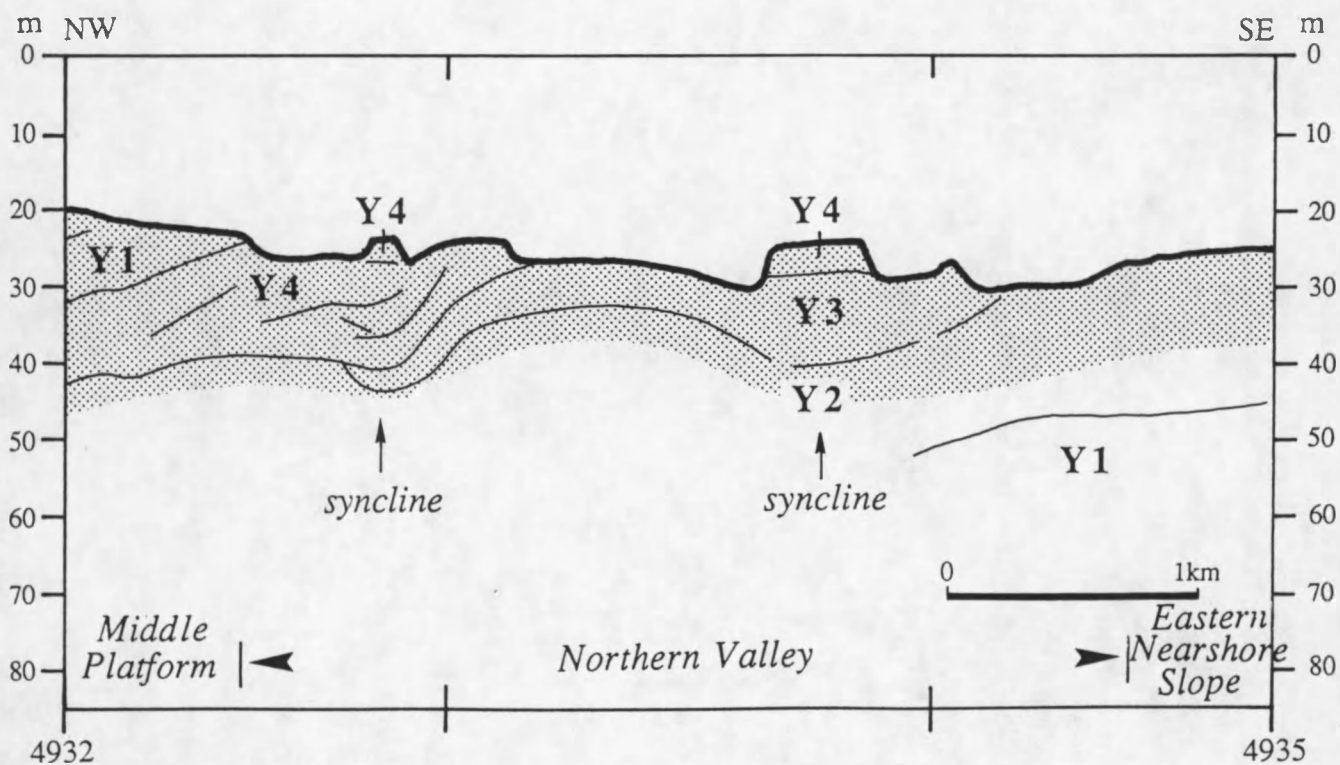
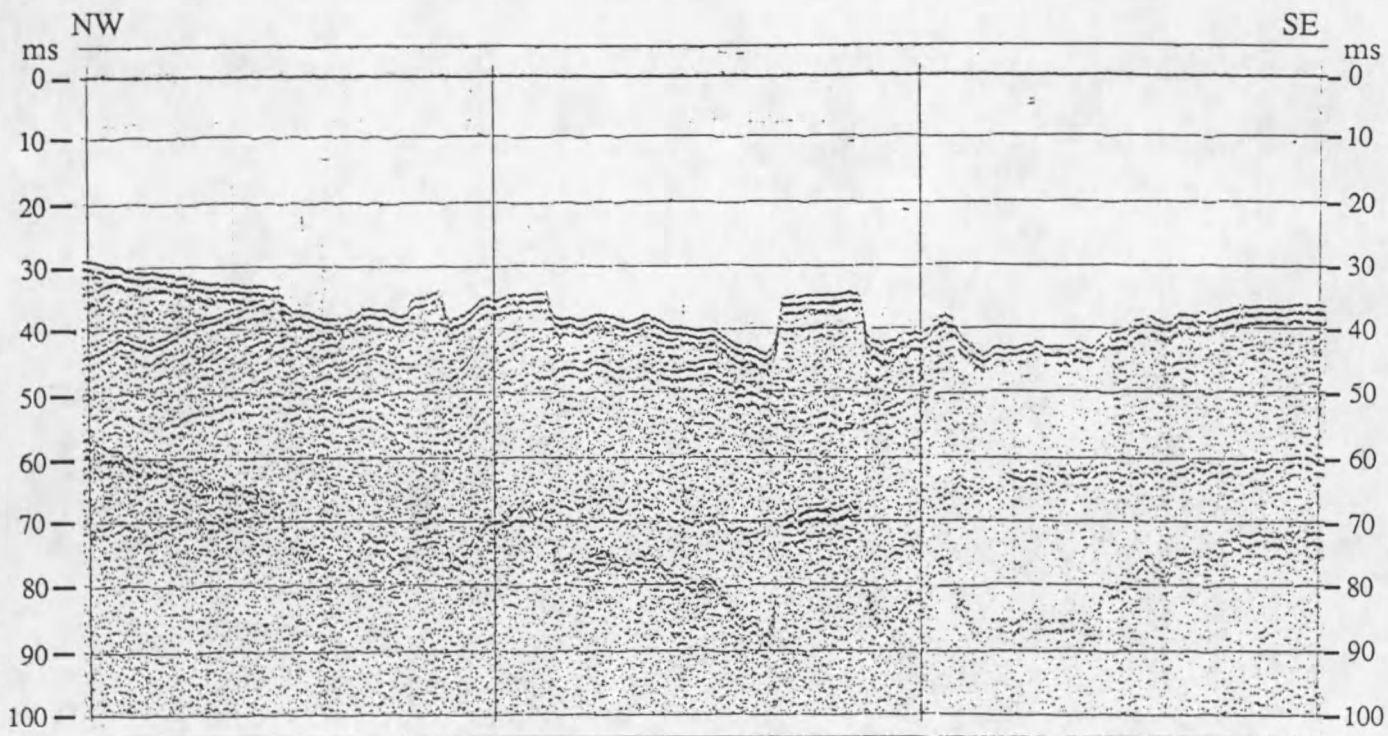


Figure 7.10 Analog record of a sparker section and interpreted line-drawing showing two weak synclines overlain by highs.

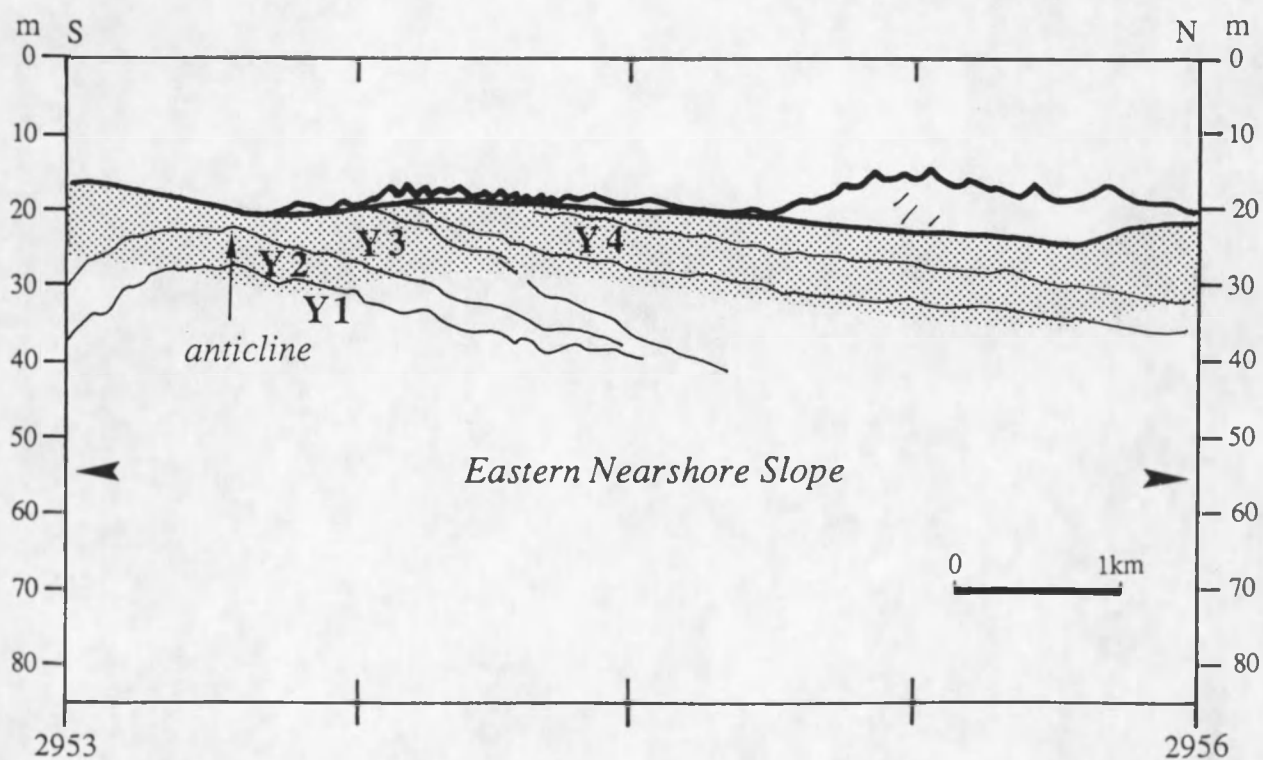
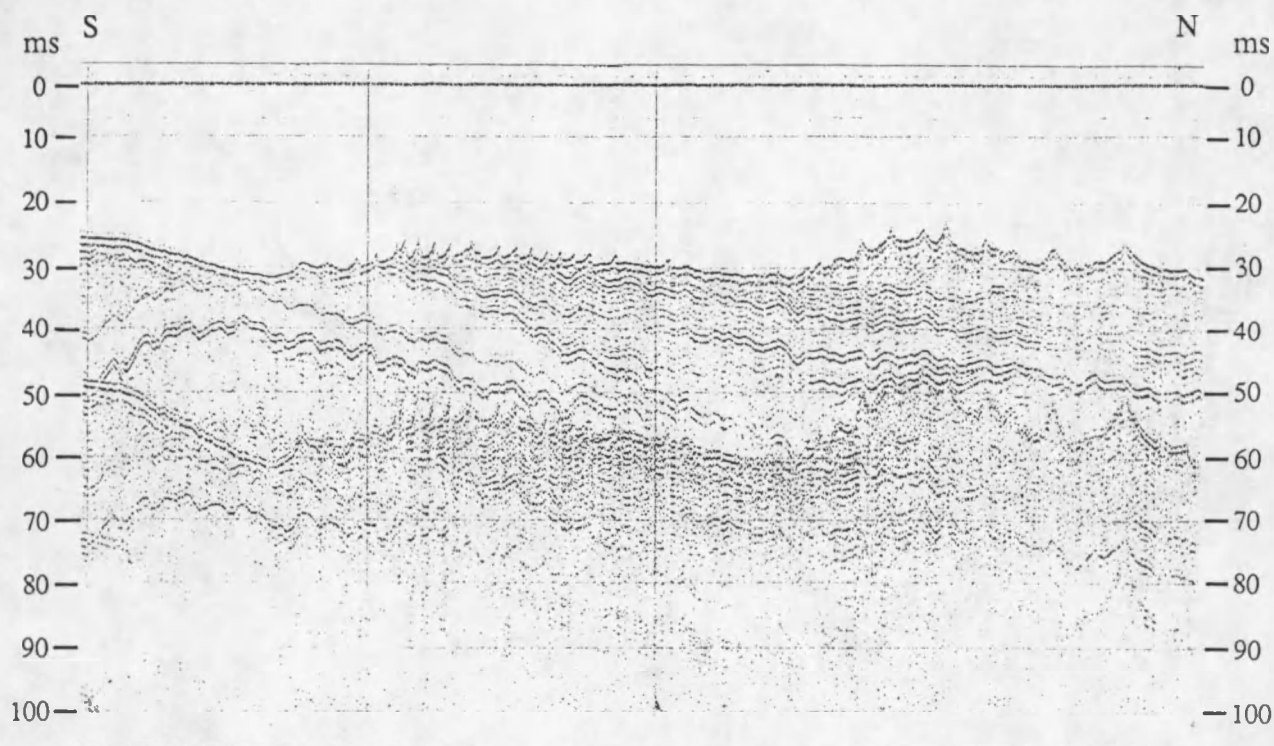


Figure 7.11 Analog record of a sparker section and interpreted line-drawing showing an anticline overlain by a depression.

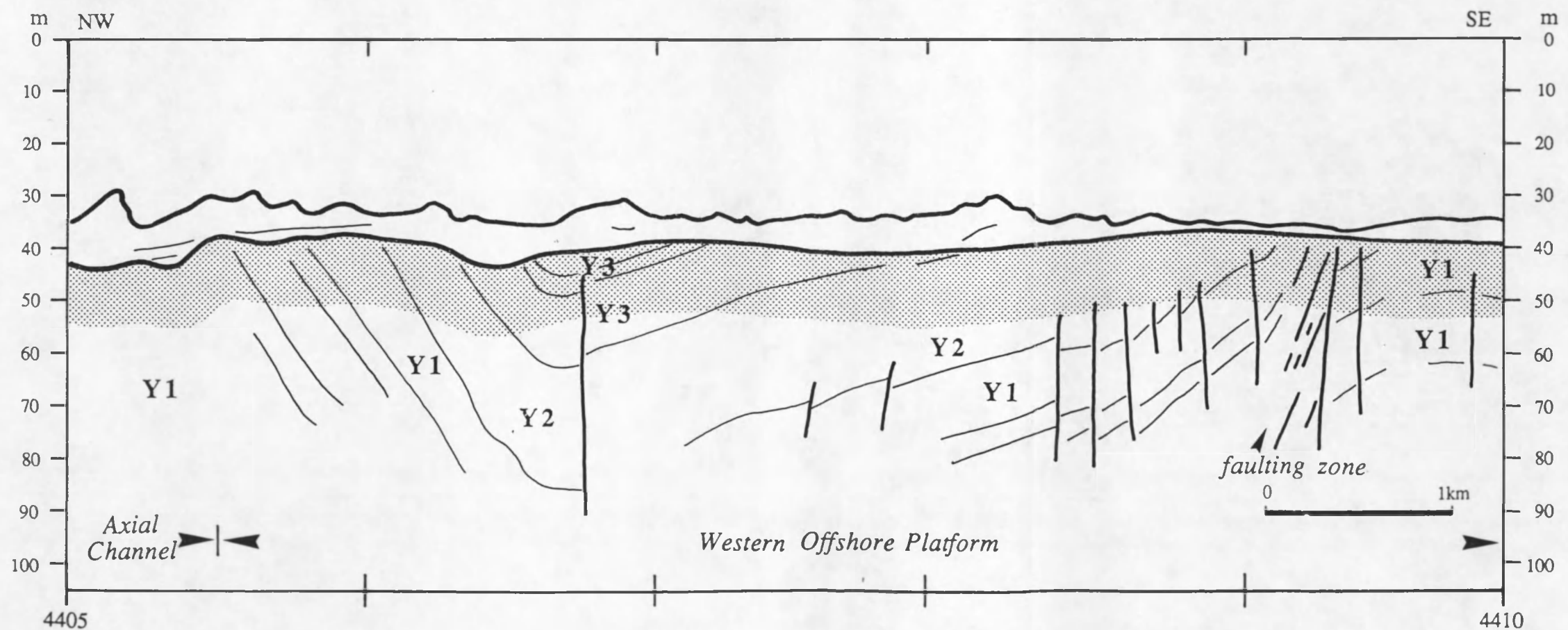
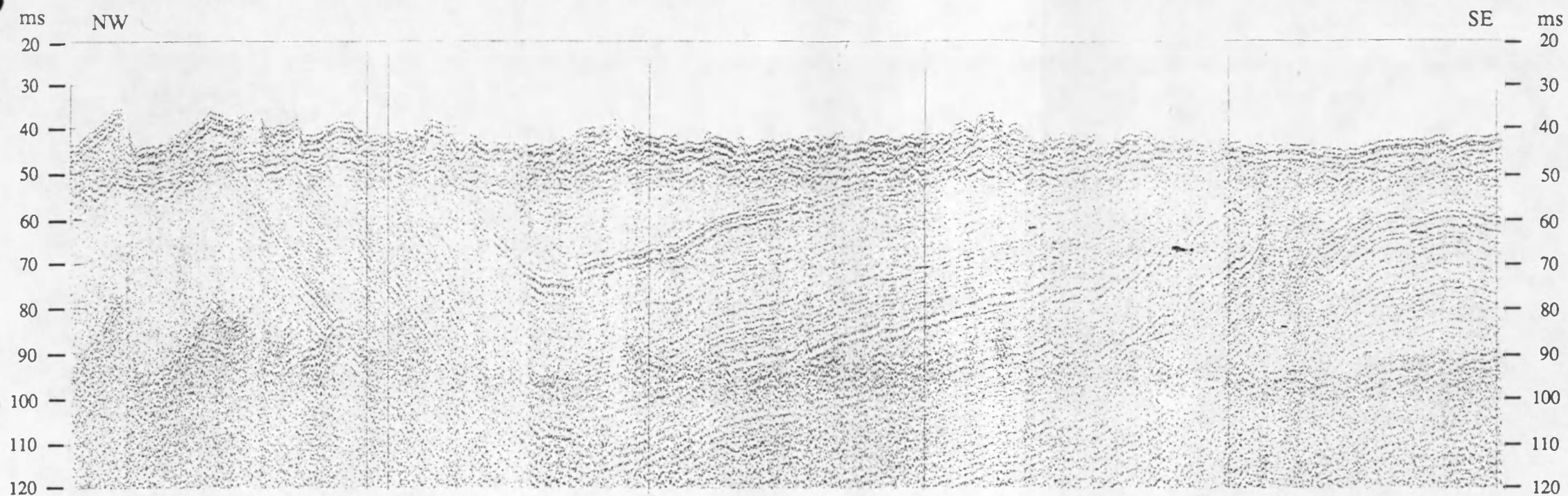


Figure 7.12 Analog record of a sparker section and interpreted line-drawing showing the most southern synclinal depression of the Noordhinder deformation zone.

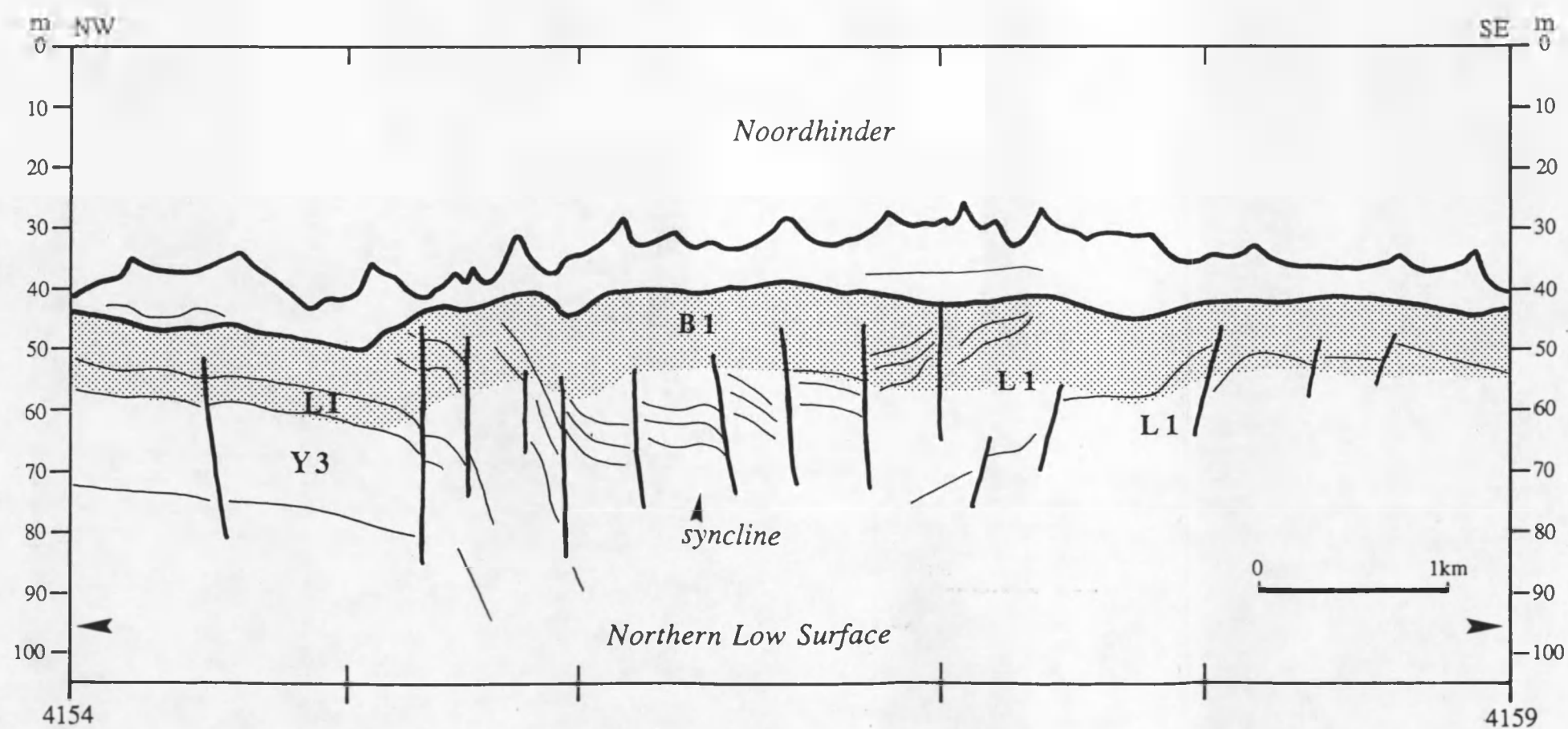
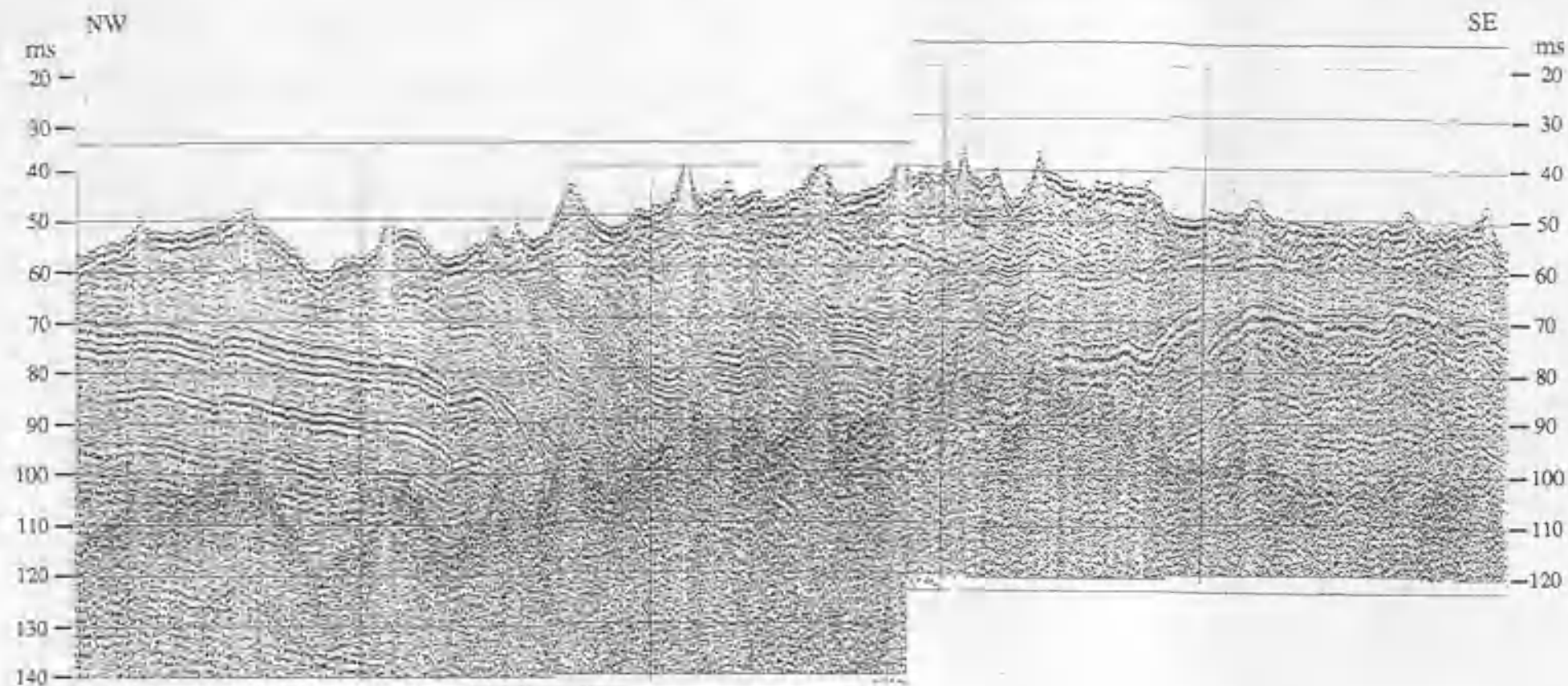


Figure 7.13 Analog record of a sparker section and interpreted line-drawing showing the northernmost central synclinal depression of the Noordhinder deformation zone.

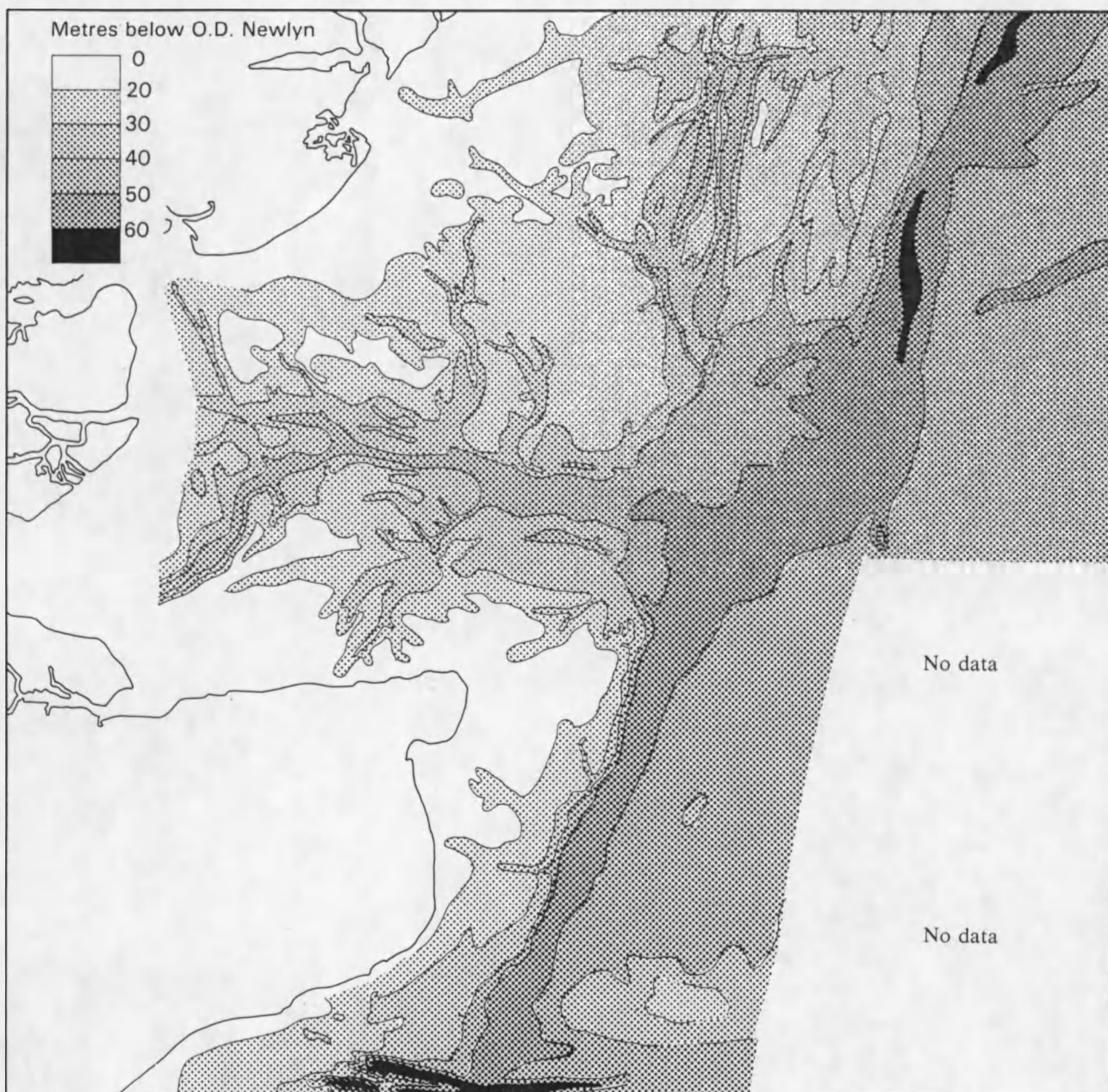


Figure 8.1 The recent Lobourg paleochannel system (after Bridgland & D'Olier, 1989).

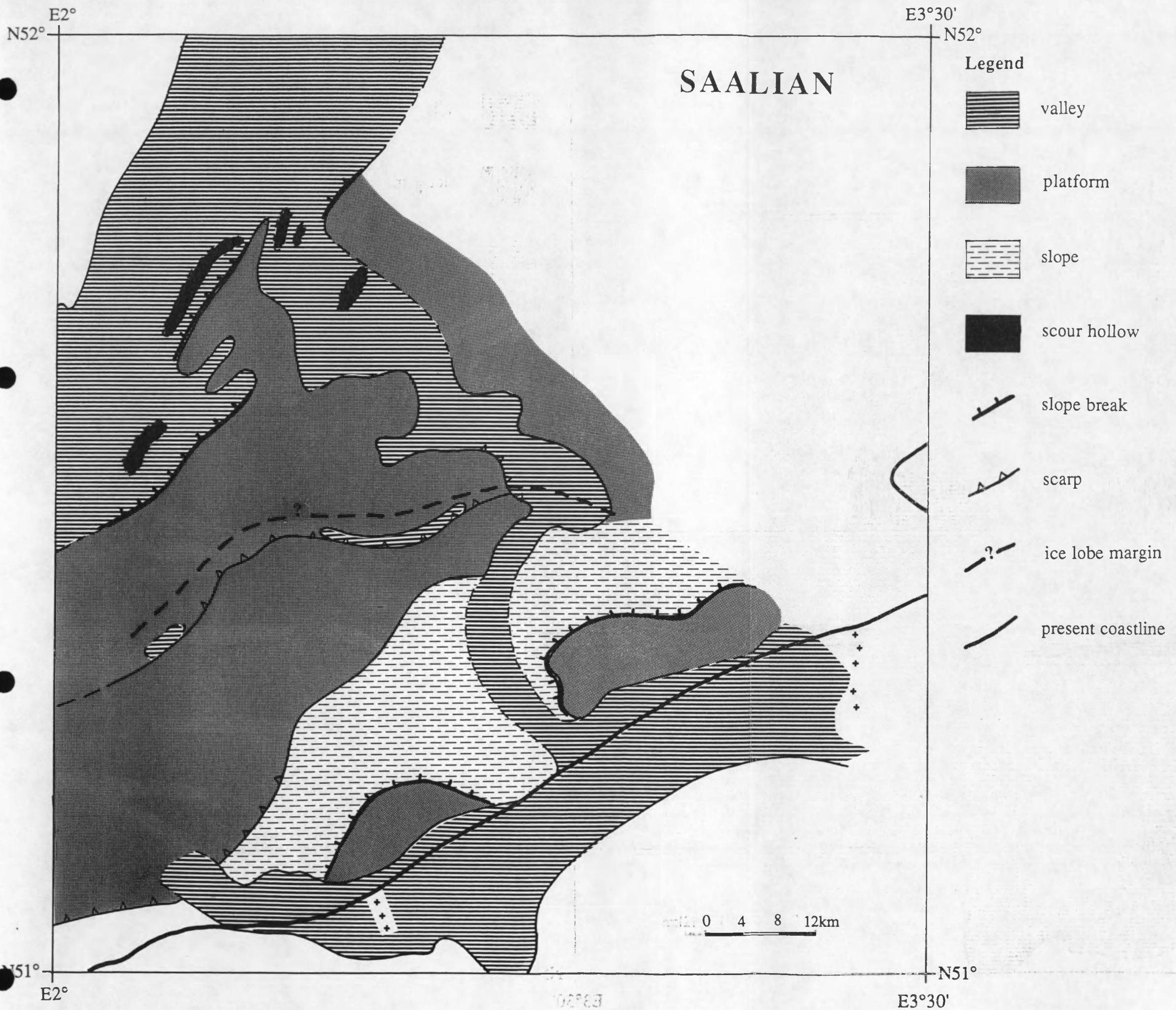


Figure 8.2 Tentative reconstruction of the study area during the Saalian.

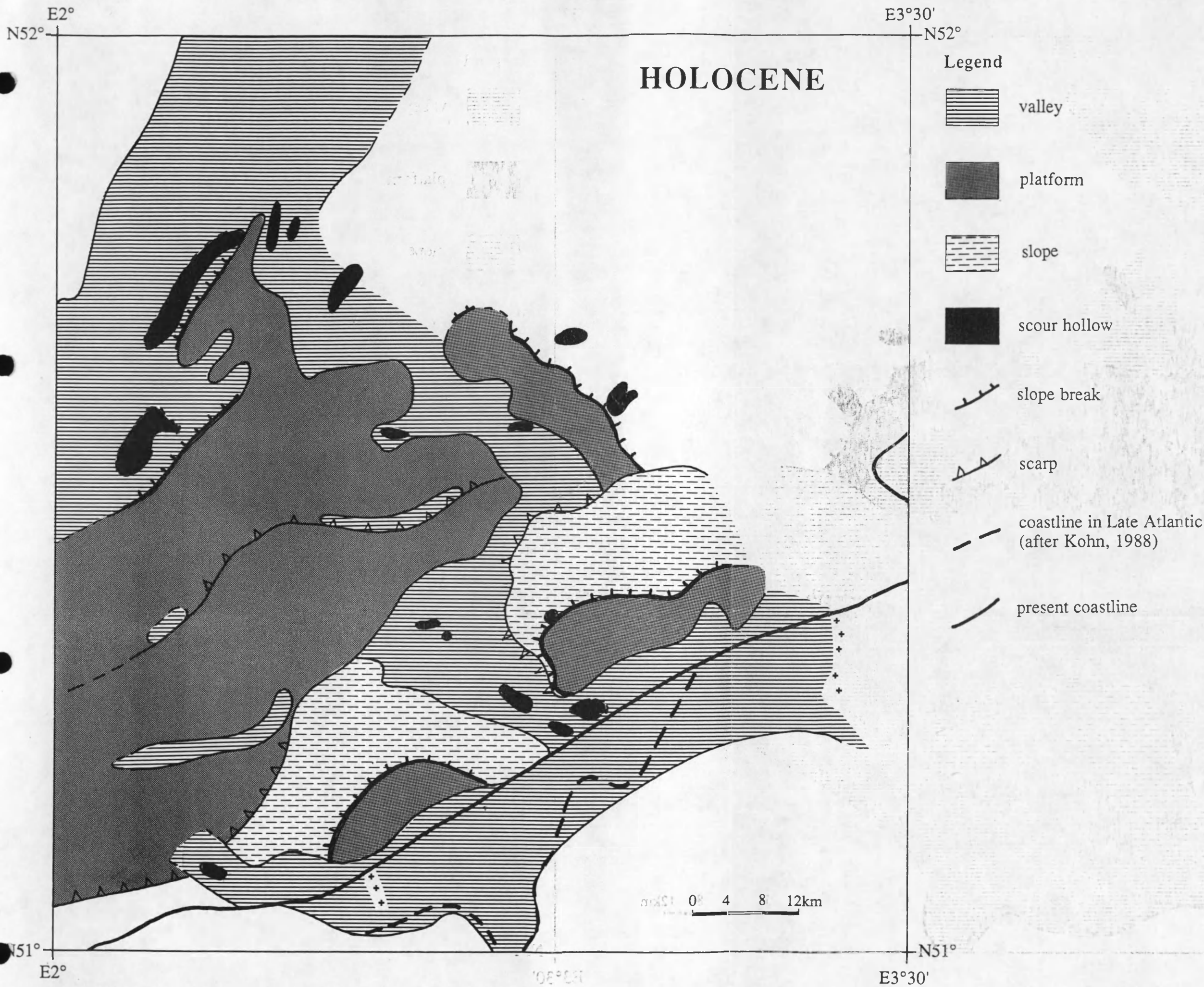


Figure 8.3 Tentative reconstruction of the study area during the Holocene.

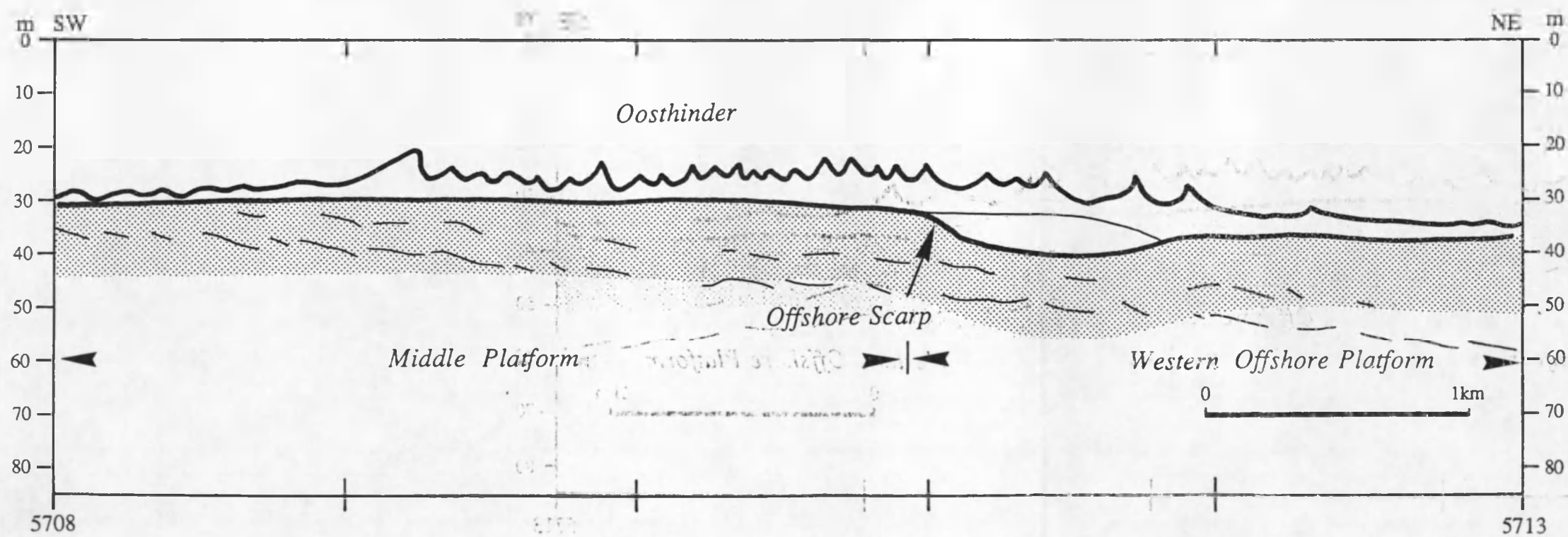
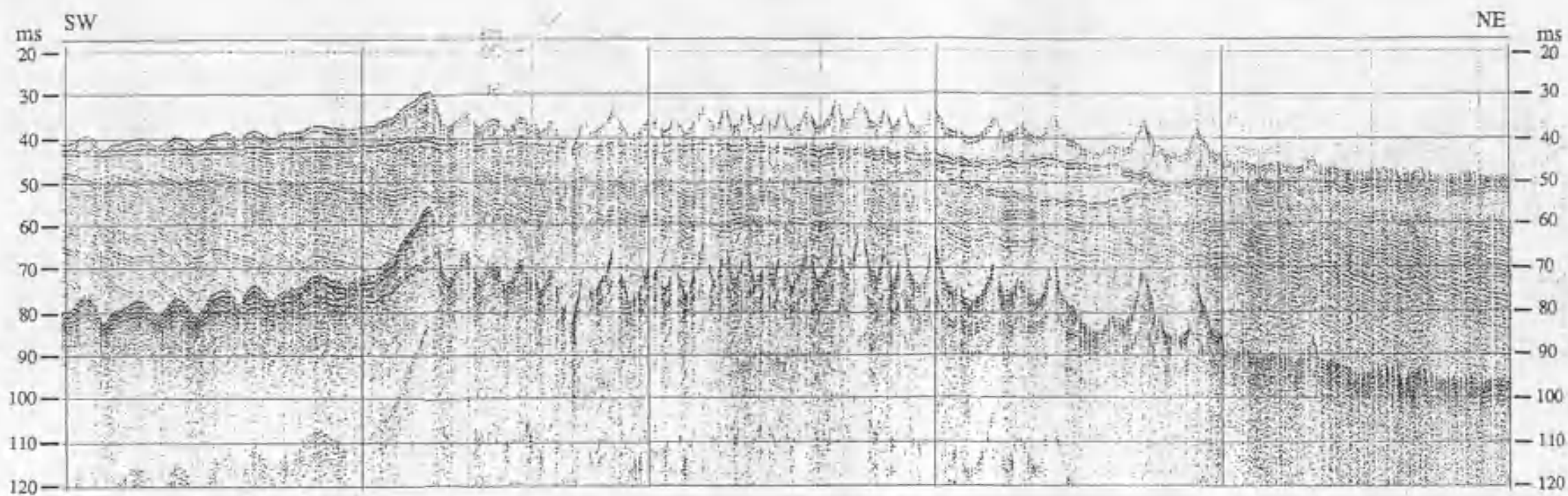


Figure 9.2 Analog record of a sparker section and interpreted line-drawing showing the Oosthinder overlying the Offshore Scarp.

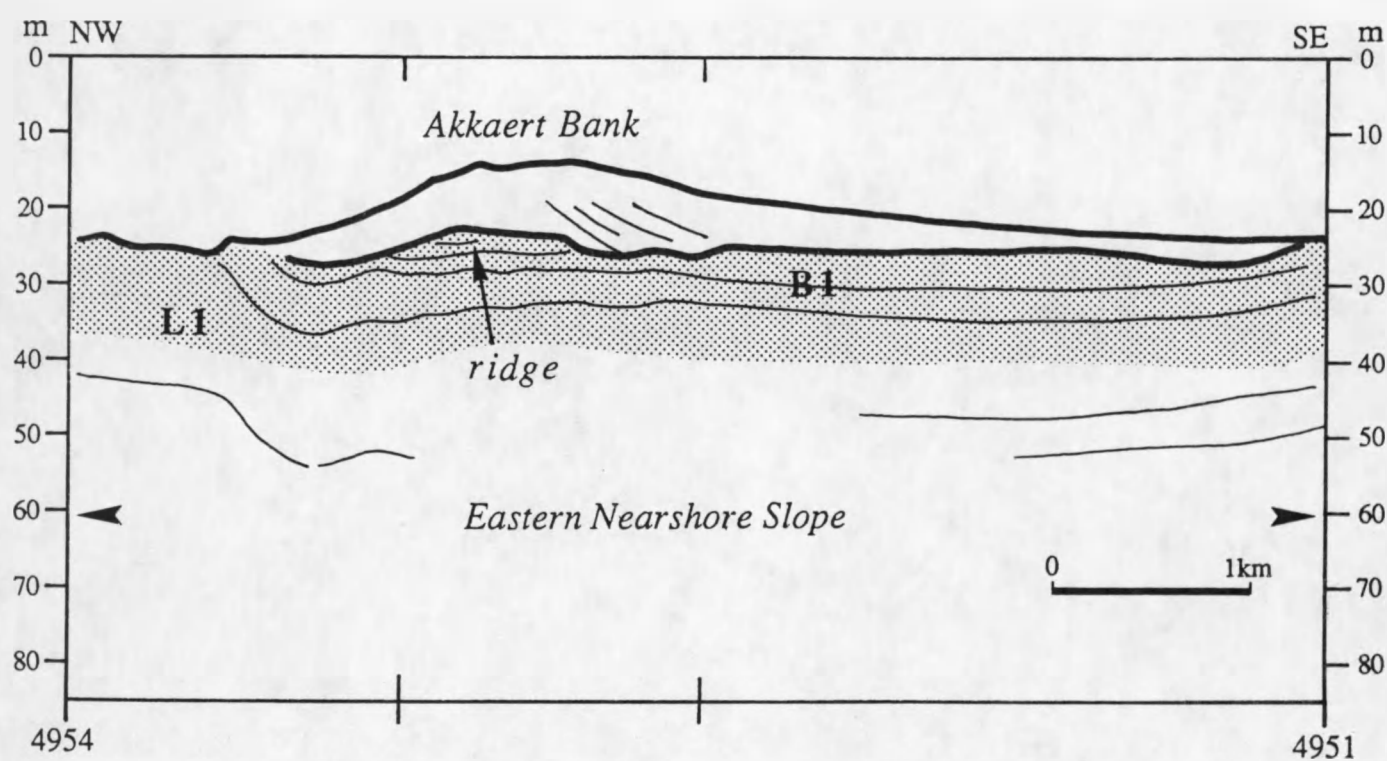
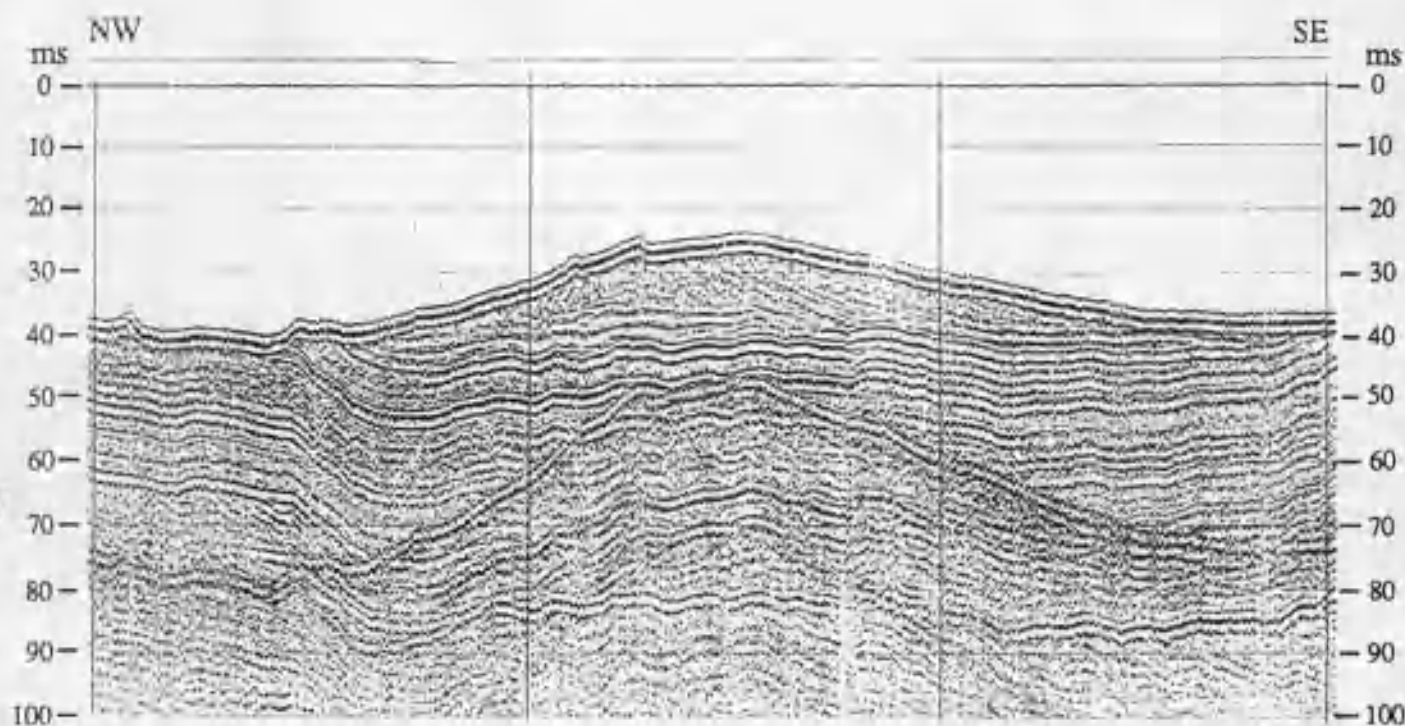


Figure 9.3 Analog record of a sparker section and interpreted line-drawing showing a ridge underlying the northern part of the Akkaert Bank.

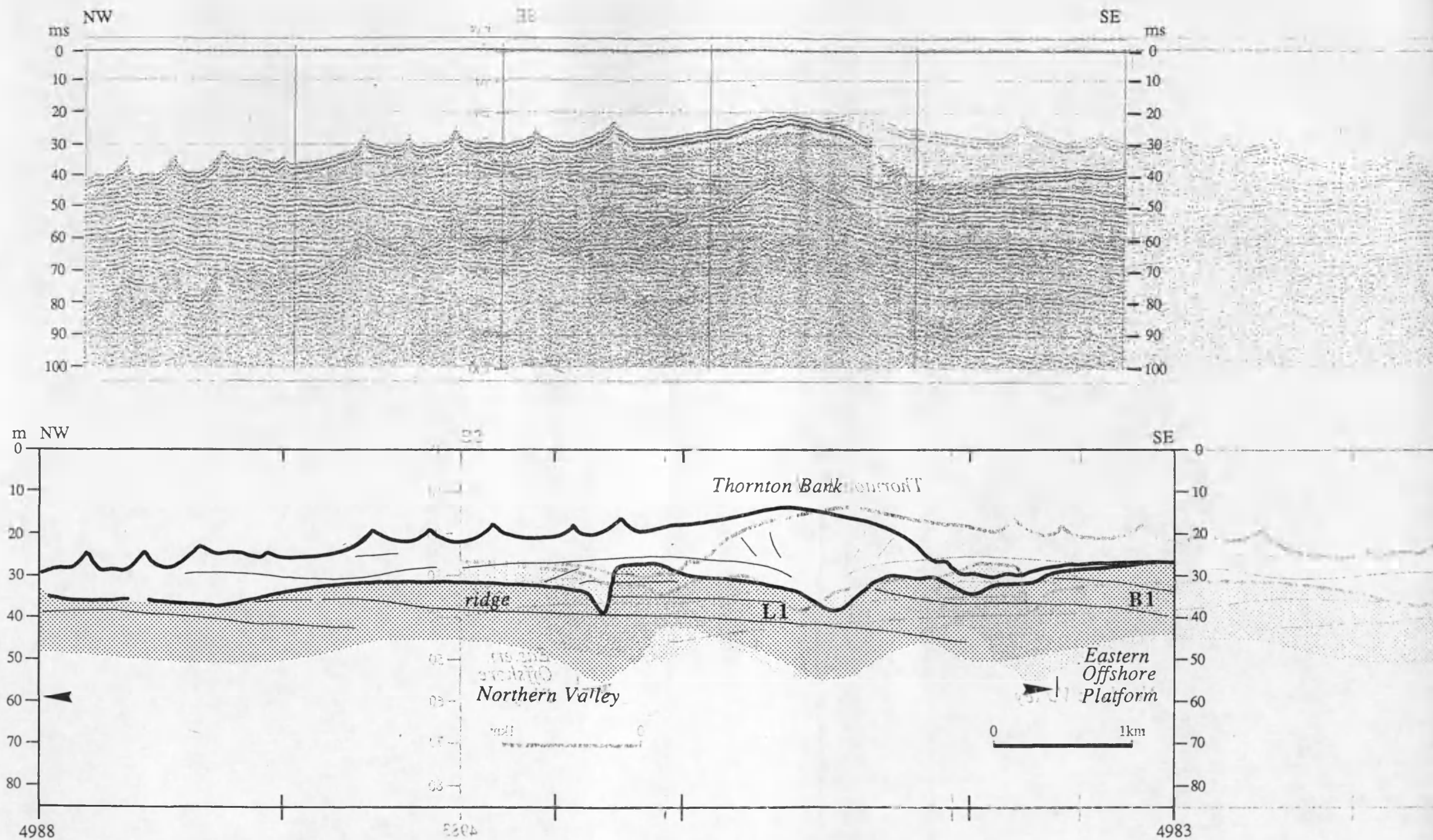


Figure 9.4 Analog record of a sparker section and interpreted line-drawing showing a broad ridge underlying the Thornton Bank.

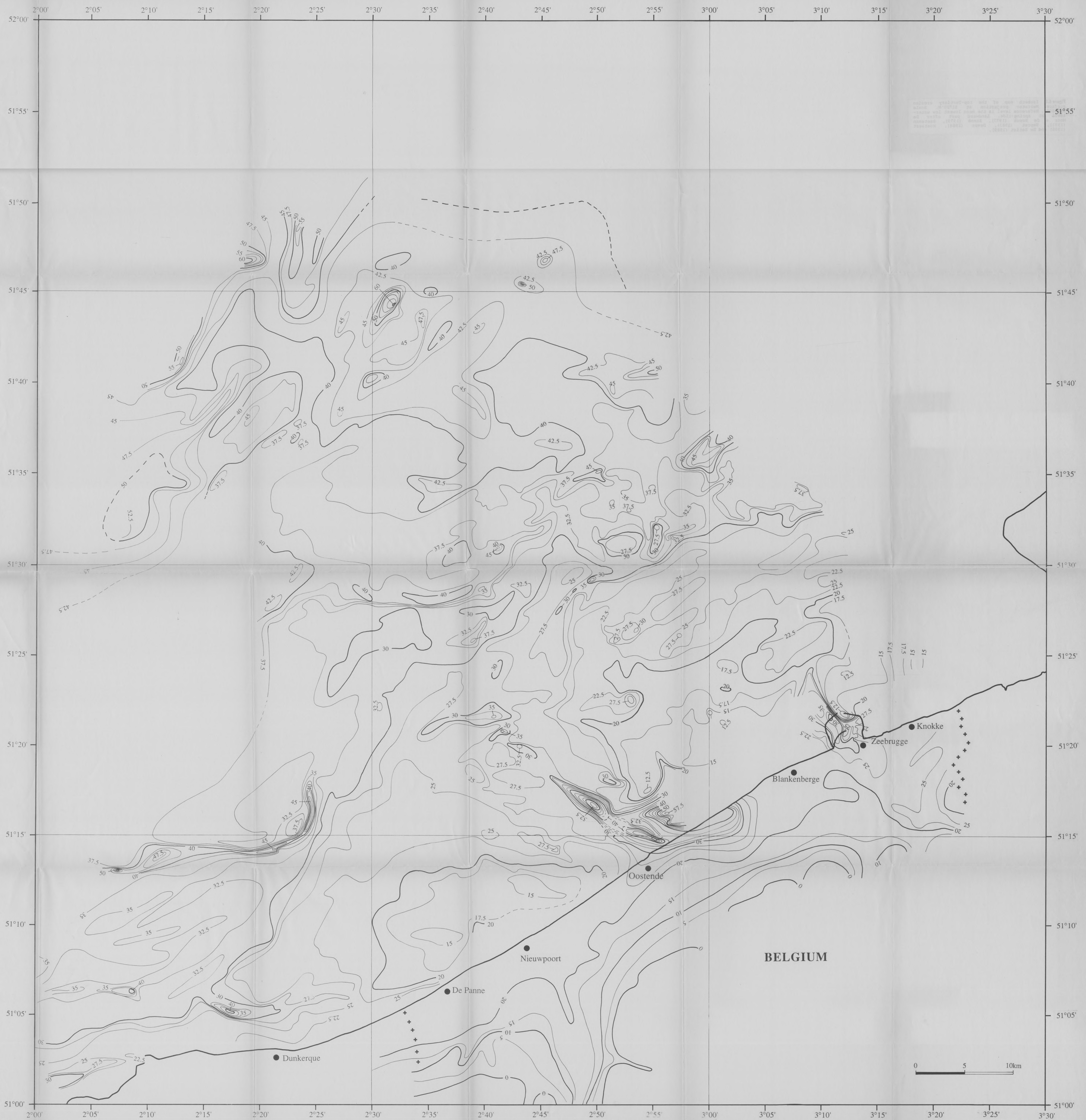


Figure 6.1 Isobath map of the top-Tertiary erosion surface. Mercator projection at 51°20'N. Scale 1/100000. Reference level is the mean lowest low water-level at spring-tide. Landward part after De Moor & De Breuk (1973), Somme (1979), Baeteman (1981), Depret (1983), Devos (1984), Mostaert (1985) and De Batist (1989).

